UNIVERSITÀ DEGLI STUDI DI CATANIA
FACOLTÀ DI SCIENZE MATEMATICHE, FISICHE E NATURALI
CORSO DI DOTTORATO IN FISICA

Emanuele Messina

Non Perturbative Renormalization of Fermion Theories

TESI DI DOTTORATO

Relatore:
Chiar.mo Prof. V. Branchina

XXIV ciclo

CONTENTS

Introduction **1**

1 Functional formalism for fermion and boson theories **7**

1.1 Gross-Neveu and Yukawa models 8

1.2 Elementary fields Green's functions and continuum limit 10

1.2.1 Green's functions of composite operators and scalar fields 13

1.3 Generating functionals for fermion theories 14

1.3.1 Generating functional for Green's functions 14

1.3.2 Generating functional for connected Green's functions 16

1.3.3 Generating functional for $1PI$ Green's functions 18

1.4 Symmetries 21

1.4.1 Symmetries in functional formalism 24

1.5 Non-interacting fermions and bosons 25

1.5.1 Free fermion theory 26

1.5.2 Free theory with fermions and scalars 30

1.6 Interactions and perturbation theory 31

1.6.1 Perturbations in fermion theories with composite operators 31

1.6.2 Perturbative expansion of Fermi theory 32

1.6.3 Perturbations in theories with fermions and scalars 36

1.6.4 Aspects of perturbative renormalization 36

1.6.5 Perturbative classification of divergences 40

1.6.6 Field theoretical renormalization of the Yukawa theory 42
1.7 Bosonization technique 45
1.7.1 The Hubbard Stratonovich transformation 45
1.7.2 Perturbation theory of the GN model in the bosonized version . . . 48
1.7.3 Non renormalizability of the bosonized theory 49

2 Non-perturbative analytical techniques I: $D-S$ equations and large N expansion 51
2.1 Dyson Schwinger equations for the GN model 52
2.1.1 Dyson series 52
2.1.2 Dyson-Schwinger equations for elementary fields 56
2.1.3 The NJL result 59
2.1.4 Dyson-Schwinger equations for theories with composite operators . 62
2.2 Large N expansion 65
2.2.1 Other bosonization tecniques 66
2.2.2 The saddle point expansion 67
2.2.3 Divergences and renormalizability of GN model at $d = 3$. 71
2.2.4 Large N behaviour of the GN model in generic dimensions, some corrections to the leading order. 73
2.3 The Scaling region, critical phenomena picture of the χSB 75
2.3.1 Critical exponents of the χSB 76
2.3.2 Large N computation of the critical exponents in the GN model . . 80
2.3.3 Equivalence with Yukawa theory 81

3 Non-perturbative analytical techniques II: Renormalization Group 85
3.1 Wilsonian effective action and blocking 87
3.2 The Wilsonian RG approach and the field theoretical epsilon expansion for the Yukawa model 88
3.2.1 The Wilsonian RG transformation: Yukawa theory 89
3.2.2 Fixed points 92
3.2.3 Callan-Symanzik equations for Yukawa theory 94
3.2.4 Fixed point structure of the Yukawa theory near the four dimension 97
3.2.5 Corrections to scaling 100

3.3 The non-perturbative *RG* approach in the *GN* model 101
3.3.1 The composite operator in the *RG* language 102
3.3.2 Derivative expansion and *LPA* approximation 106
3.3.3 Wegner-Houghton approach on renormalization group for fermions . 106
3.4 The scaling of the *GN* model in the Large N limit 109
3.4.1 Truncated potential: the Fermi constant term 109
3.4.2 Critical exponents with the RG approach 111
3.4.3 Crossover and mass generation 114
3.4.4 Analytical approximations to the RG equations 121
3.5 Critical exponents for small N values 132

4 *RG* analysis of higher powers in fermion models 139
4.1 The quartic operator in the Large-N expansion 141
4.2 RG equations for higher powers couplings 141
4.2.1 Fixed point and linearization 143
4.2.2 Anomalous dimensions 145
4.3 The impact of the $(\bar{\psi}\psi)^4$ operator and the critical behaviour near $d = 4$ . . 147
4.3.1 Analytical solutions and linearization 147
4.3.2 Flows in the language of critical phenomena 150
4.3.3 Mass flow and cross-over picture 154
4.4 Higher powers in generic N 156
4.5 The cubic operator and the onset of a first order transition 159

5 *RG* analysis of fermion-boson theories 161
5.1 Wilsonian *RG* equation for theory with fermions and bosons 162
5.2 Equations for the Yukawa theory in the LPA 162
5.3 Fermi and Yukawa theories coupled together 165
5.3.1 Two non-Gaussian solutions 167
5.3.2 Non-trivial scaling of the Yukawa coupling near and at $d = 4$ 169

6 Summary and conclusions 171

A Perturbative tricks in fermion models **177**

A.1 One loop contributions to the $1PI$ four fermion vertex 177

A.2 Correlators of the GN model in the bosonized version 178

A.3 Properties of local Grassmann vertices 180

B DS equations for the GN model **183**

B.1 DS equations for connected Green's functions 183

B.2 DS equations for $1PI$ correlators 185

C Calculation of the improved propagator **189**

C.1 Calculation at $d = 3$ 189

C.2 Sharp cut-off calculation $2 < d < 4$ 191

C.3 Sharp cut-off calculation at $d = 4$ 193

D Functional determinant computations **195**

D.1 First order corrections to the Effective action in the $1/N$ expansion 195

D.2 The RG equation for the Wilsonian potential in fermion model 196

D.3 Wilsonian RG equation for fermions and bosons 198

Bibliography **201**

INTRODUCTION

The present work is devoted to the study of the non-perturbative properties of quantum field theories (QFT) of interacting fermions. The pure fermion theories, which are theories involving only fermion degrees of freedom as well as systems of interacting fermions and bosons, are taken into account. Moreover the properties of fermion theories with the insertion of local composite operators are also widely investigated.

The use of these operators can provide important tools for the description of collective states, without involving the explicit use of scalar elementary particles. In this sense the results obtained with the Gross Neveu (GN) model [1], used as a paradigm for pure fermion theories, are compared with those obtained by studying a Yukawa type theory.

According to the (perturbative) power counting theorem [2], four-fermion interactions are non-renormalizable. They are at most regarded as effective theories, low energy limits of more fundamental ones. This is for instance the case of the Fermi theory of weak interactions [3], which is obtained as the low energy limit of the electroweak (EW) theory [4]. Although (perturbatively) non-renormalizable, it provides a very good description of physical phenomena at energies below the EW scale.

On the other hand the Yukawa theory, first introduced to describe the nuclear interaction, has found a wide application in high energy physics thanks to its (perturbative) renormalizability. The scalar field of the theory, by acquiring a non-vanishing expectation value, thus spontaneously breaking the symmetry of the model, provides an acclaimed mechanism for the generation of the particle masses [5].

In a non-perturbative framework, Nambu and Jona-Lasinio (NJL) showed that, for

values of the Fermi constant greater than a critical one, four-fermion theories undergo spontaneous breaking of chiral symmetry (χSB), thus providing dynamical generation of fermion masses [6]. Moreover, the divergences appearing in such non-perturbative analysis differ from those obtained in a perturbative approach. The specific structure of these divergences makes the non-perturbative renormalizability of the theory possible (see below).

Gross and Neveu (GN) considered a similar model in $d = 2$ dimension and found that, as a result of the instability of the perturbative vacuum, the effective potential develops non trivial minima, thus showing the occurrence of χSB. In these lower dimensions, the model turned out to be asymptotically free [1].

In this way the opportunity of describing the mass generation without involving any elementary scalar was profiled. In four fermion models a scalar excitation arises as a fermion-antifermion bound state ($\bar{\psi}\psi$) and in the Hartree approximation, it has a mass which is twice that of the fermion [6]. Many works, as for instance the studies on technicolour and top quark condensation [7], have tried to establish some compositeness conditions in the attempt to show the superiority of a purely fermionic approach.

However the strongest hint to this problem comes from the deep connection between QFT and critical phenomena.

As is well known, the generating functional of a QFT, which encodes all the quantum relativistic amplitudes, can be mapped into a correspondent partition function of a statistical system (which collects all the thermal correlators) by means of a Wick rotation.[1]

Far from being a simple mathematical curiosity, around the 70's, this analogy gave way to many QFT techniques for the study of universality properties of critical phenomena and the calculation of universal quantities [8]. But most of all it gave the possibility to interpret the renormalizability of a QFT as corresponding to the scale invariance property of a statistical system near a continuous phase transition [9]. In this sense, the renormalization program can be implemented far from the perturbative regime and the nature of divergences arising in calculations can radically change from those predicted by the perturbation theory. If two theories are acknowledged to have equal renormalizability properties, then they will show the same scaling of the correlators and in this statistical

[1] This is why all the results of this work are presented in the Euclidean path-integral formulation of the QFT.

framework are said to belong to the same universality class.

In $d = 4$ dimensions, by using the $1/N$ expansion, it is shown that the NJL and the GN models have the same divergences of Yukawa theories [10],[11],[12],[13]. Following a renormalization technique (mean field expansion) introduced by Bender and collaborators [14], the same result was also proven in [15]. In this sense, these four-fermion theories turn out to be renormalizable [10],[11],[12],[13], although they inherit from the latter the triviality problem. In $d = 3$ dimensions, Rosenstein and collaborators performed a similar computation and showed that these models are $1/N$ renormalizable [16]. Differently from the $d = 4$ case, however, in $d = 3$ the cut-off can be consistently eliminated without introducing additional counterterms in the Lagrangian.

These studies were further pursued in [17] and [18], where it was shown that, for $2 < d \leq 4$ and in the framework of the $1/N$ expansion, the GN model and the Yukawa theory belong to the same universality class.

From this point of view, χSB is nothing but the occurrence of a quantum phase transition where the order parameter is the expectation value of $\bar{\psi}\psi$, the analogous of the magnetization if one thinks of the ferromagnetic transition. In this analogy, the "temperature" is identified with $1/G$ ($1/G_c$ corresponding to the critical temperature) and a bare fermion mass plays the role of an "external magnetic field". For the GN model in d dimensions and for the corresponding Yukawa theory, the critical exponents around the non trivial fixed point G_c have been computed in the $1/N$ expansion and turned out to be the same for the two theories [19][2].

The role of the Yukawian elementary scalar is played by the fermion composite operator of the GN model which acquires a large anomalous dimension due to the quantum fluctuations.

As is well known, a profound insight in our understanding of renormalization in quantum field theories (QFT) came with the realization of its deep connection with the Wilson's theory of critical phenomena [9]. A renormalized QFT is defined around a fixed point of the RG equations in the space of the bare parameters.

In such a framework, the renormalizability of four-fermion theories is related to the existence of a non-Gaussian fixed point G_c. The breaking of chiral symmetry results from

[2]Contrary to some claims according to which the two models have a different number of parameters [20],[21].

renormalizing the theory around this point, which also turns out to be the critical point of the transition [10],[11],[12]. Finally, the fact that in the large N limit the divergences show a different structure from the one observed in the framework of the perturbation theory is understood as due to a different scaling of the bare parameters around this non-trivial fixed point. [3]

Within the Wilson renormalization group (RG) approach to critical phenomena, the critical exponents are computed by considering the behaviour of the correlation functions around the fixed points (with divergent correlation length) of the RG equations. In a QFT context, the critical exponents of the analogous quantum phase transition can also be computed once the "external fields" which correspond to the temperature and/or to other "relevant" fields (the magnetic field in the ferromagnetic case) are correctly identified [19],[22],[23].

In the present Thesis work, a generalized GN model in d dimensions with N flavours is studied within the framework of the Wilsonian RG approach (as originally implemented by Wegner and Houghton [24]) in the Local Potential Approximation (LPA).

By following [24] and [25], a new *RG* equation for a purely fermion theory is established. Then, with the help of this equation (and following the method outlined above), the critical exponents are computed in the large N limit in a purely fermion language. Our results are found to coincide with those obtained with other analytical techniques.

By introducing a running mass term (which, in the ferromagnetic analogy and near the fixed point, plays the role of an external magnetic field), it is possible to compute non-universal IR physical quantities such as the *physical* fermion mass. This soft explicit breaking of the symmetry suggests a mechanism for the generation of a finite physical mass as a *cross-over* phenomenon, thus indicating a way of performing the chiral limit in the *RG* picture.

Since our *RG* method does not depend on perturbative expansions in any small parameter ($1/N$ or coupling constants expansions), it offers the opportunity of investigating questions which remain open within the framework of these typical analytical methods. In this respect, the equivalence of the Yukawa theory and the GN model beyond the $1/N$

[3] In this respect, it is worth noting that in $d = 3$ dimensions the correspondence between the four-fermion model and the Yukawa theory is realized as a mapping between the neighbourhood of the non-trivial fixed point G_c and the neighbourhood of the Wilson-Fisher-Yukawa fixed point of the corresponding Yukawa theory, while for $d = 4$ the latter collapses onto the Gaussian fixed point.

expansion at $d < 4$ has been investigated (see chap.3). Moreover, in the Hartree approximation (large N), the triviality of the GN model in $d = 4$ dimensions, in a purely fermion language (i.e. with no reference to bosonization techniques), has been reproduced for the first time. This opens the way for addressing such a question for any value of N, an analysis which cannot be performed with the help of the usual bosonization techniques.

A novel, intriguing, result suggested by our analysis concerns the possibility that the non-Gaussian fixed point G_c triggers a non trivial physics when the theory, in addition to the Fermi interaction term, contains also a Yukawa interaction (see chap.5).

This Thesis is organized as follows. The first two chapters serve as an introduction to the subject and gives the possibility to contextualize our original RG results in a coherent way. Nevertheless, some new (albeit simple) results have also been worked out. More specifically, the first chapter contains an introduction to the path-integral formulation of theories with self-interacting fermions, involving also the presence of fermion composite operators and scalar fields. The chiral symmetry is introduced and the perturbative analyses of the GN and Yukawa models are considered. The Feynmann diagrams of these models are introduced and the triviality of the Yukawa theory is presented.

In the second chapter some classical non-perturbative techniques are considered and the celebrated NJL result is recovered in its original formulation, i.e. with the help of the Dyson-Schwinger equations in the Hartree approximation. Then the large N expansion method is considered which allows the extension of the field theoretical renormalization approach to non-perturbative (in the coupling constant) tools. The non-perturbative renormalizability of the GN model and its equivalence to the Yukawa theory is then shown.

The third chapter is mainly devoted to the presentation of our original work. Before doing that, the Wilsonian RG is introduced and the Yukawa theory is studied with the epsilon expansion method. Then, after introducing our original RG approach, the phase space of the GN model is studied in a purely fermion language. In the large N limit, its equivalence to the Yukawa theory is then recovered also in this context. Then our RG method is applied to the computation of the critical exponents of the GN model in $d = 3$ dimensions (far from the epsilon expansion domain) and for small values of N.

In this respect, it is worth to note that, within our approach, these models can be studied even far from the small epsilon domain and for small values of N. This is what

has been done at the end of this chapter.

In chapter four the impact of higher powers operators, $(\bar{\psi}\psi)^n$, in the Wilsonian potential is considered. In the large N limit, the failure of the hyperscaling and the presence of a logarithmic behaviour with the scale of the quartic operator $(\bar{\psi}\psi)^4$ are thus recovered in our *RG* fermion language. In order to study the theory for small values of N, it would be necessary to consider the impact of derivative terms, which is left for future work. However, the above mentioned scaling behaviour is obtained around a non-Gaussian fixed point, which is a new and unexpected result.

By considering the impact of odd interaction terms in the potential, the marginality of the cubic operator in $d = 3$ dimensions is recovered. The anomalous dimension of this operator is computed and found to be in agreement with results given in the literature at the next to leading order in the $1/N$ expansion.

Finally, in the fifth chapter our *RG* equation is extended to models involving fermions and bosons. Some interesting non-trivial fixed point solutions are found which would suggest a non-trivial behaviour of the Yukawa coupling in $d = 4$ dimensions.

CHAPTER 1

FUNCTIONAL FORMALISM FOR FERMION AND BOSON THEORIES

In this chapter the path integral formulation of fermion and boson field theories is adopted as a useful tool for studying the properties of those quantum systems with the same techniques adopted for studying the properties of statistical systems. A deeper insight into the renormalizability of a QFT is provided by this statistical picture.

Indeed the renormalization of a quantum field theory corresponds to the exhibition of some critical behaviour in the statistical language. On one hand this offers the possibility of interpreting the usual perturbative results within this framework, on the other hand allows the extension of the notion of renormalization beyond the perturbative regime.

By introducing the functional formalism, a perturbative analysis of the GN model and of the Yukawa theory is performed. The Feynmann diagrams, arising from the expansion in the coupling constants, are found and some basic quantities as the degree of divergence of a diagram or the scaling dimension of an operator are introduced. In such a framework, the perturbative non-renormalizability of theories with self-interacting fermions as well as the renormalizability of Yukawian interactions are shown. How the renormalizability properties of these models are modified by the use of non-perturbative techniques is the topic of the other chapters.

Finally, a way of interpreting the perturbative results for the GN model in terms of the Feynmann diagrams of a Yukawa theory is obtained with the help of the Hubbard-Stratonovich transformation [26].

1.1 Gross-Neveu and Yukawa models

The main topic of our work is the study of the properties of the GN model and of the Yukawa theory. The first one is given as an example of a purely fermion theory with fermions interacting through a quartic interaction, while the second one is a model of fermions interacting by means of a scalar. The Gross-Neveu model is thus defined by the action:

$$S_f[\psi,\bar{\psi}] = -\int d^dx \quad \left[\bar{\psi}\partial\!\!\!/\psi + \frac{G}{2}(\bar{\psi}\psi)^2\right] \tag{1.1}$$

where ψ and $\bar{\psi}$ are $U(N)$ multiplets and $U(N)$ is called the flavour group. Each fermion field possesses a Dirac index and a flavour one. There internal indices are understood.

The Yukawa theory instead is defined by the action:

$$S_{fb}[\psi,\bar{\psi},\phi] = \int d^dx \left[\quad -\bar{\psi}\left(\partial\!\!\!/ + g\phi\right)\psi + \frac{1}{2}(\partial_\mu\phi)^2 + \frac{M^2}{2}\phi^2 + \frac{\lambda}{4!}\phi^4\right]. \tag{1.2}$$

The fermion fields are always in the fundamental representation of the unitary flavour group. In addition, there is a single self-interacting scalar field ϕ.

In order to present the results with a high level of generality, one refers to $S_f[\psi,\bar{\psi}]$ as the action of a generic purely fermion theory. A generic theory involving fermions and scalars will be characterized by the action $S_{fb}[\psi,\bar{\psi},\phi]$. Both these actions are required to involve only local interactions which in statistical language corresponds to taking into account only short-range interacting systems [27],[28] .

Expanding the fermionic action in powers of the fields one finds:

$$\begin{aligned} S_f[\psi,\bar{\psi}] \;&=\; \sum_{n,m=1}^{\infty}\frac{1}{(n+m)!}\int_{x_1}\cdots\int_{x_m}\int_{y_1}\cdots\int_{y_n}\bar{\psi}(y_m)\cdots\bar{\psi}(y_1)\psi(x_1)\cdots\psi(x_m) \\ &\times\; \frac{\delta^{n+m}S_f}{\delta\psi(x_n)\ldots\delta\psi(x_1)\delta\bar{\psi}(y_m)\cdots\delta\bar{\psi}(y_1)}. \end{aligned} \tag{1.3}$$

The coefficients of the series with $(n+m) > 2$ define the vertices of the the theory. The generic $n+m$-th derivative of the r.h.s of Eq. (1.3) is represented with the diagram shown in Fig. 1.1. The locality condition is achieved by means of the factorization of a space-time delta function in front of each derivative.

The inverse of each second derivative of the action plays a prominent role in the calculations since it defines an inverse propagator. Thus, for example, the matrix $\left(\frac{\delta^2 S}{\delta\psi\delta\bar{\psi}}\right)^{-1}$

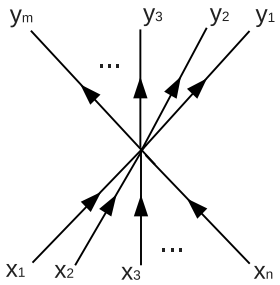

Figure 1.1: The bare vertex of a purely fermion theory with $(n+m)$ external legs, defined by the expansion in Eq. (1.3), is represented . Starting from the first label the subsequent indices follow in counterclockwise order.

is represented by an oriented line with the arrows pointing in the opposite direction to those of $\frac{\delta^2 S}{\delta\psi\delta\psi}$.

The action $S_{fb}[\psi,\bar{\psi},\phi]$ of a model involving both scalar and fermions, as for example the Yukawa theory, can be expanded in powers of ψ, $\bar{\psi}$ and ϕ. The general coefficient of the expansion of S_{fb} in powers of the fields is:

$$\frac{\delta^{n+m+r} S_{fb}}{\delta\psi(x_1)\ldots\delta\psi(x_n)\delta\bar{\psi}(y_1)\cdots\delta\bar{\psi}_{\beta_1}(y_m)\delta\phi(z_1)\cdots\delta\phi(z_r)}, \tag{1.4}$$

and it will also be represented by the diagram shown in Fig. 1.2.

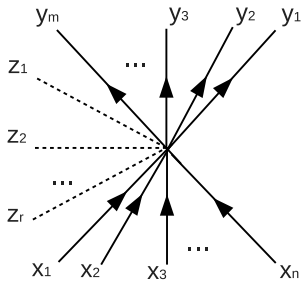

Figure 1.2: A diagram, representing either the bare vertex of a theory with elementary fermion and scalar fields, given in Eq.(1.4), or a vertex defined by the expansion in Eq. (1.5), is shown. Alternatively each dashed line represents either a scalar field or the composite operator $\bar{\psi}\psi$. Starting from the first label the subsequent indices follow in counterclockwise order.

Being interested in describing collective composite excitations, as those described by the local operator $\bar{\psi}\psi(x) = \sum_{\alpha,a} \bar{\psi}_{\alpha,a}(x)\psi_{\alpha,a}(x)$ (where α and a are respectively Dirac's

and internal indices), an alternative, quite redundant, expansion of the action S_f in powers of the composite and elementary fields can be considered. A generic coefficient of this expansion has the form:

$$\frac{\delta^{n+m+r} S_f}{\delta\psi(x_1)\dots\delta\psi(x_n)\delta\bar{\psi}(y_1)\cdots\delta\bar{\psi}_{\beta_1}(y_m)\delta\bar{\psi}\psi(z_1)\cdots\delta\bar{\psi}\psi(z_r)}, \tag{1.5}$$

which defines a vertex which turns out to be useful for further developments and can be represented with the diagram in Fig. 1.2.

The dashed line for representing both elementary scalars and composite operators was used. However, by never considering the impact of local operators in theory involving elementary scalars, misunderstandings should not occur.

1.2 Elementary fields Green's functions and continuum limit

The correlation functions or the euclidean Green's functions are the main object of the statistical parallel of a quantum field theory. For a theory of elementary fermions they are defined as:

$$G_f^{(m;n)}(y_1,\dots,y_m;x_1,\dots,x_n) = \left\langle \psi(y_1)\dots\psi(y_m)\bar{\psi}(x_1)\dots\bar{\psi}(x_n)\right\rangle. \tag{1.6}$$

They are expectation values of products of fermionic fields over the ground state. After the Wick rotation, this mean value is a quantum amplitude that in many cases can be related to observable quantities as cross sections and decay rates.

For a generic fermionic theory defined by the action $S_f[\psi,\bar{\psi}]$ the euclidean Green's functions can be written through the path-integral formalism as:

$$\begin{aligned} & G_f^{(m;n)}(y_1,\dots,y_m;x_1,\dots,x_n) \\ = \; & \frac{\int \mathcal{D}\psi\mathcal{D}\bar{\psi}\,\psi(y_1)\dots\psi(y_m)\bar{\psi}(x_1)\dots\bar{\psi}(x_n)\,e^{-S_f[\psi,\bar{\psi}]}}{\int \mathcal{D}\bar{\psi}\mathcal{D}\psi\,e^{-S_f[\psi,\bar{\psi}]}}, \end{aligned} \tag{1.7}$$

which are nothing but the momenta associated with the normalized weight function $\frac{e^{-S_f[\psi,\bar{\psi}]}}{Z[0]}$, where:

$$Z[0] = \int \mathcal{D}\psi\mathcal{D}\bar{\psi}\,e^{-S_f[\psi,\bar{\psi}]}. \tag{1.8}$$

Since the Green's functions are antisymmetric, with respect to their indices, the fermionic functions can be described by means of even elements of a Grassmann algebra. A generic Green's function is represented by the diagram shown in Fig. 1.3.

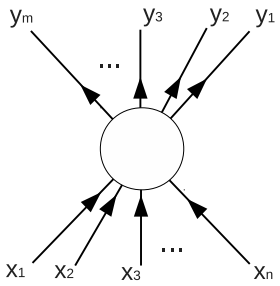

Figure 1.3: The Green's function of a purely fermion theory with (n+m) external legs, defined in Eq. (1.7), is represented . Starting from the first label the subsequent indices follow in counter-clockwise order.

Without going into technical details, defining the correlators by means of the path-integral formulation deserves some comments. Each field theory represents a system with an infinite number of degrees of freedom $(\psi, \bar{\psi})$ labeled by the spatial index x as well as as well as any internal indices. In order to define and compute a path-integral it is necessary to restrict the whole system in a finite box of volume $\mathcal{V}$ and then to discretize the space-time with a lattice of size "a". So doing, the fields are thus defined over the $\mathcal{N}$ sites x_i of the lattice. Each function $\psi(x_i)$ $(\bar{\psi}(x_i))$ with $i = 1, \ldots, \mathcal{N}$, represents a possible configuration of the system. Each configuration is weighted by $\frac{e^{-S_f[\psi,\bar{\psi}]}}{Z[0]}$ (also calculated for the discretized version of system) so that the path-integral appears as a well defined statistical sum. From the reciprocal space (momentum space) point of view the use of a finite box results in a discretization of momentum spectrum. On the other hand a discretization of the space time implies that each momentum component, say p, is bounded as $|p| \leq \frac{\pi}{a}$. Thus space time discretization is strictly related with a sharp cut-off regularization procedure in momentum space, the cut-off implied being $\Lambda = \frac{\pi}{a}$ [29]. Throughout the present work this type of regularization will be used. The statistical system associated with this regularized field theory is a usual discrete statistical system.

However the path-integral definition requires two different limits, that are:

$$\mathcal{N}, \mathcal{V} \rightarrow \infty, \quad \text{with} \quad \mathcal{N}/\mathcal{V} \quad \text{fixed}, \tag{1.9}$$

$$a \rightarrow 0, \quad \text{with finite correlators.} \tag{1.10}$$

The first limit in Eq. (1.9) has an analogy in statistical systems in the so called thermodinamic limit. It just represents a way of handling systems with an infinite number of degrees of freedom but finite density. On the other hand, performing the limit in Eq. (1.10), while all the Green's functions are to be finite, corresponds to a very particular statistical situation. In fact, the size a, from the statistical point of view, characterizes the typical length scale of the "microstates" of the system. If the "macroscopic" objects, as the correlators, are insensitive to the microscopic scale, the system turns out to be scale invariant. The simplest manifestation of scale invariance occurs for systems near a critical point. (Another example is that of conformal theories). Thus a QFT theory corresponds to a statistical system near a continuous phase transition [9].

Performing the scaling limit in Eq. (1.10) requires the fine tuning of a small number of control parameters characterizing the phase of the statistical system, such as the temperature, the external field, etc., near their critical value. This statistical fine tuning reflects in the predictive power of a QFT. A renormalizable theory is characterized by the possibility of choosing the bare parameters (the parameters appearing in the action of the theory) as functions of the cut-off in such a way that correlation functions have a large finite cut-off limit [27].

Each bare parameter in the action can be identified with the value of a certain microscopical coupling of the statistical reduced Hamiltonian. (More precisely, the reduced Hamiltonian identifies a whole class of statistical systems with the same ratio of energy for temperature). The couplings of a theory near a phase transition must directly correspond to the control parameters of the transition. The other possible interactions must be discarded from the Hamiltonian.

Thus the first parameters are called relevant, the others are defined "irrelevant" couplings. If we do not discard the irrelevant couplings it means that we are not close enough to the critical point, so that cut-off effects are not negligible.

This is what occurs when "non renormalizable" interactions are included in the action. The cut-off cannot be removed and the quantum field theory is called effective [30]. There

are many way of rephrasing this statement which will be further analyzed in the following.

1.2.1 Green's functions of composite operators and scalar fields

In the previous section the Green's functions for elementary fields have been introduced and their relation to the excitation of fermionic particles or antiparticles has been stressed. However a theory with a non-perturbative vacuum could also allow the excitations of composite fields as for example the operator $\bar{\psi}\psi$. The impact of these operators is taken into account by defining the appropriate Green's functions, according to the well known procedure introduced in [31].

A generic Green's function involving both elementary and composite fields is defined as:

$$\begin{aligned} & G_f^{(m;n;r)}(y_1,\ldots,y_m;x_1,\ldots,x_n;z_1,\ldots,z_r) \\ = \; & \left\langle \psi(y_1)\ldots\psi(y_m)\bar{\psi}(x_1)\ldots\bar{\psi}(x_n)\bar{\psi}\psi(z_1)\cdot\bar{\psi}\psi(z_r)\right\rangle \\ = \; & \frac{\int \mathcal{D}\psi\mathcal{D}\bar{\psi}\,\psi(y_1)\ldots\psi(y_m)\bar{\psi}(x_1)\ldots\bar{\psi}(x_n)\bar{\psi}\psi(z_1)\ldots\bar{\psi}\psi(z_r)\,e^{-S_f[\psi,\bar{\psi}]}}{\int \mathcal{D}\psi\mathcal{D}\bar{\psi}\,e^{-S_f[\psi,\bar{\psi}]}}. \end{aligned} \tag{1.11}$$

The correlators of composite operators are very different objects from the Green's functions of elementary operators. To recover the correlator of composite operators from that of some elementary fields requires contracting and permutating some fields and performing the limit $y_1 \to x_1$, where y_1 and x_1 are two distinct points. On the other hand, the Green's function of elementary operators can be expanded in terms of a basis of composite operators . Both these procedures are strictly related with the continuum limit. This can generate divergences showing that the two types of Green's functions require different renormalization prescriptions [32]. Thus the correlators of composite operators are completely independent quantities.

In conclusion the Green's functions of a theory with elementary fermions and scalars defined by the action S_{fb} are introduced. These correlators are as expected:

$$\begin{aligned} & G_{fb}^{(m;n;r)}(y_1,\ldots,y_m;x_1,\ldots,x_n;z_1,\ldots,z_r) \\ = \; & \left\langle \psi(y_1)\ldots\psi(y_m)\bar{\psi}(x_1)\ldots\bar{\psi}(x_n)\phi(z_1)\ldots\psi(z_r)\right\rangle \\ = \; & \frac{\int \mathcal{D}\psi\mathcal{D}\bar{\psi}\int\mathcal{D}\phi\,\psi(y_1)\ldots\psi(y_m)\bar{\psi}(x_1)\ldots\bar{\psi}(x_n)\phi(z_1)\ldots\phi(z_r)e^{-S_{fb}[\psi,\bar{\psi},\phi]}}{\int \mathcal{D}\psi\mathcal{D}\bar{\psi}\int\mathcal{D}\phi\,e^{-S_{fb}[\psi,\bar{\psi},\phi]}}. \end{aligned} \tag{1.12}$$

The diagram representing such Green's functions is shown in Fig. 1.4.

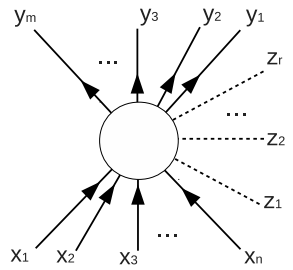

Figure 1.4: A diagram, representing the Green's functions of a theory with elementary fermion and scalar fields, given in Eq.(1.12), is shown. Each dashed line represents either a scalar field. Starting from the first label the subsequent indices follow in counterclockwise order.

1.3 Generating functionals for fermion theories

All the Green's functions that have been introduced can be calculated by means of an appropriate generating functional. The knowledge of the explicit form of the generating functional corresponds to knowing the whole theory, thus many results are presented in terms of these quantities.

1.3.1 Generating functional for Green's functions

Starting simply with the generator of the Green's functions of elementary fermion fields. For the fermion theory one defines:

$$Z_f[\eta,\bar{\eta}] \;=\; \int \mathcal{D}\psi\mathcal{D}\bar{\psi}\, e^{-S_f[\psi,\bar{\psi}]+\int\bar{\eta}\cdot\psi-\int\bar{\psi}\cdot\eta}, \tag{1.13}$$

where η and $\bar{\eta}$ are two Grassmann-valued source fields. The generic correlator $G_f^{(m;n)}$ is then obtained as:

$$\begin{aligned} & G_f^{(m;n)}(y_1,\ldots,y_m;x_1,\ldots,x_n) \\ = \;& \frac{1}{Z_f[0]}\,\frac{\delta}{\delta\bar{\eta}(y_1)}\cdots\frac{\delta}{\delta\bar{\eta}(y_m)}\,\frac{\delta}{\delta\eta(x_1)}\cdots\frac{\delta}{\delta\eta(x_n)}Z_f[\eta,\bar{\eta}]\bigg|_{\eta,\bar{\eta}=0}, \end{aligned} \tag{1.14}$$

thus Z plays the same role of a canonical partition function. After the derivatives have been performed the sources must be switched off. Often it is also useful to work with the correlators including the fluctuations induced by their own sources.

Strictly speaking the generating functional is given by the ratio $\frac{Z_f[\eta,\bar{\eta}]}{Z_f[0]}=\frac{Z_f}{Z_{f,0}}$. Actually this functional can be expanded in powers of η and $\bar{\eta}$. So the Green's functions can be read as the coefficient of this power series.

Figure 1.5: Graphic representation of the η source term coupled with the $\bar{\psi}$ elementary fermion field in the generating functional given in Eq. (1.13).

Figure 1.6: Graphic representation of the $\bar{\eta}$ source term coupled with the ψ elementary fermion field in the generating functional given in Eq. (1.13).

Representing the external sources with the diagrams shown in Figs. 1.5, 1.6, the power series of $\frac{Z_f}{Z_{f,0}}$ is diagrammatically given by the picture in Fig. .1.7.

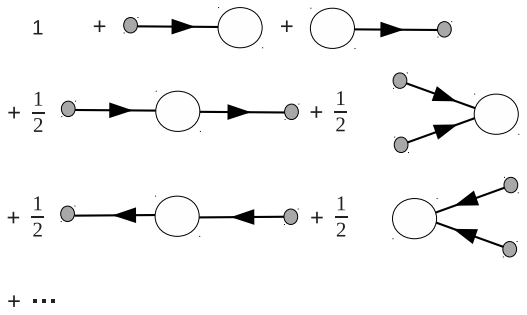

Figure 1.7: Diagrammatic representation of the series expansion of the functional $\frac{Z_f[\eta,\bar{\eta}]}{Z_f[0]} = \frac{Z_f}{Z_{f,0}}$ in powers of η and $\bar{\eta}$. The coefficient of the series are nothing but the Green's functions in Eq. (1.6).

Clearly a generating functional of Green's functions of elementary fermion and scalar fields is defined as:

$$Z_{fb}[\eta,\bar{\eta},J] \;=\; \int \mathcal{D}\psi\mathcal{D}\bar{\psi}\int \mathcal{D}\phi\, e^{-S_{fb}[\psi,\bar{\psi},\phi]+\int\bar{\eta}\cdot\psi-\int\bar{\psi}\cdot\eta+\int J\phi}, \tag{1.15}$$

so that all the previous results can be rephrased for this expression.

Finally the generating functional for the Green's functions of elementary and composite fermion operators can also be defined. Now an additional scalar source K must be introduced so that the partition function is:

$$Z_f[\eta,\bar{\eta},K] \;=\; \int \mathcal{D}\psi\mathcal{D}\bar{\psi}\, e^{-S_f[\psi,\bar{\psi}]+\int\bar{\eta}\cdot\psi+\int\bar{\psi}\cdot\eta+\int K\bar{\psi}\cdot\psi}, \tag{1.16}$$

If source term K is taken as a constant it has the impact of a bare mass term for the fermion fields. The Green's functions can be recovered as:

$$\begin{aligned} & G_f^{(m;n;r)}(y_1,\ldots,y_m;x_1,\ldots,x_n;z_1,\ldots,z_r) \\ = \;& \frac{1}{Z_f[0]}\,\frac{\delta}{\delta\bar{\eta}(y_1)}\cdots\frac{\delta}{\delta\bar{\eta}(y_m)}\frac{\delta}{\delta\eta(x_1)}\cdots\frac{\delta}{\delta\eta(x_n)}\frac{\delta}{\delta K(z_1)}\cdots\frac{\delta}{\delta K(z_r)}Z_f[\eta,\bar{\eta},K]\Big|_{\eta,\bar{\eta},K=0} \end{aligned} \tag{1.17}$$

A similar expansion to those shown in Fig. .1.7 holds also in this case.

1.3.2 Generating functional for connected Green's functions

Green's functions previously defined contain some unconnected pieces [33]. In order to obtain only connected functions of elementary fields, which cannot be written as a sum of product of other Green's functions, an appropriate generator must be defined. In purely fermion theory including the impact of elementary and composite fields it is defined by the relation:

$$Z_f[\eta, \bar{\eta}, K] = e^{W_f[\eta,\bar{\eta},K]}, \tag{1.18}$$

where Z_f is the partition function appearing in Eq. (1.16). A generic connected Green function of elementary fermion fields is obtained as:

$$\begin{aligned} & G^{(m;n)}_{C,f}(y_1, \ldots, y_m; x_1, \ldots, x_n) \\ = \; & \left\langle \psi(y_1) \ldots \psi(y_m) \bar{\psi}(x_1) \ldots \bar{\psi}(x_n) \right\rangle_C \\ = \; & \frac{\delta}{\delta\bar{\eta}(y_1)} \cdots \frac{\delta}{\delta\bar{\eta}(y_m)} \frac{\delta}{\delta\eta(x_1)} \cdots \frac{\delta}{\delta\eta(x_n)} W_f[\eta, \bar{\eta}, K]\Big|_{\eta=\bar{\eta}=K=0}. \end{aligned} \tag{1.19}$$

From the statistical point of view W is nothing but the opposite of the Helmholtz free energy of the system normalized at its own temperature. Expanding this functional in powers of the sources η and $\bar{\eta}$ and setting $K = 0$, the Green's functions of the theory are achieved as coefficients of the power series. On the other hand by deriving with respect to the source K also unconnected pieces are generated. The Green's functions of a purely fermion theory described by the action:

$$S_f^{\eta,\bar{\eta},K}[\psi, \bar{\psi}] = S_f[\psi, \bar{\psi}] - \int \bar{\eta} \cdot \psi + \int \bar{\psi} \cdot \eta - \int K\bar{\psi} \cdot \psi, \tag{1.20}$$

can also be introduced. Such a theory is affected by the impact of the source terms in the fluctuations. For example a theory involving the source K takes into account the presence of an explicit bare fermion mass term.

The connected correlators for a theory with elementary scalars and fermions are ob-

tained by defining the generator $W_{fb} = \ln Z_{fb}[\eta, \bar{\eta}, J]$. Thus one finds:

$$\begin{aligned} & G^{(m;n;r)}_{C,f}(y_1, \ldots, y_m; x_1, \ldots, x_n; z_1, \ldots, z_r) \\ = \; & \left\langle \psi(y_1) \ldots \psi(y_m) \bar{\psi}(x_1) \ldots \bar{\psi}(x_n) \phi(z_1) \phi(z_r) \right\rangle_C \\ = \; & \frac{\delta}{\delta \bar{\eta}(y_1)} \ldots \frac{\delta}{\delta \bar{\eta}(y_m)} \frac{\delta}{\delta \eta(x_1)} \ldots \frac{\delta}{\delta \eta(x_n)} \frac{\delta}{\delta J(z_1)} \ldots \frac{\delta}{\delta J(z_r)} W_f[\eta, \bar{\eta}, J] \Big|_{\eta=\bar{\eta}=J=0} . \end{aligned} \tag{1.21}$$

These correlators are graphically represented with the diagram shown in Fig. 1.8.

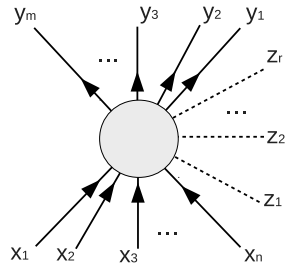

(a)

Figure 1.8: A diagram, representing the connected correlators a theory with elementary fermion and scalar fields given in Eq. (1.21), is shown. Starting from the first label the subsequent indices follow in counterclockwise order.

For our purposes, it is important to compute the the expectation values:

$$\psi_c(x) = \langle \psi(x) \rangle_C^{\eta,\bar{\eta},K} = \langle \psi(x) \rangle^{\eta,\bar{\eta},K} , \tag{1.22}$$

$$\bar{\psi}_c(x) = \left\langle \bar{\psi}(x) \right\rangle_C^{\eta,\bar{\eta},K} = \left\langle \bar{\psi}(x) \right\rangle^{\eta,\bar{\eta},K} , \tag{1.23}$$

as well as the connected correlator:

$$\bar{\psi}\psi(x)_c = \left\langle \bar{\psi}\psi(x) \right\rangle_C^{\eta,\bar{\eta},K} . \tag{1.24}$$

The latter, which is a fermion condensate, is a scalar quantity. Therefore, unlike the expectation values in Eqs. (1.22)(1.23), it can be different from zero without violating the Lorentz invariance but spontaneously breaking the chiral symmetry. More on this point in the section dedicated to the symmetries of our models. The classical fields in Eqs. (1.22)(1.23) can be written in terms of the functional generator W_f as:

$$\psi_c(x) = \frac{\delta}{\delta \bar{\eta}(x)} W_f[\eta, \bar{\eta}, K], \tag{1.25}$$

$$\bar{\psi}_c(x) = \frac{\delta}{\delta \eta(x)} W_f[\eta, \bar{\eta}, K], \tag{1.26}$$

As the classical field $\bar{\psi}\psi_c$ can be calculated by the relation:

$$\frac{\delta W_f}{\delta K}[\eta, \bar{\eta}, K] = \bar{\psi}\psi(x)_c + \bar{\psi}_c(x) \cdot \psi_c(x). \tag{1.27}$$

Deriving twice W_f the dressed fermion propagator is obtained:

$$\begin{aligned} \left\langle \psi_a \bar{\psi}_b \right\rangle_C &= \frac{\delta^2 W_f}{\delta \bar{\eta}_a \delta \eta_b} \\ &= \frac{1}{Z_f} \frac{\delta^2 Z_f}{\delta \bar{\eta}_a \delta \eta_b} - \frac{1}{Z_f^2} \frac{\delta Z_f}{\delta \bar{\eta}_a} \frac{\delta Z_f}{\delta \eta_b} \\ &= \left\langle \psi_a \bar{\psi}_b \right\rangle - \left\langle \psi_a \right\rangle \left\langle \bar{\psi}_b \right\rangle, \end{aligned} \tag{1.28}$$

where in the present case a, b collectively indicate spatial and internal indices. The imaginary poles (since the Euclidean formulation is employed) give the dressed fermion mass. In the following it will be seen in which cases a fermion mass can be generated by quantum fluctuations.

The bound states of the system can be found by studying the poles of the function [34]:

$$G^{ab}_{\bar{\psi}\psi} = \frac{\delta^2 W_f}{\delta K_a \delta K_b} = \left\langle \bar{\psi}\psi_a \bar{\psi}\psi_b \right\rangle - \left\langle \bar{\psi}\psi_a \right\rangle \left\langle \bar{\psi}\psi_b \right\rangle, \tag{1.29}$$

which, as will be seen, provides informations about the propagation of collective modes.

Finally, the generator of one particle irreducible ($1PI$) correlators is defined. With the help of this functional, the usual systematic treatment of the renormalization properties of a QFT can be extended to non-perturbative approaches.

1.3.3 Generating functional for $1PI$ Green's functions

As is well known, the $1PI$ generating functional is the Legendre transform of the generator $W_f[\eta, \bar{\eta}] = \ln Z_f[\eta, \bar{\eta}]$ with respect to the sources coupled with the elementary fields. It is so called, since it generates diagrams which cannot be separated into two pieces by cutting a single propagator line. On the other hand, this functional Γ_f can be defined, as [1]:

$$\Gamma_f[\psi_c, \bar{\psi}_c] = \Gamma_f[\psi_c, \bar{\psi}_c, K]\big|_{K=0}, \tag{1.30}$$

[1] On the other hand, the functional $\frac{\delta \Gamma_f}{\delta K}[\psi_c, \bar{\psi}_c, K]\Big|_K = 0$, generates $1PI$ functions with one $\bar{\psi}\psi$ operator insertion [27]

where:

$$\Gamma_f[\psi_c, \bar{\psi}_c, K] = -W_f[\eta, \bar{\eta}, K] + \int \bar{\eta} \cdot \psi_c - \int \bar{\psi}_c \cdot \eta. \tag{1.31}$$

While both Z and W are functional of the external sources, Γ is a functional of the classical fields, defined in Eqs. (1.25),(1.26). From a statistical point of view, it can be regarded as a sort of Gibbs potential.

By deriving Γ with respect to the classical field ψ_c one finds:

$$\begin{aligned} \frac{\delta\Gamma_f}{\delta\psi_c} &= -\frac{\delta W_f}{\delta\psi_c} - \bar{\eta} + \int \frac{\delta\bar{\eta}}{\delta\psi_c}\psi_c + \int \frac{\delta\eta}{\delta\psi_c}\bar{\psi}_c \\ &= -\bar{\eta}, \end{aligned} \tag{1.32}$$

where the identities found in Eqs. (1.25),(1.26)were applied. Similarly, it is found:

$$\frac{\delta\Gamma_f}{\delta\bar{\psi}_c} = -\eta, \tag{1.33}$$

The relations given in Eqs. (1.32),(1.33) show how Γ, in terms of its arguments, satisfies the same relations obeyed by the classical action S in the presence of external sources. For this reason Γ is also called the "effective action" and the previous equations can be regarded, with a grain of salt, as the quantum equations of motion. Further developments are found in the next chapter. From these relations it is shown that the classical values of each fields are given by the minima of the effective action.

The $1PI$ Green's functions are obtained by expanding the effective action in powers of the classical fields around $\psi_c = \bar{\psi}_c = 0$ one obtains the $1PI$ correlators. These are the coefficient of the series:

$$\begin{aligned} \Gamma_f[\psi_c, \bar{\psi}_c] &= \sum_{n,m}^{\infty} \frac{1}{(n+m)!} \int_1, \dots \int_n, \int_1, \dots, \int_m \bar{\psi}_{c,m} \cdots \bar{\psi}_{c,1} \psi_{c,n} \dots \psi_{c,1} \\ &\times \Gamma_f^{(n;m)}(x_1, \dots, x_n; y_1, \dots, y_m). \end{aligned} \tag{1.34}$$

The derivative term is represented in Eq. (1.34) Clearly the $1PI$ functions for a theory of scalars and bosons can also be defined starting from the appropriate functional Γ_{fb}; a generic correlator of a theory with elementary scalars and fermions is represented with the diagram shown in Fig. 1.9.

Returning to theories involving only elementary fermions one can see that it is possible to expand the Γ_f around a generic non zero classical configuration. Clearly, different series

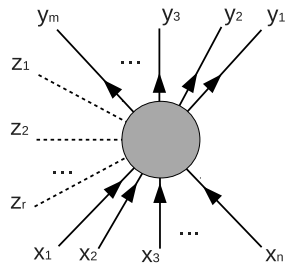

(a)

Figure 1.9: Graphical representation of the $1PI$ vertex defined by expansion of the functional Γ_{fb}. Starting from the first label the subsequent indices follow in counterclockwise order.

define different irreducible correlators. Expanding around a minimum of the functional the most interesting results are derived.

Indeed by using the identity:

$$\begin{pmatrix} \frac{\delta\psi_c}{\delta\bar{\eta}} & \frac{\delta\psi_c}{\delta\eta} \\ \frac{\delta\bar{\psi}_c}{\delta\bar{\eta}} & \frac{\delta\bar{\psi}_c}{\delta\eta} \end{pmatrix} \cdot \begin{pmatrix} \frac{\delta\bar{\eta}}{\delta\psi_c} & \frac{\delta\bar{\eta}}{\delta\bar{\psi}_c} \\ \frac{\delta\eta}{\delta\psi_c} & \frac{\delta\eta}{\delta\bar{\psi}_c} \end{pmatrix} = \begin{pmatrix} 1 & 0 \\ 0 & 1 \end{pmatrix}, \tag{1.35}$$

it is immediately found, with the help of Eqs. (1.25),(1.26) and Eqs. (1.32),(1.33):

$$\begin{pmatrix} \frac{\delta^2 W_f}{\delta\bar{\eta}\delta\bar{\eta}} & \frac{\delta^2 W_f}{\delta\eta\delta\bar{\eta}} \\ \frac{\delta^2 W_f}{\delta\bar{\eta}\delta\eta} & \frac{\delta^2 W_f}{\delta\eta\delta\eta} \end{pmatrix} = - \begin{pmatrix} \frac{\delta^2 \Gamma_f}{\delta\psi_c\delta\psi_c} & \frac{\delta^2 \Gamma_f}{\delta\bar{\psi}_c\delta\psi_c} \\ \frac{\delta^2 \Gamma_f}{\delta\psi_c\delta\bar{\psi}_c} & \frac{\delta^2 \Gamma_f}{\delta\bar{\psi}_c\delta\bar{\psi}_c} \end{pmatrix}^{-1}. \tag{1.36}$$

which shows how the second derivative of the effective action calculated for a generic field configuration is related to the inverse dressed propagators. Therefore, setting the external sources at zero, the second derivatives of the effective action calculated at the minimum are found to provide information about the particle spectrum of the theory.

Following the procedure introduced by Cornwall, Jackiw and Tomboulis CJT [31] one can eliminate both also the source K via a double Legendre transform:

$$\Gamma_f[\psi_c, \bar{\psi}_c, \bar{\psi}\psi_c] = -W_f[\eta, \bar{\eta}, K] + \int \bar{\eta}\cdot\psi_c - \int \bar{\psi}_c\cdot\eta + \int K\bar{\psi}\psi_c + \int K\bar{\psi}_c\psi_c. \tag{1.37}$$

Thus with the help of Eqs. (1.25),(1.26),(1.27) one finds:

$$\frac{\delta\Gamma_f}{\delta\bar{\psi}_c}[\psi_c, \bar{\psi}_c, \bar{\psi}\psi_c] = -\eta + K\psi_c, \tag{1.38}$$

$$\frac{\delta\Gamma_f}{\delta\psi_c}[\psi_c, \bar{\psi}_c, \bar{\psi}\psi_c] = -\bar{\eta} - K\bar{\psi}_c, \tag{1.39}$$

$$\frac{\delta\Gamma_f}{\delta\bar{\psi}\psi_c}[\psi_c, \bar{\psi}_c, \bar{\psi}\psi_c] = K. \tag{1.40}$$

These equations

1.4 Symmetries

The symmetries of the Hamiltonian, together with the field content, uniquely characterize the critical behaviour of a statistical system. Indeed the last, near a continuous transition, no more depends by microscopical details. Similarly, it is well known by some perturbative renormalization arguments, that quantum field theories are uniquely specified by the type of fields involved in the action and by their symmetry transformations [35]. This poverty of detail is a consequence of the universal behaviour implied by the scaling limit. There are some cases in literature in which a classical symmetry is violated by the quantum fluctuations [36],[37]. In this section only systems will be considered in which quantum fluctuations are consistent with the ones possessed by the action. However as in the case of the GN model and the Yukawa theory the quantum fluctuations can spontaneously break a symmetry by generating a non vanishing expectation value for the fields [38].

Briefly summarizing the symmetries of the GN model and of the Yukawa one, they turn out to be the same for both of these theories.

Clearly Lorentz and translational invariance are both symmetries of the model. It should be noted that, in the Euclidean version of the theory, the Lorentz group in d dimensions is simply the special orthogonal group $SO\,(d)$.

The set of d gamma matrices satisfying the Clifford algebra are:

$$\{\gamma^{\mu}, \gamma^{\nu}\} = 2\delta^{\mu\nu}. \tag{1.41}$$

If the dimension d of the space is even, another matrix can be constructed which extend the relations in Eq. (1.41). this matrix γ_{d+1} is defined as:

$$\gamma_{d+1} = (-i)^{d/2}\Pi_{\mu=1}^{d}\gamma_{\mu}. \tag{1.42}$$

With this position $\gamma_{d+1}^2 = 1$ and $\{\gamma_{d+1}, \gamma_{\mu}\} = 0$. In odd dimension the Clifford algebra is fulfilled only by the γ_{μ} and such a matrix cannot be constructed. Clearly the orthogonal group associated with the spinor transformation can be different from those acting on the space-time coordinates. Sometimes a four-dimensional representation of the gamma matrices is chosen also for $2 \leq d \leq 4$ for facilitating the analytical continuation of the results.

- **Spatial reflections**. In addition to the usual Poincaré invariance, the reflections are needed in order to obtain the full orthogonal group. A full reflection is given by the transformation:

$$x' = -x. \tag{1.43}$$

Now even and odd dimensions have to be distinguished.

If the dimension of the space is even the full reflection transformation is represented by:

$$\psi'(x) = \gamma_{d+1}\psi(-x), \tag{1.44}$$

$$\bar{\psi}'(x) = \bar{\psi}(-x)\gamma_{d+1}. \tag{1.45}$$

Since γ_{d+1} commutes with all the $SO(d)$ transformation the Dirac representation is reducible. (However it is an irreducible representation of the whole orthogonal group.) By means of the γ_{d+1} matrix all the other spatial reflections can be constructed in order to cover all the transformations of the $O(d)$ group. In conclusion the scalar is left unchanged by a spatial reflection, that is:

$$\phi'(x) = \phi(-x). \tag{1.46}$$

If the dimension of the space is odd, there is no γ_{d+1}. Since the matrix $-\hat{1}$ has determinant -1, then the total space reflections are represented by:

$$\psi'(x) = -\psi(-x), \tag{1.47}$$

$$\bar{\psi}'(x) = \bar{\psi}(-x). \tag{1.48}$$

(Moreover it should observed that the matrix $-\hat{1}$ also represents the other spatial reflections.) In contrast with the even dimension, under a reflection the scalar changes its sign:

$$\phi(x) = -\phi(-x), \tag{1.49}$$

thus preserving the Yukawa interaction. For odd dimensions the presence of an explicit fermion mass violates this symmetry.

- **Chiral symmetry**. However both the models possess, in even dimension, another internal symmetry which prevents an explicit mass term. By transforming the spinors as:

$$\psi'(x) = \gamma_{d+1}\psi(x), \tag{1.50}$$

$$\bar{\psi}'(x) = -\bar{\psi}(x)\gamma_{d+1}, \tag{1.51}$$

and the scalar field as:

$$\phi'(x) = -\phi(x), \tag{1.52}$$

the kinetic terms as well as the interactions are left unchanged. Conversely a fermion mass term is forbidden. One of the main purposes of this work is to investigate the generation of a fermion mass through the spontaneous symmetry breaking of this chiral symmetry or spatial reflections.

Since these are a discrete symmetries no Goldstone bosons are generated.

- **Flavour symmetry**: The introduction of an $U(N)$ symmetry in these models is a very useful tool for investigating the theory with the methods of the $1/N$ expansions. Moreover several physical situations can be described with the help of the unitary group. For historical reasons this N is referred to as a flavour number.

The spinors of the models transform in the fundamental representation according to:

$$\psi \quad \rightarrow e^{i\alpha_i T^i}\psi \tag{1.53}$$

where T^i are the $U\,(N)$ generators. The scalar ϕ transforms as a singlet of the group. This type of symmetry ensures that all the fermions acquire the same mass from the SSB mechanism.

Charge conjugation and hermitian conjugation are also discrete symmetries of the model. For further remarks the reader may refer to [27].

1.4.1 Symmetries in functional formalism

In order to describe the behaviour of the generating functionals under a general symmetry transformation a compact notation is introduced with $\phi = (\psi, \bar{\psi}, \phi)$ and $J = (\bar{\eta}, \eta, J)$.[2] The linear representation F of a generic symmetry group acts on the field as:

$$\phi \to F\phi. \tag{1.54}$$

The statement that a quantum field theory possesses a symmetry can be rephrased in the conditions:

$$S[F\phi] = S[\phi] \tag{1.55}$$

$$D(F\phi) = D\phi. \tag{1.56}$$

The first Eq. (1.55) is the condition for the classical symmetry, the Eq. (1.56) provides the quantum extension. The above equations imply that the quantum fluctuations leave all physical quantities unchanged. For the partition function:

$$\begin{aligned} Z[J] &= \int D\phi\, e^{-S[\phi]+\int J\cdot\phi} = \int D(F\phi)\, e^{-S[F\phi]+\int J\cdot F\phi} \\ &= \int D\phi\, e^{-S[\phi]+\int (F^T)J\cdot\phi} = Z[F^T J]. \end{aligned} \tag{1.57}$$

For the generating functional of the connected correlators this immediately implies that:

$$W[F^T J] = W[J]. \tag{1.58}$$

As for the classical field one finds:

$$\begin{aligned} \phi_c[F^T J] &= \frac{\delta}{\delta(F^T J)} W[F^T J] = F^{-1}\frac{\delta}{\delta J} W[F^T J] \\ &= F^{-1}\frac{\delta}{\delta J} W[J] = F^{-1}\phi_c[J], \end{aligned} \tag{1.59}$$

which, once inverted, gives:

$$F^T J[\phi_c] = J[F^{-1}\phi_c]. \tag{1.60}$$

[2] Clearly one should also require that any generic transformation preserve this structure [39].

The symmetry condition for the effective action then reads:

$$\begin{aligned}\Gamma[F^{-1}\phi_c] &= -W[J[F^{-1}\phi_c]] + \int J[F^{-1}\phi_c]\cdot F^{-1}\phi_c \\ &= -W[F^T J[\phi_c]] + \int F^T J[\phi_c]\cdot F^{-1}\phi_c \\ &= -W[J[\phi_c]] + \int J[\phi_c]\cdot\phi_c \\ &= \Gamma[\phi_c], \end{aligned} \tag{1.61}$$

which can also be written as:

$$\Gamma[F\phi_c] = \Gamma[\phi_c]. \tag{1.62}$$

Eq. (1.62) shows that the effective action obeys the same symmetries as classical action. This property turns out to be very useful whenever the computation of some correlator can be simplified with the help of symmetry arguments.

It is important to stress that, although the action possesses symmetry, the quantum fluctuations can spontaneously break this symmetry by inducing a non-vanishing expectation value in the effective action. This is exactly the way in which the chiral symmetry is broken in the considered fermion models. For the GN model, for example, the $\langle\bar{\psi}\psi\rangle$ condensate acquires a non vanishing value.

1.5 Non-interacting fermions and bosons

The first analysis of the present fermion theories is provided by the perturbation techniques. This tool gives the possibility of understanding some aspects of these models, and by means of this technique the Feynmann diagrammatic, which will be useful for further developments, can be introduced. First of all the partition functions for the non interacting theories must be calculated. Then by plugging the fermion interactions the Feynmann rules for the calculations of the correlators of elementary and composite operators can be established. In the perturbative frame a new diagrammatic representation is also introduced making it possible to distinguish the Hartree's contributions from the Fock's ones.

1.5.1 Free fermion theory

One can begin by considering the massless free fermion action:

$$S_f[\psi,\bar{\psi}] = -\int d^dx\,\bar{\psi}\cdot\not{\partial}\psi = -\int_x\int_y \bar{\psi}\,D^{-1}\,\psi. \tag{1.63}$$

According to Eq. (1.16), the corresponding generating functional $Z_f[\eta,\bar{\eta},K]$ is:

$$Z_f[\eta,\bar{\eta},K] = \int \mathcal{D}\psi\mathcal{D}\bar{\psi}\exp\left[\int_x\int_y \bar{\psi}\,(x)\,D_K^{-1}\,(x,y)\,\psi\,(y) + \int\bar{\eta}\cdot\psi - \int\bar{\psi}\cdot\eta\right], \tag{1.64}$$

where $D_K^{-1}(x,y) = (\not{\partial}+K)\delta^{(d)}(x,y)$. The Gaussian integration, extended for a Grassmann algebra, is given by the formula:

$$\int d\theta_1...d\theta_n e^{-\frac{1}{2}\theta^T A\theta+\rho^T\theta} = (\det A)^{1/2}\,e^{-\frac{1}{2}\rho^T A^{-1}\rho}, \tag{1.65}$$

where $\theta=(\theta_1,\ldots,\theta_n)$ as well as $\rho=(\rho_1,\ldots,\rho_n)$ are two different sets of Grassmann numbers and A is an antisymmetric $n\times n$ matrix. With the help of Eq. (1.65) the integrations in Eq. (1.64) can be performed obtaining:

$$\begin{aligned}
Z_f[\eta,\bar{\eta},K] &= \int\mathcal{D}\psi\mathcal{D}\bar{\psi}\exp\left[-\frac{1}{2}\int\int(\psi,\bar{\psi})\begin{pmatrix}0 & \left(D_K^{-1}\right)^T\\ -D_K^{-1} & 0\end{pmatrix}\begin{pmatrix}\psi\\ \bar{\psi}\end{pmatrix}\right.\\
&+ \left.\int(\bar{\eta},\eta)\cdot\begin{pmatrix}\psi\\ \bar{\psi}\end{pmatrix}\right]\\
&= \mathcal{N}\det\begin{pmatrix}0 & \left(D_K^{-1}\right)^T\\ -D_K^{-1} & 0\end{pmatrix}^{1/2}\\
&\times \exp\left[-\int\int\frac{1}{2}(\bar{\eta},\eta)\cdot\begin{pmatrix}0 & \left(D_K^{-1}\right)^T\\ -D_K^{-1} & 0\end{pmatrix}^{-1}\cdot\begin{pmatrix}\bar{\eta}\\ \eta\end{pmatrix}\right]\\
&= \mathcal{N}\det\begin{pmatrix}0 & \left(D_K^{-1}\right)^T\\ -D_K^{-1} & 0\end{pmatrix}^{1/2}\\
&\times \exp\left[-\frac{1}{2}\int\int(\bar{\eta},\eta)\cdot\begin{pmatrix}0 & -D_K\\ D_K^T & 0\end{pmatrix}\cdot\begin{pmatrix}\bar{\eta}\\ \eta\end{pmatrix}\right]\\
&= \mathcal{N}'\det(DD_K^{-1})\exp\left(\int\int\bar{\eta}\,D_K\,\eta\right).
\end{aligned} \tag{1.66}$$

Clearly, the pre-factors $\mathcal{N}$ or $\mathcal{N}'$ have no impact in the computation of the correlators.

The two factors appearing in Eq. (1.66) can be interpreted with the help of the diagrammatic representation introduced in Sec.1.1. Using the identity:

$$\det(A) = \exp\left(\mathrm{Trln}A\right), \tag{1.67}$$

the first factor appearing in the partition function can be rewritten as:

$$\begin{aligned}\det(DD_K^{-1}) &= \exp\left(\mathrm{Trln}\left(1+DK\right)\right) \qquad (1.68)\\ &= 1+\mathrm{Tr}(DK)+\frac{1}{2}\left(\left(\mathrm{Tr}(DK)\right)^2-\mathrm{Tr}\left(DKDK\right)\right)\\ &+ \frac{1}{6}\left(\left(\mathrm{Tr}(DK)\right)^3-3\mathrm{Tr}(DK)\mathrm{Tr}\left(DKDK\right)+2\mathrm{Tr}\left(DKDKDK\right)\right)\\ &+ \mathcal{O}(K^4). \qquad (1.69)\end{aligned}$$

The trace Tr is performed over the internal indices as well as over the space-time coordinates. For simplicity the matrix $K = K(x)\delta(x,y)$ was defined. The series in Eq. (1.68) is diagrammatically represented in Fig. 1.10. From these diagrams all the correlators of the

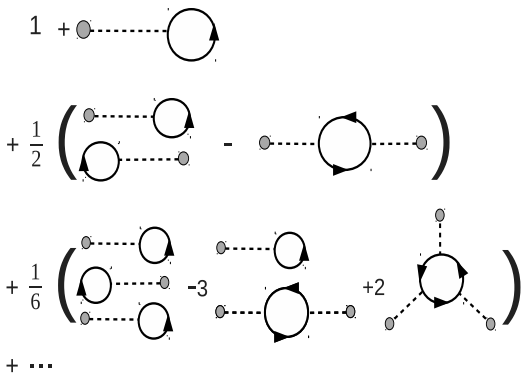

Figure 1.10: Graphical representation of the series expansion in Eq. (1.68). Loop contributions arise in the free theory because of the insertion of the $\bar{\psi}\psi$ composite field.

composite field can be extracted. On the other hand the second factor in Eq. (1.66) can be expanded as:

$$\exp\left(\bar{\eta}D_K\eta\right) = 1+\bar{\eta}D_K\eta+\frac{1}{2}(\bar{\eta}D_K\eta)^2+\mathcal{O}(\eta^3,\bar{\eta}^3). \qquad (1.70)$$

Using the operatorial expansion:

$$(A+B)^{-1} = A^{-1}-A^{-1}BA^{-1}+A^{-1}BA^{-1}BA^{-1}-\ldots, \qquad (1.71)$$

a series for the second factor appearing in Z_f is found. This is:

$$\begin{aligned}\exp\left(\bar{\eta}D_K\eta\right) &= 1+\bar{\eta}D\eta-\bar{\eta}DKD\eta+\bar{\eta}DKDKD\eta\\ &+ \frac{1}{2}\left((\bar{\eta}D\eta)^2+(\bar{\eta}DKD\eta)^2\right.\\ &- \left.2(\bar{\eta}D\eta)(\bar{\eta}DKD\eta)+2(\bar{\eta}D\eta)(\bar{\eta}DKDKD\eta)\right)+\mathcal{O}(\eta^3,\bar{\eta}^3,K^3). \qquad (1.72)\end{aligned}$$

From Eq. (1.72) the diagrams contributing to the correlators of elementary fields as well as to the correlators of composite and elementary ones can be computed. The series in Eq. (1.72) is represented with the diagrams shown in Fig. 1.11. As expected the two point

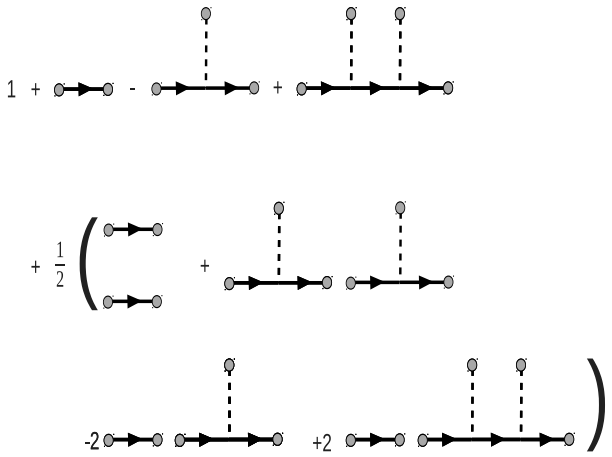

Figure 1.11: Graphical representation of the series expansion in Eq. (1.72). The massive propagator D_K comes from the resummation of an infinite series of massless propagators D with source insertions.

fermion function is nothing but the propagator D, that is:

$$G_f^{(1;1)}(x;y) = D(x,y). \tag{1.73}$$

The four point elementary function is disconnected and factorizes in the product of the two point correlators. One finds:

$$G_f^{(2;2)}(x_1,x_2;y_1,y_2) = -D_{11}D_{22} + D_{12}D_{21}. \tag{1.74}$$

The free contribution to the one point function of the composite operator is given by:

$$G_f^{(0;0;1)}(x) = \mathrm{tr}D(x,x), \tag{1.75}$$

where, in the present case, the trace covers only the internal indices. The two point composite function is given by:

$$G_f^{(0;0;2)}(x,y) = \mathrm{tr}D(x,x)\mathrm{tr}D(y,y) - \mathrm{tr}(D(x,y)D(y,x)). \tag{1.76}$$

Finally the function of two elementary fields and one composite operator is calculated. This is:

$$G_f^{(1;1;1)}(x;y;z) = D(x,y)\delta(x,z). \tag{1.77}$$

In the following how these expressions will be modified by the presence of interactions is studied.

Starting from the result of Eq. (1.66) the functional W_f can be calculated. It turns out to be:

$$W_f[\eta,\bar{\eta},K] = \int\int \bar{\eta}\, D_K\, \eta + \mathrm{Trln}\left(DD_K^{-1}\right), \tag{1.78}$$

where the trace Tr is over spatial and internal indices. Thus, with the help of the Eqs. (1.25),(1.26),(1.27) the values of the classical fields can be computed. These are:

$$\psi_c(x) = \int_z D_K(x,z)\eta(z), \tag{1.79}$$

$$\bar{\psi}_c(x) = -\int_z \bar{\eta}(z) D_K(z,x). \tag{1.80}$$

By applying the following derivative rules for operators:

$$\frac{d}{dx}\mathrm{Trln}A = \mathrm{Tr}\left(A^{-1}\frac{dA}{dx}\right), \tag{1.81}$$

$$\frac{dA^{-1}}{dx} = -A^{-1}\frac{dA}{dx}A^{-1}, \tag{1.82}$$

the first term in Eq. (1.78) becomes:

$$\frac{\delta D_K}{\delta K} = -D_K\frac{\delta D_K^{-1}}{\delta K}D_K. \tag{1.83}$$

The second term gives instead:

$$\begin{aligned}\frac{\delta}{\delta K}\mathrm{Trln}\left(DD_K^{-1}\right) &= \mathrm{Tr}\left(D_K D^{-1} D\frac{\delta D_K^{-1}}{\delta K}\right)\\ &= \mathrm{tr}D_K.\end{aligned} \tag{1.84}$$

Thus the expectation value of the composite operator is given by:

$$\left\langle\bar{\psi}\psi\right\rangle = \bar{\psi}_c\cdot\psi_c + \mathrm{tr}D_K \tag{1.85}$$

$$= \bar{\psi}_c\cdot\psi_c + \bar{\psi}\psi_c. \tag{1.86}$$

By taking $K = 0$ the second term in Eq. (1.85) vanishes so that in a free theory the expectation value of the composite operator is simply given by $\bar{\psi}_c\cdot\psi_c$. This is not the case when the interactions are taken into account.

With the help of Eqs. (1.80) and (1.80) for the classical values of the fields, the effective action defined in Eq. (1.30) can be computed. After some manipulations one finds:

$$\Gamma_f[\psi_c, \bar{\psi}_c, K] = -\int\int \bar{\psi}_c \, D_K^{-1} \, \psi_c - \mathrm{Trln}\left(D D_K^{-1}\right). \tag{1.87}$$

Setting $K = 0$ one finds that the effective action, in terms of its arguments, has the same form of the classical action as a function of the fields.

1.5.2 Free theory with fermions and scalars

Now a free theory with elementary fermion and scalar fields in considered. The action of this theory has the form:

$$S_{fb}[\psi, \bar{\psi}, \phi] = \int d^d x \, [-\bar{\psi}\partial\!\!\!/\psi + \frac{1}{2}\phi(-\partial^2 + M^2)\phi], \tag{1.88}$$

so that the partition function in Eq. (1.15) is given by two decoupled Gaussian functional integrals:

$$\begin{aligned} Z_{fb}[\eta, \bar{\eta}, J] &= \int \mathcal{D}\psi\mathcal{D}\bar{\psi} \, \exp\left[\int_x\int_y \bar{\psi} \, D^{-1} \, \psi + \int \bar{\eta}\cdot\psi - \int \bar{\psi}\cdot\eta\right] \\ &\times \int \mathcal{D}\phi \, \exp\left[-\frac{1}{2}\int_x\int_y \phi \, D_b^{-1} \, \phi + \int J\phi\right]. \end{aligned} \tag{1.89}$$

With the help of Eq. (1.65) for the integration of Grassmann variables and by applying the usual Gaussian integration formula, that is:

$$\Pi_k \int dx_k e^{-\frac{1}{2}x_i A_{ij} x_j + b_i x_i} = \mathcal{N}(\det A)^{-1/2} \exp\left(\frac{1}{2} b_i A_{ij}^{-1} b_j\right), \tag{1.90}$$

the generating functional Z_{fb} is easily computed and it is found:

$$\begin{aligned} Z_{fb}[\eta, \bar{\eta}, J] &= \mathcal{N}' e^{\left[\frac{1}{2}\int\int J \, D_b \, J\right]} e^{\left[\int\int \bar{\eta} \, D \, \eta\right]} \\ &\sim Z_b[J] Z_f[\eta, \bar{\eta}], \end{aligned} \tag{1.91}$$

which is just the product of the generating functionals of the two independent fermion and boson free theories. The generating functional of the connected Green's functions is:

$$W_{fb}[\eta, \bar{\eta}, J] = \ln Z_f[\eta, \bar{\eta}] + \ln Z_b[J] = W_f[\eta, \bar{\eta}] + W_b[J], \tag{1.92}$$

so that also the effective action can be immediately computed, giving the result:

$$\Gamma_{fb}[\psi_c, \bar{\psi}_c, \phi_c] = \frac{1}{2}\int\int \phi_c \, D_b^{-1} \, \phi_c - \int\int \bar{\psi}_c \, D^{-1} \, \psi_c. \tag{1.93}$$

Again it can be noted that the effective action is obtained from the classical one by replacing in the classical theory the elementary fields with the corresponding classical fields. mean values. The only connected functions are the two point correlators.

1.6 Interactions and perturbation theory

Once the partition function of a free theory is known, the impact of interaction terms is usually analyzed by performing a perturbative expansion in the coupling constants. Although the aim of this section is to review the perturbative diagrammatic rules for the GN and the Yukawa models, some general formulas will be worked out that can be applied to any local potential possessing certain symmetries. The one-loop amplitudes of the GN model will be worked out explicitly.

1.6.1 Perturbations in fermion theories with composite operators

The partition function for a model of fermions interacting via a local potential $V(\psi, \bar{\psi})$ is given by:

$$Z_f\left[\eta, \bar{\eta}, K\right] \;=\; \int \mathcal{D}\psi \mathcal{D}\bar{\psi}\, e^{\left[-S_G - \int V + \int \bar{\eta}\cdot\psi - \int \bar{\psi}\cdot\eta + \int K\bar{\psi}\cdot\psi\right]}, \tag{1.94}$$

where S_G is the free action given in Eq. (1.63). If only the Green's function of elementary fields given by the generating functional in Eq. (1.13) are needed, the usual perturbative formula can be applied, which is:

$$Z_f\left[\eta, \bar{\eta}\right] = \exp\left[-\int V(\delta/\delta\bar{\eta}, \delta/\delta\eta)\right] \exp\left[\int\int \bar{\eta}\, D\, \eta\right]. \tag{1.95}$$

The vertices appearing in the expansion of the first factor are represented by the diagrams in Fig. 1.1. The propagators, coming from the expansion of the second factor, are represented by the usual continuous oriented line.

In order to calculate the Green's functions of the composite operator $\bar{\psi}\psi$ the Eq. (1.94) must be considered. As is well known, the identity :

$$\begin{aligned} &\int \mathcal{D}\psi \mathcal{D}\bar{\psi}\, (\bar{\psi}\cdot\psi)\, e^{\left[-S_G + \int \bar{\eta}\cdot\psi - \int \bar{\psi}\cdot\eta + \int K\bar{\psi}\cdot\psi\right]} \\ =\; &\frac{\delta}{\delta K} \int \mathcal{D}\psi \mathcal{D}\bar{\psi}\, e^{\left[-S_G + \int \bar{\eta}\cdot\psi - \int \bar{\psi}\cdot\eta + \int K\bar{\psi}\cdot\psi\right]}, \end{aligned} \tag{1.96}$$

is the basis of perturbation theory.

Now, the potential $V(\psi,\bar{\psi}) = V(\bar{\psi}\psi)$ can be expanded in powers of the fields and of the composite operator, as shown in Eq. (1.5) then the Eq. (1.96) can be applied and the partition function in Eq. (1.94) can be rewritten as:

$$\begin{aligned} Z_f\left[\eta,\bar{\eta},K\right] &= \exp\left[-\int V\left(\frac{\delta}{\delta\bar{\eta}},\frac{\delta}{\delta\eta},\frac{\delta}{\delta K}\right)\right]\int \mathcal{D}\psi\mathcal{D}\bar{\psi}e^{\left[-S_G+\int\bar{\eta}\cdot\psi-\int\bar{\psi}\cdot\eta+\int K\bar{\psi}\cdot\psi\right]} \\ &= \exp\left[-\int V\left(\frac{\delta}{\delta\bar{\eta}},\frac{\delta}{\delta\eta},\frac{\delta}{\delta K}\right)\right] Z_G\left[\eta,\bar{\eta},K\right] \\ &= \exp\left[-\int V\left(\frac{\delta}{\delta\bar{\eta}},\frac{\delta}{\delta\eta},\frac{\delta}{\delta K}\right)\right]\det(DD_K^{-1})\exp\left(\int\int\bar{\eta}\,D_K\,\eta\right) \quad (1.97) \end{aligned}$$

where $Z_G\left[\eta,\bar{\eta},K\right]$ is the partition function of the free fermion model and has been computed in Eq. (1.66). The Feynmann rules can easily be worked out. The potential V can be symbolically expanded in powers of the derivative with respect to the sources of the elementary and of the composite fields. Then a generic vertex can be represented with the diagram shown in Fig. 1.5.

Thus the functional Z can be calculated by linking every possible vertex with the contributions given in Eqs. (1.68),(1.72).

1.6.2 Perturbative expansion of Fermi theory

The previous results are applied by evaluating some amplitudes of the GN model by means of the Feynmann diagrams. The one-loop contributions to the two point and four point functions of elementary fields are computed by applying the formula in Eq. (1.95). Then the one-loop contributions to the one point and the two point correlators of the composite operator are calculated with the help of Eq. (1.97).

Perturbation with elementary operators

By deriving the interacting part of the action of GN model one finds:

$$\frac{-\int V(\bar{\psi}\cdot\psi)}{\delta\psi_a(x)\delta\bar{\psi}_b(y)\delta\psi_c(z)\delta\bar{\psi}_d(w)} = G\left(\delta_{ab}\delta_{cd}-\delta_{ad}\delta_{bc}\right)\delta(x,y)\delta(y,z)\delta(z,w), \quad (1.98)$$

thus the vertex splits into two contributions as shown in Fig. 1.12. The first diagram is called the "direct" or Hartree term, the second one is the "exchange" or Fock term.

Now the one-loop contribution to the $1PI$ two point and four point function of elementary fields can be calculated. The one-loop correction to the $1PI$ two point function

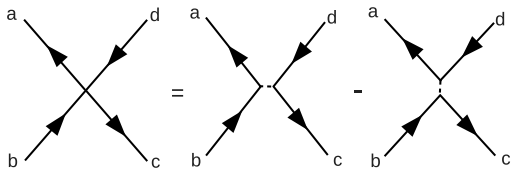

.

Figure 1.12: According to Eq. (1.98) the four fermion vertex splits in a direct (s-channel) contribution and in a exchange one (t-channel).

(the inverse propagator) is of order G in perturbation theory. The Feynmann diagrams contributing to this function are shown in Fig. 1.13. The explicit calculation of the inverse

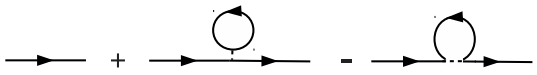

.

Figure 1.13: One loop contributions to the $1PI$ fermion-fermion amplitude. The Hartree and the Fock terms are respectively the second and the last diagram.

propagator gives:

$$\Gamma^{(1;1)}_{ab}(x,y) = D^{-1}_{ab}(x,y) + G\left[\delta_{ab}\mathrm{tr}D(z,z) - D_{ab}(z,z)\right]\delta(x,y). \tag{1.99}$$

By taking the Fourier transform of the previous expression, one finds the form of the inverse propagator in momentum space. If $\tilde{\Gamma}^{(1;1)}_{ab}(p,q)$ is the Fourier transform of $\Gamma^{(1;1)}_{ab}(x,y)$, by defining $\tilde{\Gamma}^{(1;1)}_{ab}(q)$ from $\Gamma^{(1;1)}_{ab}(p,q) = \Gamma^{(1;1)}_{ab}(q)(2\pi)^d\delta(p,q)$, one finds:

$$\tilde{\Gamma}^{(1;1)}_{ab}(q) = i\not{q}_{ab} + m_B\delta_{ab} + G\left[\delta_{ab}\int\frac{d^dp}{(2\pi)^d}\mathrm{tr}\frac{-i\not{p}+m_B}{p^2+m_B^2} - \int\frac{d^dp}{(2\pi)^d}\frac{-i\not{p}_{ab}+m_B\delta_{ab}}{p^2+m_B^2}\right] \tag{1.100}$$

where for convenience a bare mass m_B was introduced in the fermion propagator. It is important to note that the one-loop correction is momentum independent. The integral appearing in Eq. (1.100) is divergent for $d \geq 2$, thus a cut-off Λ (or another kind of regularization) is implied.

The one-loop contributions to the $1PI$ fermion four-point correlator are listed in Fig 1.14. The computation of each diagram is performed in the App. A.1. Here the result is presented after all the external momenta were settled to zero. So the correlator

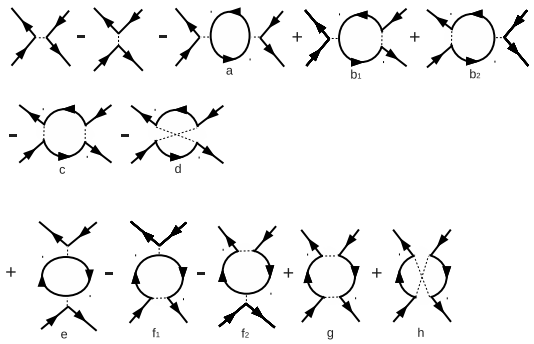

.

Figure 1.14: One loop contributions to the $1PI$ four point vertex function. The diagrams from (a) to (c) are s-channel terms, those from (e) to (g) are t-channel terms, finally (d) and (h) are u-channel terms .

in the momentum space turns out to be:

$$\Gamma^{(2;2)}_{abcd}(0,0,0,0) = (2\pi)^d\delta(0)\left[G - G^2 N \mathrm{tr}\mathbb{I}\int\frac{d^dp}{(2\pi)^d}\frac{-p^2+m_B^2}{(p^2+m_B^2)^2}\right.$$
$$\left.+G^2\int\frac{d^dp}{(2\pi)^d}\frac{m_B^2}{(p^2+m_B^2)^2}\right](\delta_{ab}\delta_{cd}-\delta_{ad}\delta_{bc})\,. \qquad (1.101)$$

The results in Eqs. (1.100),(1.101) are useful in testing the RG equations that will be derived in the following.

Perturbation theory with composite operators

According to the form of the action in Eq. (1.1), the expansion of the potential gives the result:

$$\begin{aligned}-\int_x V(\delta/\delta\bar\eta,\delta/\delta\eta,\delta/\delta K) &= \frac{G}{3}\int_x\int_y\delta(x,y)\frac{\delta}{\delta K(x)}\frac{\delta}{\delta K(y)}\\ &+ \frac{G}{3}\sum_{ab}\int_x\int_y\int_z\delta(x,y)\delta(y,z)\delta_{ab}\frac{\delta}{\delta K(x)}\frac{\delta}{\delta\bar\eta(y)}\frac{\delta}{\delta\eta(z)}\\ &+ \frac{G}{6}\sum_{abcd}\int_x\int_y\int_z\int_w\delta(x,y)\delta(y,z)\delta(z,w)\\ &\times (\delta_{ab}\delta_{cd}-\delta_{ad}\delta_{bc})\frac{\delta}{\delta\bar\eta(x)}\frac{\delta}{\delta\eta(y)}\frac{\delta}{\delta\bar\eta(z)}\frac{\delta}{\delta\eta(w)} \qquad (1.102)\end{aligned}$$

Thus the perturbative expansion for the functions of the composite operator can be obtained by linking the diagrams given in the series in Eq. (1.68) with these three different types of vertices. The diagrams contributing to the connected one point function of the composite operator are shown in Fig. 1.15.

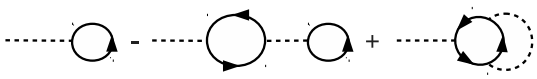

.

Figure 1.15: Graphical representation of the contributions to $\langle\bar{\psi}\psi\rangle$, given in Eq. (1.103), up to the order G in perturbation theory.

By explicitly performing the calculation the tadpole contribution is obtained, it turns out to be:

$$\begin{aligned}\langle\bar{\psi}\psi(x)\rangle &= \mathrm{tr}D(x,x) - G\int_z \mathrm{tr}\left[D(x,z)D(z,x)\right]\mathrm{tr}D(z,z) \\ &- G\int_z\int_w \mathrm{tr}\left[D(x,z)D(z,w)D(w,x)\right]. \end{aligned} \tag{1.103}$$

By evaluating the diagrams that contribute to the two-point connected correlator of the composite operator, which are displayed in Fig. 1.16, one obtains:

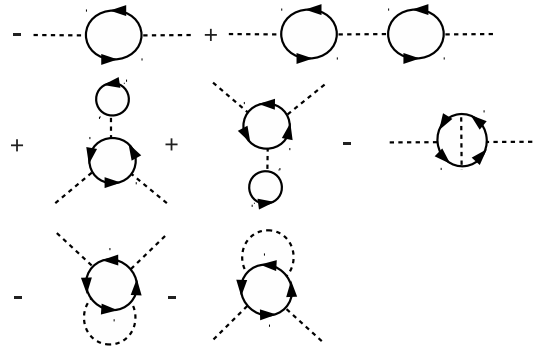

.

Figure 1.16: Graphical representation of the contributions to the two point connected correlator , given in Eq. (1.104), up to the order G in perturbation theory.

$$
\begin{aligned}
G_{\bar{\psi}\psi}(x,y) &= -\mathrm{tr}(D(x,y)D(y,x)) + G\int_z \mathrm{tr}[D(x,z)D(z,x)]\mathrm{tr}[D(z,y)D(y,z)] \\
&+ G\int_z \mathrm{tr}[D(x,z)D(z,y)D(y,x)]\mathrm{tr}[D(z,z)] \\
&+ G\int_z \mathrm{tr}[D(x,y)D(y,z)D(z,x)]\mathrm{tr}[D(z,z)] \\
&- G\int_z \mathrm{tr}[D(x,y)D(y,z)D(z,z)D(z,x)] \\
&- G\int_z \mathrm{tr}[D(x,z)D(z,z)D(z,y)D(y,x)] \\
&- G\int_z \mathrm{tr}[D(x,z)D(z,y)D(y,z)D(z,x)]. \qquad (1.104)
\end{aligned}
$$

It is important to note how the contributions in Fig. 1.15 look very similar to the one loop contributions to the scalar mean value of the Yukawa theory. On the other hand the diagrams in Fig. 1.16 are very similar to those of a scalar propagator, apart from a bare propagator term which is lacking. This not an accident, the similarity found a clear interpretation with the help of the bosonization technique.

1.6.3 Perturbations in theories with fermions and scalars

By following the same steps used in the previous sections the partition function for a theory with scalars and fermions that interact via the potential $V(\psi,\bar{\psi},\phi)$ can be computed. For this theory it turns out to be:

$$
\begin{aligned}
Z_{fb}[\eta,\bar{\eta},J] &= \int \mathcal{D}\psi\mathcal{D}\bar{\psi}\int \mathcal{D}\phi\, e^{-S_G[\psi,\bar{\psi},\phi]-\int V(\psi,\bar{\psi},\phi)+\int \bar{\eta}\cdot\psi-\int\bar{\psi}\cdot\eta+\int J\phi} \\
&= \exp\left[-\int V(\delta/\delta\bar{\eta},\delta/\delta\eta,\delta/\delta J)\right] Z_{G,fb}[\eta,\bar{\eta},J] \\
&= \exp\left[-\int V(\delta/\delta\bar{\eta},\delta/\delta\eta,\delta/\delta J)\right] \exp\left[\int\int \bar{\eta}\, D\, \eta\right] \\
&\times \exp\left[\frac{1}{2}\int\int J\, D_b\, J\right]. \qquad (1.105)
\end{aligned}
$$

In such a way the perturbative expansion can be performed.

1.6.4 Aspects of perturbative renormalization

Since the perturbative regime is considered the classification of field theories which is based on the dimensional analysis can be applied [2]. The usual results are summarized in

order to stress the basic concepts that will be applied in the study of the non-perturbative renormalizability. Some elementary quantities as the scaling dimension and the perturbative degree of divergence as well as their connection with the renormalization program are reported in the following.

Scale invariance of a theory: classical conditions

The renormalizability of a field theory is achieved once that the correlators can be made short distance insensitive by means of the fine tuning of a finite number of bare parameters [27]. This form of scale invariance is reflected on the request that the correlators must be homogeneous functions of their arguments and is related to the scaling properties of these functions under a scale transformation. Actually the renormalizability of a theory requires the invariance of the theory under a wider class of transformations. This will be the subject of chap. 3. However in some cases these are reduced to simple scale transformations. Thus it is important to analyze how the several quantities behave under a scale transformation [40].

A contraction transforms the space time coordinates as:

$$x^{'\mu} = bx^{\mu}, \tag{1.106}$$

with $b < 1$. A gradient ∂_μ and a momentum p_μ are affected by their contraction as:

$$p^{'\mu} = p^{\mu}/b, \tag{1.107}$$

$$\frac{\partial}{\partial x'^{\mu}} = b^{-1}\frac{\partial}{\partial x^{\mu}}. \tag{1.108}$$

Generally if the quantity A scales as $A' = b^{-D_A}A$ under a contraction, then its scaling dimension $[A]$ will be defined as:

$$[A] = D_A. \tag{1.109}$$

As is well known, for a free theory, the scale invariance can be simply rephrased on the condition that the Green's functions transform in such a way that the effective action as well as the action are invariant, under a scale transformation. Since the effective action of a theory of free fermions and scalars is given by Eq. (1.93) the scaling dimension of free fermion is defined through the behaviour of the fermion tree propagator. This propagator

is a homogeneous function of degree $\alpha = -1$. That is:

$$D\left(\frac{p}{b}\right) \sim b\frac{1}{i\not{p}}, \qquad p \to \infty. \tag{1.110}$$

Thus in d space-time dimensions the scaling dimension of the non interacting fermion fields is defined as:

$$[\psi] = \left[\bar{\psi}\right] = \frac{d+\alpha}{2} = \frac{d-1}{2}. \tag{1.111}$$

This means that in a free theory the fields transform as:

$$\psi(bx) = b^{\frac{(1-d)}{2}}\psi(x), \tag{1.112}$$

$$\bar{\psi}(bx) = b^{\frac{(1-d)}{2}}\bar{\psi}(x). \tag{1.113}$$

For a scalar field instead the propagator behaves as:

$$D_B\left(\frac{p}{b}\right) \sim b^2\frac{1}{p^2}, \qquad p \to \infty, \tag{1.114}$$

showing that it is an homogeneous function of degree $\alpha = -2$. Thus the scaling dimension for the scalar is given by:

$$[\phi] = \frac{d+\alpha}{2} = \frac{d-2}{2}. \tag{1.115}$$

With these positions the scale invariance of the theory is simply satisfied which also means the action and the effective action must have a vanishing scaling dimension, i.e. they must be invariants under a scaling [27].

Anomalous dimensions of elementary fields

Far from the perturbative regime the Green's functions of a renormalizable theory can acquire a different scaling law. For example the fermion dressed propagator can behave near the critical region as:

$$\Delta\left(\frac{p}{b}\right) = b^{1-\eta_\psi}\Delta(p). \tag{1.116}$$

The number η_ψ is called the anomalous dimension of the correlator since it represents the difference between the scaling of the propagator an that of the connected two point function.

In order to preserve the scale invariance of the Gaussian part of the effective action the fermion fields transform as:

$$\psi(bx) = b^{-\frac{d-1}{2}} Z_\psi^{-1/2}(b)\psi(x), \tag{1.117}$$

$$\bar{\psi}(bx) = b^{-\frac{d-1}{2}} Z_\psi^{-1/2}(b)\bar{\psi}(x). \tag{1.118}$$

Thus one finds:

$$Z_\psi = b^{\eta_\psi}. \tag{1.119}$$

From this result the scaling dimensions of the fermion fields can immediately be calculated:

$$[\psi] = [\bar{\psi}] = \frac{d-1}{2} + \frac{\eta_\psi}{2} = [\psi]_0 + \gamma_\psi. \tag{1.120}$$

Then $\gamma = \eta_\psi/2$ is called the anomalous dimension of the field. By deriving the Z_ψ function given in Eq (1.119) one obtains:

$$\frac{d\ln Z_\psi}{d\ln b} = \eta_\psi = \frac{\gamma_\psi}{2}. \tag{1.121}$$

The same arguments can be applied for a theory including a scalar. If the boson two point correlator scales as:

$$\Delta_B\left(\frac{p}{b}\right) = b^{2-\eta_\phi}\Delta_B(p), \tag{1.122}$$

the scalar field must transform as:

$$\phi(bx) = b^{-\frac{d-2}{2}} Z_\phi^{-1/2}(b)\phi(x), \tag{1.123}$$

in order to preserve the scale invariance of the effective action. This gives :

$$Z_\phi = b^{\eta_\phi}. \tag{1.124}$$

The anomalous dimension for the boson field can be calculated from the following relation:

$$\frac{d\ln Z_\phi}{d\ln b} = \eta_\phi = \frac{\gamma_\phi}{2}. \tag{1.125}$$

Perturbative scaling of the composite operator $\bar{\psi}\psi$

The canonical dimension of a local derivative operator is simply given by:

$$[\mathcal{O}]_0 = l + \sum_j [\psi_j]_0 + \sum_k [\phi_k]_0, \tag{1.126}$$

where l is the number of derivatives acting on the operator. Thus for example, the composite field $\bar{\psi}\psi$ has the dimension:

$$[\bar{\psi}\psi]_0 = 2[\psi]_0. \tag{1.127}$$

On the other hand the scaling dimension of this local operator can be defined by the one of the two point function:

$$\begin{aligned} \tilde{G}_{\bar{\psi}\psi}(q) &= \int d^d x \int d^d y \, e^{-iq(x-y)} G_{\bar{\psi}\psi}(x,y) \\ &= \int d^d x \int d^d y e^{-iq(x-y)} \mathrm{tr}(D(x,y)D(y,x)) \\ &= \int \frac{d^d p}{(2\pi)^d} \mathrm{tr}(D(p)D(p+q)) \simeq q^{(2-d)}. \end{aligned} \tag{1.128}$$

The last equalities come from an explicit calculation that will be analyzed in the following. Thus the scaling dimension of the field is given by:

$$\left[\bar{\psi}\psi\right]^2 = d - \left[G^{-1}_{\bar{\psi}\psi}\right] = 2d - 2, \tag{1.129}$$

$$\left[\bar{\psi}\psi\right] = d - 1 = 2\left[\psi\right]_0. \tag{1.130}$$

From this result it should be clear that also in the free case the canonical dimension and the scaling dimension of this composite operator coincide.

1.6.5 Perturbative classification of divergences

In a free field theory the scaling dimension coincides with its canonical or engineering dimension. The last one is simply obtained, through dimensional analysis, by measuring all the quantities in powers of an energy scale. Thus since the action is a dimensionless quantity the canonical dimensions of the fields are $[\psi]_0 = [\bar{\psi}]_0 = (d-1)/2$, and $[\phi]_0 = (d-2)/2$. This result coincide with the scaling dimensions found in Eqs. (1.111),(1.115).

Starting from the canonical dimensions of the fields the canonical one of an interacting term can be computed, so finding:

$$[m_b]_0 = 1, \tag{1.131}$$

$$\left[M^2\right]_0 = 2 \tag{1.132}$$

for the fermion and scalar masses, or

$$[G]_0 = 2 - d, \tag{1.133}$$

$$[g]_0 = \frac{4-d}{2}, \tag{1.134}$$

$$[\lambda]_0 = 4 - d. \tag{1.135}$$

for the dimensions of the Fermi coupling G of the Yukawa interaction g and of the scalar quartic coupling respectively.

From the perturbative point of view the scale invariance depends on the way in which the cut-off scale appears in each diagram. If at every order in the perturbation theory new positive powers of the cut-off scale are generated, which cannot be removed by tuning a finite number of parameters, the scaling limit cannot be performed. The origin of new cut-off effects in a diagram can be taken into account by defining the superficial degree of divergence D of a Feynman diagram. This quantity will be calculated for a theory with scalars and bosons. The degree of divergence is nothing but the power law by which a diagram seems to diverge when the cut-off is sent to infinity. [3] One finds [41]:

$$D = d - E_\psi[\psi]_0 - E_\phi[\phi]_0 - \sum_a [g_a]_0 V_a, \tag{1.136}$$

where E_ψ is the number of fermion external legs, E_ϕ the number of scalar ones and $[g_a]_0$ is the canonical dimension of the coupling associated with the a vertex.

The divergences occurring in the perturbation theory permit the classification the QFT's in the following way [27]:

- *Non-renormalizable theories:* If there is a vertex with a coupling g_a of negative (canonical) dimension (irrelevant coupling). The number V_a can be arbitrarily increased in order to obtain an infinite number of diverging diagrams.

[3] This statement must be revisited when overlapping divergences appear beyond the one loop order [2].

- *Super-renormalizable theories:* If all the vertices have couplings with positive dimension (relevant couplings) only a finite number of diagrams is divergent. The divergences can be treated by tuning only this finite number of interactions.

- *Renormalizable theories:* If the dimension of a coupling vanishes (marginal coupling) and there are no couplings with negative dimension then an infinite number of diagrams diverge. However the maximum degree of divergence does not change for fixed external legs and does not depend on additional insertions of the coupling with zero dimension.

According to these results one finds that, for $2 < d < 4$, the GN model is perturbatively non-renormalizable, while the Yuwaka theory is super-renormalizabile. At $d = 2$ the GN model became renormalizable while the Yukawa one is always super-renormalizable, conversely at $d = 4$ the Yukawa theory is renormalizable since both the coupling g and the quartic coupling λ have zero dimensions. When a theory is super-renormalizable its action is scale invariant near the perturbative region. For small values of the interactions the action satisfies:

$$[S] = 0. \tag{1.137}$$

This implies that in the perturbative regime of a super-renormalizable theory the scaling dimension of the fields and their canonical dimension coincides. Moreover from the Eq. (1.137) the scaling dimension and the canonical dimension of the couplings must coincide.

$$[g_a] \;=\; [g_a]_0 \tag{1.138}$$

In a perturbative renormalizable theory the Eq. (1.138) is no longer satisfied. Weak violations to the trivial (canonical) scaling occur and the scaling of the fields does not follow a simple power law.

Finally when a theory is non-renormalizable, in order to preserve the scale invariance of the theory, an infinite number of coupling must be introduced.

1.6.6 Field theoretical renormalization of the Yukawa theory

As already stressed, the Green's functions of a (super-)renormalizable theory are cut-off independent for an appropriate choice of a finite number of bare parameters. Also

renormalizable theories can be made cut-off independent by imposing a finite number of conditions. However, in the last case, the scaling limit cannot be performed so that the IR scales and the UV cut-off can never be completely decoupled. From a field theoretical point of view the cut-off Λ can be removed by setting a finite number of *renormalization conditions* [41]. As an example the one loop perturbative divergences of the Yukawa theory at $d = 4$ are considered. According to the formula in Eq. (1.136) the divergent diagrams are listed in Fig. 1.17. Just the $1PI$ diagrams can be considered since the

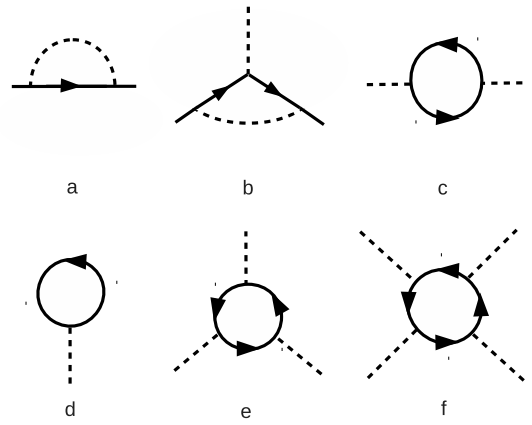

.

Figure 1.17: One loop divergent diagrams in the Yukawa theory. The (b) and the (f) diagrams correct to the coupling constants, the (c) give a correction to the scalar mass and the scalar field, while the diagrams (d) and (e) vanishes because of the symmetry. Finally only the fermion field is corrected by the (a) diagram since the correction to the fermion mass is zero.

divergent parts of reducible diagrams are products of the divergent pieces corresponding to their irreducible parts. However diagrams (b) and (e) vanish because of the symmetry of the theory. At an IR renormalization scale $\mu << \Lambda$ the renormalized connected Green's functions are defined by performing the fields transformations:

$$\psi_r(x) = Z_\psi^{-1/2}(\frac{\mu}{\Lambda}, \{g\})\psi(x), \tag{1.139}$$

$$\bar{\psi}_r(x) = Z_\psi^{-1/2}(\frac{\mu}{\Lambda}, \{g\})\bar{\psi}(x), \tag{1.140}$$

$$\phi_r(x) = Z_\phi^{-1/2}(\frac{\mu}{\Lambda}, \{g\})\phi(x), \tag{1.141}$$

so that the renormalized correlators are related with the original or bare ones by the relations:

$$\begin{aligned}&\left\langle \psi_r(x_1)\dots\psi_r(x_m)\bar{\psi}_r(y_1)\dots\bar{\psi}_r(y_n)\phi_r(z_1)\dots\phi_r(z_r)\right\rangle \\ &= Z_\psi^{-\frac{n+m}{2}} Z_\phi^{-\frac{r}{2}} \left\langle \psi(x_1)\dots\psi(x_m)\bar{\psi}(y_1)\dots\bar{\psi}(y_n)\phi(z_1)\dots\phi(z_r)\right\rangle . \end{aligned} \tag{1.142}$$

In principle these are not the same quantities appearing in Eqs. (1.117),(1.118),(1.123). Instead, they are defined by the conditions:

$$\Delta^r(p)^{-1}(p, g_r, \lambda_r, \mu, \Lambda)\big|_{p^2=-\mu^2} = 0, \tag{1.143}$$

$$\frac{d}{d\not{p}}\Delta^r(p)^{-1}(p, g_r, \lambda_r, \mu, \Lambda)\bigg|_{p^2=-\mu^2} = 1, \tag{1.144}$$

$$\Delta_B^r(p)^{-1}(p, g_r, \lambda_r, \mu, \Lambda)\big|_{p^2=-\mu^2} = 0, \tag{1.145}$$

$$\frac{d}{dp^2}\Delta_B^r(p)^{-1}(p, g_r, \lambda_r, \mu, \Lambda)\bigg|_{p^2=-\mu^2} = 1. \tag{1.146}$$

$$\tag{1.147}$$

As the bare correlators are functions of momenta, bare parameters and cut-off scale, so the renormalized ones are just functions of the momenta, of the scale μ and of the *renormalized parameters*.[4] The renormalized parameters are given by the conditions:

$$\Gamma_{\phi\psi\bar{\psi}}(\{p\}, g_r, \lambda_r, \mu, \Lambda)\big|_{s=t=u=-\mu^2} = \mu^{4-d} g_r, \tag{1.148}$$

$$\Gamma_{\phi\phi\phi\phi}(\{p\}, g_r, \lambda_r, \mu, \Lambda)|_{s=t=u=-\mu^2} = \mu^{4-d}\lambda_r, \tag{1.149}$$

where s, t and u are the three kinematic channels. If the theory had been super-renormalizable (as it is at $d = 3$) the number of arbitrary renormalization conditions equates the number of bare relevant parameters that have to be tuned in order to reach the critical region. For example, the conditions in Eqs. (1.143), (1.145) fix respectively the fermion and the boson bare masses near their critical value. Similarly, the conditions in Eqs. (1.148), (1.149) tune the Yukawa and the quartic scalar coupling near the origin. As the conditions in Eqs. (1.144), (1.146) are redundant, so they turn out to be just a simple rescaling of the fields. In this sense, near the critical point they coincide with those given in Eqs. (1.117),(1.118),(1.123). When the Yukawa theory is just renormalizable (at d=4)

[4]Eventually they may depend on terms involving the cut-off that are suppressed near the scaling region.

the scaling limit cannot be performed. The renormalization conditions tune the value of the relevant couplings, as done by Eqs. (1.143), (1.145), as well as those of the marginal ones (conditions in Eqs. (1.148), (1.149)). They give, together with the conditions in Eqs. (1.144), (1.146), the opportunity of removing the cut-off from the renormalized functions. However by the presence of the marginal couplings some logarithmic divergences arise in the bare correlators so that the cut-off can be sent to infinity just at the price of finding a non interacting theory.

1.7 Bosonization technique

As previously stated there is a strict analogy between the Green's function of a composite operator and those of an elementary scalar coupled with the elementary fermion fields. This parallel is favoured by the diagrammatic representation that was introduced but it has deeper reasons. In principle, the presence of an elementary scalar in a fermion theory and the insertion of a composite operator should describe two distinct physical situations. The inclusion of a scalar composite operator in theory should model the effects of the collective boson excitations of the system. On the other hand the use of an elementary scalar assumes that all the boson effects must be described with the introduction of a new scalar elementary particle. It is a difficult task to establish if these alternatives can produce different distinguishable effects. In this section a technical trick is introduced which allows the comparison to be clarified.

1.7.1 The Hubbard Stratonovich transformation

The Hubbard Stratonovich transformation for the Fermi interaction is obtained through the Gaussian identity [26]:

$$\int \mathcal{D}\sigma \, \exp\left[-\int \frac{1}{2G}\sigma^2 + \int \left(\frac{K}{G} + \bar{\psi}\psi\right)\sigma\right] = \mathcal{N} \exp\left[\int \frac{G}{2}\left(\bar{\psi}\psi + \frac{K}{G}\right)^2\right], \quad (1.150)$$

then for the GN model the expression in Eq. (1.16) can be rewritten as:

$$\begin{aligned} Z_f[\eta,\bar{\eta},K] &= \mathcal{N}\int \mathcal{D}\psi\mathcal{D}\bar{\psi}\int \mathcal{D}\sigma\, \exp\int\left[\bar{\psi}(\partial\!\!\!/+\sigma)\psi-\frac{\sigma^2}{2G}+\bar{\eta}\cdot\psi-\bar{\psi}\cdot\eta+\frac{K}{G}\sigma\right] \\ &\times \exp\left[-\int\frac{K^2}{2G}\right] \\ &= \mathcal{N}e^{-\int\frac{K^2}{2G}}Z_b\left[\eta,\bar{\eta},\frac{K}{G}\right]. \end{aligned} \tag{1.151}$$

Apart from a source dependent pre-factor, the partition function looks like very similar to that of a theory of elementary fermions and scalar interacting via a Yukawa term. However some additional remarks are required. First of all there is not any scalar derivative term ensuring the particle propagation; for this reason this field is often called auxiliary scalar. Moreover a scalar self-interaction lacks from the original Yukawa theory. Thus the Lagrangian has fewer bare parameters than those of a Yukawa theory. These observations could mislead. In the past, attempts were done trying to establish whether the theories without fundamental scalars could be more predictive than those with the same symmetries but involving an explicit scalar [20],[21]. Different analysis, performed in the framework of $1/N$ expansion, have shown that this is not the case [17] [18]. More on this point in the next chapter. For the moment some aspects of the Hubbard-Stratonovich trick are presented. The mean value of the composite operator in the GN theory in the presence of explicit sources, is given by:

$$\left\langle\bar{\psi}\psi\right\rangle^{\eta,\bar{\eta},K}=\frac{1}{Z_f[\eta,\bar{\eta},K]}\frac{\delta}{\delta K}Z_f[\eta,\bar{\eta},K]. \tag{1.152}$$

On the other hand the mean value of the auxiliary field can be defined as:

$$\begin{aligned} \langle\sigma\rangle^{\eta,\bar{\eta},\mathcal{J}} &= \frac{\int\mathcal{D}\psi\mathcal{D}\bar{\psi}\int\mathcal{D}\sigma\,\sigma e^{\left[-S_b[\psi,\bar{\psi},\sigma]+\int\mathcal{J}\sigma+\int\bar{\eta}\cdot\psi-\int\bar{\psi}\cdot\eta\right]}}{\int\mathcal{D}\psi\mathcal{D}\bar{\psi}\int\mathcal{D}\sigma\,e^{\left[-S_b[\psi,\bar{\psi},\sigma]+\int\mathcal{J}\sigma+\int\bar{\eta}\cdot\psi-\int\bar{\psi}\cdot\eta\right]}} \\ &= \frac{1}{Z_b\left[\eta,\bar{\eta},\mathcal{J}\right]}\frac{\delta}{\delta\mathcal{J}}Z_b\left[\eta,\bar{\eta},\mathcal{J}\right], \end{aligned} \tag{1.153}$$

where $\mathcal{J}=\frac{K}{G}$ and S_b is the action given by the Lagrangian:

$$\mathcal{L}_b=-\bar{\psi}(\partial\!\!\!/+\sigma)\psi+\frac{1}{2G}\sigma^2. \tag{1.154}$$

Now it is easy to establish the relationship between the original correlators and those of the bosonized version. Clearly one can immediately verify that the classical values ψ_c

and $\bar{\psi}_c$ as well as all the correlators made of fermionic elementary fields coincide either for the purely fermion version of the model or for the bosonized one. By deriving the original partition function one finds:

$$\langle\sigma\rangle^{\eta,\bar{\eta},\mathcal{J}} = K + G\left\langle\bar{\psi}\psi\right\rangle^{\eta,\bar{\eta},K}. \tag{1.155}$$

The result shown in Eq. (1.155) is the well known relation between the mean value of the auxiliary scalar and that one of the composite operator [6]. The source term explicitly appears. Minding the form of the partition function in Eq. (1.16) one can realize how the source term, being positive, plays the role of a bare mass for the fermion fields.

The relationship between the two point functions can also be calculated. These Green's functions are then related according to:

$$\begin{aligned}\left\langle\bar{\psi}\psi_1\ \bar{\psi}\psi_2\right\rangle^{\eta,\bar{\eta},K} &= -\frac{\delta_{21}}{G} + \frac{1}{G^2}K_1K_2 - \frac{K_1}{G^2}\langle\sigma_2\rangle_C^{\eta,\bar{\eta},\mathcal{J}} \\ &- \frac{K_2}{G^2}\langle\sigma_1\rangle_C^{\eta,\bar{\eta},\mathcal{J}} + \frac{1}{G^2}\langle\sigma_1\sigma_2\rangle^{\eta,\bar{\eta},\mathcal{J}}.\end{aligned} \tag{1.156}$$

All the detailed calculations can be found in the App. A.2.

Now some expressions are derived for the two other generating functionals and for the their own correlators.

From Eq. (1.151) one deduces:

$$W_f\left[\eta,\bar{\eta},K\right] = W_b\left[\eta,\bar{\eta},\mathcal{J}\right] - \int\frac{K^2}{2G}, \tag{1.157}$$

where clearly $Z_b = e^{W_b}$. Thus the propagator of the scalar theory is given by:

$$\frac{\delta^2 W_f}{\delta K_1\delta K_2} = -\frac{\delta_{12}}{G} + \frac{1}{G^2}\langle\sigma_1\,\sigma_2\rangle_C. \tag{1.158}$$

The effective action for the bosonized version is defined in a natural way as:

$$\Gamma_b[\psi_c,\bar{\psi}_c,\sigma_c] = -W_b\left[\eta,\bar{\eta},\mathcal{J}\right] + \int\mathcal{J}\sigma_c + \int\bar{\eta}\psi_c - \int\bar{\psi}_c\eta. \tag{1.159}$$

After some manipulations, all reported in the App. A.2, one finds:

$$\Gamma_f[\psi_c,\bar{\psi}_c,\bar{\psi}\psi_c] + \int\frac{G}{2}(\bar{\psi}\psi_c)^2 = \Gamma_b[\psi_c,\bar{\psi}_c,\sigma_c] - \int\frac{\sigma_c^2}{2G} + \int\sigma_c\,\bar{\psi}\psi_c. \tag{1.160}$$

Clearly $\bar{\psi}\psi_c$ and σ_c are not independent variables but are related according to the Eq. (1.155). A more fruitful relation is given by:

$$\frac{\delta\Gamma_f}{\delta\bar{\psi}\psi_c} = G\frac{\delta\Gamma_b}{\delta\sigma_c}. \tag{1.161}$$

Twice deriving this relation one finds that the second derivative of the two theories are related in the following way:

$$\left(\frac{\delta^2\Gamma_f}{\delta\bar{\psi}\psi_c\delta\bar{\psi}\psi_c}\right)^{-1} = G + G^2\left(\frac{\delta^2\Gamma_b}{\delta\sigma_c\delta\sigma_c}\right)^{-1}. \tag{1.162}$$

Finally the $1PI$ correlators of one composite and two elementary fields differ from the dressed Yukawian interaction simply by a proportionality factor. Indeed by deriving both sides of Eq. (1.161) one obtains:

$$\Gamma^f_{\psi\bar{\psi}\,(\bar{\psi}\psi)} = G\,\Gamma^b_{\psi\bar{\psi}\,\sigma}. \tag{1.163}$$

1.7.2 Perturbation theory of the GN model in the bosonized version

The first advantage provided by the Hubbard Stratonovich transformation is the following: The perturbartive expansion of the correlators of the GN model can be rephrased in a perturbative series for the bosonized version. The perturbative calculations for the composite operators are more simple if performed with the bosonization technique. After the shift:

$$\sigma \to \sqrt{G}\sigma, \tag{1.164}$$

and by defining:

$$G = g^2, \tag{1.165}$$

the partition function in Eq. (1.151) becomes:

$$\begin{aligned} Z_f[\eta,\bar{\eta},K] &= \mathcal{N}'\int\mathcal{D}\psi\mathcal{D}\bar{\psi}\int\mathcal{D}\sigma\,\exp\int\left[-\bar{\psi}(\partial\!\!\!/ + g\sigma)\psi - \frac{\sigma^2}{2} + \bar{\eta}\cdot\psi - \bar{\psi}\cdot\eta + \frac{K}{g}\sigma\right] \\ &\times \exp\left[-\int\frac{K^2}{2g^2}\right] \\ &= \mathcal{N}'e^{-\int\frac{J^2}{2}}Z_b\left[\eta,\bar{\eta},J\right], \end{aligned} \tag{1.166}$$

where $J = \frac{K}{g}$ was defined. According to the relation in Eq. (1.165) a term of order G^n becomes of order g^{2n} in the bosonized theory. Thus the pertubative scheme shown in Eq. (1.105) can be applied. Here the potential is $V = g\sigma\bar{\psi}\psi$ and the boson propagator is

simply $D_b(x,y) = \delta(x,y)$. All the results found from section 1.6.2 can be easily recovered. In particular the result of Eq. (1.98) finds an interesting interpretation in this language. The Hartree term looks like the direct contribution (or s channel) in a four point amplitude obtained by means of this "auxiliary" Yukawa theory. On the other hand the Fock contribution appears as the exchange term (or t channel). The relation found in Eq. (1.163), performing the appropriate rescaling becomes:

$$\Gamma^f_{\psi\bar{\psi}\,(\bar{\psi}\psi)} = g\,\Gamma^b_{\psi\bar{\psi}\,\sigma}. \tag{1.167}$$

The usual Feynmann rules can simply be applied in order to evaluate the one-loop contribution at the function $\Gamma^b_{\psi\bar{\psi}\,\sigma}$. The diagrams involved in the computation are shown in Fig. 1.18, while the amplitude turns out to be:

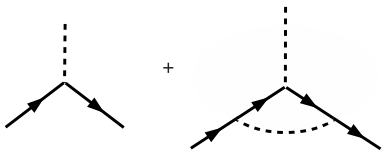

.

Figure 1.18: Diagrammatic representation of the $1PI$ $\Gamma_{\psi\bar{\psi}\sigma}$, calculated in Eq. (1.169) by means of the perturbative expansion in the bosonized version of the model.

$$\begin{aligned}\frac{\delta^3\Gamma_b}{\delta\psi_c(x)\delta\bar{\psi}_c(y)\delta\sigma_c(z)} &= g\delta(x,z)\delta(z,y) \\ &+ g^3 D(y,z)\cdot D(z,x)\delta(x,y)\end{aligned} \tag{1.168}$$

By applying the result in Eq. 1.167, the $1PI$ function of two elementary fields and one composite operator at the one-loop order can be written. This is:

$$\begin{aligned}\frac{\delta^3\Gamma_f}{\delta\psi_c(x)\delta\bar{\psi}_c(y)\delta\bar{\psi}\psi_c(z)} &= G\delta(x,z)\delta(z,y) \\ &+ G^2 D(y,z)\cdot D(z,x)\delta(x,y).\end{aligned} \tag{1.169}$$

These one-loop results will be very useful for further developments in the framework of the $1/N$ expansion.

1.7.3 Non renormalizability of the bosonized theory

A word of caution is necessary. Although the diagrammatic picture of the bosonized version could resemble that of a Yukawa theory the scaling and the pertubative divergences

of these two models are very different. It should be stressed that, at this stage, the bosonization technique was just a way of rephrasing the perturbative results, that were previously found. The perturbative classification of the divergences in the GN which is very far from that of the Yukawa theory must not be altered if all the quantities are expressed in the bosonized version. From the action S_b it can be deduced that the canonical dimension of the auxiliary field is equal to:

$$[\sigma]_0 = d/2. \tag{1.170}$$

Looking at the auxiliary propagator one obtains:

$$D_\sigma(p) = 1 = \frac{1}{p^0}, \tag{1.171}$$

consistently with Eq. (1.170). Again from the action S_b or from the relation in Eq. (1.165) the dimension of the coupling g can be calculated. This turns out to be:

$$[g]_0 = \frac{d-2}{2}. \tag{1.172}$$

Also in the bosonized version the model is perturbatively non-renormalizable.

CHAPTER 2

NON-PERTURBATIVE ANALYTICAL TECHNIQUES I: $D-S$ EQUATIONS AND LARGE N EXPANSION

The perturbative analysis has shown that self-interacting fermionic theories are not renormalizable. Thus the cut-off used in regularizing the theory cannot be sent to infinity, while keeping finite all other quantities. It represents the physical scale at which these models no longer apply. However this non-renormalizability statement must be restricted to the perturbative domain, i.e. when the bare parameters are closer to zero. Indeed, as will be seen, it is possible to find a region of the bare parameter space, far from the perturbative one, where the divergences can be removed by an appropriate tuning of the couplings. This implies a different connection from the usual one between the bare parameters and the cut-off scale.

Originally the first analytical tools used for studying the non-perturbative behaviour of fermion theories were the Dyson-Schwinger (DS) equations [42]. The generation of a fermion mass via a non trivial critical value of the Fermi constant was one of the results of the NJL analysis and it was achieved by means of the DS method [6]. Therefore the last one is introduced in this chapter in order to present the NJL results and the non-perturbative aspects of the χSB.

However, generally the DS equations cannot be solved exactly and consistent approximations are needed. A parameter expansion could be introduced making the systematic estimation of errors possible [26].

Anyway the usual perturbative expansion in the coupling constants, besides from be-

ing a simple calculation technique, also provides the scheme for establishing when the divergences arise in a theory and how to heal them. Following another type of expansion one can establish a new systematization of renormalization which is far from the perturbative region. The $1/N$ expansion can be used for this objective and will be introduced later in the chapter.

2.1 Dyson Schwinger equations for the GN model

The Dyson-Schwinger equations are a system of algebraic relations between the correlators of a theory. They can be seen as the quantum equations of motion, extending the variational principle for the classical degrees of freedom to their the quantum counterparts. Similar equations exist for statistical systems and are often applied to non equilibrium problems [43],[44]. In the construction of the DS equations the exact Green's functions of the theory are involved; however analytical approximate solutions can be found with the introduction of a small parameter expansion. As an example, if a Green's function is written in a power series of the coupling constant, at each order in the expansion, the corresponding perturbative approximation of the correlator will be found as a solution of the DS equations. On the other hand, by resumming the Feynmann diagrams up to a certain order in the coupling constant an approximate solution of the DS equation is obtained. A certain class of diagrams whose resummation satisfy the DS equations is called Dyson series which can be found by grouping diagrams in a different way from the perturbative prescription. In the following a Dyson series whose resummation gives the first order of the $1/N$ expansion, also called Hartree approximation [34], is presented. The DS equations for both elementary and composite operators are then recovered. Finally, by using the Hartree approximation, the NJL result providing the generation of a fermion mass and a relation between the fermion mass and the mass of the composite particle is found.

2.1.1 Dyson series

Now, by following the perturbative approach, an infinite class of diagrams is resummed. However the validity of this result holds beyond the perturbative hypothesis. What will be found is a truncation of the DS equations called the Hartree approximation [31].

Indeed the rule for selecting this particular class of diagrams is entirely justified in the framework of the $1/N$ expansion. This procedure was first introduced by t'Hooft in [45]. If one supposes that the coupling G is of $\mathcal{O}(1/N)$ then every Feynmann diagram will have a weight in powers of N given by the number of couplings G and the number of closed loops involved in its construction. A closed loop is a fermionic loop in which the product of propagators is traced over. Each of these loops gives a contribution of order N. As an example, the diagrams obtained in Fig. 1.13 for the corrected inverse fermionic propagator can be considered. The bare inverse propagator is of order N^0 as well as the first one loop diagram in the picture, since it is formed by a closed flavour loop and a fermionic vertex G. The last diagram instead has a weight of order $1/N$, since the propagator is not traced over, thus at the leading order in the $1/N$ expansion it can be neglected, while it has to be retained at the next order. A second example is given by the one loop contributions to the four point fermionic function shown in Fig. 1.14. The bare vertices are of order $1/N$, as well as the one loop contributions "a" and "e". The other diagrams are of order $1/N^2$ and must be neglected at the leading order. As it should be clear the $1/N$ expansion collects the diagrams in a different way from those given by the usual perturbative expansion. Indeed the bare functions and their one loop corrections are both included in the Hartree term.

The Dyson series giving the Hartree contribution to the correlators of the Gross Neveu model are now summed. In Fig. 2.1 the diagrams at $\mathcal{O}(G^2)$ giving the Hartree contribution to the two point $1PI$ function are represented. Since the $1PI$ function $\Gamma_{\psi\bar{\psi}}$ is nothing

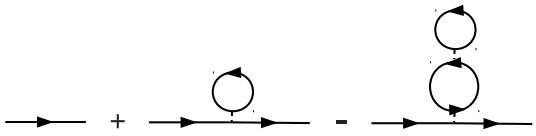

.

Figure 2.1: The Hartree contributions to the two point $1PI$ fermion function are represented up to two loop order. Such terms are often called tadpole diagrams.

but the inverse matrix of the fermionic dressed propagator $\langle \psi\, \bar{\psi} \rangle = \Delta$, the Hartree contribution at the one-loop order can be written as:

$$\Delta^{-1}_{ab} = D^{-1}_{ab} + G\, \delta_{ab} \mathrm{tr}\,(D) + \mathcal{O}\left(G^2\right), \tag{2.1}$$

where a, b are generic spatial and internal indices. On the other hand the connected two

point function satisfies at the same order:

$$\Delta = D - G\, D\mathrm{tr}\,(D)\,\Delta + \mathcal{O}\left(G^2\right), \tag{2.2}$$

where now all indices are understood. Tracing over all the internal indices one finds:

$$\mathrm{tr}\,(\Delta) = \mathrm{tr}\,(D) - G\,\mathrm{tr}\,(D\Delta)\,\mathrm{tr}\,(D) + \mathcal{O}\left(G^2\right). \tag{2.3}$$

Thus at every order in the bubble resummation, thanks to the Eq. (2.3), the series of terms in Eq. (2.2) can be replaced by a trace over the dressed propagator. The error belonging to the next order in G. So doing the following equation is obtained:

$$\begin{aligned} \Delta^{-1} &= D^{-1} + G\,\mathrm{tr}\,(D) - G^2\,\mathrm{tr}\,(D)\,\mathrm{tr}\,(D\Delta) + \mathcal{O}\left(G_\Lambda^3\right) \\ &= D^{-1} + G\,\mathrm{tr}\,(\Delta)\,. \end{aligned} \tag{2.4}$$

The second line is true at every order in the perturbation theory and represents the sum of the series.

The Dyson series for the mean value of the composite operator $\bar{\psi}\psi$ can be immediately calculated. Looking at the diagrams in Fig. 1.15 it is possible to note how the first two terms are Hartree contributions. By performing the series resummation with the help of Eq. (2.3), it is found:

$$\left\langle \bar{\psi}\psi \right\rangle = \mathrm{tr}\,(\Delta)\,. \tag{2.5}$$

Using Eq. (2.4) and Eq. (2.5) the fermionic propagator and the vacuum expectation value of the composite field are related according to:

$$\Delta^{-1} = D^{-1} + G\left\langle \bar{\psi}\psi \right\rangle. \tag{2.6}$$

Now the analysis of other series can be treated. For example, the $1PI$ 4-point function, that has been calculated at one loop level in Eq. (1.101), is considered. The Hartree contributions to it are shown in Fig. 2.2 (b). First of all it should be observed that in such a series all the diagrams group in an s channel term and in a t channel one. Indeed the four point function can be organized as:

$$\begin{aligned} \frac{\delta^4\Gamma_f}{\delta\psi_a(x)\delta\bar{\psi}_b(y)\delta\psi_c(z)\delta\bar{\psi}_d(w)} &= \mathcal{G}(x,y)\delta(y,z)\delta(z,w)\delta_{ab}\delta_{cd} \\ &- \mathcal{G}(y,z)\delta(x,y)\delta(z,w)\delta_{ad}\delta_{bc}, \end{aligned} \tag{2.7}$$

where $\mathcal{G}(x,y)$ is the same function for both these channels. Thus the series for the s and the t contributions becomes a series for the only $\mathcal{G}(x,y)$ function. First of all, one supposes that only the bubble chains diagrams give a contribution to the series. As a consequence one found the expression:

$$\begin{aligned}
\mathcal{G}(x,y) &= G\delta(x,y) - G^2 \mathrm{tr}\left(D(x,y)D(y,x)\right) \\
&+ G^3 \int_z \mathrm{tr}\left(D(x,z)D(z,x)\right) \mathrm{tr}\left(D(z,y)D(y,z)\right) + \mathcal{O}\left(G^4\right) \\
&= G\delta(x,y) - G \int_z \mathrm{tr}\left(D(x,z)D(z,x)\right) \\
&\times \left[G\delta(z,y) - G^2 \mathrm{tr}\left(D(z,y)D(y,z)\right)\right] + \mathcal{O}\left(G^4\right) \\
&= G\delta(x,y) - G \int_z \mathrm{tr}\left(D(x,z)D(z,x)\right) \mathcal{G}(z,y) \qquad (2.8)
\end{aligned}$$

In order to include all the other corrections to the fermionic propagator (the tadpole contributions) it should be observed that at every order in G the dressed propagator can be replaced for the bare one in Eq. 2.8. Finally one gets:

$$\mathcal{G}(x,y) = G\delta(x,y) - G \int_z \mathrm{tr}\left(\Delta(x,z)\Delta(z,x)\right) \mathcal{G}(z,y). \qquad (2.9)$$

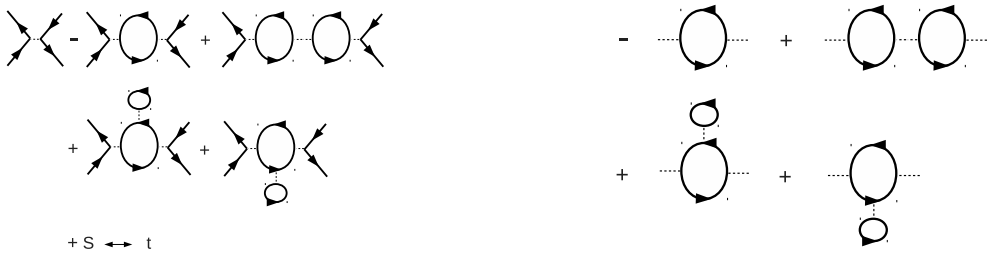

a b

Figure 2.2: (a) The Hartree type contributions to the s-channel of the four point $1PI$ fermion vertex are shown. In this approximation both tadpole and bubble diagrams are included. The t-channel contributions can be immediately worked out by a simple reflection, while all the u-channel contributions are discarded. (b) The Hartree type contributions to the connected correlator of two composite fields.

The result that has been found has also an interesting interpretation. The Hartree diagrams contributing to the connected Green's function of two composite operators $G^{(0;0;2)}_{f,C}(x,y)$, calculated at one loop level in Eq. (1.104), are shown in Fig. 2.2 (b). Looking at the diagrams in Fig. 2.2 (a) one finds that in the Hartree approximation the function

$G^{(0;0;2)}_{f,C}(x,y)$ can be related to the function $\mathcal{G}(x,y)$ defined in Eq. (2.7). This implies the equation:

$$\mathcal{G}(x,y) = G\delta(x,y) - G^2\, G^{(0;0;2)}_{f,C}(x,y), \tag{2.10}$$

which is nothing but the same relation found in Eq. (1.158). The function $\mathcal{G}(x,y)$ turns out to be the propagator of the auxiliary scalar in the bosonized version. An extension of the relation in Eq. (1.98) to the dressed functions was found. At the leading order in the large N expansion the four point fermionic function can be rewritten as the sum of the s and t channel contributions of a particular Yukawa theory. Now however the propagator in the amplitude is the function $\mathcal{G}(x,y)$ which includes all the bubbles resummation. It is often called improved propagator, since it is a correction of the trivial propagator of the auxiliary scalar [12].

Some important properties of the GN will soon be investigated by means of the DS equations. Before this the DS equations of the model will be recovered in a more rigorous procedure.

2.1.2 Dyson-Schwinger equations for elementary fields

The Dyson-Schwinger identities are derived starting from the functional identity for the partition function found in Eq. (1.96). By applying a functional operator to the partition function of elementary fermionic fields one gets:

$$\begin{aligned}
\frac{\delta S_f}{\delta\psi}\left[\frac{\delta}{\delta\bar\eta},\frac{\delta}{\delta\eta}\right] Z_f[\eta,\bar\eta] &= \int \mathcal{D}\psi\mathcal{D}\bar\psi\, \frac{\delta S_f}{\delta\psi}\left[\psi,\bar\psi\right] \\
&\times \exp\left[-S_f[\psi,\bar\psi] + \int\bar\eta\psi - \int\bar\psi\eta\right] \\
&= -\, e^{\left[-S_f[\psi,\bar\psi]+\int\bar\eta\psi-\int\bar\psi\eta\right]}\Big|_{\text{bound.}} \\
&- \int \mathcal{D}\psi\mathcal{D}\bar\psi\,\bar\eta\, e^{\left[-S_f[\psi,\bar\psi]+\int\bar\eta\psi-\int\bar\psi\eta\right]} \\
&= -\bar\eta\, Z_f[\eta,\bar\eta]
\end{aligned} \tag{2.11}$$

where an integration by parts was performed minding that the fermion fields vanish at the boundaries. Similarly, by applying the same arguments to the first derivative in $\bar\psi$ one finds the equation:

$$\left(\frac{\delta S_f}{\delta\bar\psi}\left[\frac{\delta}{\delta\bar\eta},\frac{\delta}{\delta\eta}\right] + \eta\right) Z_f[\eta,\bar\eta] = 0. \tag{2.12}$$

Now a generic functional $F[\eta,\bar{\eta}]$ is considered. The partition function Z_f can always be expressed in terms of the functional W_f as $Z_f = e^{W_f}$. For a single application of the derivative $\delta/\delta\eta$ one finds:

$$\exp\left(-W_f[\eta,\bar{\eta}]\right)\left(\frac{\delta}{\delta\eta}\right)\exp W_f[\eta,\bar{\eta}]F[\eta,\bar{\eta}] \;=\; \left(\frac{\delta}{\delta\eta}+\frac{\delta W[\eta,\bar{\eta}]}{\delta\eta}\right)F[\eta,\bar{\eta}]. \quad (2.13)$$

So that the DS equations (see Eqs.(2.11),(2.12)) can be rewritten as:

$$\left(e^{-W_f[\eta,\bar{\eta}]}\frac{\delta S_f}{\delta\psi}\left[\frac{\delta}{\delta\bar{\eta}},\frac{\delta}{\delta\eta}\right]e^{W_f[\eta,\bar{\eta}]}+\bar{\eta}\right)F[\eta,\bar{\eta}] \;=\; 0, \quad (2.14)$$

$$\left(e^{-W_f[\eta,\bar{\eta}]}\frac{\delta S_f}{\delta\bar{\psi}}\left[\frac{\delta}{\delta\bar{\eta}},\frac{\delta}{\delta\eta}\right]e^{W_f[\eta,\bar{\eta}]}+\eta\right)F[\eta,\bar{\eta}] \;=\; 0, \quad (2.15)$$

Thus applying the result found in Eq. (2.13) the DS equations for the generator of connected Green's functions W_f are immediately obtained. They are:

$$\frac{\delta S_f}{\delta\psi}\left[\frac{\delta}{\delta\bar{\eta}}+\frac{\delta W_f}{\delta\bar{\eta}},\frac{\delta}{\delta\eta}+\frac{\delta W_f}{\delta\eta}\right]+\bar{\eta}=0, \quad (2.16)$$

$$\frac{\delta S_f}{\delta\bar{\psi}}\left[\frac{\delta}{\delta\bar{\eta}}+\frac{\delta W_f}{\delta\bar{\eta}},\frac{\delta}{\delta\eta}+\frac{\delta W_f}{\delta\eta}\right]+\eta=0. \quad (2.17)$$

The DS equations for the effective action are quite involved. Using Eq. (1.22) and Eq. (1.23) the derivatives with respect to the sources can be expressed in terms of derivatives with respect to the classical fields. One finds:

$$\begin{aligned}\frac{\delta}{\delta\eta} &= \int\frac{\delta\psi_c}{\delta\eta}\frac{\delta}{\delta\psi_c}+\int\frac{\delta\bar{\psi}_c}{\delta\eta}\frac{\delta}{\delta\bar{\psi}_c}\\ &= \int\frac{\delta^2W_f}{\delta\eta\delta\bar{\eta}}\frac{\delta}{\delta\psi_c}+\int\frac{\delta^2W_f}{\delta\eta\delta\eta}\frac{\delta}{\delta\bar{\psi}_c}, \quad (2.18)\\ \frac{\delta}{\delta\bar{\eta}} &= \int\frac{\delta\psi_c}{\delta\bar{\eta}}\frac{\delta}{\delta\psi_c}+\int\frac{\delta\bar{\psi}_c}{\delta\bar{\eta}}\frac{\delta}{\delta\bar{\psi}_c}\\ &= \int\frac{\delta^2W_f}{\delta\bar{\eta}\delta\bar{\eta}}\frac{\delta}{\delta\psi_c}+\int\frac{\delta^2W_f}{\delta\bar{\eta}\delta\eta}\frac{\delta}{\delta\bar{\psi}_c}, \quad (2.19)\end{aligned}$$

so that Γ_f satisfies the following equation:

$$\begin{aligned}\frac{\delta\Gamma_f}{\delta\psi_c} &= \frac{\delta S}{\delta\psi}\left[\psi_c+\int\frac{\delta^2W_f}{\delta\bar{\eta}\delta\bar{\eta}}\frac{\delta}{\delta\psi_c}+\int\frac{\delta^2W_f}{\delta\bar{\eta}\delta\eta}\frac{\delta}{\delta\bar{\psi}_c},\right.\\ &\qquad \left.\bar{\psi}_c+\int\frac{\delta^2W_f}{\delta\eta\delta\bar{\eta}}\frac{\delta}{\delta\psi_c}+\int\frac{\delta^2W_f}{\delta\eta\delta\eta}\frac{\delta}{\delta\bar{\psi}_c}\right]. \quad (2.20)\end{aligned}$$

Here the second derivative of the W_f functional must be expressed in terms of the derivatives of the Γ_f, according to the Eqs. (1.36). As an application of these results the DS

equations for the connected and $1PI$ Green's functions for a fermionic theory, with a bare mass term and a quartic coupling in the action, are calculated. All computations are reported in the App. B.2. The physical request that odd Green's functions must vanish is motivated by the results in Sec.1.4.1. Under certain conditions if the action possesses any symmetry this cannot be violated by the quantum fluctuations. This assumption also implies that $\langle\psi_c\rangle = \langle\bar{\psi}_c\rangle = 0$, in order to preserve the Lorentz and the $U(N)$ invariance. The two point $1PI$ function satisfies the equation shown in Fig. 2.3. The diagrams represent the equation for a generic two point fermion correlator in which the classical fields are collected in the multiplet $\theta = \left(\psi_c, \bar{\psi}_c\right)$. Two types of diagrams contribute to

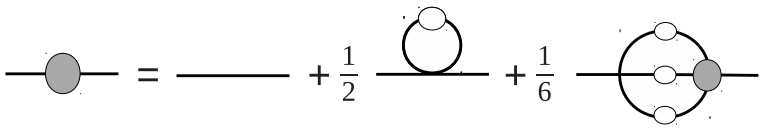

.

Figure 2.3: The DS equation for the $1PI$ fermion two point function. The exact inverse propagator is given by the sum of a tree level inverse propagator, of a one-loop Hartree-Fock diagram with a four fermion bare vertex and of a two-loop diagram involving the exact effective interaction. All loops involve the exact connected two point functions

this equation: the tadpole diagram which is the first one appearing in the figure and the saturn diagram which is the second. In the Hartree approximation the saturn diagram can be discarded. In order to trust this assumption one can expand each function in the following power series:

$$\Gamma_f^{(m;n)} = \sum_{p=0}^{\infty} \frac{1}{N^p} \Gamma_{f,p}^{(m;n)}, \tag{2.21}$$

and identify the terms of the same order. At the leading order in this expansion the same result shown in Eq. (2.4) is recovered for the two point $1PI$ fermion function.

Similar results hold also for the four point $1PI$ function. After performing the calculations one finds (see App. B.2) the result which is diagrammatically shown in Fig. 2.4. Once again all the odd contributions have been discarded. Moreover, in this case, the contribution given by the six point function was removed. One can verify that in the Hartree approximation this equation reduces to the results found in Eqs. (2.7),(2.9).

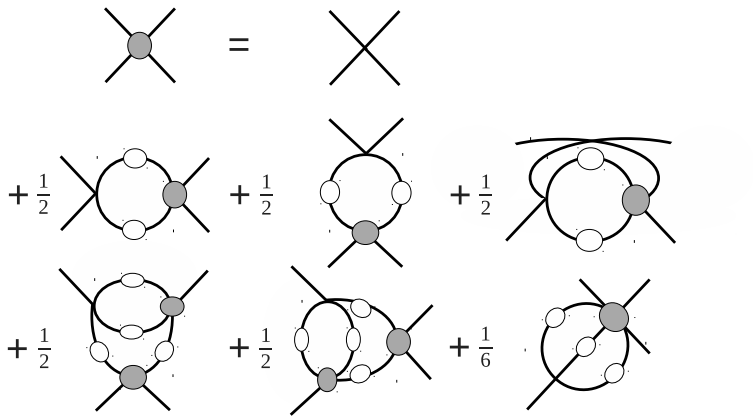

.

Figure 2.4: The DS equation for the $1PI$ fermion four point function. The r.h.s. of the equation involve: the bare fermion vertex, the three one-loop Hartree-Fock terms, giving respectively the s,t and u contributions, and the two-loop terms, made of a the bare vertex and two dressed four point functions. The term involving the six point correlator is descarded.

2.1.3 The NJL result

In this section the Nambu - Jona-Lasinio (NJL) mechanism for the generation of a fermion mass, by means of the quantum fluctuations, is recovered . Actually, this result was originally found by the authors for a model in $d = 4$ dimensions with a continuous chiral symmetry [6]. However, many of their arguments were also applied to the GN model. For the moment, only the system in four dimensions is considered. Starting with the Eq. (2.4) and writing the result in the momentum space one finds:

$$\begin{aligned}\Delta^{-1}_{\alpha\beta,ab}(p) &= D^{-1}_{\alpha\beta,ab}(p) + G\delta_{\alpha\beta}\delta_{ab}\int \frac{d^4p}{(2\pi)^4}\,\mathrm{tr}D(p), \\ &= \left(i\not{p}_{\alpha\beta} + m_B\delta_{\alpha\beta}\right)\delta_{ab} + G\delta_{\alpha\beta}\delta_{ab}\int \frac{d^4p}{(2\pi)^4}\,\mathrm{tr}D(p) \qquad (2.22)\end{aligned}$$

where the Greek letters stand for the Dirac indices while the Latin ones are used for the internal flavour space. The mass m_B must be removed in order to preserve the symmetry of the model. This procedure is usually called the chiral limit. From the perturbative analysis it is known that the corrections to the propagator are momentum independent. Since a similar loop appears in the DS equation the following ansatz is assumed:

$$\Delta^{-1}_{\alpha\beta,ab}(p) = \left(i\not{p}_{\alpha\beta} + m\delta_{\alpha\beta}\right)\delta_{ab} \qquad (2.23)$$

The equation for the inverse propagator becomes a self consistent equation for the fermionic mass. One finds:

$$m = m_B + G\int \frac{d^4p}{(2\pi)^4}\mathrm{tr}\left(\frac{1}{i\not{p}+m}\right). \tag{2.24}$$

The integration can be explicitly performed by means of a sharp momentum cut-off Λ. Thus the gap equation for the mass turns out to be:

$$m = m_B + NG\,\frac{m}{4\pi^2}\left[\Lambda^2 - m^2\ln\left(1+\frac{\Lambda^2}{m^2}\right)\right]. \tag{2.25}$$

Setting $m_B = 0$ (chiral limit), one obtains:

$$\frac{m^2}{\Lambda^2}\ln\left(1+\frac{\Lambda^2}{m^2}\right) = 1 - \frac{4\pi^2}{\Lambda^2 N\,G}. \tag{2.26}$$

Since the first member of the equation is always non-negative a non-trivial solution for the mass m exists only if:

$$G \geq G_c = \frac{4\pi^2}{\Lambda^2 N}. \tag{2.27}$$

The generation of a fermionic mass and the related χSB are triggered by a critical value of the coupling constant. This result is far from being an accident. Indeed the occurrence of a symmetry breaking has a clear interpretation in the statistical language. The critical value of the coupling is related to the occurrence of a phase-transition in the statistical system. Thus the coupling G must be related to the temperature of the system while the fermion mass should correspond to the order parameter of the transition. All these aspects will be clarified in the following.

The Eq. (2.9) involving the auxiliary field of the bosonized model is now considered. For $d = 4$, in Fourier space, it can be written as:

$$\mathcal{G}(q) = G - G\int \frac{d^4p}{(2\pi)^4}\mathrm{tr}\left(\Delta(p)\cdot\Delta(p+q)\right)\mathcal{G}(q). \tag{2.28}$$

The previous result can be immediately rewritten in terms of the inverse propagator as:

$$\mathcal{G}(q)^{-1} = 1/G + \Pi(q), \tag{2.29}$$

where:

$$\Pi(q) = \int \frac{d^4p}{(2\pi)^4} \mathrm{tr}\left(\frac{1}{i\not{p}+m}\cdot\frac{1}{i\left(\not{p}+\not{q}\right)+m}\right). \tag{2.30}$$

The evaluation of this function is quite involved. All the calculations can be found in the App. C.3. Following the NJL procedure the function $\mathcal{G}(q)$ calculated when $G = G_c$ is reported. It is found:

$$\begin{aligned}\mathcal{G}(q)^{-1} &= \frac{1}{8\pi^2}\left(q^2+4m^2\right)\left[\log\left(\frac{\Lambda^2}{m^2}\right)\right. \\ &- \left.\frac{\sqrt{q^2+4m^2}}{q}\log\left(\frac{1+\frac{q}{\sqrt{q^2+4m^2}}}{1-\frac{q}{\sqrt{q^2+4m^2}}}\right)-3\right].\end{aligned} \tag{2.31}$$

This expression shows that the propagator has a pole in $q^2 = -4m^2$. Minding that the Euclidean version of the model is used, one finds that in the Hartree approximation the collective bosonic excitation possess the mass:

$$M = 2m. \tag{2.32}$$

For a long time this result was considered as evidence that a purely fermionic model is more predictive than a model with an explicit scalar. However it will be seen how a fixed ratio between the boson and the fermion masses can be found also in the usual Yukawa theory.

Another important observation concerns the presence of the logarithmic divergence in Eq. (2.31). Since the dimension is fixed at $d = 4$ the Π function in Eq. (2.30) has both quadratic and logarithmic divergences. However while the leading divergence was canceled by the use of the gap equation it was not possible to remove the sub-leading one. At the critical point when $m = 0$ one obtains:

$$\mathcal{G}(q) = \frac{4\pi^2}{q^2 \ln\left(\frac{\Lambda}{q}\right)}, \tag{2.33}$$

Thus the theory remains effective. The scaling of the function is very different from the perturbative case. In [15] Tamvakis and Guralnik, with the help of the bosonization technique introduced by Bender et al. [14], have shown that the divergences of self-interacting fermionic theories in four dimension are equal to those of certain Yukawa

models in the perturbative region. The presence of this logarithm was related to the triviality of the Yukawa theory. The renormalization of the bosonized version of the theory can be performed at every order in the perturbative $1/N$ expansion by adding a finite number of counter-terms in the Lagrangian. The number of renormalization conditions are equal for both the bosonized GN model and the Yukawa theory. More on this point later.

2.1.4 Dyson-Schwinger equations for theories with composite operators

A complete study of the phenomenon of χSB involves the mean value of the $\bar{\psi}\psi$ condensate. Also the two point function of this composite operator plays an important role. Thus the DS equations satisfied by the Green's functions of composite operators will be explicitly derived. It will be seen how the bosonization technique is a necessary tool in order to establish these relations. First of all by applying the same arguments used in the previous sections and by following the same passages the DS equations for a theory involving fermionic and bosonic degrees of freedom are given by:

$$\left(\frac{\delta S_{fb}}{\delta\psi}\left[\frac{\delta}{\delta\bar{\eta}},\frac{\delta}{\delta\eta},\frac{\delta}{\delta J}\right]+\bar{\eta}\right)Z_{fb}[\eta,\bar{\eta},J]=0, \tag{2.34}$$

$$\left(\frac{\delta S_{fb}}{\delta\bar{\psi}}\left[\frac{\delta}{\delta\bar{\eta}},\frac{\delta}{\delta\eta},\frac{\delta}{\delta J}\right]+\eta\right)Z_{fb}[\eta,\bar{\eta},J]=0, \tag{2.35}$$

$$\left(\frac{\delta S_{fb}}{\delta\phi}\left[\frac{\delta}{\delta\bar{\eta}},\frac{\delta}{\delta\eta},\frac{\delta}{\delta J}\right]-J\right)Z_{fb}[\eta,\bar{\eta},J]=0. \tag{2.36}$$

The partition function of the elementary and composite fermionic operators of the GN model can be rewritten in a bosonized version according to Eq. (1.166). In principle the results in Eqs. (2.34),(2.35),(2.36) can be applied also to the bosonized version of this model. Since these DS equations are indeed satisfied by the functional Z_b.

By following the same arguments applied in Eq. (2.13) one finds:

$$\begin{aligned} e^{-\int\frac{J^2}{2}}\left(\frac{\delta}{\delta J}\right)e^{\int\frac{J^2}{2}}Z_f &= \left(\frac{\delta}{\delta J}+J\right)Z_f \\ &= \mathcal{N}'e^{-\int\frac{J^2}{2}}\left(\frac{\delta}{\delta J}\right)Z_b. \end{aligned} \tag{2.37}$$

Thus applying the first derivatives of the bosonized action S_b to the generating functional

Z_f one derives:

$$\left(\frac{\delta S_b}{\delta\psi}\left[\frac{\delta}{\delta\bar{\eta}},\frac{\delta}{\delta\eta},\frac{\delta}{\delta J}+J\right]+\bar{\eta}\right)Z_f[\eta,\bar{\eta},K]=0, \tag{2.38}$$

$$\left(\frac{\delta S_b}{\delta\bar{\psi}}\left[\frac{\delta}{\delta\bar{\eta}},\frac{\delta}{\delta\eta},\frac{\delta}{\delta J}+J\right]+\eta\right)Z_f[\eta,\bar{\eta},K]=0, \tag{2.39}$$

$$\left(\frac{\delta S_b}{\delta\phi}\left[\frac{\delta}{\delta\bar{\eta}},\frac{\delta}{\delta\eta},\frac{\delta}{\delta J}+J\right]-J\right)Z_f[\eta,\bar{\eta},K]=0. \tag{2.40}$$

These are the DS equations for correlators of elementary and composite functions. The DS equations for the connected Green's functions can also be calculated. They turn out to be:

$$\frac{\delta S_b}{\delta\psi}\left[\frac{\delta}{\delta\bar{\eta}}+\frac{\delta W_f}{\delta\bar{\eta}},\frac{\delta}{\delta\eta}+\frac{\delta W_f}{\delta\eta},\frac{\delta}{\delta J}+\frac{\delta W_f}{\delta J}+J\right]+\bar{\eta} = 0, \tag{2.41}$$

$$\frac{\delta S_b}{\delta\bar{\psi}}\left[\frac{\delta}{\delta\bar{\eta}}+\frac{\delta W_f}{\delta\bar{\eta}},\frac{\delta}{\delta\eta}+\frac{\delta W_f}{\delta\eta},\frac{\delta}{\delta J}+\frac{\delta W_f}{\delta J}+J\right]+\eta = 0, \tag{2.42}$$

$$\frac{\delta S_b}{\delta\phi}\left[\frac{\delta}{\delta\bar{\eta}}+\frac{\delta W_f}{\delta\bar{\eta}},\frac{\delta}{\delta\eta}+\frac{\delta W_f}{\delta\eta},\frac{\delta}{\delta J}+\frac{\delta W_f}{\delta J}+J\right]-J = 0. \tag{2.43}$$

By using Eq. (2.43) the equations for the one and the two point functions of composite scalars can be calculated. After some brief manipulations and the appropriate rescalings the equation becomes:

$$\frac{\delta W_f}{\delta K}-\mathrm{tr}\left(\frac{\delta^2 W_f}{\delta\eta\delta\bar{\eta}}\right)-\mathrm{tr}\left(\frac{\delta W_f}{\delta\eta}\frac{\delta W_f}{\delta\bar{\eta}}\right)=0, \tag{2.44}$$

which can simply be rewritten as:

$$\left\langle\bar{\psi}\psi\right\rangle=\bar{\psi}_c\cdot\psi_c+\mathrm{tr}\left(\Delta\right). \tag{2.45}$$

The diagrammatic representation of this result is shown in Fig. 2.5. It is an extension of the Eq. (1.85) to the interacting theory but it also represents the same result found in Eq. (2.5). In the present case a non-vanishing expectation value is induced by a non-trivial propagator.

It is possible to look at this result with the help of Eq. (2.42). Performing some straight calculations one finds:

$$D^{-1}\frac{\delta W_f}{\delta\bar{\eta}}+G\frac{\delta^2 W_f}{\delta K\delta\bar{\eta}}+K\frac{\delta W_f}{\delta\bar{\eta}}+G\frac{\delta W_f}{\delta K}\frac{\delta W_f}{\delta\bar{\eta}}=\eta. \tag{2.46}$$

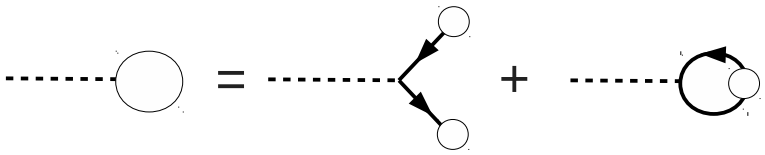

.

Figure 2.5: The DS equation for the expectation value of the $\bar{\psi}\psi$ composite field. The first contribution in the r.h.s. involves the mean values of the elementary fields. It must vanish in order to preserve the Lorentz invariance of the theory. The second one is a one-loop tadpole contribution including the dressed fermion propagator.

Most people prefer working with the directly with the DS equations for the bosonized theory. By deriving the Eq. (2.35) and setting to zero all the external sources and the mean values of the elementary fields one obtains the DS equation for the improved propagator. This is:

$$\Delta = D - D\,g\,\langle\sigma\rangle\,\Delta - D\,g\,\frac{\delta^3 W_b}{\delta\eta\delta\bar{\eta}\delta J}. \tag{2.47}$$

The result is represented in Fig. 2.6. The last term of the Eq. (2.47) vanishes in the

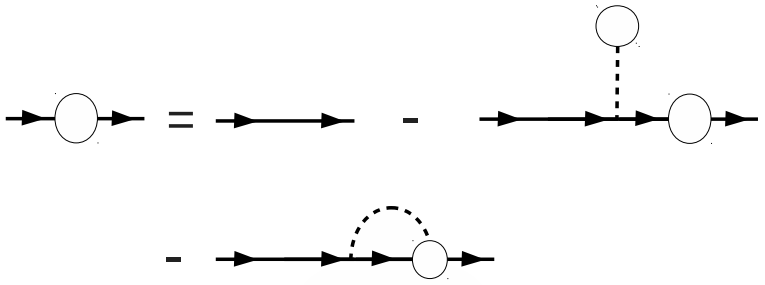

.

Figure 2.6: The DS equation for the dressed fermion propagator. Apart from the tree level term two other diagrams appear in the r.h.s of the equation. The first one involve the auxiliary scalar expectation value. It suggest a relationship between the generation of a fermion mass and fermion condensate.

ladder approximation, the first one is nothing but the same tadpole contribution shown in Eq. (2.3). Indeed once the classical value of the scalar field, given by Eq. (2.45) through Eq. (1.155), is replaced in Eq. (2.47), where $\bar{\psi}_c = \psi_c = 0$, the self-consistent gap equation for the fermionic propagator is recovered. In the ladder (Hartree) approximation the fermionic mass generation is immediately related to a non-zero fermionic condensate in a similar way as that theorized for superconductors [46]. Finally the correlator of two

auxialary fields is calculated. Deriving Eq. (2.36), with respect to the source J, one obtains:

$$\frac{\delta^2 W_b}{\delta J \delta J} = g\,\mathrm{tr}\left(\frac{\delta^3 W_b}{\delta J \delta\eta \delta\bar{\eta}}\right) + g\,\mathrm{tr}\left(\frac{\delta W_f}{\delta\eta}\frac{\delta^2 W_f}{\delta J\delta\bar{\eta}}\right) + g\,\mathrm{tr}\left(\frac{\delta^2 W_f}{\delta J\delta\eta}\frac{\delta W_f}{\delta\bar{\eta}}\right). \tag{2.48}$$

Thus by setting $\psi_c = \bar{\psi}_c = 0$ it is immediately found:

$$G^{(0;0;2)}_{f,C}(x,y) \;=\; g\,\mathrm{tr}\,G^{(1;1;1)}_{f,C}(x;x;y). \tag{2.49}$$

2.2 Large N expansion

The large N technique has been the most fruitful method applied for investigating the non-perturbative aspects of the self-interacting fermionic theories. It has shown how the Dyson-Schwinger equations can also be treated by means of a certain expansion, however, in principle, there is no natural small parameter which could be used. Moreover, relying on the validity of expansion it could become a bit cumbersome. For example, the idea that the impact of the quartic self-interaction $\frac{G}{2}(\bar{\psi}\psi)^2$ can be replaced with the effective term $G\left\langle\bar{\psi}\psi\right\rangle\bar{\psi}\psi - \frac{G}{2}\left\langle\bar{\psi}\psi\right\rangle^2$ is justified only if the fluctuations of the composite field $\bar{\psi}\psi$ are much smaller then those of the fermionic field itself [47]. This cannot be expected a priori from the DS analysis. Instead the large N expansion, formulated in terms of the bosonization tool, provides a solution to this problem in the spirit of the central limit theorem. When the flavour number N is large, an $U(N)$ scalar as the composite field $\bar{\psi}\psi$ will be a sum of many terms and therefore have small fluctuations from its mean value. In this sense, the bosonization technique is just a way of rewriting the theory in terms of the collective degrees of freedom, in such a way that the main contribution to the partition function is given by the mean value $\left\langle\bar{\psi}\psi\right\rangle$. For this reason the leading order of the mean field expansion, around this collective excitation, is also called Hartree contribution [31]. In the following section the large N techniques for the study of the Gross-Neveu model are presented. The results found by means of the DS equations are recovered and extended. First of all some of the usual bosonization tools will be introduced, then by performing the $1/N$ expansion the NJL result, found at $d = 4$, will be extended to $2 \leq d \leq 4$. With the help of the large N techniques a systematic analysis of the divergences of the model can also be provided; the theory turns out to be renormalizable at $2 \leq d < 4$ [19],[22],[23].

However, thanks to the systematic nature of the $1/N$ tool, the corrections to the leading order can also be computed. How this can be done will also be illustrated.

2.2.1 Other bosonization tecniques

The simplest bosonization technique is the Hubbard-Stratonovich transformation. It has also been introduced in the previous chapter. By using the result shown in Eq. (1.151) and following the relation between the mean value of the auxiliary scalar and that of the composite operator $\bar{\psi}\psi$, found in Eq. (1.155), when the source term has been switched off, one can replace:

$$\frac{G}{2}(\bar{\psi}\psi)^2 \to G\left\langle\bar{\psi}\psi\right\rangle\bar{\psi}\psi - \frac{G}{2}\left\langle\bar{\psi}\psi\right\rangle^2. \tag{2.50}$$

This position is justified when the fluctuations of the field σ can be discarded.

However the Hubbard-Stratonovich trick requires a quadratic interaction in powers of $\bar{\psi}\psi$. In order to evaluate the impact of the higher powers of the composite field in the potential another method is required. Thus the bosonization technique for a generic potential $V(\bar{\psi}\psi)$ which is a function of the composite fermionic operator is presented [47]. In this case the functional in Eq. (1.16) is given by:

$$Z_f\left[\eta,\bar{\eta},K\right] = \int \mathcal{D}\psi\mathcal{D}\bar{\psi}\, e^{\left[\int\bar{\psi}\partial\!\!\!/\psi - \int V(\bar{\psi}\psi) + \int\bar{\eta}\psi - \int\bar{\psi}\eta + \int K\bar{\psi}\psi\right]}. \tag{2.51}$$

Inserting a delta function, an auxiliary field X can be introduced so that the generating functional Z_f can be rewritten as:

$$Z_f\left[\eta,\bar{\eta},K\right] = \int \mathcal{D}\psi\mathcal{D}\bar{\psi}\int\mathcal{D}X\,\delta(X-\bar{\psi}\psi)\, e^{\left[\int\bar{\psi}\partial\!\!\!/\psi - \int V(X) + \int\bar{\eta}\psi - \int\bar{\psi}\eta + \int KX\right]}. \tag{2.52}$$

For a generic real parameter x the delta function is represented in terms of a Fourier transform as:

$$\delta(x) = \int_{-i\infty}^{i\infty}\frac{dk}{2\pi i}\, e^{-kx}, \tag{2.53}$$

where the variable k belongs to the imaginary axis. By extending this result to the path-integral formalism the partition function turns out to be:

$$\begin{aligned} Z_f\left[\eta,\bar{\eta},J\right] &= \mathcal{N}\int\mathcal{D}\psi\mathcal{D}\bar{\psi}\int\mathcal{D}\Phi \\ &\quad \int\mathcal{D}X\; e^{\left[\int\bar{\psi}(\partial\!\!\!/+\Phi)\psi - \int\Phi X - \int V(X) + \int\bar{\eta}\psi - \int\bar{\psi}\eta + \int JX\right]}. \end{aligned} \tag{2.54}$$

With these positions the fermionic degrees of freedom appear just as quadratic terms. Thus they can be completely integrated out, then generating an effective action made only by the collective auxiliary fields X and Φ. Differently from the Hubbard Stratonovich approach, in this case two auxiliary fields are needed. However the correlators of the field X can be immediately related to those of the composite field $\bar{\psi}\psi$.

2.2.2 The saddle point expansion

Since the GN model is investigated the Hubbard-Stratonovich transformation, giving the expression in Eq. (1.151), is resumed. As was anticipated, a systematic large N expansion relies on the assumption that, when the number of flavours is very large, the invariants of the $U(N)$ group self average, as for example the composite operator $\bar{\psi}\psi$. Thus for example using Eq. (2.50) one finds:

$$\left\langle (\bar{\psi}\psi)^2 \right\rangle - \left\langle \bar{\psi}\psi \right\rangle^2 = 0, \tag{2.55}$$

showing that fluctuations around the mean value are negligible. Now, the way to implement this assumption is analyzed. First of all the generating functional of elementary fields and the auxiliary scalar shown in Eq. (1.166) is considered. Then the fermionic source multiplets η and $\bar{\eta}$ are chosen having just one non-vanishing component. Since the theory is symmetric under the $U(N)$ group, all the results, written in terms of the group invariants, will not depend on this particular position. Integrating out the $(N-1)$ fermionic degrees of freedom which are not coupled with the sources one obtains:

$$\begin{aligned} Z_b\left[\eta,\bar{\eta},\mathcal{J}\right] &= \int \mathcal{D}\psi \int \mathcal{D}\bar{\psi} \int \mathcal{D}\sigma \, e^{\int\int \bar{\psi}\, D_\sigma^{-1}\, \psi - S_{eff.}[\sigma] + \int \bar{\eta}\psi - \int \bar{\psi}\eta + \int \mathcal{J}\sigma} \\ &= \int \mathcal{D}\psi \int \mathcal{D}\bar{\psi} \int \mathcal{D}\sigma \, e^{-S_{eff.}[\psi,\bar{\psi},\sigma] + \int \bar{\eta}\psi - \int \bar{\psi}\eta + \int \mathcal{J}\sigma}, \end{aligned} \tag{2.56}$$

where $D_\sigma^{-1} = \not{\partial} + \sigma$ and:

$$S_{eff.}[\sigma] = \int \frac{\sigma^2}{2g^2} - \mathrm{Trln}\left(\Delta\Delta_\sigma^{-1}\right), \tag{2.57}$$

was defined. A functional f of the form:

$$f(j) = \int_{-\infty}^{\infty} dx \, e^{-\frac{s(x)}{\epsilon} + jx}, \tag{2.58}$$

can be calculated by expanding the argument of the exponent around its maximum x_0 as:

$$\begin{aligned} -\frac{s(x)}{\epsilon}+jx &= -\frac{s(x_0)}{\epsilon}+j\,x_0-\frac{1}{2\epsilon}\,\frac{\delta^2 s}{\delta x^2}\bigg|_{x=x_0}(x-x_0)^2+\ldots \\ &= -\frac{s(x_0)}{\epsilon}+j\,x_0-\frac{1}{2}\,\frac{\delta^2 s}{\delta x^2}\bigg|_{x=x_0}y^2+\mathcal{O}(\sqrt{\epsilon}), \end{aligned} \tag{2.59}$$

where $\sqrt{\epsilon}y = x - x_0$ and the small parameter ϵ has been explicitly shown. By retaining terms up to the first order in ϵ one finds: Thus obtaining:

$$\begin{aligned} f(j) &= \epsilon^{1/2}e^{-\frac{s(x_0)}{\epsilon}+j\,x_0}\int_{-\infty}^{\infty}dy\,e^{-\frac{1}{2}f_0''y^2-\frac{\epsilon^{1/2}}{3!}f_0^{(3)}y^3-\frac{\epsilon}{4!}f^{(4)}y^4+\mathcal{O}(\epsilon^{3/2})} \\ &= \epsilon^{1/2}e^{-\frac{s(x_0)}{\epsilon}+j\,x_0}\int_{-\infty}^{\infty}dy\,e^{-\frac{1}{2}s_0''y^2}\left[1-\frac{\epsilon}{24}s^{(4)}y^4+\frac{\epsilon}{72}\left(s_0^{(3)}\right)^2y^6+\mathcal{O}(\epsilon^2)\right] \\ &= \sqrt{2\pi\epsilon}e^{-\frac{s(x_0)}{\epsilon}+j\,x_0-\frac{1}{2}\ln[(s_0'')^{-1}]}\left[1-\frac{\epsilon}{8}(s_0'')^{-3}s_0^{(4)}+\frac{5\epsilon}{24}(s_0'')^{-3}(s_0^{(3)})^2\right]+\ldots, \end{aligned} \tag{2.60}$$

where the usual Gaussian integrations were performed. From this calculation it can be immediately verified that at the leading order, when:

$$f(j) \simeq e^{-\frac{s(x_0)}{\epsilon}+j\,x_0}, \tag{2.61}$$

one gets:

$$\langle x\rangle_j = \frac{1}{f(j)}\frac{\delta f}{\delta j} = x_0. \tag{2.62}$$

Now by applying the same arguments to the path-integral in Eq. (2.56) one can verify that the action in Eq. (2.57) is of order N thus the position $\epsilon = \frac{1}{N}$ can be done. The saddle point condition reads:

$$-\int\int\bar{\psi}_0\,\frac{\delta D_\sigma^{-1}}{\delta\sigma}\bigg|_{\sigma_0}\psi_0+\frac{\delta S_{eff.}}{\delta\sigma}\bigg|_{\sigma_0} = \mathcal{J} \tag{2.63}$$

$$\int D_{\sigma_0}\psi_0 = \eta \tag{2.64}$$

$$\int\bar{\psi}_0 D_{\sigma_0} = -\bar{\eta}. \tag{2.65}$$

Expanding around this configuration and discarding terms up to the second order in the fluctuations, the partition function is approximated by:

$$Z_b = e^{-S_{eff.}[\psi_0,\bar{\psi}_0,\sigma_0]-\frac{1}{2}S\mathrm{Trln}\left(S^{(2)}\big|_0\right)+\int\bar{\eta}\psi_0-\int\bar{\psi}_0\eta+\int\mathcal{J}\sigma_0}, \tag{2.66}$$

where the matrix $S^{(2)}$ is the super-matrix:

$$S^{(2)} = \begin{pmatrix} S_{\sigma\sigma} & S_{\bar{\psi}\sigma} & S_{\psi\sigma} \\ S_{\sigma\bar{\psi}} & S_{\bar{\psi}\bar{\psi}} & S_{\psi\bar{\psi}} \\ S_{\sigma\psi} & S_{\bar{\psi}\psi} & S_{\psi\psi} \end{pmatrix}, \tag{2.67}$$

and where $S\mathrm{Tr}$ designs the super-trace. With some involved calculations reported in the App. D.1 the form of the effective action at the next to leading order is calculated. It turns out to be:

$$\begin{aligned} \Gamma[\psi_0, \bar{\psi}_0, \sigma_0] &= S_{eff.}[\psi_0, \bar{\psi}_0, \sigma_0] + \frac{1}{2}\mathrm{Trln}\left(\frac{\delta^2 S_{eff.}}{\delta\sigma\delta\sigma}\bigg|_0\right) - \mathrm{Trln}\left[D_{\sigma_0}^{-1}\right] \\ &+ \frac{1}{2}\mathrm{Trln}\left(1 - 2\left(\frac{\delta^2 S_{eff.}}{\delta\sigma\delta\sigma}\right)^{-1}\bigg|_0 \bar{\psi}_0 D_{\sigma_0}\psi_0\right). \end{aligned} \tag{2.68}$$

The form of the $1PI$ Green's function for the fermionic fields and the auxiliary scalar can be obtained by expanding this expression. It should be emphasized that the trace over the logarithm of the fermionic propagator appearing in Eq. (2.68) runs only over the Dirac indices, and not over the flavour ones, since the $N-1$ spinors were previously integrated out. Often people prefer to include this last term in the definition of the action $S_{eff.}$ for the reasons which will be clarified soon. The mean field expansion has an important diagrammatic interpretation that can simplify the calculations. Indeed a saddle expansion is always a loop expansion. It is well known [41] of the number of loops L is equal to:

$$L = P - V + 1, \tag{2.69}$$

where P is the number of propagators and V is the number of vertices. Looking at the action of the example in Eq. (2.60) one finds that the leading order of the expansion has no internal line nor vertices thus corresponding to tree level contributions. By this way:

$$\mathcal{O}(\epsilon) = L - 1. \tag{2.70}$$

However this loop expansion is very different from the ordinary one. Indeed the propagators and the vertices implied are derived by the action $S_{eff.}$, not by the original action of the model S_f. As an example the bosonic "tree" propagator $S^{-1}_{\sigma\sigma}$ is the so called "improved propagator" obtained from the infinite resummation of Hartree type diagrams given in Eq. (2.9)). This propagator is represented by the diagram shown in Fig. 2.7. The induced or improved bosonic vertices can be read off by expanding the action $S_{eff.}$. For example

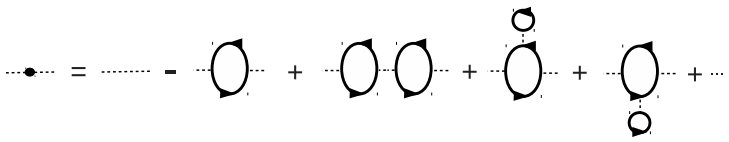

.

Figure 2.7: The leading order contribution in the $1/N$ expansion, defining an improved bosonic propagator for the auxiliary field. A comparison with the digrams in Fig. 2.2 (a) shows that, in this approximation, the four point function can be rewritten as the sum of two tree level channels involving the improved propagator.

. .

Figure 2.8: The three point and the four point scalar vertices, arising in the improved action $S_{eff.}$, are shown. Their presence affects only the higher orders contributions of the $1/N$ expansion.

the diagrammatic representation of the cubic and quartic scalar interactions, giving contributions at two loop order, are shown respectively in Figs. 2.8 (a) and (b). The fermionic propagator is massive and is given by:

$$\Delta(p) = (i\not{p} + \sigma_0)^{-1}. \tag{2.71}$$

It is represented with the ordinary solid line. The computation of the improved vertex gives:

$$\frac{\delta^3 S_{eff}}{\delta\psi_a(x)\delta\bar{\psi}_b(y)\delta\sigma(z)} = -\delta_{ab}\delta(x,y)\delta(x,z). \tag{2.72}$$

It is the only vertex linking boson and fermion lines and it will be represented as a usual Yukawian interaction. One more observation. The one loop contribution in Eq. (2.68) involves the one loop diagrams containing fermionic bubble and tadpoles, represented by the trace over the logarithm of the fermion improved propagator, as shown in Fig. 1.10. If this contribution is absorbed in the redefinition of the action S_{eff} these types of graphs have to be discarded from the corrections to the leading order.

Finally it is important to stress how the systematic expansion also provides a criterion for the renormalizability of the theory. By studying the form of the $1PI$ primitive divergences one can establish if all divergences can be systematically removed. An example of this procedure is described in the following section.

2.2.3 Divergences and renormalizability of GN model at $d = 3$.

A proof of the renormalizability of the GN model at $d = 3$ was given by [16]. From the saddle point condition, stated in Eqs. (2.63),(2.64),(2.65), by setting $\psi_0 = \bar{\psi}_0 = 0$, the gap equation for the fermion mass is obtained, representing the analogous at $d = 3$ of the result in Eq. (2.24). It turns out to be:

$$\frac{\sigma_0}{G} = \int \frac{d^3p}{(2\pi)^3} \mathrm{tr}\left(\frac{1}{i\not{p} + \sigma_0}\right). \tag{2.73}$$

As found in Sec. 2.1.4, a non trivial expectation value of the auxiliary field induces a non trivial fermion mass, so that one can simply replace $m = \sigma_0$.

The comparison with the Eq. (2.24) also shows how the bare mass m_B does not appear in Eq. (2.73). Indeed since m_B must be identified with the source term, it has been removed. More precisely one should set $m_B = \frac{\mathcal{K}}{g}$. The critical value for the coupling G is obtained by setting $\sigma_0 = 0$ thus finding:

$$\frac{1}{G_c} = N \mathrm{tr}\,\mathbb{I} \int \frac{d^3p}{(2\pi)^3} \frac{1}{p^2} = \frac{N \mathrm{tr}\,\mathbb{I}\Lambda}{2\pi^2}. \tag{2.74}$$

The auxiliary improved propagator $\mathcal{G}(q)^{-1}$ can be calculated by deriving the effective action in Eq. (2.68). Since only the leading order of the expansion is considered it can be simply found by twice deriving the $S_{eff.}[\sigma]$ and Fourier transforming the result. Thus one obtains:

$$\mathcal{G}^{-1}(q) = \frac{1}{G} + \int \frac{d^3p}{(2\pi)^3} \mathrm{tr}\left(\frac{1}{i\not{p}+\sigma_0} \frac{1}{i(\not{p}+\not{q})+\sigma_0}\right). \tag{2.75}$$

The integral appearing in the gap equation (Eq. (2.73)) is linearly diverging, as the integral in Eq. (2.75). Both these integrals are regularized by means of a sharp cut-off. However by replacing in Eq. (2.75) the value of the coupling G found in Eq. (2.73) the divergences are removed, leaving a finite result when $\Lambda \to \infty$. When the scaling limit is taken the coupling G approaches its critical values. So one finds:

$$\mathcal{G}^{-1}(q) = \left(q^2 + 4\sigma_0^2\right) \arctan\left(\frac{q}{2\sigma_0}\right) \frac{N \mathrm{tr}\,\mathbb{I}}{8\pi q}. \tag{2.76}$$

As in four dimensions the propagator has a pole in $q^2 = -4\sigma^2$.

One can also calculate the ratio:

$$\left.\frac{\mathcal{G}^{-1}(q^2)}{\frac{d\mathcal{G}^{-1}(q^2)}{dq^2}}\right|_{q^2=0} = \frac{4\sigma_0^2 \frac{N \mathrm{tr}\,\mathbb{I}}{16\pi\sigma_0}}{\frac{N \mathrm{tr}\,\mathbb{I}}{24\pi\sigma_0}} = 6\sigma_0^2, \tag{2.77}$$

that will be useful for further applications.

It has shown how, by tuning the coupling G at its critical value (and by setting the external sources at zero), all the divergences have been removed in the Hartree approximation. A systematic proof of the renormalizability of the theory at every order of the $1/N$ expansion was given by Rosenstain in [16] Here some of the arguments are reported. The scaling dimension of the fermionic fields does not change from its canonical value, as can be found from Eq. (2.71). Thus $[\psi] = [\bar{\psi}] = 1$. On the other hand in the large momentum limit (at the critical region) the two point correlator of the auxiliary field behaves as:

$$\mathcal{G}(q) \sim \frac{1}{q}, \tag{2.78}$$

thus the scaling dimension of the auxiliary field is $[\sigma] = 1$. The result is very different from the usual trivial dimension found in Eq. (1.171) but also from the behaviour of a free propagating scalar and it has been interpreted as the appearance of a bound state in the model. The scaling dimension of the improved vertex defined in Eq. (2.72) can easily be calculated. Since at the leading order the effective action is scale invariant, the dimension of the vertex is achieved by requiring:

$$[S_{eff}] = 0 \Rightarrow \; -d + [\sigma] + [g] + 2[\psi] = 0, \tag{2.79}$$

which gives $[g] = 0$. The corrections to the leading order scaling have to be calculated by applying the procedure explained in Sec. 2.2.2. The divergences arising at every order in the loop expansion are taken into account by defining the appropriate superficial degree of divergence:

$$D = d - E_\psi[\psi] - E_\phi[\phi] - [g] = 3 - E_\psi - E_\phi, \tag{2.80}$$

obtained from the result in Eq. (1.136) by replacing the canonical dimension of the fields with the scaling dimension found in the Hartree approximation. With the help of the diagrammatic rules established in Sec. 2.2.2 and by using the Eq. (2.80), one finds that the primitive divergent [2] graphs are those shown in Fig 2.9. The symmetric case in which $\sigma_0 = 0$ can be considered and a procedure similar to that described in Sec. 1.6.6 is followed. The diagrams (d) and the the diagram (e) in Fig 2.9 identically vanish since these diagrams respectively involve a trace over one and over three Dirac matrices. Also

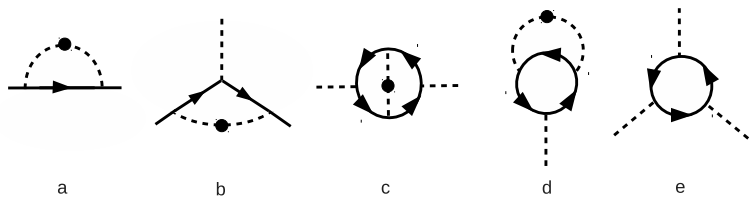

.

Figure 2.9: Primitive divergences arising in the $1/N$ expansion of the GN model at $d = 3$. In the fourth-dimension also the fourth-point scalar vertex has to be considered.

the momentum independent part of the diagram (a) is zero since the symmetric phase is considered. Finally the diagram (a) gives a correction to the scaling of the $\bar{\psi}\partial\!\!\!/\psi$ operator, the diagram (b) gives a correction to the scaling of $\bar{\psi}\psi\sigma$ operator while the graph (c) produces a correction only to the scalar mass term coupled with the operator σ^2. It is important to stress that, differently from the $d = 4$ case presented in Sec. 2.1.3, there are no momentum dependent divergences in the scalar propagator. In order to heal the divergences only counter-terms generated by operators given in the original action S_f are needed.

2.2.4 Large N behaviour of the GN model in generic dimensions, some corrections to the leading order.

The result in Eq. (2.73) can be generalized, for generic d dimension, with $2 < d < 4$.

The gap equation at the leading order turns out to be:

$$\frac{\sigma_0}{G} = \int \frac{d^d p}{(2\pi)^d} \frac{1}{i\not{p} + \sigma_0}, \tag{2.81}$$

which leads to the result:

$$\frac{1}{G} = \frac{2N \mathrm{tr}\,\mathbb{I}}{(4\pi)^{d/2}(d-2)} \left[\frac{\Lambda^{d-2}}{\Gamma(d/2)} - \sigma_0^{d-2} \Gamma\left(2 - \frac{d}{2}\right) \right]. \tag{2.82}$$

And immediately one finds the critical value:

$$\frac{1}{G_c} = \frac{2N \mathrm{tr}\,\mathbb{I} \Lambda^{d-2}}{(4\pi)^{d/2}(d-2)\Gamma(d/2)}. \tag{2.83}$$

The bosonic improved propagator is given by the expression:

$$\begin{aligned} \mathcal{G}^{-1}(q) &= \frac{1}{G} + \Pi(q) \\ &= \frac{1}{G} + \int \frac{d^d p}{(2\pi)^d} \mathrm{tr} \left(\frac{1}{i\not{p} + \sigma_0} \frac{1}{i(\not{p} + \not{q}) + \sigma_0} \right). \end{aligned} \tag{2.84}$$

A simple power counting analysis gives that near G_c the correlator has the following behaviour:

$$\mathcal{G}(q) \sim \frac{1}{q^{d-2}} = \frac{1}{q^{2-\eta_\sigma}}. \tag{2.85}$$

The direct computation is obtained by replacing the gap equation (see Eq. (2.81)) and performing some algebraic manipulation (see App. C.2) thus finding:

$$\begin{aligned} \mathcal{G}^{-1}(q) &= \frac{N'}{2}(q^2+4\sigma_0^2)\int \frac{d^dp}{(2\pi)^d}\frac{1}{(p^2+\sigma_0^2)[(p+q)^2+\sigma_0^2]} \\ &= \frac{N'\Gamma(2-d/2)}{2(4\pi)^{d/2}}\frac{(q^2+4\sigma_0^2)}{\sigma_0^{4-d}}2F_1\left(1,2-\frac{d}{2};\frac{3}{2};-\frac{q^2}{4\sigma_0^2}\right). \end{aligned} \tag{2.86}$$

When $d=3$ the result in Eq. (2.76) is recovered. At the leading order the anomalous dimension of the scalar field is given by $\eta_\sigma = 4-d$. When d reaches the four dimension the simple power law scaling is lost and weak logarithmic corrections to the free canonical scaling appear as shown in Eq. (2.33).

Some examples of corrections to the leading order are given. In order to calculate the correction to the two point fermionic function the contribution of the diagram (a) in Fig. 2.9 must be added to the tree level term. Thus one finds:

$$\Gamma_{\psi\bar{\psi}}(p) = i\not{p} + \sigma_0 - G\int \frac{d^dq}{(2\pi)^d}\frac{1}{i(\not{p}+\not{q})+\sigma_0}\mathcal{G}(q). \tag{2.87}$$

Also the gap equation at the next to leading order can be calculated by adding to Eq. (2.81) the contribution of the (e) diagram shown in Fig. 2.9. The result is:

$$\frac{\sigma_0}{G} = \int_p \mathrm{tr}\frac{1}{i\not{p}+\sigma_0} + \int_p\int_q \mathrm{tr}\left(\frac{1}{(i\not{p}+\sigma_0)(i(\not{p}+\not{q})+\sigma_0)}\right)\mathcal{G}(q) \tag{2.88}$$

where $\int_p = \int \frac{d^dp}{(2\pi)^d}$.

The scaling of the composite operator

Finally the behaviour of the two point correlator of the composite field is calculated by means of the result in Eq. (1.158). By Fourier transforming this equation one finds:

$$G_{\bar{\psi}\psi}(p,q) = -\frac{(2\pi)^d\delta^d(p+q)}{G} + \frac{1}{G^2}\langle\sigma(p)\sigma(q)\rangle_C \tag{2.89}$$

Thus by defining: $G_{\bar{\psi}\psi}(p,q) = (2\pi)^d\delta^d(p+q)G_{\bar{\psi}\psi}(q)$ it is obtained:

$$G_{\bar{\psi}\psi}(q) = -\frac{1}{G} + \frac{1}{G^2}\mathcal{G}(q). \tag{2.90}$$

Using the result found in Eq. (2.84) this Green's function turns out to be:

$$\begin{aligned} G_{\bar{\psi}\psi}(q) &= -\frac{1}{G}\Pi(q)\frac{1}{1/G+\Pi(q)} \\ &= -\frac{1}{G}\Pi(q)\mathcal{G}(q). \end{aligned} \tag{2.91}$$

In the scaling region the function $\Pi(q)$ can be replaced with its divergent part for $2 < d < 4$ or with the leading divergence at $d = 4$ [18] thus getting:

$$G_{\bar{\psi}\psi}(q) \simeq \frac{1}{G_c^2}\mathcal{G}_{\Lambda=\infty}(q)\,. \tag{2.92}$$

A part from the $1/G^2$ factor, near the critical region the composite field two point correlator has the same momentum behaviour of the auxiliary scalar one; however the different divergences arising in these improved propagators are reflected in the different form of the $Z_{\bar{\psi}\psi}$ function and of the Z_σ one.

2.3 The Scaling region, critical phenomena picture of the χSB

In the following section a detailed comparison between the theory of the critical phenomena and the chiral symmetry breaking mechanism in the Yukawa and Gross Neveu model is explored. At this scope the corresponding quantities to the order parameter, the critical temperature and so on are introduced for these QFT . Moreover the relation between the non-perturbative renormalizability of these models and the anomalous scaling behaviour of the correlators is analyzed. Thus the critical exponents, acknowledging the features of a theory around the critical region, are defined.

Although the GN model and the Yukawa one should be in principle two different theories, they have shown the same renormalizability properties (in the $1/N$ framework) after the bosonization of the first model. It could be objected that the Yukawa theory has two more bare parameters (the quartic scalar coupling and the scalar derivative term), however when these parameters are necessary in order to renormalize the theory at $d = 4$ they must be introduced for the bosonized GN model too. Conversely it will be found that these parameters play no role near the scaling region for $2 < d < 4$ thus showing that the two models have the same predictive power. Using the critical phenomena terminology one can say that they belong to the same universality class in the framework of the large

N expansion. This clearly holds for the $d = 4$ case, as said. Similar situations arise in the description of a ferromagnetic phase transition. Two of the models describing the emergence of a spontaneous magnetization are the Ising model and the Landau-Wilson one. The first theory simply modeling the interactions between the spins of the material while the second one involves the interactions of scalar quantity representing a local magnetization intensity. One should expect that the first description is more accurate than the second one, since it investigates the structure of the interactions in the material. However near the second order phase transition these details are lost. As explained in Sec. 1.4 the symmetries and the dimension of the order parameter are sufficient to predict the behaviour of the correlators.

2.3.1 Critical exponents of the χSB

The description of the χSB transition needs the definition of an appropriate order parameter. This quantity should be the mean value of any field whose non-vanishing value is a signal of the occurence of the transition. As it is clear from the previous section the first candidate for the bosonized version of the GN model is the expectation value of the auxiliary field σ. A non-vanishing $\langle\sigma\rangle$ induces a fermion mass violating the symmetry. The result in Eq. (1.155) suggests that in terms of a purely fermionic language the order parameter is the expectation value of the composite operator $\bar{\psi}\psi$. The NJL result described in Sec.2.1.3 identifies the critical value of the coupling G as it discriminates between the symmetric and the broken phase. Since the χSB occurs when $G > G_c$ the inverse of the Fermi coupling, $1/G$ should be interpreted as the temperature of the model. Thus the reduced temperature τ is given by:

$$\tau = \frac{1}{G} - \frac{1}{G_c}. \tag{2.93}$$

Once the order parameter and the temperature have been identified one more quantity is needed in order to complete the parallel between the χSB and a continuous transition. In analogy with the ferromagnetic models one has to search for the external (magnetic) field. This is nothing but the external source K introduced in Eq. (1.16). As previously stated it can be interpreted as a bare mass term that linearly couples with the operator $\bar{\psi}\psi$, explicitly breaking the symmetry of interest. Setting the bare mass equal to zero (chiral limit) as was done in Eq. (2.81) it is possible to determining the critical temperature G_c

and the onset of the transition. On the other hand the presence of a small non-vanishing bare mass changes the continuous transition into a cross-over phenomenon. As explained in Sec. 1.3.2 a complete parallel with the critical phenomena picture needs the study of the correlators calculated with the effect of small sources.

The gap equation, approximated by the Eq. (2.81) in the large N limit, relates the order parameter of the transition with the temperature and the external field. It is nothing but the equation of state in the statistical language. At $\tau = 0$ and $J = m_B = 0$ the phase transition occurs, thus the coordinates $G = G_c$ and $m_B = 0$ in the parameter space identify the critical point of the transition. The coupling G and the mass m_B are the only two relevant parameters of the transition, any other coupling in the hyper-surface $G = G_c$ and $m_B = 0$ belongs to the critical surface of the system.

The behaviour under scale transformations of the correlation functions (euclidean Green's functions) near the phase transition depends on the scaling of the relevant parameters: near the critical point, the Green's functions follow a power law behaviour described by the so called critical exponents. Here the usual definition of the critical exponents for the GN model [19],[22],[23] is presented. The exponent β, which gives the scaling of the order parameter around the critical value of the Fermi constant, is defined through the equation:

$$\left\langle \bar{\psi}\psi \right\rangle \quad \sim \quad \tau^{\beta} \,, \tag{2.94}$$

while δ is defined by considering the scaling of $\left\langle \bar{\psi}\psi \right\rangle$ in the presence of a small bare mass when $G = G_c$:

$$\left\langle \bar{\psi}\psi \right\rangle\big|_{\tau=0} \quad \sim \quad m_B^{\frac{1}{\delta}} \,. \tag{2.95}$$

Another fundamental quantity in the description of our critical phenomena is the two point connected function of the operator $\bar{\psi}\psi$. It is related with the improved propagator of the auxiliary field, $\langle \sigma(x)\sigma(0) \rangle$, by means of the Eq. (1.158). Near the critical region they follow the same momentum behaviour as explicitly shown in Eq. (2.92). It is generally assumed that:

$$G_{\bar{\psi}\psi}(q) \simeq \frac{1}{G^2} \left\langle \sigma(q)\sigma(-q) \right\rangle . \tag{2.96}$$

The susceptibility χ is related to the two point correlation function from the fluctuation-dissipation theorem according to the equation:

$$\chi = G \int d^d x \left\langle \bar{\psi}\psi\left(x\right) \bar{\psi}\psi\left(0\right)\right\rangle_C , \tag{2.97}$$

since $1/G$ is the temperature of the model. Performing a Fourier transformation near the critical region one finds:

$$\chi^{-1} = G\mathcal{G}\left(0\right)^{-1} , \tag{2.98}$$

The exponent γ gives the scaling of χ near $G = G_c$:

$$\chi \sim \left|\tau\right|^{-\gamma} . \tag{2.99}$$

The exponent η, which governs the scaling of $\mathcal{G}\left(q\right)$ for large momenta at $G = G_c$, is defined by:

$$\mathcal{G}\left(q\right)\big|_{\tau=0} \;\sim\; \frac{1}{q^{2-\eta_\sigma}} . \tag{2.100}$$

It is nothing but the anomalous dimension of the function also found in Eq. (1.122). The square correlation length ξ_σ^2 for the auxiliary correlator may be defined [48] by:

$$2d\xi_\sigma^2 = \frac{\int d^d x \;\left|x\right|^2 \left\langle\sigma(x)\sigma(0)\right\rangle}{\int d^d x \;\left\langle\sigma(x)\sigma(0)\right\rangle}, \tag{2.101}$$

which is based on the result found in Eq. (2.77). With this position the correlation length is nothing but the inverse of the induced fermion mass. Alternatively it can be defined as the inverse of the composite boson mass.

By using Eq. (2.101) it turns out to be:

$$\xi = \sqrt{G}\left.\frac{d\mathcal{G}^{-1}}{dq^2}\right|_0^{1/2} \chi^{-1/2} . \tag{2.102}$$

Finally, the exponent ν is defined from:

$$\xi \;\sim\; \tau^{-\nu}. \tag{2.103}$$

Hyperscaling

As has often been said, the critical behaviour is obtained by tuning the bare parameters in such a way that the dimensionless correlation length of the system $\frac{\xi}{a}$ diverges. Indeed by supposing that under a scale transformation the correlation length transforms according to its canonical dimension one finds:

$$\xi' = \frac{\xi}{b}, \tag{2.104}$$

so that at the critical point the condition $\xi' = \xi$ is fulfilled by a divergent correlation length.[1] This property corresponds to the request that masses of the fermions and of the the scalar in the model, both proportional to the order parameter σ, are decoupled from the ultraviolet cut-off scale Λ, so that $\sigma/\Lambda << 1$. However, there is another property characterizing the critical domain. Since the correlation length diverges at the critical point, near the phase transition it has become sufficiently large with respect to the other scales involved. Thus all the correlators should be expressed in terms of simple scale ratios, thus becoming homogeneous functions of their arguments. This leads to the conclusion that at the critical point the system is scale invariant.

The way in which the correlators scale under dilatations near the critical point is reflected on the relations between the different critical exponents. They are called "hyperscaling relations". Using the hyperscaling hypothesis, that is supposing that the correlators are homogeneous functions one can derive [40]:

$$\frac{\beta}{\nu} = -\frac{1}{2}(2 - d - \eta_\sigma), \tag{2.105}$$

$$\frac{\gamma}{\nu} = 2 - \eta_\sigma, \tag{2.106}$$

$$\frac{\beta\delta}{\nu} = \frac{1}{2}(2 + d - \eta_\sigma), . \tag{2.107}$$

Only two different critical exponents are arbitrary numbers, reflecting the fact that two relevant parameters characterize the critical domain, and will be related to the behaviour of the temperature of the external field in the following chapter.

[1] Conversely an arbitrary large dilatation drives the system towards an uncorrelated ($\xi = 0$) configuration.

2.3.2 Large N computation of the critical exponents in the GN model

Once the critical exponents are defined it is possible to calculate them for a generic d dimension with $2 < d < 4$ by using the results found in Sec. 2.2.4. The gap equation in Eq. (2.81), written in the presence of an external source $\mathcal{J}$ is:

$$\frac{\sigma_0}{G} = \int \mathrm{tr}\frac{1}{i\not{p} + \sigma_0} + \mathcal{J}, \tag{2.108}$$

calculating the integral and replacing the critical value given in Eq. (2.83) one finds:

$$\frac{1}{G} - \frac{1}{G_c} = -\left[\frac{2N\mathrm{tr}\,\mathbb{I}}{(4\pi)^{d/2}(d-2)}\Gamma\left(2-\frac{d}{2}\right)\right]\sigma_0^{d-2} + \frac{\mathcal{J}}{\sigma_0}. \tag{2.109}$$

Thus setting $J = 0$ the following relation is obtained:

$$\tau \sim \sigma_0^{d-2} \Rightarrow \beta = \frac{1}{d-2}. \tag{2.110}$$

on the other hand taking $\tau = 0$ one gets:

$$\mathcal{J} \sim \sigma_0^{d-1} \Rightarrow \delta = d-1. \tag{2.111}$$

From Eq. (2.86) when $q^2 = 0$ one finds, using the relation in Eq. (2.98):

$$\chi^{-1} = G\frac{N'}{2^{d-1}\pi^{d/2}}\Gamma(2-d/2)\sigma_0^{d-2} \tag{2.112}$$

$$\Rightarrow \chi^{-1} \sim \sigma_0^{d-2}. \tag{2.113}$$

Since from Eq. (2.110) $\sigma \sim \tau^{\frac{1}{d-2}}$ one obtains $\gamma = 1$. From Eq. (2.77) extended for a generic d dimension it is found:

$$\xi^{-1} \simeq \sigma \Rightarrow \nu = \beta = \frac{1}{(d-2)}. \tag{2.114}$$

Finally the η_σ exponent has been calculated in Eq. (2.85). It is $\eta_\sigma = 4 - d$.

The first correction in the $1/N$ expansion to the leading order of exponents just calculated. was computed by Hands et al. [19],[22],[23]. Here the result is briefly reported. By defining:

$$A_d = \frac{4}{\Gamma\left(2-\frac{d}{2}\right)\Gamma\left(\frac{d}{2}\right)B\left(\frac{d}{2},\frac{d}{2}-1\right)}, \tag{2.115}$$

these exponents turn out to be:

$$\begin{aligned}
\beta &= \frac{1}{d-2}, && (2.116)\\
\delta &= (d-1)\left[1+\frac{A_d}{N'}\right], && (2.117)\\
\gamma &= 1+\frac{(d-1)}{(d-2)}\frac{A_d}{N'}, && (2.118)\\
\nu &= \frac{1}{(d-2)}\left[1+\frac{(d-1)}{d}\frac{A_d}{N'}\right], && (2.119)\\
\eta &= 4-d-\frac{2(d-1)}{d}\frac{A_d}{N'}. && (2.120)\\
& && (2.121)
\end{aligned}$$

One can easily verify that the hyperscaling relations in Eq. (2.105) are fulfilled. The results could suggest that in the fourth dimension the GN model becomes trivial at any order in the $1/N$ expansion. Actually in order to trust the result at this specific order in the expansion the higher corrections should be negligible. If the triviality remains also for small values of N is in our opinion an open question.

2.3.3 Equivalence with Yukawa theory

The large N expansion techniques is now applied in order to show that near the critical region the GN model and the Yukawa theory give the same predictions [17]: The action of the Yukawa theory was given in Eq. (1.2). Integrating out the $N-1$ fermionic fields with the procedure described in Sec.2.2.2 the following action is obtained:

$$\begin{aligned}
S_{eff.}[\psi,\bar{\psi},\phi] &= \int\left[-\bar{\psi}(\not{\partial}+\phi)\psi+\frac{1}{2g^2}(\partial_\mu\phi)^2+\frac{M^2}{2g^2}\phi^2+\frac{\lambda}{4!g^4}\phi^4\right]\\
&- \mathrm{Trln}\left(\Delta\Delta_\phi^{-1}\right), && (2.122)
\end{aligned}$$

where the shift $\phi\to g\phi$ was performed and $\Delta_\phi^{-1}=\not{\partial}+\phi$ was defined. In order to compute the large N expansion both g^2 and λ are assumed to be of $\mathcal{O}(N)$. Thus the saddle point condition leads to a modified gap equation:

$$\frac{M^2}{g^2}\phi_0+\frac{\lambda}{6g^4}\phi_0^3-\frac{N'}{(2\pi)^d}\phi_0\int\frac{d^dq}{q^2+\phi_0^2}=0, \qquad (2.123)$$

and $N' = (N-1)\mathrm{tr}\,\mathbb{I} \simeq N\mathrm{tr}\,\mathbb{I}$. The critical coupling corresponding to the critical temperature of the system can be obtained by setting $\phi_0 = 0$, thus one finds:

$$\frac{M_c^2}{g^2} = \frac{N'}{(2\pi)^d}\int \frac{d^dq}{q^2}. \tag{2.124}$$

The boson mass term allows the distinction of the symmetric phase, characterized by a zero expectation value ϕ_0, from the broken one, with a non-vanishing order parameter. The reduced temperature is defined as:

$$\tau = \frac{M^2}{g^2} - \frac{M_c^2}{g^2}. \tag{2.125}$$

Thus using Eqs. (2.123),(2.124), one derives:

$$\tau + \frac{\lambda}{6g^4}\phi_0^2 + \frac{N'}{(2\pi)^d}\phi_0^2\int \frac{d^dq}{q^2(q^2+\phi_0^2)} = 0. \tag{2.126}$$

For $2 < d < 4$ the explicit calculation gives:

$$\tau + \frac{\lambda}{6g^4}\phi_0^2 - \left[\frac{2N'}{(4\pi)^{d/2}(d-2)}\Gamma\left(2-\frac{d}{2}\right)\right]\phi_0^{d-2} = 0. \tag{2.127}$$

This shows that for small values of the order parameter, i.e. in the critical region, the last term is more singular than the second, which provides a correction to the critical behaviour. Discarding this term the same expression found in Eq, (2.109) is recovered once the auxiliary field of the bosonized GN model with the scalar field of the Yukawa theory have been identified and the inverse coupling $\frac{1}{G}$ is associated with the ratio $\frac{M^2}{g^2}$. The second derivative of the action in Eq. (2.122) gives the inverse bosonic improved propagator. Using the Eq. (2.123) it is obtained:

$$\Delta_\phi(q^2) = \frac{q^2}{g^2} + \frac{\lambda}{3g^4}\phi_0^2 + \frac{N'}{2}(q^2+4\phi_0^2)\int \frac{d^dp}{(2\pi)^d}\frac{1}{(p^2+\phi_0^2)[(p+q)^2+\phi_0^2]} \tag{2.128}$$

In the scaling region, when $\sigma, p << \Lambda$, the integral gives again the dominant contribution. Thus the bosonic propagator has the same form as the correlator of the auxiliary field in the GN model found in Eq. (2.86). Since the fermion mass is given by $m = \phi_0$ thus near the critical point $M_\sigma^2 = 4\phi_0^2 = 2m^2$. This condition fixes the ratio $\frac{\lambda_c}{3g_c^4} = 4$; when corrections to scaling are included the pole depends on the value of λ. It is found that at the leading order in the $1/N$ expansion all the exponents of the Yukawa theory coincide with those of the GN model. Since these two theories have the same critical

behaviour one says that they belong to the same universality class. The coupling λ and g as well as the kinetic term of the scalar play no role near the scaling region for $d < 4$, thus they are considered irrelevant couplings. Here there is a non-perturbative example of what was expressed in Sec. 1.2. A renormalizable theory is characterized by the scale invariance of its correlation functions. The scale invariance can be achieved near a critical point by searching for the onset of a second order phase transition. The parameters in the Lagrangian of a "renormalizable" theory are just the relevant parameters of the transition since if the system is very close to the critical point any other irrelevant couplings should be discarded. Conversely if the irrelevant couplings are retained the corrections to the critical behaviour have been taken into account. Thus the cut-off effects arise and the theory becomes non-renormalizable.

By discarding the irrelevant couplings of the Yukawa theory near the critical region its actions become equal to that of the bosonized version of the GN model, with a Fermi coupling given by $G = g^2/M^2$. Both the GN and the Yukawa theory possess the same numbers of relevant parameters. On the other hand the GN model seems to have fewer bare parameters than those of the Yukawa theory. However when $d = 4$ the subleading divergences affect the equations giving important corrections to the hyperscaling laws. These corrections are reflected in the divergences appearing in the term $\mathrm{trln}(\partial + \sigma)$ of the $S_{eff.}$ in Eq. (2.57).

In order to avoid these divergences appearing in the GN at $d = 4$ the tuning of these operators must be considered too. Thus the same number of parameters found in the Yukawian Lagrangian are needed [17].

CHAPTER 3

NON-PERTURBATIVE ANALYTICAL TECHNIQUES II: RENORMALIZATION GROUP

In the previous chapter the properties of some fermion models together with their possibility of providing a χSB mechanism were analyzed. The common aspects between the scaling properties of a QFT and the behaviour of a statistical system, when a SSB mechanism occurs in the vicinity of a critical point, were also stressed. The non perturbative character of the chiral transition was investigated with the help of the method of the large N expansion.

One of the main results of this analysis is that, in the framework of the $1/N$ expansion, the GN model and the Yukawa theory belong to the same universality class. From a theoretical point of view this means that a theory of self-interacting fermions produces the same measurable effects of a theory in which an elementary scalar is the mediator of the forces.

The easiest check for this assumption is to compare the critical exponents of both of these models. This comparison has been done in the previous chapter up to the $\mathcal{O}(1/N)$ and it was shown how the scaling of their correlators coincides near the critical region. On the other hand the number N of spinor components characterizing most of the unitary symmetry groups of the Standard Model physics is relatively small. Thus another technical tool should be found in order to check the equivalence of the description of the χSB phenomenon in terms of elementary or composite scalars.

At this scope the renormalization group represents one of the main non-perturbative

tools which are able to catch the main aspects of the critical behaviour of a system. The application of this technique to the fermion theories also represents our main original contribution to the study of fermion chiral theories.

However, there is no natural expansion parameter which can be used in order to systematically implement this procedure. The starting point is often suggested by the other analytical methods.

The following chapter is organized as follows. First of all, the main ideas concerning the Wilsonian renormalization group transformation are applied to the description of the χSB mechanism. The critical point of the transition will represent a fixed point of the *RG* transformations. It has been seen that the $d = 4$ case represents the upper critical dimension for the chiral phase transition since the critical exponents of both the bosonized version of the GN model and of the Yukawa theory acquire their mean field values. When this occurs the scaling dimension of the fields approaches its canonical value, although weak logarithmic corrections are also present. The critical region is described by the bare parameters near the origin and the theory is called trivial. By following the arguments in .. the calculus of the *RG* equations of the Yukawa model is performed by means of the epsilon expansion technique. With the help of the Callan and Symanzik 's equations the critical exponents and the scaling of the two point correlator are evaluated. Finally our main result will be introduced. The *RG* equations for chiral theories of self-interacting fermions without the help of any bosonization technique are calculated, extending a procedure also followed by Clark et. al. [25]. The computation is limited to the so called local potential approximation (LPA) which neglects the contributions of fluctuations at non-zero momentum. However as will be shown also in this approximation it is possible to reproduce the critical exponents of the GN model in the Hartree approximation for $2 < d < 4$. They are obtained following the running of an explicit fermion mass term and calculating the appropriate chiral limit. Using our technique all the physical quantities at zero momentum as the order parameter of the transition or the susceptivity can be calculated. With the appropriate approximation the NJL gap equation is recovered, then other approximations are suggested which best fit the *RG* improvement. Finally the critical exponents at any value of N are calculated by means of our technique. At $d = 3$ the results are compared with those found by means of lattice numerical simulations and of other analytical methods. The agreement with the numerical simulations is very

satisfactory.

3.1 Wilsonian effective action and blocking

The first step of the Wilsonian procedure is based on considering the impact of the higher momentum degrees of freedom [9]. Before applying this Wilsonian idea to the study of the fermion models the Wilsonian effective action for a generic scalar field theory is presented [49]. The partition function of a scalar theory is given by:

$$Z[J] = \int \mathcal{D}\phi \, e^{-S[\phi]+\int J\phi}. \tag{3.1}$$

There are different ways of selecting the degrees of freedom of a theory. The simplest and direct way is obtained by separating the Fourier modes of the fields in fast and slow components with respect to an arbitrary scale $0 \leq k \leq \Lambda$. The field $\phi(x)$ splits as:

$$\phi = \phi^- + \phi^+. \tag{3.2}$$

The field ϕ^- is made of those Fourier modes with $p \leq k$ while ϕ^+ has only momenta $p > k$. The partition function can be rewritten as:

$$Z[J] = \int \mathcal{D}\phi^- \int \mathcal{D}\phi^+ \, e^{-S[\phi^-+\phi^+]+\int J(\phi^-+\phi^+)}. \tag{3.3}$$

It should be stressed that the path-integral measure was split into two since each product containing fast and slow components vanishes. Now the fast Fourier modes, encoding the effects of the higher momenta fluctuations, can be integrated out by defining the Wilsonian effective action as:

$$e^{-S_{eff.}[\phi^-]} = \int \mathcal{D}\phi^+ \, e^{-S[\phi^-+\phi^+]+\int J\phi^+} \tag{3.4}$$

By this way the partition function can be described only in terms of the slow components and of the Wilsonian effective action as :

$$Z[J] = \int \mathcal{D}\phi^- \, e^{-S_{eff.}[\phi^-]+\int J\phi^-}. \tag{3.5}$$

The present procedure is called decimation since some of the degrees of freedom have been simply eliminated. Clearly the definition of the Wilsonian action is purely symbolic and generally cannot be evaluated until some approximations have been done.

However the knowledge of the Wilsonian action provides a way for calculating the generating functional of $1PI$ correlators. Indeed, one finds that the effective action Γ of the theory is given by:

$$e^{-\Gamma[\phi_c]} = \int \mathcal{D}\phi \, e^{-S[\phi]+\int J(\phi-\phi_c)}, \tag{3.6}$$

so that, by performing the shift $\phi \to \phi - \phi_c$, it turns out to be:

$$e^{-\Gamma[\phi_c]} = \int \mathcal{D}\phi \, e^{-S[\phi+\phi_c]+\int J\phi}. \tag{3.7}$$

When $k = \Lambda$ there are no fast components in the scalar field since the last one is composed of only its slow degrees of freedom ($\phi = \phi^-$). In this case the Wilsonian action in Eq. (3.4) coincides with the bare action of the theory. It is found:

$$S_{eff.}[\phi] \to S[\phi]. \tag{3.8}$$

Conversely when $k = 0$ most degrees of freedom have been integrated out. The right hand side of the Eq. (3.4) essentially coincides with that one of the Eq. (3.7) except for the integration over every possible constant field configuration. Thus when the classical field ϕ_c is constant the effective action calculated in this configuration is well approximated by the Wilsonian action calculated in its maximum. It is found:

$$S_{eff.}[\phi_c] \to \Gamma[\phi_c]. \tag{3.9}$$

In principle the Wilsonian action interpolates between the bare action of the theory when the scale k, also called running scale, coincides with the cut-off scale Λ and the effective action of theory when the running scale reaches zero value.

3.2 The Wilsonian RG approach and the field theoretical epsilon expansion for the Yukawa model

In this section the RG properties of the Yukawa model near the fourth dimension are analyzed.

The Wilsonian renormalization group transformations are introduced for this model and their application to the study of the chiral transition is stressed. The steps providing the renormalization group transformations for the Yukawa model are summarized. This

offers the opportunity of extending the notion of relevant and irrelevant parameters, beyond the perturbation theory, and provides the possibility of defining the non-perturbative renormalizability of a QFT. All the *RG* technical tools providing a description of the chiral phase transitions are also introduced.

However another way of implementing the *RG* transformations, closer to the spirit of the field theoretical renormalization, is presented. By applying this method the beta functions governing the flow of the parameters of the theory can be calculated by means of epsilon expansion technique. The original idea introduced by Wilson and Fisher is based on a double expansion in terms of the coupling constants of the model and in the parameter $\epsilon = 4 - d$ [50], [51]. Since at $d = 4$ the Yukawa theory is trivial, near this dimension the perturbative epsilon expansion and the Wilsonian *RG* approach give the same results.

As an application of the procedure, a series of flow equations for the couplings of the theory will be found.

3.2.1 The Wilsonian *RG* transformation: Yukawa theory

The renormalization group procedure is made of three essential steps. First of all, as shown in the previous section, the impact of the higher energy degrees of freedom must be evaluated by integrating out all the Fourier modes above a certain scale $k = b\Lambda$, with $b \leq 1$. This procedure is called decimation, [40]. In order to compare the original system, defined at the cut off scale Λ, with the new effective one, defined at the scale k, the unit measure must be rescaled by a factor b and the value of the fields needs an appropriate rescaling too.

Decimation

The Wilsonian action, introduced in Eq. (3.4) was calculated by integrating out the scalar modes with $b\Lambda \leq p \leq \Lambda$. Thus $k = b\Lambda$. For a theory with scalars and fermions one should separate fast and slow components for both scalar and fermion fields and then defining the Wilsonian action as:

$$\begin{aligned} e^{-S^k_{fb}[\psi^-,\bar{\psi}^-,\phi^-]} &= \int \mathcal{D}\psi^+ \mathcal{D}\bar{\psi}^+ \int \mathcal{D}\phi^+ \, e^{-S_{fb}[\psi^- + \psi^+, \bar{\psi}^- + \bar{\psi}^+, \phi^- + \phi^+]} \\ &\times \quad e^{\int \bar{\eta}\psi^+ - \int \bar{\phi}^+ \eta + \int J\phi^+}, \end{aligned} \tag{3.10}$$

A perturbative calculation of the Wilsonian action in Eq. (3.10) can be performed in a perturbative way. The methods introduced in Sec. 1.6.3 can be applied, although, since the integration involves only the fast components, the internal momenta of the loops belong to the shell $b \leq p \leq \Lambda$. In this sense the expansion is organized in terms of a sufficiently small b parameter. Each diagram has a weight given by the number of loops involved and by a b dependence of the bare parameters [1]. Clearly situations far from the usual perturbative one can be explored. The $1PI$ correlators, arising from such a calculation, represent the coefficients of the expansion of the Wilsonian action in series of the slow components. By expanding each of these coefficients around the momentum scale $p = k$ one could find [41]:

$$\begin{aligned} S^k_{fb}[\psi,\bar{\psi},\phi] &= \int_{|p|\leq k} d^dx \quad [-\bar{\psi}\left(Z_\psi^{-1}\not{\partial} + (g+\delta g)\phi\right)\psi \\ &+ \frac{Z_\phi^{-1}}{2}(\partial_\mu\phi)^2 + \frac{(M^2+\delta M^2)}{2}\phi^2 \\ &+ \frac{(\lambda+\delta\lambda)}{4!}\phi^4 + \dots], \end{aligned} \tag{3.11}$$

As a consequence, each parameter in the original Yukawa Lagrangian receives an appropriate correction produced by the diagrammatic contributions. Also other operators are generated by the integration as those corresponding to higher power couplings and to non-local interactions. The introduction of the non-vanishing source terms, as given in Eq. (3.10), could generate contributions which explicitly break the symmetry. However for a theory near the chiral transition this is not the case. More on this point later.

Rescaling

. The effective action in Eq. (3.11) is defined at a cut-off scale $b\Lambda$. In order to restore the original cut-off scale one can perform the rescaling:

$$x' = bx, \tag{3.12}$$

$$p' = \frac{p}{b}, \tag{3.13}$$

So that the momenta belong again to the range $0 \leq p \leq \Lambda$. Since the limit in Eq. (1.9) must be performed, this procedure also preserves the number of degrees of freedom thanks

[1] inherited by their a priori dependence on the cut-off scale

to a rescaling of the Lagrangian density. Thus the Wilsonian action can be rewritten as:

$$\begin{aligned} S^k_{fb}[\psi,\bar{\psi},\phi] &= \int_{|p|\leq\Lambda} d^dx' b^{-d}\Big[\quad -\bar{\psi}(x)\left(Z_\psi^{-1} b \not{\partial}' + (g+\delta g)\phi(x)\right)\psi(x) \\ &+ \frac{1}{2} Z_\phi^{-1}\, b^2(\partial'_\mu\phi(x))^2 + \frac{(M^2+\delta M^2)}{2}\phi^2(x) \\ &+ \frac{(\lambda+\delta\lambda)}{4!}\phi^4(x) + \ldots\Big]. \end{aligned} \tag{3.14}$$

Field renormalization

After the decimation and rescaling are performed a field transformation is defined according the rule:

$$\psi'(bx) = b^{\frac{1-d}{2}} Z_\psi^{-1/2}(b)\psi(x), \tag{3.15}$$

$$\bar{\psi}'(bx) = b^{\frac{1-d}{2}} Z_\psi^{-1/2}(b)\bar{\psi}(x), \tag{3.16}$$

$$\phi'(bx) = b^{\frac{2-d}{2}} Z_\phi^{-1/2}(b)\phi(x), \tag{3.17}$$

Again the Z factors appearing in this transformation should not be in principle confused either with those defined in Eqs. (1.117), (1.118),(1.123), or with those in Eqs. (1.139), (1.140),(1.141). However all these quantities coincide under certain conditions to be clarified soon. After the field rescaling the Wilsonian action reduces to:

$$\begin{aligned} S'^k_{fb}[\psi',\bar{\psi}',\phi'] &= \int_{|p|\leq\Lambda} d^dx' \Big[\quad -\bar{\psi}'(x')\left(\not{\partial}' + g'\phi'(x')\right)\psi'(x') \\ &+ \frac{1}{2}(\partial'_\mu\phi'(x'))^2 + \frac{M'^2}{2}\phi'^2(x') + \frac{\lambda'}{4!}\phi'^4(x') + \ldots\Big], \end{aligned} \tag{3.18}$$

where:

$$g' = Z_\phi^{1/2} Z_\psi^1 b^{\frac{d-4}{2}} g - \delta g = Z_\phi^{1/2} Z_\psi^1 b^{\frac{d-4}{2}} Z_g^{-1} g, \tag{3.19}$$

$$M'^2 = Z_\phi^1 b^{-2} M^2 - \delta M^2 = Z_\phi^1 b^{-2} Z_{M^2}^{-1} M^2, \tag{3.20}$$

$$\lambda' = Z_\phi^2 b^{d-4}\lambda - \delta\lambda = Z_\phi^2 b^{d-4} Z_\lambda^{-1}\lambda. \tag{3.21}$$

The relations in Eqs. (3.19),(3.20),(3.21) are the *RG* discrete transformations for the couplings of the theory. Thus for example, the effective Yukawa coupling or the effective four scalar interaction, according to the previous prescriptions, satisfy the relations:

$$S'^k_{\phi\psi\bar{\psi}}(\{p\})\Big|_{s=t=u=-k^2} = k^{4-d} g', \tag{3.22}$$

$$S'^k_{\phi\phi\phi\phi}(\{p\})\Big|_{s=t=u=-k^2} = k^{4-d}\lambda', \tag{3.23}$$

very similar to those given in Eqs. (1.148), (1.149).

The partition function in Eq.(3.10) becomes:

$$\begin{aligned} Z[\eta,\bar{\eta},J] &= \mathcal{N}(b,\Lambda,\eta,\bar{\eta},J,\{g\})\int \mathcal{D}\psi'\mathcal{D}\bar{\psi}'\int \mathcal{D}\phi'\, e^{-S'^{k}_{fb}[\psi',\bar{\psi}',\phi']} \\ &\times \exp\left[\int dx' b^{\frac{d+1}{2}} Z_{\psi}^{1/2}\bar{\eta}(x)\psi'(x') - \int dx' b^{\frac{d+1}{2}} Z_{\psi}^{1/2}\bar{\psi}(x')\eta(x)\right. \\ &+ \left.\int dx' b^{\frac{d+2}{2}} Z_{\phi}^{1/2} J(x)\phi'(x')\right] \\ &\equiv \mathcal{N}(b,\Lambda,\eta,\bar{\eta},J,\{g\})Z'[\eta',\bar{\eta}',J'], \end{aligned} \tag{3.24}$$

while the sources transform according to:

$$\eta'(bx) = b^{-\frac{d+1}{2}} Z_{\psi}^{1/2}\eta(x), \tag{3.25}$$

$$\bar{\eta}'(bx) = b^{-\frac{d+1}{2}} Z_{\psi}^{1/2}\bar{\eta}(x), \tag{3.26}$$

$$J'(bx) = b^{-\frac{d+2}{2}} Z_{\phi}^{1/2} J(x). \tag{3.27}$$

3.2.2 Fixed points

Clearly the procedure can be reiterated so that the whole *RG* transformation is represented by the mapping:

$$S^{k}_{fb}[\psi_k,\bar{\psi}_k,\phi_k] \to S'^{k-\delta k}_{fb}[\psi_{k-\delta k},\bar{\psi}_{k-\delta k},\phi_{k-\delta k}]. \tag{3.28}$$

Where now $b = 1 - \delta k/k$. One can think to the renormalization group transformation as a mapping defined on the space of all possible couplings. Each integration produces a new set of effective couplings. The boundary value of these transformations at $k = \Lambda$ is provided by the value of the couplings appearing in the original action S_{fb} in Eq. (1.2). It is clear that the flow of the whole parameter space cannot be followed in practice. The truncation scheme that should be adopted is justified by the possibility of neglecting those parameters which are naturally suppressed after a recursion.

It can be immediately verified that a generic connected correlator transforms as:

$$G^{(m;n;r)}_{k-\delta k,C}(\{p\};\{q\};\{l\}) = b^{\frac{d+1}{2}(n+m)} Z_{\psi}^{-\frac{n+m}{2}} b^{\frac{d+2}{2}r} Z_{\phi}^{-\frac{r}{2}} G^{(m;n;r)}_{k,C}(\{bp\};\{bq\};\{bl\}), \tag{3.29}$$

plus an additional function which decreases after many integrations. By taking the limit $\delta k \to 0$ [2] an infinitesimal transformation in the dilatation parameter b is generated. Thus

[2] this procedure requires attention especially in the sharp-cut off regularization scheme, cite

a generic parameter v_i of the action transforms according to the equation:

$$\frac{dv_i}{dt} = \beta_i\left(\{v_j\}\right), \tag{3.30}$$

where $t = -\ln b = \ln\frac{\Lambda}{k}$ was defined.

A fixed point of the *RG* equations is defined so that:

$$S^k_{fb}[\psi_k, \bar{\psi}_k, \phi_k] = S'^{k-\delta k}_{fb}[\psi_{k-\delta k}, \bar{\psi}_{k-\delta k}, \phi_{k-\delta k}], \tag{3.31}$$

$$J^k(x) = J^{k-\delta k}(x). \tag{3.32}$$

This implies that the correlators $G_{k-\delta k}$ and G_k in Eq. (3.29) become the same function, while the *RG* transformation acts as a simple rescaling. As well known, each regular map, after many recursions, flows towards a fixed point (which can be finite or infinite).

When a fixed point is reached, the correlation length of the system is either zero or divergent according to Eq. (2.104). At this point the system becomes scale invariant. The critical behaviour of the Yukawa model near the chiral transition, has to be described by the *RG* trajectories around a fixed point which is characterized by infinite correlation length (a vanishing fermion mass), that is a critical point.

All the actions connected by the same *RG* flow belong to the same universality class. Each point of the parameter space which belongs to the same universality class of a critical fixed point defines the so called critical surface. In other words a point belonging to a trajectory which starts on the critical surface flows towards this critical fixed point. Thus each point on the critical surface represents a system at the critical point of the transition.

The fixed point condition on the *RG* equations for the couplings reads:

$$\beta_i\left(\left\{v_j^*\right\}\right) = 0, \tag{3.33}$$

thus $\{v_j^*\}$ is the fixed point of the transformations in the parameter space.

Expanding the β_i's around the solution $\{v_j^*\}$ the system can be linearized. By defining the, Jacobian matrix as: $J_{ij} = \frac{\partial \beta_i}{\partial v_j}\Big|_{\{v\}=\{v\}^*}$. and by setting $\underline{\mathrm{v}} = \{v_j\}$ the equations can be rewritten in a vectorial form as:

$$\frac{d\underline{\mathrm{v}}}{dt} = J\left(\underline{\mathrm{v}} - \underline{\mathrm{v}}^*\right). \tag{3.34}$$

A generic solution of the linearized system has the general form:

$$\underline{\mathrm{v}} = \underline{\mathrm{v}}^* + \sum_i C_i e^{\lambda_i t}\underline{\mathrm{v}}_i. \tag{3.35}$$

The $\underline{v}_i$'s are the eigenvectors of the Jacobian matrix, associated with their own eigen-operators. The presence of a critical fixed point makes possible to extend the systematic renormalization presented in Sec.1.6.4 to a non-perturbative regime. In the present case only real eigenvalues are considered [27].

- The eigen-operators, corresponding to eigenvalues $\lambda_i > 0$, are related to the relevant couplings. Fixing the boundary conditions of the flow in the eigen-space spanned by one of these directions, the trajectory moves away from the fixed point. In order to reach the fixed point it has to be set $C_i = 0$ for all the relevant couplings. For this reason the relevant couplings should be identified with the control parameters of the transition as: the temperature, the external field and so on.

- The eigen-operators corresponding to eigenvalues $\lambda_i < 0$ identify the irrelevant couplings. The space spanned by the linear combination of these irrelevant couplings is the first approximation (the tangent hyperplane) of the critical surface. Near the critical region the flow of the irrelevant couplings should be discarded by setting all the irrelevant directions at their fixed point value. If the flow of the irrelevant parameter is included, the corrections to the critical behaviour will be taken into account and the cut-off effects will be no more negligible.

- When $\lambda_i = 0$ the linearization fails to work. Usually this means that the eigen-direction approaches or leaves the fixed point in a logarithmic way.

- The kinetic operators $\bar{\psi}\partial\!\!\!/\psi$ and $(\partial_\mu\phi)^2$, which realize the fields renormalization do not change under the *RG* transformation. They are called redundant.

In the following some information on the scaling of correlators of the Yukawa theory are extracted by means of the linearization around the fixed point.

3.2.3 Callan-Symanzik equations for Yukawa theory

Here a different formulation of the renormalization group transformation, first formulated by Callan and Symanzik [52],[53],[54], is considered. This is closer to the spirit of the usual field theoretical renormalization, although it will be suggested in which sense, under certain conditions, the Wilsonian and the field theoretical pictures coincide. According to the perturbative results of Sec. 1.6.5 the Yukawa theory at $d = 4$ is trivial while

at $d = 3$ is super-renormalizable. However a double expansion called "epsilon expansion" can be performed in series of the couplings and of the parameter $\epsilon = 4 - d$. Thanks to this procedure the different behaviour of the system can be shown. Since a perturbative expansion has been introduced, at every order some renormalized Green's functions can be defined. For example at an IR scale $\mu << \Lambda$ the renormalization conditions introduced in Sec. 1.6.6 can be applied.

The renormalized connected Green's functions defined at the scale μ are related to the bare ones according to the equation:

$$G_{r,C}^{(m;n;r)}(\{p\};\{q\};\{l\};\{g_\mu\},\mu,\Lambda) = Z_\psi^{-\frac{n+m}{2}} Z_\phi^{-\frac{r}{2}} G_C^{(m;n;r)}(\{p\};\{q\};\{l\};\{g\},\Lambda). \quad (3.36)$$

A renormalizable theory is such that cut-off dependence of the renormalized Green's functions is suppressed by performing the scaling limit. Under the same conditions one can realize how at $k = \mu$ the Wilsonian action coincides with the effective action of the theory as explained in Sec.3.1. Thus the effective parameters defined with the Wilsonian procedure should resemble those defined through the renormalization conditions. Finally the Eq. (3.36), after a trivial rescaling, should correspond to Eq. (3.29).

The relation between the renormalized and the bare couplings can be deduced by requiring that the renormalized Green's functions do not depend on the cut-off scale.

This reads:

$$\frac{d}{d\Lambda} G_{r,C}^{(m;n;r)} = 0. \quad (3.37)$$

Solution of $C - S$ equations and critical exponents

The condition in Eq. (3.37) implies that the bare correlation functions satisfy the equation:

$$\left[\Lambda\frac{\partial}{\partial\Lambda} + \beta_g\frac{\partial}{\partial g} + \beta_\lambda\frac{\partial}{\partial\lambda} + \beta_{M^2}\frac{\partial}{\partial M^2} + \frac{(n+m)}{2}\eta_\psi + \frac{r}{2}\eta_\phi\right] G_{r,C}^{(m;n;r)} = 0. \quad (3.38)$$

Where for the generic coupling g_i it was defined:

$$\beta_{g_i} = \Lambda\frac{dg_i}{d\Lambda} = \frac{dg_i}{dt} \equiv ([g_i]_0 + \gamma_{g_i})\, g_i, \quad (3.39)$$

and:

$$\eta_\psi = -\Lambda\frac{d\ln Z_\psi}{d\Lambda} = \frac{d\ln Z_\psi}{d\ln b}, \quad (3.40)$$

$$\eta_\phi = -\Lambda\frac{d\ln Z_\phi}{d\Lambda} = \frac{d\ln Z_\phi}{d\ln b}. \quad (3.41)$$

The epsilon expansion or any other perturbative series, together with its own renormalization conditions allows the computation of the beta functions of the parameters. These results should coincide with the Wilsonian *RG* equations in Eq. (3.30) when the same perturbative region is investigated.

The case of the two point scalar correlator $\mathcal{G}(q)$ is considered. Since it has a dimension of $(momentum)^{-2}$ the dependence on the cut-off scale can be converted in a momentum dependence by writing:

$$\mathcal{G}(q) = \frac{1}{q^2} f\left(\frac{q^2}{\Lambda^2}\right). \tag{3.42}$$

Thus Eq. (3.38) reduces to:

$$\left[-q\frac{\partial}{\partial q} + \beta_g \frac{\partial}{\partial g} + \beta_\lambda \frac{\partial}{\partial \lambda} + \beta_{M^2}\frac{\partial}{\partial M^2} - (2-\eta_\phi)\right]\mathcal{G}(q) = 0. \tag{3.43}$$

Introducing an appropriate dilatation parameter $t = \ln\frac{\Lambda}{q}$ the Eq. (3.43) can be solved using the characteristics method. The solution is:

$$\mathcal{G}(q) = \frac{h\left(\bar{\lambda}, \bar{g}, \bar{M}^2\right)}{q^2} \exp\left(\int_p^\Lambda d\ln(\Lambda/p') \quad \eta_\phi\right), \tag{3.44}$$

where h is an arbitrary function. Its arguments, which are generically denoted by $\{\bar{g}\}$, are the solutions of the equations:

$$\frac{d\bar{g}_i}{dt} = \beta_{\bar{g}_i}(\{\bar{g}\}). \tag{3.45}$$

and:

$$\eta_\phi = \eta_\phi(\{g\}). \tag{3.46}$$

Now it is possible to calculate the critical behaviour of the system by using the *RG* group equations. A critical fixed point is expected to be found corresponding to the chiral phase transition. As was shown in Sec. 2.3.3 the reduced temperature of the chiral transition is given by the difference $\tau = M^2 - M_c^2$. Thus one of relevant directions, found by means of the linearization procedure around the critical fixed point, should be approximately equal to the bare mass direction.

By linearizing the mass equation near such a point it should be found:

$$M^2(k) = M^{2*} + C\left(\frac{\Lambda}{k}\right)^{\lambda_{M^2}}, \tag{3.47}$$

where $C = M^2(\Lambda) = M^{2*}$. Thus the reduced temperature transforms according to:

$$\tau' = b^{-\lambda_{M^2}}\tau. \tag{3.48}$$

Since the correlation length scales with its canonical dimension, that is $\xi' = b\xi$, one immediately obtains:

$$\nu = \frac{1}{\lambda_{M^2}}. \tag{3.49}$$

On the other hand, as proved in the large N framework, the λ and the g couplings play no role near the phase transition, thus they should be irrelevant also with respect to the *RG* classification. The critical region is found by discarding their running. Explicit calculations show that η_ϕ near the critical point does not depend on the relevant directions, thus the scalar correlator in Eq. (3.44) scales as:

$$\mathcal{G}(q) \simeq \frac{1}{q^{2-\eta_\phi(\lambda^*,g^*)}}. \tag{3.50}$$

The other critical exponents can be calculated by means of the hyperscaling relations given in Sec. 2.3.1.

On the other hand, at $d = 4$ the hyperscaling is violated because of the triviality of the theory. By means of the *RG* methods also the corrections to trivial scaling can be calculated as will be seen in the next paragraph.

3.2.4 Fixed point structure of the Yukawa theory near the four dimension

The computation of the beta functions at one loop order in ϵ expansion was performed in [17] by using $N' = 4N$. They are:

$$\beta_\lambda = \epsilon\lambda - \frac{1}{8\pi^2}\left(\frac{3}{2}\lambda^2 - 24Ng^4 + 4N\lambda g^2\right), \tag{3.51}$$

$$\beta_{g^2} = \epsilon g^2 - \frac{2N+3}{8\pi^2}g^4, \tag{3.52}$$

$$\beta_{M^2} = [2 - \frac{1}{8\pi^2}(\frac{\lambda}{2} + 2Ng^2)]M^2. \tag{3.53}$$

In addition the anomalous dimensions of the fields turn out to be:

$$\gamma_\phi = \frac{Ng^2}{8\pi^2}, \tag{3.54}$$

$$\gamma_\psi = \frac{g^2}{32\pi^2}. \tag{3.55}$$

The system in Eqs. (3.51),(3.52),(3.53) has four solutions,[55]. They are:

- The Gaussian solution: $g^{2*} = \lambda = M^{2*} = 0$.
- The wilson-fisher fixed point: $M^{2*} = g^{2*} = 0, \lambda^* = \frac{16\pi^2}{3}\epsilon$,
- And the non trivial solutions $M^{2*} = 0$, $g^{2*} = \frac{8\pi^2\epsilon}{2N+3}$ and $\lambda^*_\pm = 8\pi^2\epsilon\tilde{\lambda}^*_\pm$,

where:

$$\tilde{\lambda}^*_\pm = \frac{1}{3(2N+3)}[-(2N-3) \pm \sqrt{4N^2+132N+9}]. \tag{3.56}$$

Each of these results deserve to be commented. First the case in which $d < 4$ is considered. Linearizing around the Gaussian solution the couplings, as expected, scale with their trivial behaviour. One finds:

$$\lambda_{M^2} = 2, \tag{3.57}$$

$$\lambda_{g^2} = \epsilon, \tag{3.58}$$

$$\lambda_\lambda = \epsilon. \tag{3.59}$$

Since $\epsilon > 0$ all these directions are relevant. This reflects the fact that around the origin the Yukawa theory is super-renormalizable, as also has been found with the perturbative treatment. Replacing the solution in Eqs. (3.54),(3.55) both the anomalous dimensions vanish. Thus the correlators scale according to their canonical behaviour.

The second solution is an extension of the well known Wilson-Fisher fixed point. The linearization around this solution gives the eigenvalues:

$$\lambda_\tau = 2 - \frac{\epsilon}{3}, \tag{3.60}$$

$$\lambda_\lambda = -\epsilon, \tag{3.61}$$

$$\lambda_{g^2} = \epsilon. \tag{3.62}$$

As in the case of the Gaussian fixed point, the eigenvalues do not depend on N. The first eigenvalue is associated with the reduced temperature of the ferromagnetic transition. By using the Eq. (3.49) and calculating the scalar anomalous dimension at the fixed point it is found:

$$\nu^{-1} = 2 - \frac{\epsilon}{3}, \tag{3.63}$$

$$\eta_\phi = 0. \tag{3.64}$$

However, since the Yukawa interaction is associated with a relevant direction, this model requires an additional fine-tuning to the ones prescribed in the usual ferromagnetic models. The presence of a small interaction between the fermions and the scalar drives the system away from the critical surface.

The non-trivial solution with λ_-^* has two relevant directions so cannot describe the chiral transition. Finally the non-trivial solution with λ_+^* is considered. For simplicity it will be denoted with λ^*. The linearization around this solution gives the eigenvalues:

$$\lambda_\tau = 2 - \epsilon\frac{10N+3+\sqrt{4N^2+132N+9}}{6(2N+3)}, \tag{3.65}$$

$$\lambda_2 = -\epsilon, \tag{3.66}$$

$$\lambda_3 = -\epsilon\frac{\sqrt{4N^2+132N+9}}{2N+3}. \tag{3.67}$$

Expanding in powers of $1/N$ one obtains:

$$\nu^{-1} = d-2+(d-4)\frac{3}{2N}+\mathcal{O}(1/N^2), \tag{3.68}$$

while the anomalous dimension of the scalar is given by:

$$\eta_\phi = \frac{2N\epsilon}{3+2N} = 4-d+(d-4)\,\frac{3}{2N}+\mathcal{O}(1/N^2). \tag{3.69}$$

These results are consistent with those found in Sec. 2.3.2. However by means of the epsilon expansion technique the critical exponents of the Yukawa theory also for small values of N can be calculated near $d=4$. This point will be further investigated. The critical point is an IR attractor along the λ and the g directions. For a generic choice of the initial bare parameters after many recursions the renormalized ones are frozen to their fixed point value. On the other hand the in the IR region a tree level calculation can be performed giving the boson mass $M_\phi^2 = \lambda^*\phi_c^2/3$ the fermion mass $m_\psi = g^*\phi_c$. Thus the ratio of the squared masses is given by:

$$\frac{M_\phi^2}{m_\psi^2} = \frac{\lambda^*}{3g^{2*}} = \frac{-(2N-3)+\sqrt{4N^2+132N+9}}{9} \simeq 4-30\frac{1}{N}+\mathcal{O}(1/N^2). \tag{3.70}$$

Once again it seems that a fixed mass ratio is a consequence of the irrelevance of these couplings.

3.2.5 Corrections to scaling

With the help of the *RG* equations it was shown that the critical exponent of the Yukawa theory take their mean field value at any value of the flavour number. Indeed the result is independent from the particular choice of N showing that this theory is trivial at $d = 4$. When the theory reaches its upper critical dimension the linearization around the fixed point fails. However corrections to scaling can be calculated in the following way. The equations Eq. (3.51) can be analytically solved by setting $\epsilon = 0$. The solution gives for the Yukawa coupling:

$$g(t)^2 \simeq \frac{8\pi^2}{(2N+3)t+c}, \tag{3.71}$$

while the anomalous dimension is given by:

$$\eta_\phi = 2\gamma_\phi = \frac{2N}{(2N+3)+c} \tag{3.72}$$

Thus evaluating the expression in Eq. (3.44) one finds:

$$e^{-\int_0^t dt' \eta_\phi} = \left(1 + \frac{3+2N}{c}t\right)^{-\frac{2N}{3+2N}}. \tag{3.73}$$

According to this result, the bosonic correlator scales in the large N limit as:

$$\mathcal{G}(q) \simeq \frac{1}{q^2 \ln\left(\frac{\Lambda}{q}\right)}, \tag{3.74}$$

which is the same result found in Eq. (2.33).

For large t values the coupling constants become:

$$g(t)^2 \simeq \frac{8\pi^2}{(2N+3)t}, \tag{3.75}$$

$$\lambda(t) \simeq \frac{8\pi^2 \tilde{\lambda}_*}{t} \tag{3.76}$$

The behaviour of the correlation length is encoded in the function:

$$\nu^{-1}(\lambda(t), g(t)) = 2 + \gamma_{M^2} = 2 - \frac{\tilde{\lambda}_*}{2t} - \frac{2N}{(2N+3)t} \simeq 2 - \frac{1}{t} + \dots \tag{3.77}$$

3.3 The non-perturbative RG approach in the GN model

The present section is devoted to introducing our original RG approach for the analysis of self-interacting fermion theories.

A generalized GN model in d dimensions with N flavours is studied, where the interaction term is replaced by a more general potential $U(\bar{\psi}\psi)$, within the framework of the Wilsonian RG approach as originally implemented by Wegner and Houghton [24].

By applying the same techniques considered in [25] (where the $N = 1$ case for a boson-fermion system was considered), first of all an RG equation for the Wilsonian potential for generic N is established, then the large N limit is considered.

In this limit, by truncating the potential to the Fermi constant term alone (and successively to the mass and Fermi constant terms), it is found that the theory possesses a non-trivial fixed point (beyond the Gaussian one). This generalizes to large N a result which, in this Wilsonian setup, was first obtained for $N = 1$ in [56].

Then the RG equations for the running mass $m(k)$ and Fermi constant $G(k)$ (k is the running scale) are linearized around this non-trivial fixed point and both m and G are found to be relevant eigendirections, i.e. they both are UV repulsive directions. From the corresponding eigenvalues (the magnetic and temperature exponents in the analogy with the ferromagnetic case), the hyperscaling relations for the GN model are established in the fermion language. Then, with the help of these relations, the critical exponents are computed, finding that our results are in agreement with those obtained in the $1/N$ expansion [19],[22],[23]. Naturally, a word of caution has to be said for the $d = 4$ case (the upper critical dimension), where weak violations to the scaling laws are expected [57],[27]. If these relations are used even in the $d = 4$ case, the critical exponents turn out to coincide with their mean field values. Up to weak scaling violations, however, they give the correct behaviour for the correlation functions near the critical point.

Successively, the impact of the presence of an (infinitesimal) bare mass, which is nothing but the boundary value $m(\Lambda)$ for the flow of $m(k)$ at the UV scale Λ, on the renormalized theory, is studied. i.e. the connection between the renormalized mass, the value of $m(k)$ at $k = 0$, and the bare mass $m(\Lambda)$ (IR-UV connection) is analyzed. To this end, one can consider for the bare Fermi constant $G_B = G(\Lambda)$ (the UV boundary for

the running of $G(k)$) values such that $G(\Lambda) > G_c$ and $G(\Lambda) < G_c$, where G_c is the fixed point value for $G(k)$. Choosing the same value for the bare mass $m_B = m(\Lambda)$ in the two cases, it is found that when $G(\Lambda) > G_c$ the renormalized mass turns out to be orders of magnitude greater than the corresponding renormalized mass obtained with $G(\Lambda) < G_c$. In other words, when $G(\Lambda) < G_c$, if the bare mass is infinitesimal, the renormalized mass turns out to be infinitesimal too. On the contrary, when $G(\Lambda) > G_c$, the renormalized mass turns out to be orders of magnitudes larger than the bare mass, thus giving the possibility for the generation of a finite fermion mass.

This interesting result suggests a mechanism for the generation of a finite physical mass as a *cross-over* phenomenon. For values of the Fermi constant greater than the critical value G_c, the quantum fluctuations provide an enormous amplification mechanism which results in the generation of a finite physical mass from an infinitesimal bare mass. In the ferromagnetic analogy, this corresponds to the fact that for $T < T_c$ an infinitesimal external magnetic field is sufficient to trigger a finite spontaneous magnetization of the ferromagnetic material.

Then, analytical approximate solutions to our RG equations are studied. At a first stage, it is shown that, by considering a simple approximation of the RG equation for the running fermion mass $m(k)$, it is possible to recover the celebrated NJL result.

Successively, by considering more elaborated approximations, it is possible to recover with a very good degree of accuracy the entire profile of $m(k)$ (previously obtained numerically) in the whole IR-UV range. This is also an interesting result, as the knowledge of the profile of $m(k)$ should be relevant for phenomenological applications.

Finally the critical exponents for small value of N are computed and the comparison with other numerical and analytical approaches is performed at $d = 3$.

3.3.1 The composite operator in the *RG* language

In analyzing the χSB mechanism of the Yukawa theory it was supposed that the sources of the elementary fields do not affect the behaviour of the system. This assumption was then corroborated by the direct calculations performed with the epsilon expansion method. The anomalous scaling of the two point bosonic Green's function is driven by the large anomalous dimension acquired by the scalar field near the critical point. The source term of the scalar field is not affected by the quantum fluctuations and its scaling is defined by

the relation in Eq. (3.27).

A similar situation can be found in the Landau-Wilson theory of the ferromagnetic phase transition. As previously said, this transition can be described by means of the behaviour of a lambda-phi-fourth theory around the non-trivial Wilson-Fisher fixed point. On the other hand, it is well known, how the spontaneous magnetization can also be depicted with the Ising model. Near the critical region these two models become equivalent, they predict the same critical exponents or in other words belong to the same universality class [35],[51].

What happens is very similar to the equivalence of the Yukawa theory and the GN model in the large N framework. More precisely also the Ising and the Landau-Wilson models can be related by means of an Hubbard Stratonovich transformation near the critical region.

However the divergences arising in the Ising model are different from those appearing in the Wilson-Fisher theory. Indeed in the Ising model, it is the external magnetic field, coupled with the spin field, receiving the large correction from the statistical fluctuations and which is accountable for the anomalous dimension of the two point correlator. But in the end, the anomalous scaling of the source term and that of the field have to be balanced. This is a necessary condition in order to preserve the scale (RG) invariance of the effective action of the theory. Conversely, when the scaling violations are taken into account the condition is not fulfilled, and the way in which the field and the source renormalize is different. However below the upper critical dimension, the hyperscaling relations are satisfied near the critical region and the critical exponents, calculated by considering the RG transformation of the magnetic field, coincide with those found for the Landau-Wilson model.

In the present section it will be shown that this is also the case for the GN when a functional RG approach in a purely fermion language is adopted. The major role is played by the introduction of an explicit mass term coupled with the $\bar{\psi}\psi$ composite operator.

Callan-Symanzik equations

The generating functional of fermion elementary and composite fields was defined in Eq. (1.16). After the integration over the fast field components it turns out to be:

$$Z_f[\eta,\bar{\eta},K] = \mathcal{N}\int \mathcal{D}\psi\mathcal{D}\bar{\psi}\, e^{-S_{eff.}[\psi,\bar{\psi}]+\int\bar{\eta}\psi-\int\bar{\psi}\eta+\int Z_K^{-1}K\bar{\psi}\psi}, \tag{3.78}$$

where the $S_{eff.}$ is including all the effects of the integration, except for the correction to the source term. This merged into the $\bar{\psi}\psi$ operator. The integration over the external fields could also produce any corrections which explicitly violate the symmetry of the Wilsonian action. However one should expect that near the critical region of continuous transition this is not the case. A similar statement can be explicitly verified in the real space *RG* group of the Ising model. The explicit integration of a non-zero magnetic field converts the continuous transition in a sharp cross-over phenomenon.

Similarly in the case of our treatment of the chiral transition it will be shown that within our approximation scheme the fermion running mass, in the linearization region, decouples from the other interactions.

Now the rescaling and the field renormalization can be applied to Eq. (3.78), in such a way:

$$Z_f[\eta,\bar{\eta},K] = \mathcal{N}\int \mathcal{D}\psi'\mathcal{D}\bar{\psi}'\, e^{-S'_{eff.}[\psi',\bar{\psi}]+\int Z_\psi^{1/2}\bar{\eta}\psi'+\int Z_\psi^{1/2}\eta\bar{\psi}'+\int Z_{\bar{\psi}\psi}+K\bar{\psi}'\psi'} \tag{3.79}$$

where:

$$Z_{\bar{\psi}\psi} = Z_K^{-1}Z_\psi, \tag{3.80}$$

was defined. Which means that the Eq. (3.80) extends the transformations of elementary operators in Eqs. (3.15),(3.15),(3.17) to the case of the composite field field $\bar{\psi}\psi$ so that:

$$\bar{\psi}\psi'(bx) = b^{-[\bar{\psi}\psi]_0}Z^{-1}_{\bar{\psi}\psi}\bar{\psi}\psi(x), \tag{3.81}$$

thus immediately giving:

$$\gamma_{\bar{\psi}\psi} = 2\gamma_\psi - \gamma_K. \tag{3.82}$$

On the other hand, the composite operator renormalization can be defined in the framework of any perturbative scheme which allows the introduction of the appropriate

renormalization conditions devoted to removing the divergences in the correlators of the composite field itself.

Again, choosing these conditions at a scale $\mu << \Lambda$, the renormalized and the bare Green's functions are related according to:

$$G_r^{m;n;r} = Z_\psi^{-(n+m)/2} Z_{\bar{\psi}\psi}^{-r/2} G^{m;n;r}. \tag{3.83}$$

By requiring that the renormalized functions do not depend on the cut-off scale, it is found:

$$\Lambda \frac{d}{d\Lambda} \left[Z_\psi^{-(n+m)/2} Z_{\bar{\psi}\psi}^{-r/2} G^{m;n;r} \right]. \tag{3.84}$$

Thus the C-S equations for the correlators with composite operator insertion reads:

$$\left[\Lambda \frac{\partial}{\partial \Lambda} + \beta_G \frac{\partial}{\partial G} + \frac{(n+m)}{2} \eta_\psi + \frac{r}{2} \eta_{\bar{\psi}\psi} \right] G_r^{(m;n;r)} = 0. \tag{3.85}$$

Wilsonian effective action

As in the case of the Yukawa theory, an appropriate Wilsonian action can be used for extracting information on the critical behaviour of the system with elementary and composite fermion fields. Indeed it defines the way in which the bare parameters transform in order to preserve the scale invariance. But it also provides a method for calculating some IR quantities as the order parameter of the transition or the susceptivity when the running scale is close to zero. This can be shown by splitting the fermion fields in fast and slow components, then by defining the Wilsonian action as:

$$\begin{aligned} e^{-S_{eff.}[\psi^-, \bar{\psi}^-, K]} &= \int \mathcal{D}\psi^+ \mathcal{D}\bar{\psi}^+ \, e^{-S_f[\psi^- + \psi^+, \bar{\psi}^- + \bar{\psi}^+]} \\ &\times \exp\left[\int \bar{\eta}\psi^+ - \int \bar{\psi}^+ \eta + \int K \left(\bar{\psi}^+ \psi^+ + \bar{\psi}^- \psi^- \right) \right]. \end{aligned} \tag{3.86}$$

With this position when $k = \Lambda$ the Wilsonian action converge to:

$$S_{eff.}[\psi, \bar{\psi}, K] \to S_f[\psi, \bar{\psi}] + \int K \bar{\psi}\psi, \tag{3.87}$$

which is the action of the model plus an additional bare mass term. On the other hand when $k = 0$ it is found:

$$S_{eff.}[\psi, \bar{\psi}, K] \to \Gamma[\psi_c, \bar{\psi}_c, K]. \tag{3.88}$$

That should converge to the effective action of the GN model once $K = 0$ is set.

3.3.2 Derivative expansion and LPA approximation

In order to study the critical fixed point of the Yukawa theory the epsilon expansion was introduced. This was possible since near $d = 4$ the critical behaviour of the system is not so far from the origin. Unfortunately in a purely fermion language there is no natural expansion that can be used for the computation of the beta functions near the fourth dimension. However if one is searching for a constant vacuum, as found in GN in the $1/N$ expansion, the analysis can be conducted by means of a gradient expansion of the Wilsonian action [49].

By expanding the Wilsonian action at a scale k around a constant field configuration one finds for a fermion theory:

$$S_k[\psi, \bar{\psi}] = \int d^d x \left[U_k(\bar{\psi}\psi) - Z_k(\bar{\psi}\psi)\bar{\psi}\partial\!\!\!/\psi + \mathcal{O}(\partial^2) \right]. \tag{3.89}$$

The form of the U_k and the Z_k functions have been restricted by imposing both the Lorentz and the $U(N)$ invariance of the model. However, in order to study the χSB mechanism the even powers as well as of the odd ones of the $\bar{\psi}\psi$ operator are included.

Since both ψ and $\bar{\psi}$ are slowly varying at the scale $k - \delta k$ one can imagine they split as:

$$\psi(x) = \psi_0^-(x) + \psi^+(x), \tag{3.90}$$

$$\bar{\psi}(x) = \bar{\psi}_0^-(x) + \bar{\psi}^+(x), \tag{3.91}$$

with $\psi_0^-(x) = \psi^- + \epsilon(x)$ and $\bar{\psi}_0^-(x) = \bar{\psi}^- + \bar{\epsilon}(x)$. so that the Wilsonian action at the scale $k - \delta k$ can be expanded in gradients of the field too.

In the present work the analysis is limited to the simplest approximation. Only the running of the Wilsonian potential is taken into account while the Z function is frozen to the value $Z_\Lambda(\bar{\psi}\psi) = 1$. For this reason this procedure is called Local Potential Approximation (LPA).

3.3.3 Wegner-Houghton approach on renormalization group for fermions

By following the techniques of [25] (where the $N = 1$ case for a boson-fermion system is considered), in the present section the RG equation for the Wilsonian potential $U_k(\bar{\psi}\psi)$

of a generalized N flavours GN model are derived within the framework of the local potential approximation (LPA). As will be seen, this equation contains a Hartree and a Fock contribution. Neglecting the latter, the leading order approximation to this equation in the $1/N$ expansion will be obtained.

The Wilsonian action $S_k\left[\Psi,\bar{\Psi}\right]$ is defined at the (energy) scale k and the field Ψ (as well as $\bar{\Psi}$) contains Fourier modes up to k. In order to define $S_{k-\delta k}$, the Wilsonian action at an infinitesimally lower scale $k-\delta k$, the field $\Psi(x)$ is decomposed in a component $\psi(x)$ with modes in the range $[0,k-\delta k]$ and a component $\xi(x)$ with modes in the infinitesimal shell $[k-\delta k,k]$:

$$\Psi(x)\equiv\psi(x)+\xi(x)=\sum_{|p|\leq k-\delta k}\frac{e^{-ip\cdot x}}{V}\psi_p+\sum_{k-\delta k\leq|p|\leq k}\frac{e^{-ip\cdot x}}{V}\xi_p\,, \tag{3.92}$$

where Ψ is an $U(N)$ multiplet with N Dirac spinors and V is the quantization volume. An analogous decomposition holds for $\bar{\Psi}(x)$. $S_{k-\delta k}\left[\psi,\bar{\psi}\right]$ is defined through the integration over the modes ξ_p ($\bar{\xi}_p$):

$$e^{-S_{k-\delta k}\left[\psi,\bar{\psi}\right]}\;=\;\mathcal{N}_d\int\mathcal{D}\xi\mathcal{D}\bar{\xi}e^{-S_k\left[\psi+\xi,\bar{\psi}+\bar{\xi}\right]}\;, \tag{3.93}$$

where $\mathcal{D}\xi=\Pi_p d\xi_p$ (analogously $\mathcal{D}\bar{\xi}=\Pi_p d\bar{\xi}_p$) and $\mathcal{N}_d$ is a constant which takes care of the dimensions of the ξ_p's. In order to perform the ξ ($\bar{\xi}$) integration, $S_k\left[\psi+\xi,\bar{\psi}+\bar{\xi}\right]$ is expanded in Eq. (3.93) in powers of ξ and $\bar{\xi}$ around $\xi=\bar{\xi}=0$ and keep only terms up to the quadratic ones, as higher powers give vanishing contributions [24]:

$$\begin{aligned}S_k\left[\psi+\xi,\bar{\psi}+\bar{\xi}\right]=S_k\left[\psi,\bar{\psi}\right]&+\int d\,x\,\left(\xi(x)\frac{\delta S_k}{\delta\psi(x)}+\bar{\xi}(x)\frac{\delta S_k}{\delta\bar{\psi}(x)}\right)\\&+\frac{1}{2}\int d\,x\,d\,y\,\left(\frac{\delta^2S_k}{\delta\bar{\psi}(x)\delta\bar{\psi}(y)}\bar{\xi}(y)\bar{\xi}(x)+\frac{\delta^2S_k}{\delta\psi(y)\delta\bar{\psi}(x)}\bar{\xi}(x)\xi(y)\right.\\&\left.+\frac{\delta^2S_k}{\delta\psi(y)\delta\bar{\psi}(x)}\bar{\xi}(x)\xi(y)+\frac{\delta^2S_k}{\delta\psi(y)\delta\psi(x)}\xi(x)\xi(y)\right).\end{aligned} \tag{3.94}$$

The RG equation for $U_k(\bar{\psi}\psi)$ in the LPA is obtained by plugging in Eq.(3.94) the ansatz

$$S_k\left[\Psi,\bar{\Psi}\right]=\int d^dx\left[-\bar{\Psi}\left(x\right)\not{\partial}\,\Psi\left(x\right)+U_k\left(\bar{\Psi}\cdot\Psi\right)\right], \tag{3.95}$$

and choosing for the background field $\psi(x)$ ($\bar{\psi}(x)$) the constant mode: $\psi(x)=\psi_0$ ($\bar{\psi}(x)=\bar{\psi}_0$). With this choice, due to Fourier orthogonality, the linear term in ξ ($\bar{\xi}$) in Eq.(3.94)

disappears. As for the quadratic terms, the integration in x and y in the second and third line of Eq. (3.94) is easily performed and gives:

$$\frac{1}{2V^2}\sum_{p,q}\left(\bar{\xi}_p,\xi_p\right)\cdot\,\Delta^{-1}\,\delta_{p,q}\cdot\begin{pmatrix}\bar{\xi}_q\\ \xi_q\end{pmatrix}\,, \tag{3.96}$$

where Dirac and flavour indices are understood and Δ^{-1} is defined as:

$$\Delta^{-1}=\begin{pmatrix}\frac{\delta^2 U_k}{\delta\bar{\psi}_0\delta\bar{\psi}_0} & -i\not{p}+\frac{\delta^2 U_k}{\delta\psi_0\delta\bar{\psi}_0}\\ -i\not{p}^T+\frac{\delta^2 U_k}{\delta\bar{\psi}_0\delta\psi_0} & \frac{\delta^2 U_k}{\delta\psi_0\delta\psi_0}\end{pmatrix}\,. \tag{3.97}$$

Eq. (3.93) then reduces to a Gaussian integral and for $U_{k-\delta k}$ it is found:

$$U_{k-\delta k}=U_k-\frac{1}{2}\int'\frac{d^dp}{(2\pi)^d}\,\mathrm{trln}\left(\frac{\Delta^{-1}}{k}\right)\,, \tag{3.98}$$

where the trace refers to flavour and Dirac indices and the superscript $'$ indicates that the integration is extended to the shell $[k-\delta k,k]$ only.

If one now defines $\rho=\bar{\psi}\psi=\sum_{c,\alpha}\bar{\psi}_{c,\alpha}\psi_{c,\alpha}$, where $c=1,\ldots,N$ is the flavour index and α the Dirac one, after some manipulations reported in the App. D.2, taking the $\delta k\to 0$ limit, finally the RG equation for $U_k(\rho)$ are obtained (the lower index is omitted as well as the argument in $U_k(\rho)$):

$$k\frac{dU}{dk}=k^dC_d\left(N\mathrm{tr}\,\mathbb{I}\ln\left(\frac{k^2+U_\rho^2}{k^2}\right)-C_d\ln\left(1+\frac{2\rho\,U_\rho U_{\rho\rho}}{k^2+U_\rho^2}\right)\right)\,, \tag{3.99}$$

where $\mathrm{tr}\,\mathbb{I}$ is the trace of the identity matrix in the Dirac space ($\mathrm{tr}\,\mathbb{I}=2^{d/2}$ for even values of d and $\mathrm{tr}\,\mathbb{I}=2^{(d-1)/2}$ for odd values), $C_d=\frac{1}{(4\pi)^{d/2}\Gamma(d/2)}$ and U_ρ means the derivative of $U_k(\rho)$ w.r.t. ρ. In the r.h.s. of Eq. (3.99), it is possible to recognize a Hartree and a Fock term, the first and the second one respectively. Being neglected in the large N limit the Fock term, Eq. (3.99) becomes:

$$k\frac{dU}{dk}=k^dC_dN\mathrm{tr}\,\mathbb{I}\ln\left(\frac{k^2+U_\rho^2}{k^2}\right)\,. \tag{3.100}$$

Eq.(3.100) corresponds to the ladder approximation for our RG equation. For our purposes, it is also convenient to write this equation in terms of dimensionless quantities. If one defines $t=\ln(k_0/k)$, where k_0 is an arbitrary scale, together with the dimensionless field and potential, $\sigma=k^{1-d}\rho$ and $V(\sigma,t)=k^d\,U_k(\rho)$, the RG equation for the $V(\sigma,t)$ turns out to be:

$$\frac{\partial}{\partial t}V=d\,V-(d-1)\,\sigma V_\sigma-C_dN\mathrm{tr}\,\mathbb{I}\ln\left(1+V_\sigma^2\right)\,, \tag{3.101}$$

where again V_σ is the derivative of $V(\sigma, t)$ w.r.t. σ.

Eq. (3.101) (or, equivalently, Eq. (3.100)) is the starting point of our following analysis.

3.4 The scaling of the GN model in the Large N limit

3.4.1 Truncated potential: the Fermi constant term

Our study begins by truncating the potential $V(\sigma, t)$ in Eq. (3.101) to the GN (or Fermi) term alone:

$$V(\sigma, t) = -\frac{G(t)}{2}\sigma^2 \,, \tag{3.102}$$

where $G(t)$ is the dimensionless Fermi constant. With this truncation, Eq. (3.101) becomes an RG equation for $G(t)$ ($d \geq 2$):

$$\frac{dG}{dt} \;=\; (2-d)\, G + 2N \mathrm{tr}\, \mathbb{I} C_d G^2 \,. \tag{3.103}$$

For $d = 2$, this is nothing but the equation found by Gross and Neveu [1]. The beta function vanishes at $G = 0$ and the theory turns out to be asymptotically free: $G = 0$ is an UV stable fixed point.

For $d > 2$, the beta function vanishes at

$$G = 0 \qquad \text{and} \qquad G = G_c = \frac{d-2}{2\, N \mathrm{tr}\, \mathbb{I} C_d} \tag{3.104}$$

and the solution to Eq.(3.103) is:

$$G\,(t) = \frac{G_c}{1 - Be^{(d-2)t}} \,, \tag{3.105}$$

where B is an arbitrary integration constant. Now the two cases $B < 0$ and $B > 0$ have to be distinguished.

The $B < 0$ case. In this case, $G\,(t)$ flows for $t \to -\infty$ ($k \to \infty$) towards G_c, while in the IR ($t \to \infty$ or $k \to 0$), $G\,(t)$ vanishes. Therefore, G_c turns out to be a UV fixed point and $G = 0$ an IR fixed point.

The $B > 0$ case. In this case, $G\,(t)$ again flows towards G_c in the UV. In its flow towards the IR, however, $G(t)$ diverges at a finite value of k, $k = k_c$ ($t = t_c$) (see Fig. 3.1). As first noted by GN, this is also what happens for the IR flow of $G(t)$ in the $d = 2$ case.

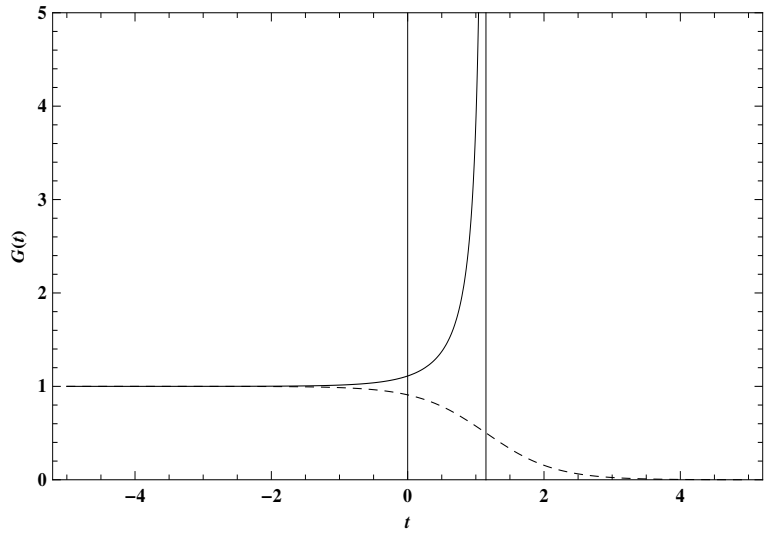

Figure 3.1: Using a rescaled coupling (so that $G_c = 1$), the running of $G(t)$ for $B = -0.1$ is shown (dashed line) and $B = 0.1$ (solid line), representing the symmetric and the broken phase respectively.

By computing the effective potential for their model in $d = 2$, they were actually able to relate the divergence of $G(t)$ at a finite value of the running scale with the existence of χSB and the consequent generation of a fermion mass.

In this respect, it should be observed that the appearance of such a divergence in the RG flow of the theory is nothing but the precursor of the transition to the broken phase which occurs when the boundary value of $G(t)$ at the UV scale Λ are chosen (say $G(t = 0)$ with $k_0 = \Lambda$) such that: $G(t = 0) > G_c$. This shows that G_c has to be identified with the critical point of the transition. In this case, the approximation of the potential with a polynomial expansion (a single term in the truncation of Eq. (3.102)) turns out to be a poor approximation.

As fluctuations of a longer and longer wavelength (i.e. the RG equations are runt towards the IR) being included, the system starts to develop an instability which eventually manifests itself in the divergence of the coupling constants. A clear illustration of this behaviour can be found in [58], where the same phenomenon was considered for a scalar theory.

Our next goal is to show that it is possible to describe the phase transition with the help of Eq. (3.101). In particular, in the next section, it will be seen that by means of our RG equations the critical exponents previously obtained in the framework of the $1/N$ expansion [19],[22],[23] can be reproduced.

3.4.2 Critical exponents with the RG approach

Now going back to Eq. (3.101) and considering the truncation, $V(\sigma,t) = -m(t)\sigma - \frac{G(t)}{2}\sigma^2$, for the potential $V(\sigma,t)$. Plugging this truncation in Eq. (3.101), the system of RG equations for $m(t)$ and $G(t)$ is found to be:

$$\frac{dm}{dt} = m + 2N\mathrm{tr}\,\mathbb{I}C_d\frac{Gm}{1+m^2}, \tag{3.106}$$

$$\frac{dG}{dt} = (2-d)\,G + 2N\mathrm{tr}\,\mathbb{I}C_d G^2\frac{1-m^2}{(1+m^2)^2}. \tag{3.107}$$

As for the truncation considered in the previous section, the above RG system has two fixed points: the Gaussian one ($m=0\,,\,G=0$) and the non-Gaussian one:

$$m = 0, \tag{3.108}$$

$$G = \frac{d-2}{2N\mathrm{tr}\,\mathbb{I}C_d}\,. \tag{3.109}$$

Note that Eq. (3.109) is nothing but G_c found in Eq. (3.104), when the truncation for $V(\sigma,t)$ given in Eq. (3.102) is considered , i.e. the truncation with the Fermi term only.

Linearizing Eqs. (3.106) and (3.107) around the Gaussian fixed point it is found:

$$\frac{dm}{dt} = m, \tag{3.110}$$

$$\frac{dG}{dt} = (2-d)\,G, \tag{3.111}$$

which show that both m and G are eigen-directions for the RG flow around the Gaussian fixed point, with eigenvalues given by ($m(t)\sim e^t$, $G(t)\sim e^{(2-d)t}$):

$$\lambda_m = 1, \tag{3.112}$$

$$\lambda_G = 2-d\,. \tag{3.113}$$

From Eqs. (3.112) and (3.113), one can see that, for $d>2$, m is a relevant direction, while G is irrelevant, this latter property being related to the perturbative non-renormalizability of the theory.

Linearizing now around the non-Gaussian fixed point one obtains:

$$\frac{dm}{dt} = [1+(d-2)]m, \tag{3.114}$$

$$\frac{d(G-G_c)}{dt} = [(2-d)+(2d-4)](G-G_c), \tag{3.115}$$

which show that, as for the case of the Gaussian fixed point, m and G are eigendirections for the RG flow. However, this time the eigenvalues are given by:

$$\lambda_m = d-1, \tag{3.116}$$

$$\lambda_G = d-2, , \tag{3.117}$$

which means that around this fixed point:

$$m(t) \sim e^{(d-1)t} \quad , \quad G(t) - G_c \sim e^{(d-2)t}. \tag{3.118}$$

As was anticipated, from Eqs. (3.116) and (3.117) (or from Eq. (3.118)), it is possible to see that around the non-Gaussian fixed point, for $d > 2$, *both* m and G are relevant couplings. Technically, it should be said that, within such a truncation, the (G, m) plane is a "UV critical surface" for the non-Gaussian fixed point ($G = G_c$, $m = 0$). This means that the coupling constants, whatever boundary conditions are considered in the (G, m) plane, flow towards the UV always reach the point ($G = G_c$, $m = 0$). From this more technical point of view, the theory is said to be "asymptotically safe" [59]. This is nothing but an extension of the notion of asymptotic freedom for the case when the UV fixed point, towards which the dimensionless coupling constants flow in the UV, is not the Gaussian one.

From Eqs. (3.110), (3.111), (3.112) and (3.113) it can be noted that the eigenvalues λ_m and λ_G around the Gaussian fixed point are nothing but the *canonical dimensions* of the coupling constant m and G. By comparing now with Eqs. (3.114), (3.115), (3.116) and (3.117), it is found that the *anomalous dimensions* γ_m and γ_G of m and G are:

$$\gamma_m = d-2, \tag{3.119}$$

$$\gamma_G = 2(d-2)\,. \tag{3.120}$$

In passing, one can note that, in ladder approximation, it is $\gamma_G = 2\gamma_m$, which was found.

As already stressed, the non-Gaussian fixed point is the critical point of the χSB transition and, from Eqs. (3.116) and (3.117), one can see that m and G are both relevant directions around this point. Moreover, in the ferromagnetic analogy, the eigenvalues λ_m and λ_G correspond to D_h and D_t, the critical exponents related to the magnetic field and the temperature respectively.

Now the hyperscaling relations which relate the different critical exponents β, δ, ... defined through Eqs. (2.94)-(2.103), can be obtained. These relations are verified under very general conditions [52],[53],[54]: the scale invariance of the $1PI$ vertex functions of elementary and/or composite operators, the existence of a fixed point and the possibility of linearizing the RG equations around the fixed point [3]. Under these conditions, the critical exponents are expressed in terms of the exponents related to the parameters relevant at the transition (m and G in this case, the magnetic field and the temperature in the ferromagnetic case).

Therefore, by following the same steps which gives the possibility of finding the hyperscaling relations related to the ferromagnetic phase transition [41], thus the analogous relations for the χSB transition in a fermion language are achieved:

$$\begin{aligned} \beta &= \frac{d-\lambda_m}{\lambda_G}, \qquad \delta = \frac{\lambda_m}{d-\lambda_m}, \\ \gamma &= \frac{2\lambda_m - d}{\lambda_G}, \qquad \nu = \frac{1}{\lambda_G}, \\ \eta &= 2 + d - 2\lambda_m. \end{aligned} \tag{3.121}$$

By replacing in Eqs. (3.121) the values of λ_m and λ_G found in Eqs. (3.116) and (3.117), it is finally obtained for the critical exponents:

$$\beta = \frac{1}{d-2}, \tag{3.122}$$

$$\delta = d-1, \tag{3.123}$$

$$\gamma = 1, \tag{3.124}$$

$$\nu = \frac{1}{d-2}, \tag{3.125}$$

$$\eta = 4-d\,. \tag{3.126}$$

These values coincide with those obtained in the leading order of the $1/N$ expansion [19], [22],[23].

As is well known, $d = 4$ is the upper critical dimension: for $d > 4$, the theory becomes free and the mean field results are exact. At $d = 4$, the correlation functions get weak logarithmic corrections to simple power law behaviour. However, the approximation that

[3] This means that the cases when the operators are either relevant or irrelevant are considered excluding the case when marginal operators appear. When this happens, as is well known, weak violations to the scaling relations appear. In this case, the behaviour of the vertex functions is not described by simple power laws.

is considered, the LPA, does not allow the detection of the corresponding hyperscaling violations. The latter are actually due to non-local contributions, which are absent in the LPA. Nevertheless, the occurrence of the transition can be observed already at this stage of the approximation. This is exactly what was seen. For a more detailed study, the presence of non-local terms needs to be considered. Work is in progress in this direction.

3.4.3 Crossover and mass generation

In the previous section, it was seen how the RG equations for $m(t)$ and $G(t)$ allows the computation of the critical exponents which give the behaviour of the correlators for values of G close to the critical point. To this end, it was sufficient to study the linearized equations in the neighborhood of the non trivial fixed point ($G = G_c, m = 0$). In this section the previous analyses are extended to the study of the G and m flows in the whole (G, m) plane. As will be seen, these flows show interesting features in connection with the problem of the generation of fermion masses.

The starting point of our analysis is the coupled system of RG equations, Eqs. (3.106) and (3.107), which are here reproduced for readers' convenience:

$$\frac{dm}{dt} = m + 2N\mathrm{tr}\,\mathbb{I}C_d\frac{Gm}{1+m^2}, \tag{3.127}$$

$$\frac{dG}{dt} = (2-d)\,G + 2N\mathrm{tr}\,\mathbb{I}C_dG^2\frac{1-m^2}{(1+m^2)^2}. \tag{3.128}$$

The flows of m and G obtained by solving Eqs. (3.127) and (3.128) are governed by the presence of the two fixed points found in the previous section, the Gaussian and the non trivial one. For definiteness, in the following these solutions are drawn for the $d = 4$ case, although similar flows also hold for other values of d in the range $2 < d < 4$.

In Fig. 3.2 the numerical solutions of Eqs. (3.127) and (3.128) are shown, in the (G, m) plane, for different boundary values. For convenience, the parameters are rescaled in a manner which amounts to set $N = C_d = \mathrm{tr}\,\mathbb{I} = 1$ (for $d = 4$, this gives $G_c = 1$). As has already been seen, the non-trivial fixed point is IR repulsive, while the Gaussian one has an irrelevant direction (G) and a relevant one (m). Therefore, all the flows emanate from the non trivial fixed point at $k = \infty$ and move towards the IR, asymptotically converging to the $G = 0$ axis.

In each of these trajectories, the bare couplings have to be identified with values of m and G near the non trivial fixed point (UV region), the renormalized ones with those

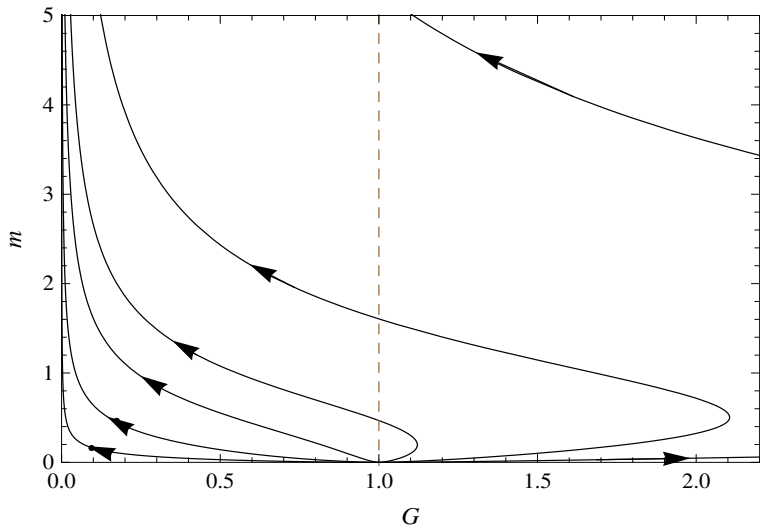

Figure 3.2: The three trajectories which lie entirely on the left of the $G = G_c$ axis are obtained for $G_B = G_c - 0.1 < G_c$ and $m_B = 0.1, 0.01, 2 * 10^{-3}$ (from top to bottom respectively). The three other trajectories are obtained by setting $G_B = G_c + 0.1 > G_c$ for the same values of m_B (again from top to bottom).

in the IR region. Moreover, as seen in the previous section from the linearization of Eqs. (3.127) and (3.128) around the fixed points, while the IR flow is governed by the Gaussian scaling, so that the (renormalized) couplings in this region scale according to their canonical dimension, in the UV the (bare) couplings acquire an anomalous scaling (see Eqs. (3.119) and (3.120)) due to the presence of the non trivial fixed point. By considering again the analogy with the ferromagnetic phase transition, this is exactly what happens to the relevant coupling in that case. Around the critical point of the transition (Wilson-Fisher fixed point), the squared mass (bare value of the coupling) has an anomalous scaling while in the IR its renormalized value (the inverse square correlation length) scales with the canonical dimension [50],[51].

A close inspection to the trajectories of Fig. 3.2 shows that they are of four different types. Two of them lie on the G axis and correspond to the flows already studied in Section 3. Starting with the UV boundaries $m = 0$ and $G < G_c$, the trajectory flows along the G axis (from the right to the left) towards the Gaussian fixed point. If, on the contrary, one starts with the UV boundaries $m = 0$ and $G > G_c$, the flow proceeds along the G axis towards the right side and reaches $G = \infty$ at a finite value of t (finite value of k). These flows correspond to the symmetric and broken phases respectively.

If instead the UV boundary $m \neq 0$ is chosen, the two following types of trajectories

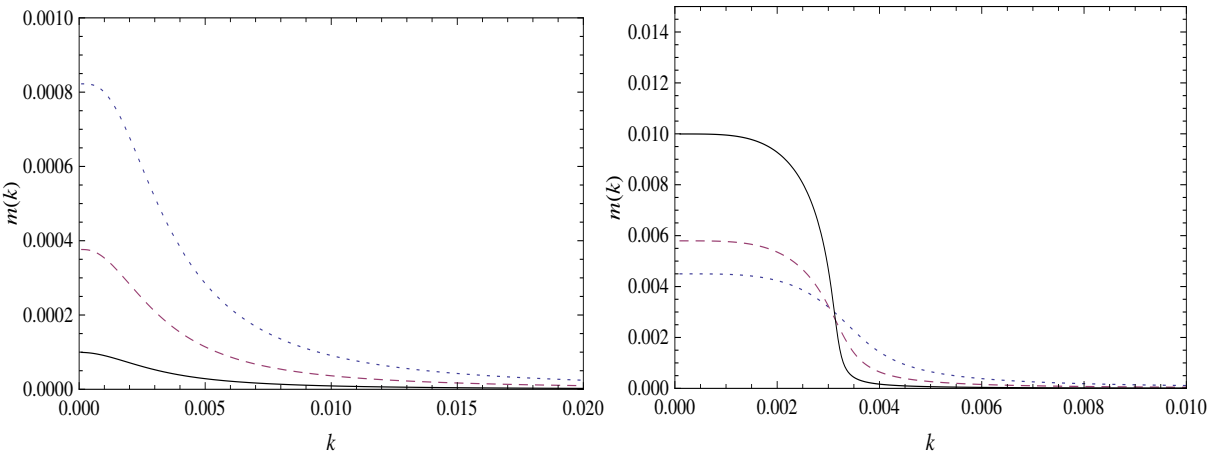

Figure 3.3: (a): The running dimensionful mass obtained by setting, at $k = \Lambda = 1$, $G_B = G_c - 10^{-5}$ and $m_B = 10^{-8}, 4 * 10^{-9}, 10^{-9}$ (dotted, dashed and solid lines, respectively). (b): The running dimensionful mass obtained by setting, at $k = \Lambda = 1$, $G_B = G_c + 10^{-5}$ and $m_B = 10^{-8}, 4 * 10^{-9}, 10^{-9}$ (dotted, dashed and solid lines, respectively). All quantities are expressed in cut-off units.

arise. For the UV boundary $G < G_c$, the flow proceeds from right to left asymptotically converging on the m axis. When, on the contrary, the UV boundary $G > G_c$ is chosen, the trajectory initially flows from left to right, moving away from the $G = G_c$ axis. Then, after creating a more or less pronounced horizontal bell, it turns back, crosses the $G = G_c$ axis and eventually converges asymptotically on the m axis as in the previous case.

These latter two types of trajectories are very interesting for our analysis. Let us choose an *infinitesimal* value as UV boundary for m. When the corresponding UV boundary for G is $G < G_c$, the trajectory runs very close to the G axis from the right to the left for a long "RG time interval", eventually escaping to reach the m axis asymptotically. The smaller the initial value of m, the closer the trajectory is to the G axis. If the UV boundary for G is $G > G_c$, the trajectory initially runs very close to the G axis (as in the previous case, but in the opposite sense) for a long "RG time", then it creates a *very elongated bell* (before turning back to reach asymptotically the m axis). For smaller and smaller initial values of m, the bell becomes more and more elongated. By comparing these trajectories with those obtained for the limiting UV boundary $m = 0$, it can immediately be seen that the limiting case of the first kind of trajectories corresponds to the (strictly) unbroken phase, while the limiting case of the second kind of trajectories corresponds to the (strictly) broken phase.

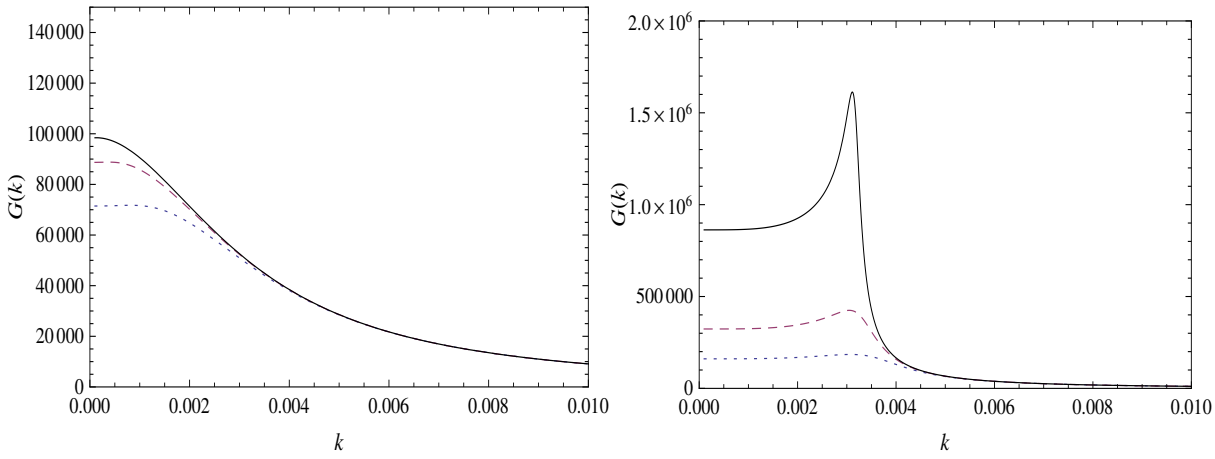

(a) (b)

Figure 3.4: (a): The running of the dimensionful coupling $G(k)$ obtained by setting, at $k = \Lambda = 1$, $G_B = G_c - 10^{-5}$ and $m_B = 10^{-8}, 4*10^{-9}, 10^{-9}$ (dotted, dashed and solid lines, respectively). (b): The running of the dimensionful coupling $G(k)$ obtained by setting, at $k = \Lambda = 1$, $G_B = G_c + 10^{-5}$ and $m_B = 10^{-8}, 4*10^{-9}, 10^{-9}$ (dotted, dashed and solid lines, respectively). All quantities are expressed in cut-off units.

In order to understand better the physics related to these two types of trajectories, the flows of the corresponding dimensionful running mass $m(k)$ and Fermi constant $G(k)$ is considered. The RG equations for $m(k)$ and $G(k)$ can be obtained from Eqs. (3.127) and (3.128) by noting that: $m(k) = k\, m(t)$ and $G(k) = G(t)/k^2$. Alternatively, these equations can be directly calculated from Eq. (3.100) by truncating the dimensionful potential $U(\sigma)$ as: $U(\sigma) = m(k)\,\sigma - \frac{G(k)}{2}\,\sigma^2$. Specifying to the $d = 4$ case, it it found (NG is redefined as G):

$$\frac{dm}{dk} = -\frac{k^3}{2\pi^2}\frac{Gm}{k^2+m^2}, \tag{3.129}$$

$$\frac{dG}{dk} = -\frac{k^3}{2\pi^2}\frac{G^2\,(k^2-m^2)}{(k^2+m^2)^2}. \tag{3.130}$$

Now the present task is to solve Eqs. (3.129) and (3.130) numerically. Before doing that, however, it is worth noting that, although it is not possible to find the exact solution for this system, it is easy to get the asymptotic IR ($k \to 0$) and UV ($k \to \infty$) analytical behaviour for $m(k)$ and $G(k)$:

$$k \to 0: \quad m(k) \sim \overline{m} = \text{Const.} \quad ; \quad G(k) \sim \overline{G} = \text{Const.} \tag{3.131}$$

$$k \to \infty: \quad m(k) \sim \frac{1}{k^2} \quad ; \quad G(k) \sim \frac{1}{k^2}\,. \tag{3.132}$$

This asymptotic behaviour can be easily checked against the numerical solutions presented in Figs. 3.3 and 3.4.

Now the Eqs. (3.129) and (3.130) are numerically solved. By choosing at the UV boundary $k = \Lambda$ an infinitesimal value for the bare mass $m(\Lambda)$, the running of the equations is considered once for $G(\Lambda) < 1/\Lambda^2$ and once for $G(\Lambda) > 1/\Lambda^2$ (remember that $G_c = 1$ for our choice). The units are so chosen that $\Lambda = 1$. The results for the running of $m(k)$ are shown in Fig. 3.3. In the left panel (a) the solutions obtained by taking $G(\Lambda) < 1/\Lambda^2$ are presented for different values of $m(\Lambda)$, in the right panel (b) those for $G(\Lambda) < 1/\Lambda^2$ are related to the same values of the bare masses.

By comparing the figures in these two panels, it immediately found that the smaller the initial (UV) value of the bare mass, the larger the difference between the renormalized masses, i.e. the values of $m(k)$ at $k = 0$.

Physically this is very interesting. It means that if in the UV ($k = \Lambda$) an infinitesimal value for the bare mass $m(\Lambda)$ is set, when $G(\Lambda) < 1/\Lambda^2$, the renormalized mass $m(k = 0)$ turns out not to be much different from the initial bare value. On the contrary, when $G(\Lambda) > 1/\Lambda^2$, a magnification mechanism triggers the generation of a finite value for the fermion mass.

Let us look, for instance, at the continuous line in Fig. 3.3(b). Starting from the UV, one should observe that, for a long RG time, $m(k)$ runs very close to the $m = 0$ axis. At a certain value of k, however, it climbs up steeply to its IR (renormalized) value. From the continuous line in Fig. 3.3(a), the corresponding picture for $G(\Lambda) < 1/\Lambda^2$, one can see that in this case no such mechanism is operating.

In Fig. 3.4 the corresponding flows for the running of $G(k)$ are presented. The left panel (a) shows the $G(\Lambda) < 1/\Lambda^2$ case, the right panel (b) the $G(\Lambda) > 1/\Lambda^2$ one. The continuous lines in Figs. 3.4(b) and 3.3(b) are obtained for the same boundary values of G and m. The running Fermi constant $G(k)$ has a peak in correspondence of the "step" in $m(k)$.

Turning back to Fig. 3.1, where the flows were studied in the plane of the dimensionless parameters $m(t)$ and $G(t)$, one can understand that the elongated horizontal bells on the right of the $G = G_c$ axis are the reflection of the steepness of $m(k)$ (and the peak of $G(k)$) at a finite value of k . They are more or less elongated according to the degree of steepness of $m(k)$ (and to the height of the peak of $G(k)$), which in turn depends on the

value of the bare mass.

The physical picture of what was found should be clear by now. This is the presence of a crossover phenomenon. As in the case of the strict unbroken-broken phase transition, for values of G_B greater than a critical value, the fermion system is unstable against quantum fluctuations. The presence of an even infinitesimal bare fermion mass triggers an amplification mechanism which resolves the instability through the generation of a finite fermion mass.

In our opinion, such a mechanism is physically more grounded than the picture obtained with a strictly vanishing m_B. The reason is explained in the following. Apart from the Theory of Everything (TOE), every quantum field theory (QFT) is an effective theory valid up to a certain scale Λ, the physical cut-off. Actually, QFTs are organized in a hierarchical manner, each having a lower and lower range of validity. The way the TOE gives rise to this chain of lower-energy effective theories is easily pictured if one thinks of the RG flow in the TOE coupling constants space. This flow emanates from the UV fixed point of the TOE. Following the Wilson-Kadanoff approach, in the original (UV) lagrangian any coupling constant should be considered, i.e. any operator, whatever is needed in physics, even those of condensed matter [4]. The RG flow (the renormalized trajectory) then dictates the relevance or irrelevance of the different coupling constants in the various energy regimes. In its way towards the infrared, the renormalized trajectory actually approaches several fixed points. These points create basins of attractions for the RG flow, so giving rise to the lower energy theories as the electroweak theory, QCD, QED, ... Within such a Wilson-Kadanoff picture, operators which are relevant in a certain energy regime become irrelevant at different scales and vice-versa [58].

In the present case, a non-trivial fixed point for a simple fermion theory was found. Within the above picture, this means that there is a certain energy range where the flow is governed by this fixed point. The RG trajectory passes close to this point. Therefore, when the renormalized trajectory is in this region, the mass term is very small, although not strictly vanishing. As has been seen above, if one also has a bare value of the Fermi constant greater than a certain value, then a dynamical mechanism is operating to generate a finite value of the fermion mass.

[4] Naturally, all these terms are generally complicated composite operators in terms of the fundamental degrees of freedom of the TOE.

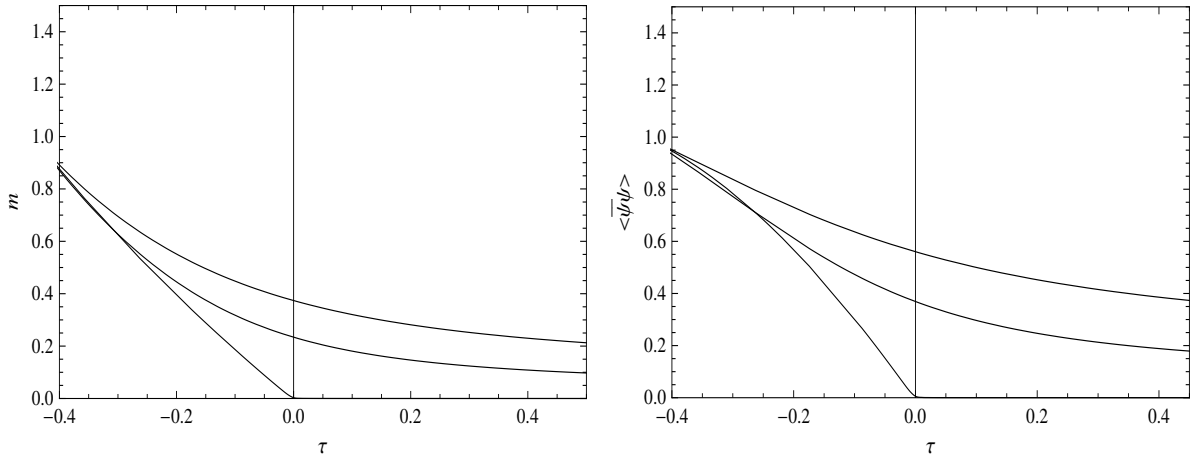

Figure 3.5: Different phase diagrams showing the normalized mass (a) and the vev $\langle\bar{\psi}\psi\rangle$ (b) as functions of $\tau = 1/G_B - 1/G_c$. The different lines correspond (from top to bottom) to the choices: $m_B = 10^{-1}, 5 * 10^{-2}, 10^{-4}$. All quantities are expressed in cut-off units.

What was found is reminiscent of what happens in the ferromagnetic case. In the presence of a weak external magnetic field, if the temperature is higher than the critical temperature, $T > T_c$, the spin alignment is just the one produced by the weak magnetic field. A weak magnetization of the ferromagnetic material, which is basically of the same order of the applied external field, should be observed. On the contrary, when the temperature is lower than the critical temperature, $T < T_c$, due to large fluctuations, an even infinitesimal external field h can trigger a macroscopic alignment of spins, so that the resulting magnetization of the ferromagnetic material is macroscopic, much greater than the applied external field.

In this respect, it is interesting to note that, if a two dimensional Ising model is considered, where in addition to the nearest-neighbourhood interactions the magnetic field coupled to the spins is taken into account, the RG trajectories in the (J, h) plane closely resemble the RG trajectories in the (G, m) plane [35].

Finally, in order to appreciate better how this cross-over picture contains all the physical features of a phase transition, the dependence of the physical fermion mass on the "reduced temperature" $\tau = 1/G_B - 1/G_c$ is studied. In the analogy with the ferromagnetic transition, this corresponds to the dependence of the magnetization M on $T - T_c$. Alternatively, as in the Hartree approximation one can easily obtain the relation

$$m = m_B - G_B \langle\bar{\psi}\psi\rangle \ , \tag{3.133}$$

and also consider the dependence on τ of $\langle\bar{\psi}\psi\rangle$. The results are shown in Fig. 3.5, where it is possible to see how, depending on the value of m_B, the system passes from a smoother cross-over picture to a sharper one (for smaller values of m_B), the latter having all the features of a strict symmetry breaking transition, actually being indistinguishable from it for very small values of m_B. In the authors' opinion, Fig. 3.5 clearly shows how this cross-over picture is perfectly suited for implementing the phase transition, with the consequent dynamical generation of fermion masses.

In the coming Section, it is shown that it is possible to find very good approximate analytical solutions to our RG equations, thus providing the profile of $m(k)$ (and $G(k)$) in the whole k range.

3.4.4 Analytical approximations to the RG equations

In the previous section the numerical solutions of Eqs.(3.129) and (3.130) were studied and it was found that the chiral transition is described in a very satisfactory manner in terms of a cross-over phenomenon.

Now it will be shown how different degrees of analytical approximations to our RG equations can be obtained. At first, it will be seen that it is possible to reproduce the NJL result with a simple approximation, which (for obvious reasons) is called the NJL approximation. Despite of its simplicity, this approximation contains the qualitative features which describe the chiral transition.

For the present analysis, this is an important point. On the one hand, it shows that the NJL (non-perturbative) approach is already efficient in grasping the physical mechanism behind the dynamical breaking of the symmetry, i.e. in describing the physics of the transition. On the other hand, it will be shown that the NJL result is well understood as an approximate solution to the RG equations, which are naturally designed to take into account, in a systematic manner, the non-perturbative dynamics of the quantum fluctuations responsible for the transition.

Finally, higher order analytical approximations are considered, which reproduce not only the qualitative but also the quantitative predictions of the full RG equations.

NJL approximation

First of all the NJL approximation is considered. Their well known gap equation is easily obtained from Eq. (3.129) for the dimensionful mass $m(k)$ once for the r.h.s. (right-hand-side) of this equation the two approximations indicated in the following are considered.

In the previous section, the IR and the UV asymptotic behaviour of $m(k)$ and $G(k)$ was found. In particular, it has been seen that the solution to the equation for $G(k)$ in the UV gives: $G(k) \sim 1/k^2$. By considering now a UV scale $k = \Lambda$, the running Fermi constant $G(k)$ in the r.h.s. of Eq. (3.129) is approximated with its UV value $G(\Lambda)$.

The second step of this approximation consists in replacing in the r.h.s. of Eq. (3.129) the running mass $m(k)$ with its IR value $\overline{m} = m(0)$. This latter approximation can be partially justified for the denominator $k^2 + m(k)^2$. In fact, in the IR the dominating term is the mass term, which has already almost saturated to its IR value $\overline{m}^2$, while in the UV the dominating term is k^2 (and the actual value of $m(k)^2$, which anyhow in the UV vanishes as $1/k^2$) does not really matter. As for the numerator, this approximation is justified only in the IR. As already noted, in fact, in the UV the mass runs as $1/k^2$.

None of these approximations for $m(k)$ and $G(k)$ can be justified in the entire IR-UV range. As was anticipated, however, despite the fact that these are somehow crude approximations, they retain some of the important features of the non-perturbative RG equations. For this reason, they are able to grasp the fundamentally non-perturbative nature of the dynamical mechanism which is responsible for the transition from the unbroken to the broken phase.

Then by inserting these approximations in the r.h.s. of Eq. (3.129). Defining the dimensionless Fermi constant $\tilde{G}_\Lambda = G_\Lambda \, \Lambda^2$, Eq. (3.129) is then approximated as:

$$\frac{dm(k)}{dk} = -\frac{k^3}{2\pi^2} \, \overline{m} \, \frac{\tilde{G}_\Lambda}{\Lambda^2} \, \frac{1}{k^2 + \overline{m}^2} \, . \tag{3.134}$$

Integrating this equation between $k = 0$ and $k = \Lambda$ one obtains:

$$m\,(\Lambda) - m\,(0) = -\frac{m\tilde{G}_\Lambda}{4\pi^2} \left[\Lambda^2 - m^2 \ln\left(1 + \frac{\Lambda^2}{m^2}\right) \right] \, . \tag{3.135}$$

Eq. (3.135), where $m(0)$ is nothing but $\overline{m}$, is already the NJL result. In fact, once one identifies $m(\Lambda)$ with the bare mass, $m(\Lambda) = m_B$, and note that $\Lambda^2/\overline{m}^2 >> 1$, Eq. (3.135)

is immediately written as:

$$\overline{m} - m_B = \frac{\overline{m}\,\tilde{G}_\Lambda}{4\pi^2}\left(1 - \frac{\overline{m}^2}{\Lambda^2}\ln\frac{\Lambda^2}{\overline{m}^2}\right), \tag{3.136}$$

Finally, if the bare mass vanishes, which is the requirement for a massless chiral invariant bare theory, it is obtained:

$$\frac{4\pi^2}{\tilde{G}_\Lambda} = 1 - \frac{\overline{m}^2}{\Lambda^2}\ln\frac{\Lambda^2}{\overline{m}^2}\,, \tag{3.137}$$

which is indeed the celebrated NJL result. For values of $\tilde{G}_\Lambda$ greater than $G_c = 4\pi^2$, Eq. (3.137) admits a non vanishing solution for the fermion mass $\overline{m}$, while for values of $\tilde{G}_\Lambda$ smaller than $G_c = 4\pi^2$, the only solution for $\overline{m}$ is $\overline{m} = 0$.

Although Eq. (3.137) does not provide a profile function for the running mass $m(k)$, still, through the connection between the UV value of the mass $m(\Lambda) = m_B = 0$ and its IR value $m(0) = \overline{m}$, the transition from the unbroken to the broken phase can be described. It is worth noting that a non vanishing solution for $\overline{m}$ can also be found for non-vanishing values of $m(\Lambda) = m_B$. This is somewhat closer in spirit to our result, where it was shown that for finite values of the scale Λ, $m(\Lambda)$ is of order $1/\Lambda^2$ rather than being strictly vanishing. Again it is important to stress that, even though the entire profile of $m(k)$ is missing (which is intrinsically in the nature of the approximation that we are considering), the possibility of it still being in one of the two phases is given by the connection between the UV value of the mass $m(\Lambda)$ and the corresponding IR value $\overline{m}$.

Beyond the NJL approximation

Now it is shown that it is possible to find approximate analytical solutions to Eqs. (3.129) and (3.130) which go beyond the NJL approximation considered in the previous subsection and provide, to some extent, quite accurate estimates of the exact numerical results that we found in Section 5. For the sake of definiteness, again the $d = 4$ dimensions are chosen, although the following reasoning applies to any dimension.

For the readers' convenience, Eqs. (3.129) and (3.130) are written again:

$$\frac{dm}{dk} = -\frac{k^3}{2\pi^2}\frac{Gm}{k^2+m^2}, \tag{3.138}$$

$$\frac{dG}{dk} = -\frac{k^3}{2\pi^2}\frac{G^2\left(k^2-m^2\right)}{\left(k^2+m^2\right)^2}\,, \tag{3.139}$$

where, as already noted, N has been absorbed in the redefinition of G.

First of all the Eq. (3.139) is considered. It has already been noted (see Eqs. (3.131) and (3.132)) that for $k \to \infty$, $m(k) \sim 1/k^2$ and for $k \to 0$, $m(k) \sim \overline{m} = \text{Const.}$. Therefore, one should expect that, if in the r.h.s. of Eq. (3.139), $m(k)$ is replaced with its IR value $\overline{m}$, a quite good approximation to this equation should be found. In the UV regime, in fact, k^2 is by far the dominant term when compared to $m(k)^2$ and it should not change much either the actual value $m(k)$ or the approximated one, $\overline{m}$ are considered. In the IR, on the other hand, $m(k)$ converges to $\overline{m}$. Therefore, in these asymptotic regimes (IR and UV), this is certainly a good approximation. Clearly, one cannot expect that it describes the intermediate regimes with the same degree of accuracy , i.e. the region of k where $m^2(k)$ is of the order of k^2. As will be seen, however, it still provides a profile for $G(k)$ which is in good qualitative and quantitative agreement with the exact numerical results.

Performing then this replacement in Eq. (3.139), the integration is easily done and one obtains:

$$G(k) = \frac{\overline{G}}{1 + \frac{\overline{G}}{4\pi^2}\left[k^2 - 3\overline{m}^2 \ln\left(1 + \frac{k^2}{\overline{m}^2}\right) + 2\overline{m}^2 - \frac{2\overline{m}^4}{k^2+\overline{m}^2}\right]}\,, \tag{3.140}$$

where $\overline{G}$ is the IR value of $G(k)$: $\overline{G} = G(k=0)$.

It is easy to see that the IR and UV limits of Eq. (3.140) are:

$$k \to 0 \quad : \qquad G(k) \sim \overline{G} + \frac{\overline{G}^2}{8\pi^2\overline{m}^2}k^4 \tag{3.141}$$

$$k \to \infty \quad : \qquad G(k) \sim \frac{4\pi^2}{k^2}\,, \tag{3.142}$$

in agreement with the expectations. Some comments on these results.

First of all it can be noted that Eq. (3.140) has a maximum for $k = \overline{m}$. If this result is compared with the numerical solutions for $G(k)$ and $m(k)$ shown in Figs. 3.4(b) and 3.3(b), one can see that, while it is true that the maximum of $G(k)$ is obtained for k of the order of $\overline{m}$, the actual value k_{max} where $G(k)$ has a maximum does not coincide with $\overline{m}$. As one can see from Fig. 3.3(b), k_{max} is also close to the inflection point of $m(k)$: in the region around these values of k, the flows of $m(k)$ and $G(k)$ change from their UV to their IR scaling. Actually, for lower values of k, $m(k)$ and $G(k)$ rapidly saturate to their IR values. This latter observation is a general feature of the RG flow equations. When the flows reach the region where $m^2(k)$ is of the order of k^2, the coupling constants rapidly saturate to their IR values so that they get practically frozen.

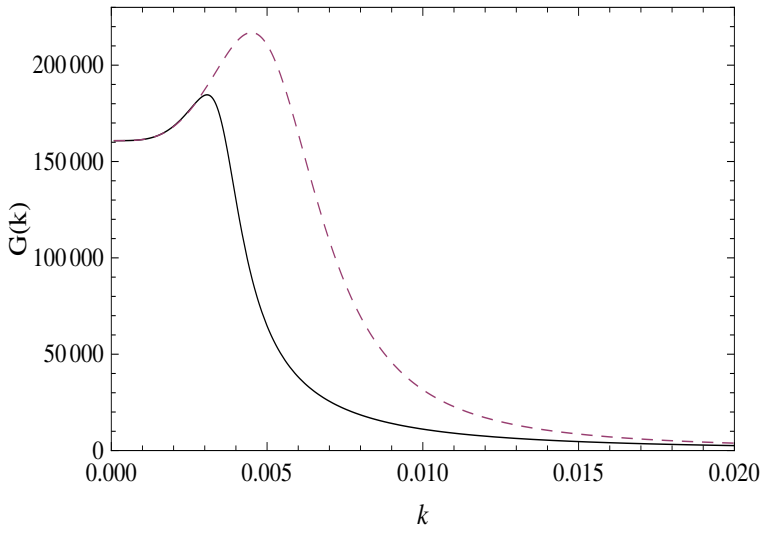

Figure 3.6: The numerical solution (solid line) of Eq. (3.139) for the broken phase where $m_B = 10^{-8}$ and $G_B = G_c + 10^{-5} = 1 + 10^{-5}$ ($\overline{m} = 4.50 \cdot 10^{-3}$, $\overline{G} = 1.61 \cdot 10^5$) and the corresponding analytical approximation (dashed line) Eq. (3.140).

The fact that the maximum of $G(k)$ is not exactly at $k = \overline{m}$ clearly shows what was observed above: in the intermediate region, the analytical approximation Eq. (3.140) cannot reproduce all the quantitative details of the exact $G(k)$ profile (in the IR and in the UV, on the contrary, as shown in Eqs. (3.141) and (3.142), Eq.(3.140) provides a very good approximation for $G(k)$).

However, as shown in Fig. 3.6, where the numerical solution of Eq. (3.139) is compared with the corresponding approximation Eq. (3.140) for $\overline{m} = 4.50 \cdot 10^{-3}$ and $\overline{G} = 1.61 \cdot 10^5$, the two curves are in quite good agreement. They coincide in the IR and UV ends, while in the intermediate region the analytical approximation somehow overestimates $G(k)$.

From Eq. (3.141) it has been seen that, near $k = 0$, $G(k)$ is always increasing. As it is known that, for higher values of k, this function decreases, it is clear that $G(k)$ has always a maximum. The location of the maximum and the height of $G(k)$ at the maximum depend on $\overline{m}$. In Section 5, where our cross-over picture was presented, it was learned that infinitesimal values of the IR mass $\overline{m}$ correspond to the unbroken phase. In this case, the maximum is a hardly detectable disturbance on the top of the already saturated value $\overline{G}$ of $G(k)$ in the IR region (see Fig. 3.4 (a)). Finite values of the IR mass, on the contrary, correspond to very pronounced maxima for $G(k)$ (see Fig. 3.4 (b)) and are related to the broken phase. For the limiting case $\overline{m} \to 0$, the maximum is reached at

$k = 0$. In this case, in fact, replacing $m = 0$ in Eq. (3.139), this equation can immediately be integrated and gives:

$$G(k) = \frac{\overline{G}}{1 + \frac{\overline{G}}{4\pi^2}k^2} = \frac{4\pi^2}{k^2 + \frac{4\pi^2}{\overline{G}}} = \frac{4\pi^2}{k^2 + M_1^2}\,, \tag{3.143}$$

where $M_1^2 = \frac{4\pi^2}{\overline{G}}$ has been defined.

Now Eq. (3.138) is considered. In the IR region, where $G(k)$ and $m(k)$ have essentially saturated to their IR values $\overline{G}$ and $\overline{m}$, Eq. (3.138) can be approximated with:

$$\frac{dm(k)}{dk} \;=\; -\frac{\overline{G}}{2\pi^2\,\overline{m}}\,k^3, \tag{3.144}$$

which is immediately integrated:

$$m(k) = \overline{m} - \frac{\overline{G}}{8\pi^2\,\overline{m}}\,k^4\,. \tag{3.145}$$

Eq. (3.145) gives the behaviour of $m(k)$ near $k = 0$ and shows the way $m(k)$ approaches $\overline{m}$ at $k = 0$. As for the UV region, it is already known that in the r.h.s. of Eq. (3.138) it is possible to replace $G(k)$ with $\frac{4\pi^2}{k^2}$ and neglect $m(k)^2$ in the denominator. The solution in this region is then:

$$m(k) = m(k_*)\,\frac{k_*^2}{k^2}\,, \tag{3.146}$$

where k_* is any UV value of k, i.e. a value of k where the above UV approximations for $m(k)$ and $G(k)$ are valid. In Eq. (3.146), $m(k_*)\,k_*^2$ is the integration constant. As in solving Eq. (3.138) it has already used the boundary condition $m(k = 0) = \overline{m}$ (see Eq. (3.145)), this constant is virtually known. The reason why, at this stage, it is unknown is that the UV approximation of Eq. (3.138) has been integrated and the matching condition between this UV tail of $m(k)$ and its IR part is unknown, Eq. (3.145). As long as these asymptotic (IR and UV) regions are considered, it cannot do better.

In order to get an analytical approximation for $m(k)$ in the whole range of k, one could try to integrate Eq. (3.138) where in the r.h.s. $G(k)$ is replaced with its approximation given by Eq. (3.140). The resulting equation, however, is still too complicated and an analytical solution to this equation was not still found.

Nevertheless, a very good approximation of Eq. (3.140) can be considered which is suited for our aim of making the analytical integration of Eq. (3.138) possible. This is obtained by dividing the whole $[0, \infty)$ k range in three regions: an IR $[0, k_1]$, an

intermediate $[k_1, k_2]$ and a UV $[k_2, \infty)$ region. In the first region, $G(k)$ is approximated with $\overline{G}$. In the intermediate region,$G(k)$ is approximated with the Lorentzian which is obtained by expanding the denominator of Eq. (3.140) around $k_{max} = \overline{m}$ up to quadratic terms in k. In the UV region, $G(k)$ is approximated by $\frac{4\pi^2}{k^2}$. Therefore, the approximation to Eq. (3.140) is:

$$G(k) = \overline{G}\theta\left(k_1 - k\right) + \frac{8\pi^2\theta\left(k - k_1\right)\theta\left(k_2 - k\right)}{\left(k - \overline{m}\right)^2 + M_2^2} + \frac{4\pi^2\theta\left(k - k_2\right)}{k^2}\,, \tag{3.147}$$

where

$$M_2^2 = \frac{8\pi^2}{\overline{G}}\left(1 + \frac{\overline{G}\,\overline{m}^2}{4\pi^2}(2 - 3\ln 2)\right) \tag{3.148}$$

The values of k_1 and k_1 are chosen in such a way that Eq. (3.140) is well reproduced by Eq. (3.147).

Inserting Eq. (3.147) in Eq. (3.138) and replacing in the denominator of the r.h.s. of this latter equation $m(k)$ with $\overline{m}$, Eq. (3.138) is easily integrated. The result is:

$$\begin{aligned}
m(k) &= \overline{m}\exp\left(-\theta\left(k_1 - k\right)\frac{\overline{G}}{4\pi^2}\left(k^2 - \overline{m}^2\ln\left(1 + \frac{k^2}{\overline{m}^2}\right)\right)\right.\\
&- \theta\left(k - k_1\right)\theta\left(k_2 - k\right)\frac{2}{4M_2\overline{m}^4 + M_2^5}\left(M_2^5\ln\left(1 + \frac{k^2 - 2k\overline{m}}{\overline{m}^2 + M_2^2}\right)\right.\\
&+ 4M_2\overline{m}^4\left(\ln\left(1 + \frac{k^2 - 2k\overline{m}}{\overline{m}^2 + M_2^2}\right) + \tan^{-1}\left(\frac{k}{\overline{m}}\right)\right)\\
&+ M_2^3\overline{m}^2\left(\ln\left(1 + \frac{k^2 - 2k\overline{m}}{\overline{m}^2 + M_2^2}\right) - \ln\left(1 + \frac{k^2}{\overline{m}^2}\right)\right)\\
&+ 2M_2^4\overline{m}\left(\tan^{-1}\left(\frac{k - \overline{m}}{M_2}\right) + \tan^{-1}\left(\frac{\overline{m}}{M_2}\right)\right)\\
&- 2M_2^2\overline{m}^3\left(\tan^{-1}\left(\frac{k - \overline{m}}{M_2}\right) + \tan^{-1}\left(\frac{\overline{m}}{M_2}\right)\right)\\
&+ 4\overline{m}^5\left(\tan^{-1}\left(\frac{k - \overline{m}}{M_2}\right) + \tan^{-1}\left(\frac{\overline{m}}{M_2}\right)\right)\Bigg)\\
&- \left.\theta\left(k - k_2\right)\ln\left(\frac{k^2}{\overline{m}^2} + 1\right)\right)\,.
\end{aligned} \tag{3.149}$$

In Figs. 7(b) and 8(b) two specific examples for Eq. (3.149) are plotted by considering the same values of $\overline{G}$ and $\overline{m}$ used in Fig. 3.6 (broken and symmetric phase respectively).

First of all the broken phase is considered. In Fig. 3.7(a) three curves are shown which reproduce the numerical solution of Eq. (3.139) (solid line), the corresponding analytical

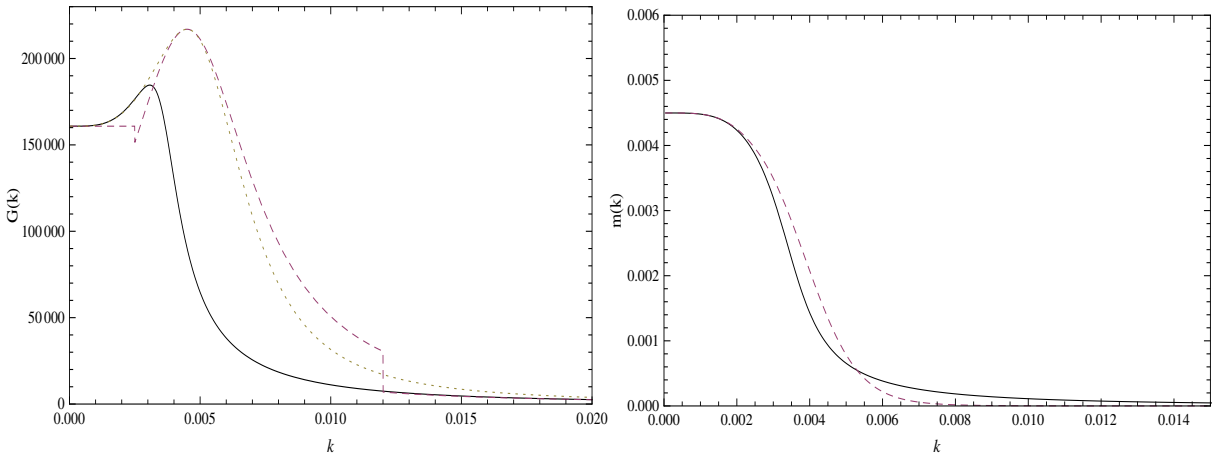

(a) (b)

Figure 3.7: (a) The dotted line is the approximation to $G(k)$ given in Eq. (3.140), in the broken phase, for $\overline{m} = 4.50 \cdot 10^{-3}$ and $\overline{G} = 1.61 \cdot 10^{5}$. The dashed line is the approximation to Eq. (3.140) given in Eq. (3.147) with the appropriate choice of k_1 and k_2. For comparison, the numerical solution (solid line) of Eq. (3.139) is also plotted. The values of $\overline{m}$ and $\overline{G}$ are as in Fig. 3.6. (b) The dashed line is the analytical approximation to $m(k)$ given in Eq. (3.149) for the same values of the parameters. The corresponding numerical solution (solid line) to Eq. (3.138) is also plotted.

approximation Eq. (3.140) (dotted line) and the approximation of Eq. (3.140) (dashed line) given by Eq. (3.147) obtained with the values of $\overline{G}$ and $\overline{m}$ used in Fig. 3.6. From Fig. 3.7(a), it is clear that Eq. (3.147) provides a very good estimate of Eq. (3.140).

In Fig. 3.7(b) the analytical approximation to $m(k)$ is plotted Eq. (3.149) (dashed line) (which is related to Eq. (3.147) plotted in Fig. 3.7(a) (dashed line)) and it is compared with the corresponding numerical result (solid line). From the above findings, it is immediately clear that the approximated analytical solution is in excellent agreement with the exact profile of $m(k)$.

Now the symmetric phase is taken into account. Again the values of $\overline{m}$ and $\overline{G}$, considered in Fig. 3.6, are chosen. In Fig. 3.8(a) four curves are shown: the numerical solution of Eq. (3.139) (solid line), the analytical approximation Eq. (3.140) (dotted line), the approximation given in Eq. (3.147) of Eq. (3.140) (dashed line) and finally the approximation Eq. (3.143) (dotted-dashed line). One can note that in this case, in addition to Eq. (3.147), Eq. (3.143) provides quite a good approximation to Eq. (3.140) too. The reason has been explained above (see the discussion leading to Eq. (3.143)). For the symmetric case, it is then possible to consider another analytical approximation for $m(k)$ if one solves

Eq. (3.138) by inserting in this equation the approximation Eq. (3.143) for $G(k)$. More precisely, if this replacement is performed and, in addition, in the denominator of the r.h.s. of Eq. (3.138) $m(k)$ with $\overline{m}$ is replaced, this latter equation is easily integrated and ($M_1^2 = \frac{4\pi^2}{\overline{G}}$) is found:

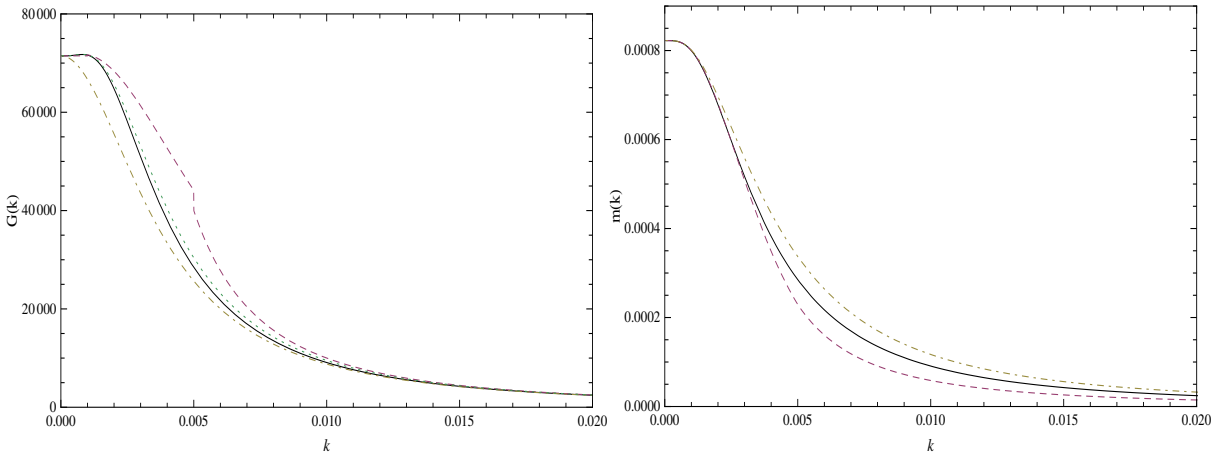

(a) (b)

Figure 3.8: (a) The dotted line is the approximation to $G(k)$ given in Eq. (3.140), in the symmetric phase, for $\overline{m} = 8.22 \cdot 10^{-4}$ and $\overline{G} = 7.15 \cdot 10^4$. The dashed line is the approximation to Eq. (3.140) given in Eq. (3.147) with the appropriate choice of k_1 and k_2. For comparison, the numerical solution (solid line) of Eq. (3.139) is also plotted. The dotted-dashed line is the approximation of $G(k)$ given by Eq. (3.143). (b) Dashed line: analytical approximation, Eq. (3.149), to $m(k)$ for the same values of the parameters. Solid line: the corresponding numerical solution, Eq. (3.138). Dotted-dashed line: analytical approximation, Eq. (3.150), to Eq. (3.138).

$$m(k) = \overline{m} \exp\left(- \frac{M_1^2 \ln\left(1 + \frac{k^2}{M_1^2}\right) - \overline{m}^2 \ln\left(1 + \frac{k^2}{\overline{m}^2}\right)}{M_1^2 - \overline{m}^2} \right) \tag{3.150}$$

In Fig. 3.8(b) the analytical approximation Eq. (3.149) to $m(k)$ (dashed line) is shown, this is obtained with the help of the analytical approximation Eq. (3.147) for $G(k)$ and the analytical approximation Eq. (3.150) (dotted-dashed line) obtained with the help of the analytical approximation Eq. (3.143). These two curves are compared with the corresponding numerical solution (solid line) to Eq. (3.138). Once again, one can see that the correspondence between the exact results and the analytical approximations is excellent.

Before ending this section, it will be shown that an analytical approximation to $m(k)$ can also be obtained by noting that the specific form of the approximate solution Eq. (3.140) to Eq. (3.139), together with all the previous considerations and results.

This suggests that one could try to approximate $G(k)$ with a Lorentzian profile of the kind:

$$G\left(k\right) = \frac{4\pi^2}{\left(k-a\right)^2 + M_3^2}\,, \tag{3.151}$$

where a serves to locate the value of k for which $G(k)$ has a maximum (which is vanishing or essentially vanishing for the "symmetric phase"), and M_3 allows the determination of the IR value of $G(k)$.

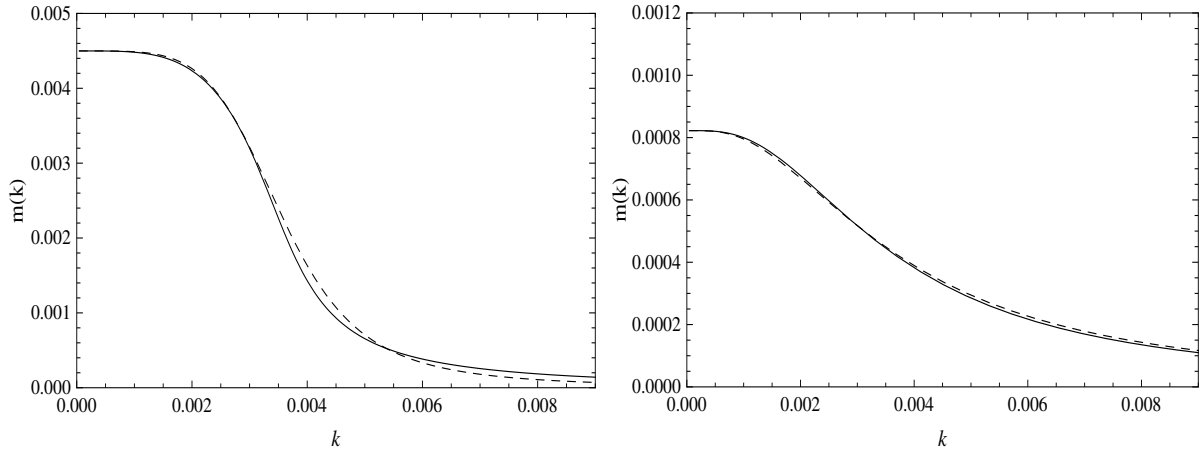

(a) (b)

Figure 3.9: (a) The analytical approximation, Eq. (3.152), to $m(k)$ (dashed line), for the broken phase, is compared with the corresponding numerical solution (solid line) plotted in Fig. 3.7(b): $a = 3.26 \cdot 10^{-3}$ and $M_3 = 1.94 \cdot 10^{-3}$. (b) The same approximation, Eq. (3.152), to $m(k)$ (dashed line), for the symmetric phase, is compared with the corresponding numerical solution (solid line) plotted in Fig. 3.8(b): $a = 0$ and $M_3 = 3.31 \cdot 10^{-3}$.

If the above approximation for $G(k)$ is now plugged in the RG equation for $m(k)$, Eq. (3.138), where again in the r.h.s. $m(k)$ is frozen to its IR value $\overline{m}$, Eq. (3.138) can be solved and gives:

$$\begin{aligned} m\left(k\right) \;= \overline{m}\exp\Bigg(&-\frac{1}{a^4+2a^2\left(\overline{m}^2+M_3^2\right)+\left(\overline{m}^2-M_3^2\right)^2}\Big(\overline{m}^2\left(-a^2+\overline{m}^2-M_3^2\right)\ln\left(\tfrac{k^2}{\overline{m}^2}+1\right)\\ &+\left(a^4+a^2\left(3\overline{m}^2+2M_3^2\right)-\overline{m}^2M_3^2+M_3^4\right)\ln\left(\tfrac{k^2-2ak}{a^2+M_3^2}+1\right)\\ &+\frac{2a\left(a^4+a^2\left(\overline{m}^2+2M_3^2\right)-3\overline{m}^2M_3^2+M_3^4\right)}{M_3}\left(\tan^{-1}\left(\tfrac{k-a}{M_3}\right)+\tan^{-1}\left(\tfrac{a}{M_3}\right)\right)\\ &+4a\overline{m}^3\tan^{-1}\left(\tfrac{k}{\overline{m}}\right)\Big)\Bigg)\,. \end{aligned} \tag{3.152}$$

This analytical approximation for $m(k)$ can be checked against the numerical solutions shown in Figs. 3.7(b) and 3.8(b) for the broken and the symmetric phase respectively.

In the left panel of Fig. 3.9 the numerical solution of Eq. (3.138) in the broken phase, where, in cut-off units, $G_B = G_c + 10^{-5} = 1 + 10^{-5}$ and $m_B = 10^{-8}$, is compared with the corresponding analytical solution obtained for $a = 3.26 \cdot 10^{-3}$ and $M_3 = 1.94 \cdot 10^{-3}$. Note that the IR values of $G(k)$ and $m(k)$ are: $\overline{G} = 1.61 \cdot 10^5$ and $\overline{m} = 4.50 \cdot 10^{-3}$. As the broken phase is considered, $\overline{m}$ turns out to be order of magnitudes greater than the bare mass. As one can easily see, the two profiles are almost superimposed. In the right panel, the system in the unbroken phase is taken into account and the exact numerical solution (where, in cut-off units, $G_B = G_c - 10^{-5} = 1 - 10^{-5}$ and $m_B = 10^{-8}$) has been compared with the corresponding analytical approximation Eq. (3.152) obtained for $a = 0$ and $M_3 = 3.31 \cdot 10^{-3}$.

The above results show that replacing $G(k)$ with Eq. (3.151) provides a very good analytical profile for $m(k)$, given by Eq. (3.152), once the appropriate values of a and M_3 are taken into account. Moreover, the IR and UV limits of the analytical approximation to $m(k)$ as given by Eq. (3.152) show quite interesting features.

Indeed, by expanding Eq. (3.152) for small values of k one finds:

$$m(k) \sim \overline{m} - \frac{k^4}{2\overline{m}\,(a^2 + M_3^2)}\,, \tag{3.153}$$

which is exactly the result previously obtained, Eq. (3.145), once it is noted that, in the notations of this section, $\overline{G} = \frac{4\pi^2}{a^2+M_3^2}$. On the other hand, for large values of k:

$$m(k) = \frac{\overline{m}}{(M_3^2)^{-\alpha}(a^2 + M_3^2)^{-\beta}}\,\frac{1}{k^2}, \tag{3.154}$$

where:

$$\begin{aligned} \alpha &= \frac{\overline{m}^2(-a^2 + \overline{m}^2 - M_3^2)}{a^4 + 2a^2(\overline{m}^2 + M_3^2) + (\overline{m}^2 - M_3^2)^2}, \\ \beta &= \frac{a^4 + a^2(3\overline{m}^2 + 2M_3^2) - \overline{m}^2 M_3^2 + M_3^4)}{a^4 + 2a^2(\overline{m}^2 + M_3^2) + (\overline{m}^2 - M_3^2)^2}, \\ \alpha + \beta &= 1\,. \end{aligned} \tag{3.155}$$

Eq. (3.154) is quite interesting as it not only provides the already known correct asymptotic behaviour of $m(k)$ for large values of k, $m(k) \sim 1/k^2$ (Eq. (3.146)), but also gives the coefficient of $1/k^2$ in terms of the IR parameters of the theory. As already noted, the coefficient of $1/k^2$ in Eq. (3.146) could not be determined because the $m(k)$ profile in the intermediate region is unknown. As Eq. (3.154) is the UV limit of Eq. (3.152), which is an

approximation to $m(k)$ in the *whole* k range, this coefficient, which is a parameter that characterizes the UV behaviour of the theory, is now known and given in terms of the IR parameters of the theory. This provides a interesting example of the IR-UV connection that has been already mentioned in this work.

Finally, one can note that Eq. (3.152) appears to be a very good fit for both the unbroken and the broken phases, the unbroken one being obtained by taking $a = 0$.

3.5 Critical exponents for small N values

The analysis of the critical behaviour of the GN model for small values of N is considered. Different analytical methods have been introduced in order to deal with the χSB phenomenon. However each of these methods has a very definite applicability limit. As an example the critical exponents calculated in the framework of the $1/N$ expansion were shown in Sec. 2.3.2, while those computed with the ϵ expansion method were presented in Sec. 3.2.4. These two techniques can be compared by performing a double expansion in ϵ and in $1/N'$. Consistently it is found:

$$\nu = \frac{1}{2} + \frac{\epsilon}{4} + \frac{3}{2}\frac{\epsilon}{N'} + \dots \tag{3.156}$$

$$\eta_\sigma = \epsilon - 6\frac{\epsilon}{N'} + \dots, \tag{3.157}$$

for both the cases. On the other hand the region when $d = 3$ and N is very small needs another tool to be explored. In this sense the Wilsonian *RG* group could compensate for this lack.

Clearly this method is also limited by its own approximations which rely on the derivative expansion as explained in Sec. 3.3.2. However far from the upper critical dimension one should expect that the derivative contributions can be discarded since, as was suggested in the previous chapter, they do not play any role in determining the critical behaviour.

The complete version of Eq. (3.101) can be calculated by writing the Eq. (3.99) in terms of dimensionless quantities. It is found:

$$\frac{\partial}{\partial t}V = d\,V - (d-1)\,\sigma V_\sigma - C_d N \mathrm{tr}\,\mathbb{I}\ln\left(1+V_\sigma^2\right) + C_d \ln\left(1 + \frac{2\sigma V_\sigma V_{\sigma\sigma}}{1+V_\sigma^2}\right), \tag{3.158}$$

Then by considering again the truncation for the potential $V(\sigma,t)$ with the mass term and the Fermi coupling only the following system is worked out:

$$\begin{aligned}\frac{dm}{dt} &= m+\frac{2N\mathrm{tr}\,\mathbb{I}C_dGm}{1+m^2}-\frac{2C_dGm}{1+m^2},\\ \frac{dG}{dt} &= (2-d)G+\frac{2N\mathrm{tr}\,\mathbb{I}C_dG^2\left(1-m^2\right)}{\left(1+m^2\right)^2}-\frac{4C_dG^2\left(1-2m^2\right)}{\left(1+m^2\right)^2}.\end{aligned} \tag{3.159}$$

The search for a fixed point of these equations gives, as expected, two possible solutions. The Gaussian solution, which was already found in Sec. 3.4.2, and the extension of the non-Gaussian one, which was used for the description of the chiral transition in the Hartree approximation. So the non-Gaussian solution is:

$$m = 0, \tag{3.160}$$

$$G = \frac{d-2}{2C_d(N\mathrm{tr}\,\mathbb{I}-2)}\,. \tag{3.161}$$

$$\tag{3.162}$$

By linearizing around this fixed point two relevant eigendirections are found. Their scaling law is encoded in the two eigenvalues:

$$\lambda_m = \frac{N\mathrm{tr}\,\mathbb{I}(d-1)-d}{N\mathrm{tr}\,\mathbb{I}-2}, \tag{3.163}$$

$$\lambda_G = d-2. \tag{3.164}$$

$$\tag{3.165}$$

As also found in the ladder approximation, the first eigendirection coincides with the fermion mass axis, while the second one is nothing but the G axis. The anomalous dimension of the local operators coupled with these parameters can immediately be worked out. One obtains:

$$\left[\bar\psi\psi\right] = \left[\bar\psi\psi\right]_0-\gamma_m = 1+\frac{(d-2)}{N\mathrm{tr}\,\mathbb{I}-2}, \tag{3.166}$$

$$\left[(\bar\psi\psi)^2\right] = \left[(\bar\psi\psi)^2\right]_0-\gamma_G = 2. \tag{3.167}$$

Their proportionality can be recovered in the large N limit. By using the same procedure described in Sec. 3.4.2 the critical exponents are calculated. Indeed the eigenvalues in

Eqs. (3.163),(3.164) can be replaced in the Eq. (3.121) thus giving:

$$\beta = \frac{1}{(d-2)} + \frac{1}{N'-2}, \tag{3.168}$$

$$\delta = (d-1) + \frac{d(d-2)}{N'-d}, \tag{3.169}$$

$$\gamma = 1 + \frac{2}{N'-2}, \tag{3.170}$$

$$\nu = \frac{1}{d-2}, \tag{3.171}$$

$$\eta = (4-d) + \frac{2(d-2)}{2-N'}. \tag{3.172}$$

Near $d = 2$ a check of these results can be done. Indeed by performing a double expansion in $1/N'$ and $\epsilon' = d - 2$ one finds:

$$\nu^{-1} = \epsilon' + \mathcal{O}(1/N'^2, \epsilon'^2), \tag{3.173}$$

$$\eta = 2 - \epsilon' - 2\frac{\epsilon'}{N'} + \mathcal{O}(1/N'^2, \epsilon'^2). \tag{3.174}$$

Which are exactly the same expressions that can be found by expanding the exponents in Sec. 2.3.2.

One should deduce that the higher derivative terms can be really neglected near $d = 2$, i.e. near the lower critical dimension of the chiral transition. On the other hand, the same contributions cannot be discarded near $d = 4$, showing how the LPA is too crude near the upper critical dimension.

However this approximation has a range of validity even wider. Indeed one could ask what happens in the intermediate region between the lower and the upper critical dimension, that is at $d = 3$. In order to test the high degree of accuracy of the LPA at $d = 3$ it is possible to compare the value of the critical exponents, calculated with the $1/N$ expansion, with those obtained by means of the functional RG. For a large enough N' both these methods give in practice the same results. This is not the case for the ϵ expansion method, which being performed near $d = 4$, should not be extended up to this range.

In advocating these statements the values of ν^{-1} and η, as functions of $1/N'$ and calculated at $d = 3$, have been shown in Figs. 3.10 (a) and 3.10 (b) respectively.

The solid line was used for representing the value of the critical exponents given in the large N expansion, which should provide a basis for the reliability of our original results.

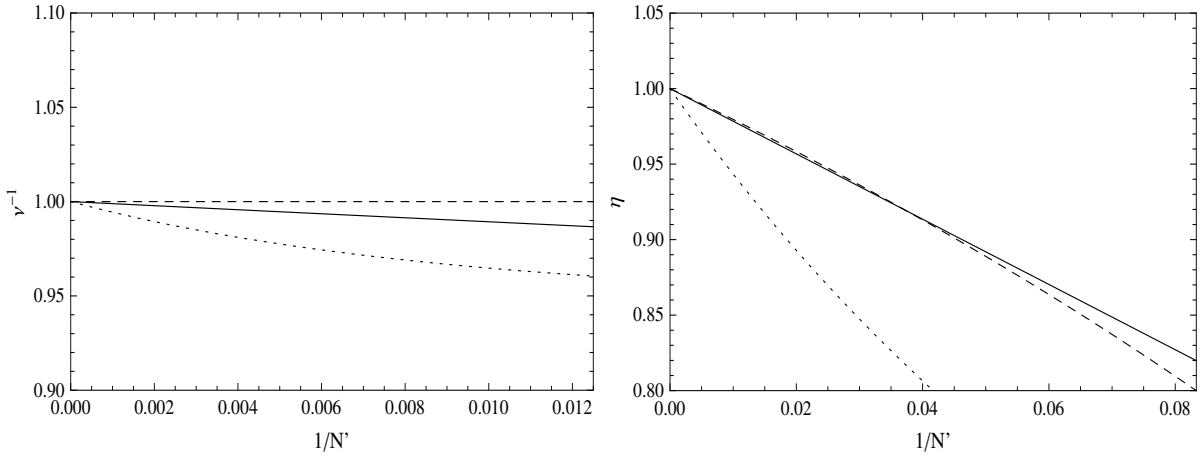

Figure 3.10: (a) The solid line shows the value of the ν^{-1} for different value of $1/N'$ and calculated at the next to leading order in the $1/N$ expansion, as shown in Sec. 2.3.2. The dashed line represents the same quantity calculated by means of the Wilsonian *RG* method, the result is given in Eq. (3.171). The dotted line is ν^{-1} as provided by the epsilon expansion technique, performed near $d = 4$ (Eq. (3.68). (b) The solid line shows the value of the exponent η for different value of $1/N'$, calculated at the next to leading order in the $1/N$ expansion, as shown in Sec. 2.3.2. The dashed line represents the same quantity calculated by means of the Wilsonian *RG* method, the result is given in Eq. (3.172). The dotted line is η as provided by the epsilon expansion technique, performed near $d = 4$ (Eq. (3.68)).

The dashed line gives the same exponents calculated with our *RG* method, while in the dotted one they are computed with the ϵ expansion tool. The Wilsonian *RG* method is nearest to the predictions of the $1/N$ expansion which, for sufficiently large N, should be the best analytical approach in this dimension.

For small N value the critical exponents were computed with numerical simulations, performed by means of Monte Carlo (MC) algorithms, in a lattice. The results for $N' = 8$ were given in [60], while at $N' = 16$ can be found in [61]. By choosing $\mathrm{tr}\,\mathbb{I} = 4$ they correspond to the cases $N = 2$ and $N = 4$. The numerical results are thus compared with the different analytical approaches respectively in Tab. 3.1 (a) and Tab. 3.1 (b). For completeness the value of some critical exponents at $N' = 12$ (N=3) and $N' = 48$ (N=12) are also reported in Tab. 3.1 (b) and Tab. 3.1 (c). In this comparison also the critical exponents calculated by means of a functional *RG* method using a bosonized version of the *GN* model are reported [62].

From these results it seems that our *RG* method provides a qualitative but also a very good quantitative description of the critical region of the *GN* model at $d = 3$ even in the

(a) $N = 2$

Technique	ν	γ	γ/ν	β	β/ν	η_σ
MC simulations	1.00(4)	1.253∗	1.246(8)	0.881∗	0.877	0.75∗
fermion Wilsonian *RG*	1.000	1.333	1.333	0.833	0.833	0.667
ϵ-expansion	0.954	1.364	1.429	0.750	0.785	0.571
$1/N$-expansion	0.829	1.041	1.256	0.723	0.872	0.744
functional bosonized *RG*	0.961	1.384	1.440	0.745	0.775	0.561

(b) $N = 3$

Technique	ν	γ	γ/ν	β	β/ν	η_σ
MC simulations	.	.	.	.	?	.
fermion Wilsonian *RG*	1.000	1.200	1.200	0.900	0.900	0.800
ϵ-expansion	1.000	1.333	1.333	0.833	0.833	0.667
$1/N$-expansion	0.942	1.105∗	1.174	0.860∗	0.913	0.826∗
functional bosonized *RG*	1.041	1.323	1.271	0.903	0.867	0.710

(c) $N = 4$

Technique	ν	γ	γ/ν	β	β/ν	η_σ
MC simulations	0.98(2)	1.131∗	1.152	0.910∗	0.927	0.848
fermion Wilsonian *RG*	1.000	1.143	1.143	0.929	0.929	0.857
ϵ-expansion	1.023	1.303	1.273	0.884	0.864	0.727
$1/N$-expansion	0.982	1.112	1.131	0.918	0.934	0.868
functional bosonized *RG*	1.010	1.228	1.213	0.910	0.901	0.789

(d) $N = 12$

Technique	ν	γ	γ/ν	β	β/ν	η_σ
MC simulations	.	.	.	.	.	
fermion Wilsonian *RG*	1.000	1.043	1.043	0.978	0.978	0.956
ϵ-expansion	1.049	1.161	1.111	0.991	0.944	0.889
$1/N$-expansion	1.013	1.058	1.045	0.991	0.978	0.955
functional bosonized *RG*	1.023	1.075	1.051	0.998	0.971	0.936

Table 3.1: Some of the critical exponents as well as some of their ratios are shown in the present table for different value of N ($\mathrm{tr}\,\mathbb{I} = 4$ has been set). The results obtained by applying different analytical methods are compared. In (a) and (c) the values obtained by means of numerical simulations are also reported.

LPA.

CHAPTER 4

RG ANALYSIS OF HIGHER POWERS IN FERMION MODELS

As in the previous chapter the χSB is analyzed , for $2 < d \leq 4$, by means of the Wilsonian *RG* equation found in Sec. 3.3.3 and the results are discussed using the language of the critical phenomena.

In the following sections the study is focused on the impact of the higher powers of $\bar{\psi}\psi$ in determining the behaviour of the chiral transition.

Clearly all the results are limited to the framework of the LPA approximation. The Eq. (3.101) (or, equivalently, Eq. (3.100)) is the starting point of the present work.

Again the Hartree approximation of the Wilsonian potential is made possible by considering fermion multiplets of the $U(N)$ flavour group. This procedure allows the comparison of the *RG* results with the ones found with large N techniques. There are two ways of extending the GN model to higher local operators. Since the theory can be rephrased in its bosonized version, the first extension is represented by the usual Yukawa theory. Some *RG* results were reported in Sec. 3.2.4 and 3.2.5 with the epsilon expansion techniques. Other approaches, always in the bosonized language, can be found [62].

Another extension is achieved by directly adding the operator $(\bar{\psi}\psi)^4$ to the Lagrangian of the non-bosonized model. In the large N expansion, this second option can also be handled with the bosonization techniques introduced in Sec.2.2.1. An example of this procedure will be found in the first section of this chapter. The addition of several powers of the $\bar{\psi}\psi$ operator is also the way in which the extension is treated by means of our *RG*

method.

In the present chapter the critical region is investigated at first by discarding the mass effects so that only even powers of the composite operator are considered in the potential. Moreover the Hartree approximation is performed and a critical point is found for $2 < d < 4$. It will be shown that while there is a relevant eigendirection, which will be related to the temperature of the system, and an irrelevant one.

In this sense the result is consistent with the predictions given by the Yukawa theory. It is well known [19], [17] how the behaviour of the critical fixed point in the Yukawa theory, describing the chiral transition, closely resembles that of the Wilson-Fisher fixed point, which is related to the ferromagnetic transition. Clearly the two theories are very different since they predict different critical behaviour even at $d =$ [63]. However many common features can be stressed. For example, the scalar mass is related, for both these theories, to the reduced temperature of the correspondent transition. Also the behaviour of the fixed points near $d = 4$ is very similar. These collapse into the origin so that both of the two theories become trivial. Some operators which are irrelevant for $d < 4$ became marginal at the upper critical dimension.

With these premises one could ask if some aspects of the triviality of the GN model may be worked by studying how the quartic operator $(\bar{\psi}\psi)^4$ scales near $d = 4$. At this scope the non-Gaussian fixed point found with the Wilsonian fermion RG equations, is compared to the Wilson-Fisher fixed point near and at the four dimension. The presence of a marginal direction found by linearizing around the critical fixed point of the GN model is highlighted at $d = 4$ in the large N approximation. In this sense this point turns out to be an example of a trivial non-gaussian fixed point at $d = 4$.

A more accurate analysis shows that, because of identical cancellations occurring at $d = 4$, the impact of the Fock' s terms should be taken into account. Despite this the marginal direction is again recovered in the large N limit.

The analysis near the critical domain is also performed by the introduction of an explicit mass term to the even powers. A cross-over picture very similar to that described in the previous chapter is recovered.

Finally the impact of the cubic power of $\bar{\psi}\psi$ is considered and the results are in agreement with those found in the literature [64].

4.1 The quartic operator in the Large-N expansion

By applying the techniques of Sec.2.2.1 for the potential:

$$V(X) = -\frac{G}{2}X^2 + \frac{g_4}{4!}X^4, \tag{4.1}$$

the saddle point equations turn out to be:

$$-\frac{g_4}{6}X^3 + GX - \Phi + K = 0, \tag{4.2}$$

$$-X + N'\Phi \int \frac{d^dp}{(2\pi)^d}\frac{1}{p^2+\Phi^2} = 0. \tag{4.3}$$

The request for a spontaneous symmetry breaking is achieved by setting $J = 0$. If the g_4 coupling can be discarded the Eqs. (4.2),(4.3) are reduced to the system:

$$X = \frac{\Phi}{G}, \tag{4.4}$$

$$-\frac{\Phi}{G} + N'\Phi \int \frac{d^dp}{(2\pi)^d}\frac{1}{p^2+\Phi^2} = 0. \tag{4.5}$$

Eq. (4.5) is nothing but the Eq. (2.81), the constraint in Eq. (4.5) resembles the relation between the $\bar{\psi}\psi$ operator and the composite field. However, as is seen from Eq. (4.3), near the critical region the system can be rewritten as:

$$-\frac{g_4}{G^4}\Phi^3 + N'\frac{\Phi}{G}\int \frac{d^dp}{(2\pi)^d}\frac{1}{p^2+\Phi^2} + \frac{\Phi}{G} \simeq 0, \tag{4.6}$$

$$\frac{X}{\Phi} \simeq \frac{1}{G}. \tag{4.7}$$

The result found in Eq. (4.7) is very similar to that shown in Eq. (2.123). It suggests the identity:

$$\frac{\lambda}{g^4} \simeq -\frac{g_4}{G^4}, \tag{4.8}$$

which shows that near the critical region $g_4 = \mathcal{O}(1/N^3)$ in order to be a correction to the scaling behaviour.

4.2 RG equations for higher powers couplings

Now the impact of higher order parameters is described by means of the *RG* methods. In the previous chapter the comparison between the χSB and a second order phase transition was established by thinking of the bare mass m_B as a seed of an external magnetic

field and at the Fermi coupling G_B (which corresponds to the boundary value $G(\Lambda)$ for the flow of $G(k)$ at the UV scale Λ) as the inverse of a temperature. Thus it was implicitly understood that both these couplings were the only relevant parameters of the model.

However, this assumption relies on the hypothesis that the effect of all other couplings near the fixed point can be neglected, or more precisely that they turn out to be irrelevant parameters. Clearly this assumption is well corroborated by the result found with the other analytical methods.

Inspite of this a consistent internal check of our RG approach is required by evaluating the impact of the higher powers in the Wilsonian potential.

The expansion up to the fourth power of σ is considered. Thus the following truncation is chosen for the potential $V(t)$:

$$V(\sigma,t) = -m(t)\sigma - \frac{G(t)}{2}\sigma^2 - \frac{g_3(t)}{3!}\sigma^3 + \frac{g_4(t)}{4!}\sigma^4. \tag{4.9}$$

With this position, by inserting this expression into the Eq. (3.101), the RG equations for the couplings turn out to be, in the Hartree approximation:

$$\frac{dm}{dt} = m + \frac{2C_d G m N \mathrm{tr}\,\mathbb{I}}{m^2+1}, \tag{4.10}$$

$$\begin{aligned}\frac{dG}{dt} &= (2-d)G + \frac{2C_d g_3 m N \mathrm{tr}\,\mathbb{I}}{m^2+1} \\ &- \frac{2C_d G^2 \left(m^2-1\right) N \mathrm{tr}\,\mathbb{I}}{\left(m^2+1\right)^2},\end{aligned} \tag{4.11}$$

$$\begin{aligned}\frac{dg_3}{dt} &= (3-2d)g_3 + \frac{6C_d g_3 G \left(1-m^2\right) N \mathrm{tr}\,\mathbb{I}}{\left(m^2+1\right)^2} \\ &- \frac{2C_d g_4 m N \mathrm{tr}\,\mathbb{I}}{m^2+1} + \frac{4C_d G^3 m \left(m^2-3\right) N \mathrm{tr}\,\mathbb{I}}{\left(m^2+1\right)^3},\end{aligned} \tag{4.12}$$

$$\begin{aligned}\frac{dg_4}{dt} &= (4-3d)g_4 - \frac{24C_d g_3 G^2 m \left(m^2-3\right) N \mathrm{tr}\,\mathbb{I}}{\left(m^2+1\right)^3} \\ &- \frac{8C_d g_4 G \left(m^2-1\right) N \mathrm{tr}\,\mathbb{I}}{\left(m^2+1\right)^2} + \frac{6C_d g_3^2 \left(m^2-1\right) N \mathrm{tr}\,\mathbb{I}}{\left(m^2+1\right)^2} \\ &+ \frac{12C_d G^4 \left(m^4-6m^2+1\right) N \mathrm{tr}\,\mathbb{I}}{\left(m^2+1\right)^4}.\end{aligned} \tag{4.13}$$

Starting from this result the critical behaviour of the extension of the GN model can be studied by setting $g_3 = 0$. However for the sake of completeness the the whole system

is considered still for a while.

4.2.1 Fixed point and linearization

The system of Eqns. from (4.10) to (4.13) cannot be analytically solved. The first qualitative and quantitative description of its behaviour can be given by searching for the fixed points.

For a generic dimension $2 < d < 4$ and $d \neq 3$ the Eqns. from (4.10) to (4.13) allow two fixed points: the Gaussian one $m = G = g_3 = g_4 = 0$ and the non-Gaussian

$$\begin{aligned} m &= 0, \\ G &= \frac{d-2}{2N\mathrm{tr}\,\mathbb{I}C_d}, \\ g_3 &= 0, \\ g_4 &= \frac{3(d-2)^4}{4(d-4)N^3\mathrm{tr}\,\mathbb{I}^3C_d^3}. \end{aligned} \tag{4.14}$$

Both these fixed point are the natural extension of those found in Sec. 3.4.2 for the m and G couplings alone.

It can be observed that the fixed point value for the couplings associated with odd powers of σ, that are m and g_3, is always zero, while the couplings related to the even powers are non-vanishing.

Some important details are needed. By explicitly studying the equations Eqs. from (4.10) to (4.13) at $d = 3$, an infinite number of fixed point solutions is found By replacing in Eq. (4.12) the fixed point values for m and G given in Eqs. (4.14),(4.14) a multiplicity of solutions is obtained due to an identical cancellation in the equation itself. Clearly this is an unpleasant result since a fixed point preserving the chiral symmetry is required. However this degeneracy disappears in the right and in the left limit for $d \to 3$. Moreover this problem is simply circumvented when also the Fock's contributions are taken into account. It can be anticipated that this identical cancellation simply reveals that the cubic operator is marginal at $d = 3$. More on this point will be clarified later.

Similar to what was found at $d = 3$, by considering the Eqs. (4.10) in the case $d = 4$ and by replacing in Eqs. (4.13 the values given in Eqs. (4.14),(4.14) for m,G and g_3) a residual term of order $1/N^3$ is left which prevents the beta function to vanish .

This seems to be an even worse result than that obtained at $d = 3$. However also in this case the identical cancellation is related to the appearance of a marginal direction.

A deeper insight in these statements needs the evaluation of the eigenvalues related to the linearization of the *RG* equations.

First of all by linearizing around the Gaussian fixed point, it is found:

$$\begin{aligned} \lambda_1 &= 1, \\ \lambda_2 &= 2-d, \\ \lambda_3 &= 3-2d, \\ \lambda_4 &= 4-3d. \end{aligned} \tag{4.15}$$

As shown in Sec. 1.6.5 these exponents, are related to the canonical dimension of each coupling.

On the other hand the linearization around the non-Gaussian fixed point given in Eqs. (4.14) returns:

$$\begin{aligned} \lambda_1 &= d-1, \\ \lambda_2 &= d-2, \\ \lambda_3 &= d-3, \\ \lambda_4 &= d-4. \end{aligned} \tag{4.16}$$

It is important to stress that the eigendirections associated with these eigenvalues do not coincide with the canonical basis but are the vectors:

$$\begin{aligned} v_1 &= \left(\frac{2(d-4)C_d^2}{3(d-2)^3}, 0, 1, 0\right), \\ v_2 &= \left(0, -\frac{(d-4)C_d^2}{6(d-2)^3}, 0, 1\right), \\ v_3 &= (0,0,1,0), \\ v_4 &= (0,0,0,1). \end{aligned} \tag{4.17}$$

At $d=3$ the eigenvalue λ_3 vanishes as a clear signal that its corresponding operator, v_3, is marginal. Some terms disappear in Eq. (4.12), giving a multiplicity of fixed point solutions, due to this marginal behaviour. The apparent degeneracy is just the signal that the linearization has lost its validity.

A more accurate analysis requires the introduction of the Fock's contributions.

For the same reason the vanishing of the λ_4 eigenvalue at $d = 4$ corresponds to the marginality of the v_4 direction. In this case the identical cancellation in Eq. (4.13) seems to be related to the disappearance of the fixed point.

Actually, as will be seen, the fixed point solution also survives in the Hartree approximation, but one of the coordinates of the FP becomes infinite so that a specific analysis is needed. Although the Hartree approximation gives the correct scaling in the large N limit the residual terms of order $1/N^3$ suggest that neglecting the Fock's contribution should not be correct.

4.2.2 Anomalous dimensions

Once the eigenvalues in Eqs.(4.16) have been computed by linearizing of Eqs. (4.10) around the non trivial fixed point, the anomalous dimension of each composite operator can be evaluated.

By comparing the eigenvalues in Eqs. (4.15) with those in Eqs. (4.16) the *anomalous dimensions* γ_1, γ_2, γ_3 and γ_4 are derived. Clearly the anomalous dimension does not describe the scaling of a given power of $\bar{\psi}\psi$ since the eigendirections do not coincide with the canonical basis. So the anomalous dimensions are:

$$\begin{aligned} \gamma_1 &= d-2, \\ \gamma_2 &= 2(d-2), \\ \gamma_3 &= 3(d-2), \\ \gamma_4 &= 4(d-2). \end{aligned} \tag{4.18}$$

The anomalous dimensions γ_1 and γ_2 are equal to the γ_m and γ_G, previously calculated in Eqs. (3.119),(3.120), and satisfy the relations $\gamma_2 = 2\gamma_1$. A proportionality relation, which is a typical result of the ladder approximation [65], holds also for the other anomalous dimensions. Indeed $\gamma_3 = 3\gamma_1$ and $\gamma_4 = 4\gamma_1$.

By knowing the anomalous dimension of each eigendirection it is possible to calculate the scaling dimensions of the local operators arising when successive powers of $\bar{\psi}\psi$ are taken into account. As explained in Sec. 3.3.1, the scaling dimension $[\mathcal{O}_n]$ of the operator , $\mathcal{O}_n$, associated with the eigendirection v_n is given, in the LPA approximation, by:

$$[\mathcal{O}_n] + [v_n] = d. \tag{4.19}$$

By knowing the scaling dimension of the operators $\mathcal{O}_n$ the scaling of each power of $\bar{\psi}\psi$ can be deduced by a simple linear combination.

Since the anomalous dimensions of the different couplings are proportional, the scaling dimensions of the operators $\mathcal{O}_n$ are connected by proportionality relations. Indeed, they are:

$$\begin{aligned}
[\mathcal{O}_1] &= \left[\bar{\psi}\psi\right]_0 - \gamma_1 = 1, \\
[\mathcal{O}_2] &= 2\left[\bar{\psi}\psi\right]_0 - \gamma_2 = 2, \\
[\mathcal{O}_3] &= 3\left[\bar{\psi}\psi\right]_0 - \gamma_3 = 3, \\
[\mathcal{O}_4] &= 4\left[\bar{\psi}\psi\right]_0 - \gamma_4 = 4,
\end{aligned} \tag{4.20}$$

where $\left[\bar{\psi}\psi\right]_0$ is the canonical dimension of the operator $\bar{\psi}\psi$.

This means that the operator $\mathcal{O}_n$ is the n-th power of the operator $\mathcal{O}_1$.

By comparing these results with those found in Sec. 3.2.4 it can be noted that the scaling dimension of the operator $\mathcal{O}_1$ is the same of those of the scalar operator ϕ of the Yukawa near the Wilson-Fisher-Yukawa FP. This is another way of thinking that the GN model and the Yukawa theory belong, in the large N limit, to the same universaltity class. The impact of the quantum fluctuations destroys the classical relationship between the elementary fields ψ and $\bar{\psi}$ and the composite local operator $\bar{\psi}\psi$. In this sense, the operator $\bar{\psi}\psi$ (or more precisely the operator $\mathcal{O}_1$) plays the same role of the scalar operator ϕ in the Yukawa theory.

Now, by using the relations in Eqs. 4.20, one finds that at $d = 4$ the scaling dimension of $\mathcal{O}_1$, which does not depend on the dimension d, coincides with the canonical dimension of the scalar operator ϕ at $d = 4$. From the point of view of the Yukawa theory or equivalently from that of the bosonised version of the GN model (as found by the large N techniques) this is the sign of triviality behaviour, since the scaling dimension differs from the canonical one for a logarithmic correction.

The operator $\mathcal{O}_4$ of this extended GN model is marginal as the ϕ^4 or the $\phi\bar{\psi}\psi$ operators of the Yukawa theory are marginal. Also the marginality of the operator $\mathcal{O}_4$ results in logarithmic scaling as will be shown in the following sections.

However, in the Yukawa theory at $d = 4$ the logarithmic divergences arise also in the operators $(\partial_\mu\phi)^2$ and $\bar{\psi}\partial\!\!\!/\psi$, leading to a weak correction of the scalar and of the fermion

fields. This correction cannot be calculated in our LPA approach but should be achievable when some higher derivative terms are taken into account.

4.3 The impact of the $(\bar{\psi}\psi)^4$ operator and the critical behaviour near $d = 4$

In the previous section the impact of higher couplings of the Wilsonian potential was analyzed by linearizing the RG equations around their fixed points. It was found a non-Gaussian FP which is an extension of that given in Sec.3.4.2. Once again, the important features of the χSB mechanism can be found if the fixed point itself is regarded as the critical point of a phase transition. As widely stressed the relevant directions of the fixed point are related with the external parameters characterizing the critical domain.

At risk of repeating well known statements some of the results of the previous chapter are summarized in order to analyze how they apply in the present case.

The critical exponents of the GN model were computed by considering both the first and the second power in σ of the Wilsonian potential. These terms are nothing but the mass m and the coupling G which are related respectively with the external magnetic field and the temperature of the statistical system. The FP solution $(0, G_c)$ was regarded as the critical point of the transition. Setting $m = 0$ the system shows two different behaviours depending on the boundary conditions chosen for the running coupling G. For $G < G_c$ the system flows towards the Gaussian fixed point while running mass term is always zero; this situation characterizes the symmetric phase. On the other hand when $G > G_c$ the system develops an instability and the equations diverge before that the value $k = 0$ is reached. This behaviour is related with the occurrence of the symmetry breaking. In following section the statistical language will be choose as a tool for interpreting the impact of the higher powers of $\bar{\psi}\psi$. First of all the critical region is studied when the external field (i.e. the bare mass) is strictly zero. Then the impact of a small mass term is taken into account for extending our cross-over picture at this case.

4.3.1 Analytical solutions and linearization

First of all, only the Eq. (4.11) and the Eq. (4.13) are considered. The odd terms as the mass or the cubic couplings have been switched off. With this assumption it was

found:

$$\frac{dG}{dt} = (2-d)G + 2G^2, \tag{4.21}$$

$$\frac{dg_4}{dt} = (4-3d)g_4 + 12G^4 + 8Gg_4, \tag{4.22}$$

where the G and g_4 couplings have been recalled as if N, C_d, $\mathbb{I} = 1$ were set. This rescaling will also be applied to represent the trajectories in the following pictures.

The system in Eqs. (4.21),(4.22) can be exactly integrated. One finds the solutions:

$$G = \frac{(d-2)/2}{1 - Be^{(d-2)t}}, \tag{4.23}$$

$$g_4 = \frac{1}{(1 - Be^{(d-2)t})^4}\left[\frac{3}{4}\frac{(d-2)^4}{(4-d)} + Ce^{(d-4)t}\right]. \tag{4.24}$$

for $2 < d < 4$, where B and C are the two arbitrary parameters.

When $B = C = 0$ the system is at one of its the fixed points, which is the same result given in Eqs. (4.14),(4.14). Thus expanding up to the first power in B and C the Eqs. (4.23),(4.24) become:

$$G = \frac{(d-2)}{2} + Be^{(d-2)t}, \tag{4.25}$$

$$g_4 = \frac{3}{4}\frac{(d-2)^4}{(4-d)} - 6\frac{(d-2)^3}{(d-4)}Be^{(d-2)t} + Ce^{(d-4)t}, \tag{4.26}$$

which are nothing but the linearized solutions consistent with the result found in Sec. 4.2.1.

At $d = 4$ the solution is instead:

$$G = \frac{1}{1 - Be^{2t}}, \tag{4.27}$$

$$g_4 = \frac{1}{(1 - Be^{2t})^4}\left[12t + C\right], \tag{4.28}$$

which clearly shows that the marginality, found through the analysis of eigenvalues in Eqs. (4.16), turns into the logarithmic behaviour of Eq. (4.28.

This supports the statement of the previous section: at $d = 4$ the theory is trivial. However it is not very clear what happened to the fixed point. The Eqs. (4.14) and Eq.(4.26) suggest that the fixed point goes to infinity along the v_4 direction as $d \to 3$. However the Eq. (4.26) and the Eq. (4.28) are not analytically related so that further studies are required.

The Eq. (4.21) can be rewritten in terms of a new coordinate $x = g_4^{-1}$ as:

$$\frac{dG}{dt} = (2-d)G + 2G^2, \tag{4.29}$$

$$\frac{dx}{dt} = (3d-4)x - 12G^4x^2 - 8Gx. \tag{4.30}$$

Now the beta functions vanish at the point $S \equiv (G = 0, x = 0)$, at $I \equiv (G = (d-2)/2, x = 0)$ and at the point C given by:

$$G = (d-2)/2, \tag{4.31}$$

$$x = \frac{4}{3}\frac{(4-d)}{(d-2)^4}. \tag{4.32}$$

The last corresponds to the non-Gaussian solution in Eq. (4.14). Clearly the Gaussian solution $O \equiv (G = 0, g_4 = 0)$ was lost, but two new solutions S and I have appeared, representing two points at $g_4 = \infty$. Near S the two parameters G and x scale with their canonical dimension, while near the point I the linearization provides the eigenvalues $\lambda_G = (2-d)$ and $\lambda_x = 4-d$. The Jacobian matrix is diagonal for both the cases, thus the eigendirections coincide with the canonical basis. At the $d = 4$ it is found that the critical point C collapses in the fixed point solution I. Thus what happens at the upper critical dimension becomes clear.

Thinking of the substitution $g_4 = x^{-1}$ as a change of coordinates one finds that, for $d < 4$, the point C has a finite value if expressed in terms of the coupling g_4 or of the coupling x. It is the critical fixed point associated with χSB, the v_2 vector representing again the direction of the reduced temperature. However as $d \to 4$ the fixed point value expressed in the x coordinate decreases while that expressed in the g_4 one increases. At $d = 4$ the fixed point value in x is zero while one of the eigendirections becomes marginal. The critical point C collapses into the point I which is at $g_4^* = \infty$. Finally for $d \leq 4$ the point I inherits the properties of the critical point. On the other hand the fixed point C cannot be used for describing the chiral transition since it acquires another relevant direction.

Investigating further on the scaling at $d = 4$, the Eqs. (4.31) can be explicitly solved giving:

$$G = \frac{1}{1 - Be^{2t}}, \tag{4.33}$$

$$x = (1 - Be^{2t})^4 \left(\frac{x_0}{1 + 12x_0t}\right). \tag{4.34}$$

Taking $B = 0$ and $x_0 = 0$ the fixed point solution is found. At the critical point when the coupling G is frozen at its fixed point value ($G = G_c = 1$), the flow of Eqs. (4.33) becomes:

$$x = \frac{x_0}{1 + 12x_0 t}, \tag{4.35}$$

The flow of the x coupling in Eq. (4.35) closely resembles the behaviour of the quartic scalar coupling or of the Yukawa one near the origin, as found in Sec.3.2.5.

4.3.2 Flows in the language of critical phenomena

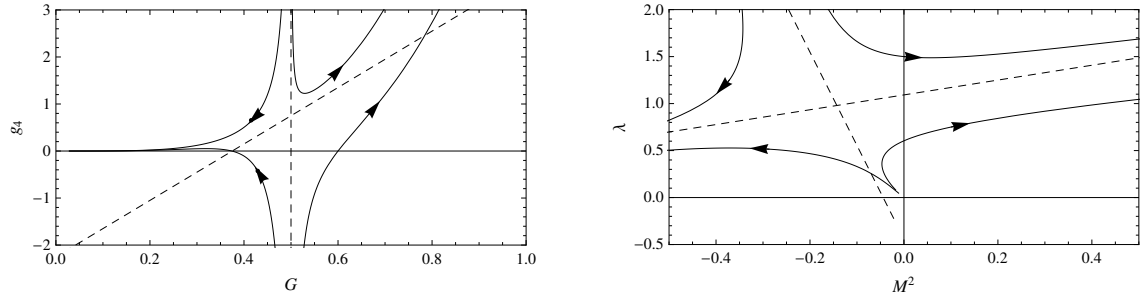

(a) (b)

Figure 4.1: (a) Four trajectories near the non-Gaussian fixed point of the Eqs. (4.21),(4.22), which describes the χSB at $d = 3$, are represented in the (G, g_4) plane. They are obtained by choosing the boundaries $G(t = 0) = 0.55, 0.6, 0.45, 0.45$ and $g_4 = 1.3, 0, -1, 1.2$ respectively. The dashed lines represent the eigendirections found through the linearization. Since both these directions are relevant the point cannot describe the χSB. (b) Four trajectories near the Wilson-Fisher fixed point, found by analyzing the Eqs. (4.36),(4.37) at $d = 5$, are shown in the (M^2, λ) plane. They are obtained by choosing the boundaries $M^2(t = 0) = -0.25, 0.1, -0.4, 0$ and $\lambda = 0.5, 0.751.1, 1.5$ respectively. The eigendirections are represented by the two dashed lines.

Once the exact solutions of Eqs. (4.21) were found, the flows in the whole (G, g_4) plane can be analyzed by varying the dimension d.

A useful insight in the description of the χSB, by using a Wilsonian *RG* method, is given by the comparison between the critical behaviour of the GN model around its critical fixed point and that one of the scalar theory around the non-trivial Wilson-Fisher fixed point.

The fact that the coupling G is related to the inverse of a temperature and the introduction of the g_4 coupling leads to an irrelevant parameter for $d < 4$ (marginal at $d = 4$) recalls what happens to the ferromagnetic systems when a scalar mass M^2 and a quartic

coupling λ are considered. The scalar system is thus analyzed by considering the *RG* equations for the scalar mass and the quartic coupling which can be found in [66]. For simplicity, these parameters are properly rescaled so that the system takes the form:

$$M^{2'} = 2M^2 + \frac{\lambda}{4(1+M^2)}, \tag{4.36}$$

$$\lambda' = (4-d)\lambda - \frac{3\lambda^2}{4(1+M^2)^2}. \tag{4.37}$$

It is important to stress that the following parallel is just an analogy between the two theories since their critical exponents are different.

The trajectories shown in Fig. (4.1) are the starting point for for the analysis at $d = 3$. On the left panel (Fig. (4.1) (a)) four trajectories in the (G, g_4) plane are shown, while in the right panel (Fig. (4.1) (b)) the flows of the square mass M^2 and the quartic coupling λ of the scalar theory can be found.

Both these pictures show the trajectories obtained by choosing four different boundary conditions and following the flows near the corresponding non-Gaussian fixed point. Thus in the case of the GN model (Fig. (4.1) (a)) the figure represents the linearization region (and beyond) around the solution in Eq. (4.14). Conversely, for the scalar model, the flows near the non-trivial W-F fixed point are considered [50]. The eigendirections obtained by the linearization are represented by the dashed lines; thus each fixed point lies on the intersection of its own lines. For the GN the line parallel to the g_4 axis and passing through the FP is the linear approximation of the critical surface. Since this space is generated by the eigendirection related to the irrelevant parameter each flows starting from this line falls on the fixed point.

Any other trajectory escapes from the FP by the effect of the relevant component. This component, in the linearization region, is represented by the dashed-oblique-line; it turns out to be the direction of the inverse temperature. Although this axis is tilted with respect to the G axis the critical value G_c is left unchanged by the addition of the g_4 parameter and also the exponent D_τ is the same. The critical line separates two possible regions on the plane: the region with $G < G_c$ and that one with $G > G_c$. The region in which $G < G_c$ represents the symmetric phase. Trajectories starting from this region fall towards the origin. The origin is an attractor for the plane since both G and g_4 are irrelevant directions. For $G > G_c$ the system is in the broken phase. After some *RG*

recursions the equations diverge for a finite value of $k > 0$. This is the same result that was found in Sec. 3.4.1.

In the scalar theory the direction of the temperature in the linearization region is represented by the dashed line almost parallel to the M^2 axis. This is the well known correction to the mean-field theory which assumes a reduced temperature proportional to the squared mass.

The other dashed line is the critical surface.

Thus a trajectory starting from the symmetric region ($M^2 > M_c^2$) flows towards the infrared and is flattened along the relevant axis.

After many RG recursions the M^2 and the λ parameters take their Gaussian scaling. Now the square mass can be identified with the inverse of the squared correlation length.

For $M^2 < M_c^2$ the system is on broken phase as for the fermion theory it develops an instability and the equations diverge due to the failure of a polynomial expansion around the false vacuum. Finally it is clear that in contrast with the fermion case, here the Gaussian fixed point is a UV attractor for the plane which is nothing but the RG formulation of the perturbative super-renormalizability of the scalar theory in $d = 3$.

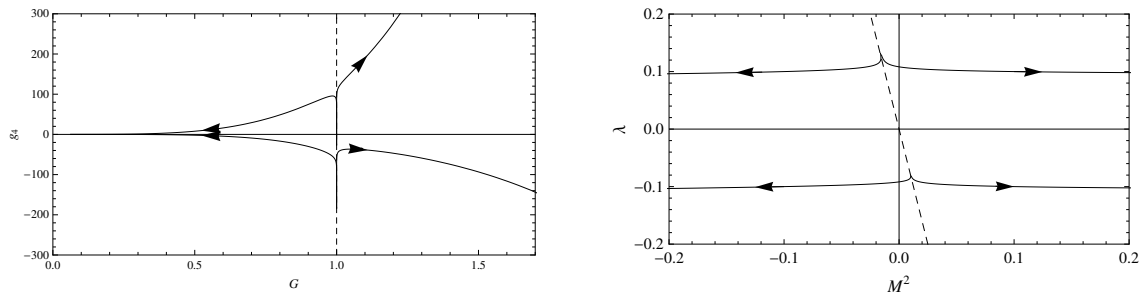

(a) (b)

Figure 4.2: (a) Four trajectories, found by running the Eqs. (4.21),(4.22) and describing the onset of the χSB at $d = 4$, are represented in the (G, g_4) plane. They are obtained by choosing the boundaries $G(t = 0) = 1.0002, 0.995, 1.0002, 0.995$ and $g_4 = -63, -63, 93, 93$ respectively. The dashed lines represent the eigendirections found through the linearization. (b) Four trajectories near the origin, found by analyzing the Eqs. (4.36),(4.37) at $d = 4$, are shown in the (M^2, λ) plane. They are obtained by choosing the boundaries $M^2(t = 0) = -0.1, 0.1, 0.1, -0.1$ and $\lambda = 0.1, 0.1, -0.1, -0.1$ respectively. The eigendirections are represented by the two dashed lines.

Now what happens at $d = 4$ can be considered. In the scalar theory the value of the Wilson-Fisher fixed point decreases and turns out to coincide with the origin. As a consequence, the irrelevant direction become marginal and the hyperscaling is violated

by the effect of the logarithmic scaling of the quartic coupling. However the quartic λ coupling is weakly irrelevant and thus the Gaussian point can be interpreted as a critical fixed point.

Conversely in the GN model the value of the non-Gaussian fixed point increases along the g_4 direction and goes to infinity at $d = 4$. What happens to the trajectories is shown in Fig. 4.2

The fixed point C, associated with the χSB, has become $G = G_c$ and $g_4 = \infty$. This result is expressed by the fact that the line $G = G_c$, which was previously identified with the critical surface at $d = 3$, again separates the plane into a symmetric region (on the left) and into a broken one (on the right). The component of a generic trajectory along the G axis leaves the critical surface when $t \to \infty$. Thus the G axis coincides with the direction of the inverse temperature.

It was shown in Eq. (4.28) that the component of the trajectory along the g_4 axis has marginal logarithmic behaviour. The marginality of this operator cannot immediately be related to the hyperscaling violation, although it signals the onset of the triviality [63],[67]. As can be seen in the Fig. 4.2 and in Eq. (4.28) the marginal component is attracted by infinity, starting with a trajectory belonging to the upper plane $g_4 > 0$. This shows how the fixed point $C \equiv I$ again possesses the features of a critical point.

However starting a trajectory with $g_4 < 0$ the "point" at $g_4 = -\infty$ is IR attractive, thus anticipating the behaviour that will be found for $d > 4$.

As is well known, at $d = 5$ the non trivial fixed point of the scalar theory, now shown in Fig. (4.3) (b), lies on the lower half plane $\lambda < 0$ [40]. The linearization near this point shows how both the two eigendirections are relevant. Thus this is no more the critical point associated with the ferromagnetic transition. Instead, the properties of the critical point are inherited from the origin. At this fixed point, while the mass direction has always remained relevant, the quartic coupling has become irrelevant.

However for $d > 4$, since the critical point is the Gaussian one, the scaling dimension of the parameters coincides with the canonical one.

Also in the fermion theory, as can be seen in Fig. (4.3) (a), the non trivial fixed point lies, at $d = 5$, on the lower half-plane. Moreover the linearization shows the appearance of two relevant directions. As in the ferromagnetic case this fixed point cannot be interpreted as the critical point of the transition.

Conversely the point I at $G = G_c$ and $g_4 = \infty$ possesses one relevant and one irrelevant direction. It has acquired the properties of a critical fixed point for the chiral transition.

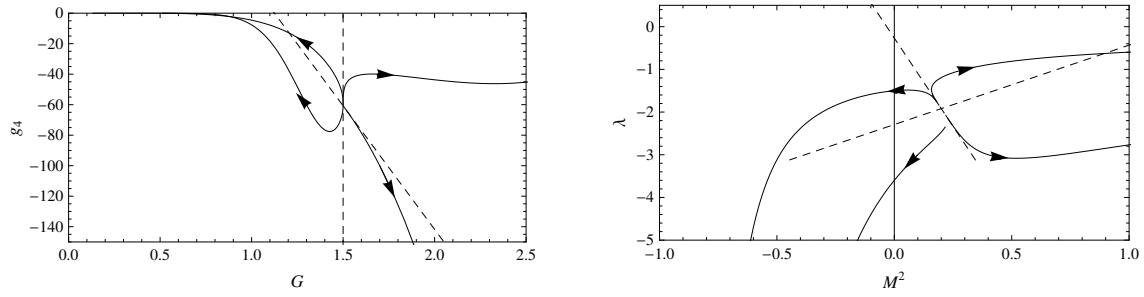

Figure 4.3: (a) Four trajectories near the non-Gaussian fixed point of the Eqs. (4.21),(4.22) at $d = 5$ are represented in the (G, g_4) plane. They are obtained by choosing the boundaries $G(t = 0) = 1.3, 1.3, 1.7, 1.7$ and $g_4 = -20, -60, -100, -40$ respectively. The dashed lines represent the eigendirections found through the linearization. (b) Four trajectories near the Wilson-Fisher fixed point, found by analyzing the Eqs. (4.36),(4.37) at $d = 5$, are shown in the (M^2, λ) plane. They are obtained by choosing the boundaries $M^2(t = 0) = 0.1, 0.3, 0.4, 0.1$ and $\lambda = -1.5, -1, -3, -3$ respectively. The eigendirections are represented by the two dashed lines. The ferromagnetic transition is instead described by the flows near the origin.

4.3.3 Mass flow and cross-over picture

In the previous section the flows in the parameter space of the GN model were analyzed by considering only the impact of the even powers in the effective potential. This procedure approximates well the behaviour of the flows near the non-trivial fixed point. However, when the system is in broken phase, the equations cannot be solved up to $k = 0$. They develop an instability, which resolves in a divergence of the system. In the previous chapter it was shown how such a stiffness can be solved by the introduction of an explicit running mass term. The explicit symmetry breaking of the model is obtained by taking the chiral limit as explained in Sec. 3.4.3. In the following,the results of the previous section are extended by considering the flow of a mass term m , together with those of the Fermi coupling G and of the quartic coupling g_4.

Actually, the extension is straightforward. As explained in Sec. 4.2.1 both the fixed points of the complete system, which involves m, G and g_4 are found by setting $m = 0$. Thus the results of Sec. 4.3.1 and Sec. 4.3.2 show nothing but the behaviour of the other bare parameters after that $m = 0$ was set as boundary. However since the m parameter is relevant thus the whole description of the critical region needs the introduction of this

mass term. The behaviour of the system in the symmetric and in the broken phase

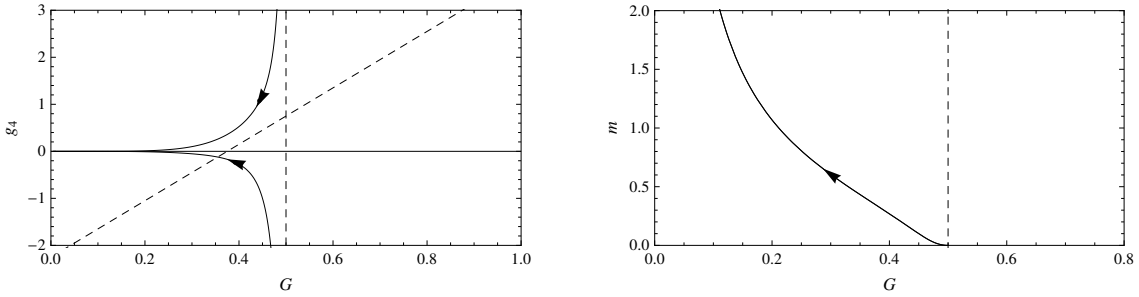

(a) (b)

Figure 4.4: (a) The projection in the (G, g_4) plane of the two trajectories belonging to in the symmetric region is represented. This region is defined by the linearization around the non-Gaussian fixed point found for the system including m, G and g_4 at $d = 3$. The flows are obtained by choosing the boundaries $G(t = 0) = 0.45, 0.45$ and $g_4 = -1, 1.2$ respectively, which are the same given for the trajectories in the symmetric region of Fig. 4.1, and by setting $m(t = 0) = 0.1$. (b) In this panel, the projection in the (G, m) plane of the two trajectories belonging to the symmetric region is represented. The flows are obtained by choosing the boundaries $G(t = 0) = 0.45, 0.45$ and $g_4 = -1, 1.2$ respectively, which are the same given for the trajectories in the symmetric region of Fig. 4.1, and by setting $m(t = 0) = 0.1$. The trajectories in the picture closely resemble those in the symmetric region of the Fig. 3.2

is studied at $d = 3$, in order to compare the results with those found in Sec. 4.3.2. The symmetric region is shown in Figs. 4.4 (a), (b). In the left panel (Fig. 4.4 (a)) two trajectories are found to be very similar to the symmetric ones given in Fig. 4.1 (a). They are obtained by choosing the boundary conditions for G and g_4 equal to to those given for the trajectories in Fig. 4.1 (a) and by setting $m(k = \Lambda) = 0.1$. In conclusion the introduction of the running mass does not affect the behaviour of the system. The projection of the trajectories in the (G, m) plane is shown in Fig. 4.4 (b). Both the flows coincide and as expected correspond to the usual symmetric trend.

Conversely the results in the broken phase are shown in Figs. 4.5 (a), (b). In the left panel (Fig. 4.5 (a)) one can find the two trajectories corresponding to those represented in the broken region of the Fig. 4.1 (a).

Once again, the first are obtained by imposing for G and g_4 the same boundary conditions chosen for the latter and by setting a small boundary value for the mass ($m(k = \Lambda) = 0.1$). However in the case of the broken phase the mass term plays a prominent role in determining the evolution of the trajectories.

The introduction of a mass term produces in the (G, m) plane those bells shown in Fig. 4.5 (b) thus preventing the divergence of the trajectories, as was explained in Sec.3.4.3.

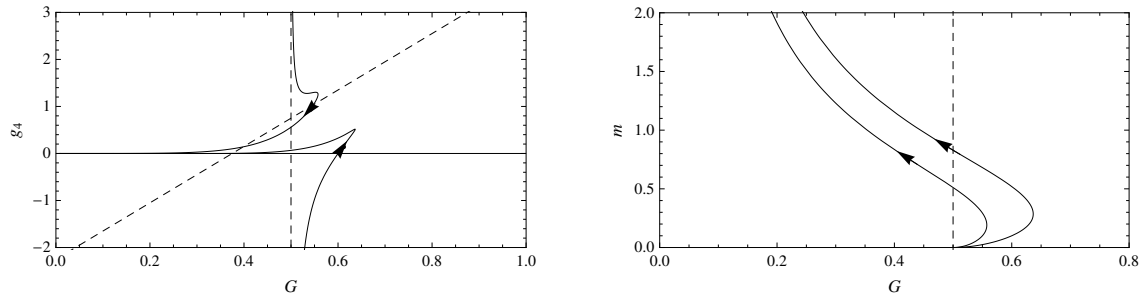

(a) (b)

Figure 4.5: (a) The projection in the (G, g_4) plane of the two trajectories belonging to in the broken region is represented. This region is defined by the linearization around the non-Gaussian fixed point found for the system including m, G and g_4 at $d = 3$. The flows are obtained by choosing the boundaries $G(t = 0) = 0.55, 0.6$ and $g_4 = 1.3, 0$ respectively, which are the same given for the trajectories in the broken region of Fig. 4.1, and by setting $m(t = 0) = 0.1$. (b) In this panel, the projection in the (G, m) plane of the two trajectories belonging to the broken region is represented. The flows are obtained by choosing the boundaries $G(t = 0) = 0.55, 0.6$ and $g_4 = 1.3, 0$ respectively, which are the same given for the trajectories in the broken region of Fig. 4.1, and by setting $m(t = 0) = 0.1$. The trajectories in the picture closely resemble those in the broken region of the Fig. 3.2

Similarly, the stiffness affecting the trajectories in the broken region of the Fig. 4.1 (a) is healed by the presence of an explicit mass. Indeed, in Fig. 4.5 (a) it is shown how such trajectories, rather than diverge, are captured by the origin thus leading the whole system to its IR behaviour.

4.4 Higher powers in generic N

Until now the impact of the higher powers has been analyzed in the Hartree approximation. This has favoured the comparison with the other analytical approaches, since in the large N limit some aspects of the triviality of the model can be rephrased, in a purely fermion language, by looking at the behaviour of the fermion couplings around the non-Gaussian fixed point. On the other hand, it is natural to ask what happens beyond this approximation. The *RG* equation for the Wilsonian potential has been worked out without any sort of expansion in the N parameter, thus the results can be trusted, inside the range of validity of the LPA, for any value of the flavour number. Using the

dimensionless version of the Eq. (3.99), one finds:

$$\begin{aligned}
\frac{dm}{dt} &= m + \frac{2C_d G m N \mathrm{tr}\,\mathbb{I}}{m^2+1} - \frac{2C_d G m}{m^2+1}, \\
\frac{dG}{dt} &= (2-d)G + \frac{2C_d g_3 m N \mathrm{tr}\,\mathbb{I}}{m^2+1} - \frac{4C_d g_3 m}{m^2+1} \\
&- \frac{2C_d G^2 (m^2-1) N \mathrm{tr}\,\mathbb{I}}{(m^2+1)^2} + \frac{4C_d G^2 (2m^2-1)}{(m^2+1)^2}, \\
\frac{dg_3}{dt} &= \frac{6C_d g_3 G (1-m^2) N \mathrm{tr}\,\mathbb{I}}{(m^2+1)^2} + \frac{6C_d g_3 G (7m^2-3)}{(m^2+1)^2} \\
&- \frac{2C_d g_4 m N \mathrm{tr}\,\mathbb{I}}{m^2+1} + \frac{6C_d g_4 m}{m^2+1} + \frac{4C_d G^3 m (m^2-3) N \mathrm{tr}\,\mathbb{I}}{(m^2+1)^3} \\
&+ \frac{4C_d G^3 m (15-13m^2)}{(m^2+1)^3} + (3-2d) g_3, \\
\frac{dg_4}{dt} &= -\frac{24 C_d g_3 G^2 m (m^2-3) N \mathrm{tr}\,\mathbb{I}}{(m^2+1)^3} + \frac{528 C_d g_3 G^2 m (m^2-1)}{(m^2+1)^3} \\
&- \frac{8C_d g_4 G (m^2-1) N \mathrm{tr}\,\mathbb{I}}{(m^2+1)^2} + \frac{16 C_d g_4 G (5m^2-2)}{(m^2+1)^2} \\
&+ \frac{6C_d g_3^2 (m^2-1) N \mathrm{tr}\,\mathbb{I}}{(m^2+1)^2} + \frac{24 C_d g_3^2 (1-3m^2)}{(m^2+1)^2} \\
&+ \frac{12 C_d G^4 (m^4-6m^2+1) N \mathrm{tr}\,\mathbb{I}}{(m^2+1)^4} \\
&- \frac{96 C_d G^4 (5m^4-9m^2+1)}{(m^2+1)^4} + (4-3d) g_4,
\end{aligned} \tag{4.38}$$

which represent the extension of the Eqns. from (4.10) to (4.13) to the region of small N values.

Once again two fixed points are found. The Gaussian FP, which does not depend on the flavour number N, provides the the usual scaling exponents also given in Eqs. 4.15. The other solution is the non-Gaussian FP associated with the χSB mechanism. This is:

$$m = 0, \tag{4.39}$$

$$G = \frac{d-2}{2C_d(N\mathrm{tr}\,\mathbb{I}-2)}, \tag{4.40}$$

$$g_3 = 0, \tag{4.41}$$

$$g_4 = \frac{3(d-2)^4 (N\mathrm{tr}\,\mathbb{I}-8)}{4C_d^3 (N\mathrm{tr}\,\mathbb{I}-2)^3 (N\mathrm{tr}\,\mathbb{I}(4-d)+10d-24)}. \tag{4.42}$$

It is important to stress that the fixed point solution is found at any value of $2 \leq d \leq 4$ and without presenting the pathologies found in the Hartree approximation. Despite

this the fourth dimension is very special and again can be regarded as the upper critical dimension for the chiral transition. The linearization around this fixed point gives the eigenvalues:

$$\lambda_1 = \frac{N\mathrm{tr}\,\mathbb{I}(d-1)-d}{N\mathrm{tr}\,\mathbb{I}-2}, \tag{4.43}$$

$$\lambda_2 = d-2, \tag{4.44}$$

$$\lambda_3 = \frac{N\mathrm{tr}\,\mathbb{I}(d-3)-5d+12}{N\mathrm{tr}\,\mathbb{I}-2}, \tag{4.45}$$

$$\lambda_4 = \frac{N\mathrm{tr}\,\mathbb{I}(d-4)-10d+24}{N\mathrm{tr}\,\mathbb{I}-2}. \tag{4.46}$$

The corresponding eigenvectors are instead:

$$v_1 = \left(\frac{2C_d^2(N\mathrm{tr}\,\mathbb{I}-2)^2(N\mathrm{tr}\,\mathbb{I}2d-6)(N\mathrm{tr}\,\mathbb{I}(4-d)-10d+24)}{3(d-2)^3((N\mathrm{tr}\,\mathbb{I})^2+N\mathrm{tr}\,\mathbb{I}(2d-11)-13d+36)},0,1,0\right), \tag{4.47}$$

$$v_2 = \left(0,\frac{C_d^2(N\mathrm{tr}\,\mathbb{I}-2)^2(N\mathrm{tr}\,\mathbb{I}+4d-10)(N\mathrm{tr}\,\mathbb{I}(4-d)+10d-24)}{6(d-2)^3(N\mathrm{tr}\,\mathbb{I}-8)(N\mathrm{tr}\,\mathbb{I}+3d-8)},0,1\right), \tag{4.48}$$

$$v_3 = (0,0,1,0), \tag{4.49}$$

$$v_4 = (0,0,0,1). \tag{4.50}$$

These results are extremely useful in order to study the problems related with the marginality of some the operators found in the Hartree approximation. The impact of the cubic operator will be studied in the following section, in the present one only the behaviour of the quartic operator is taken into account. By expanding the fixed point in powers of $1/N'$ in Eq. (4.42) one obtains:

$$g_4^* = \frac{3(d-2)^4}{4(4-d)C_d^3}\frac{1}{N'^3}+\frac{6(d-2)^5}{(4-d)^2C_d^3}\frac{1}{N'^4}+\mathcal{O}(1/N'^5). \tag{4.51}$$

The first term in the expansion gives the same result found in Eq. (4.14). The lower critical dimension ($d=2$) that is the first dimension in which the fixed point can be used for describing a critical phenomena and the upper critical dimension ($d=4$), after which the FP loses its critical properties are clearly highlighted. At every order in the $1/N$ expansion the g_4^* diverges at $d=4$. The reason is that the value of g_4 at the fixed point, given in Eq. (4.42) has a term of the type $N\mathrm{tr}\,\mathbb{I}$, thus an inverse power of $\epsilon=4-d$ is generated at every order in the $1/N$ expansion. Returning to Eq. (4.42) and setting $d=4$, the expansion of the fixed point solution in powers of $1/N'$ turns out to be:

$$g_4^* = \frac{3}{4C_4^3}\frac{1}{N'^2}-\frac{3}{2C_4^3}\frac{1}{N'^3}+\mathcal{O}(1/N'^4), \tag{4.52}$$

showing that at $d = 4$ the fixed point has become of order $1/N^2$, rather than $1/N^3$, in the large N limit. Perhaps this is a sign of the failure of the LPA approximation at $d = 4$, although also in this approximation the operator turns out to be marginal in the large N limit. Indeed the eigenvalue in Eq. (4.46) can be rewritten as:

$$\lambda_4 = d - 4 + \frac{8(d-2)}{2/N' - 1}\frac{1}{N'}. \tag{4.53}$$

4.5 The cubic operator and the onset of a first order transition

Until now, the behaviour of the cubic coupling was only considered in the framework of the general analysis performed in Sec.4.2 and Sec.4.4. A systematic treatment of the cubic interaction at $d = 3$ was performed by G. Gat. et al. [64] by using the large N expansion method. Here some of their results are briefly summarized permitting the comparison with our *RG* methods. They were able to calculate the beta function of the cubic coupling at the next to leading order in the $1/N$ series. At the leading order, the authors found that the cubic operator $(\bar{\psi}\psi)^3$ is marginal, while the operator $(\bar{\psi}\psi)$ and $(\bar{\psi}\psi)^2$ are both relevant. They suggest that the behaviour of the cubic operator near the non trivial fixed point of the GN model is similar to that one of the ϕ^6 operator near the Gaussian fixed point in the scalar theory [68], [69],[70], [71]. Both these operators are trivial near the corresponding fixed point. As is well known, in the scalar case this is a signal of a first order transition occurring when the bare parameters are chosen in the vicinity of the origin. Conversely when corrections to the leading order are included the operator turns out to be irrelevant.

The value of the anomalous dimension of the σ^3 operator near the critical FP was also computed, thus giving:

$$[\sigma^3] = 3 + \frac{32}{\pi^2 N'} \simeq 3 + 3.24\frac{1}{N'}. \tag{4.54}$$

The same results can be achieved and immediately extended by means of the Wilsonian *RG* technique. The eigenvalue in Eq. (4.45) can be rewritten as:

$$\lambda_3 = (d-3) + \frac{3(d-2)}{2 - N'}, \tag{4.55}$$

which clearly shows the marginality of the operator $\mathcal{O}_3$ in the Hartree approximation. Starting from this expression the anomalous dimension can also be calculated giving the result:

$$\gamma_3 = 3(d-2) + \frac{3(d-2)}{2-N'}, \tag{4.56}$$

thus the scaling dimension of $\mathcal{O}_3$ turns out to be:

$$[\mathcal{O}_3] = 3(d-1) - \gamma_3 = 3 + \frac{3(d-2)}{N'-2} \simeq 3 + 3\frac{1}{N'}. \tag{4.57}$$

Up to the first order in the $1/N'$ expansion the result agrees with those found in Eq. (4.54), enforcing the statement that the critical region also at $d = 3$ is well described by the LPA.

.

CHAPTER 5

RG ANALYSIS OF FERMION-BOSON THEORIES

The present chapter is a brief review of some interesting results which can be found by extending our Wilsonian *RG* methods to the study of a system of interacting fermions and bosons via a potential of the form $U(\bar{\psi}\psi\phi)$.

Clearly such a potential can include the Yukawa coupling as well as purely fermion self-interactions. The case $N = 1$ and $d = 4$ was first analyzed by [25].

These authors showed how, even in the LPA approximation, quite a good description of the triviality of the Yukawa model can be recovered. Indeed, analyzing the critical behaviour of the Yukawa model at $d = 4$, they have considered trajectories, in bare parameter space, which lie near the Gaussian fixed point, finding results which are consistent with the perturbative prescriptions. [1]

In the following, where the study is extended to $d < 4$ and for every N value, it will be shown, on the opposite, that the LPA is not able to grasp all the features of the chiral transition. The reasons for this will also be analyzed.

Successively, our studies, even if incomplete, are devoted to the behaviour of systems including both fermion self-interactions and interactions coupling fermions with bosons. A very interesting result is found. Unusual behaviour for the Yukawa coupling is noticed as the result of a non-Gaussian fixed point triggered by the presence of an explicit Fermi interaction. Such a fixed point persists at $d = 4$. The scaling of the Fermi coupling resembles that found for the GN model in chap.3, while the Yukawa coupling follows a

[1] However an accurate description requires the inclusion of the field strength renormalization.

simple power law scaling.

5.1 Wilsonian RG equation for theory with fermions and bosons

First of all, the Wilsonian RG equation for a chiral theory with N fermions and a single scalar can be worked out easily for generic d dimension. The result will be an extension of the equation found in [25]. The LPA approximation is obtained by assuming the following ansatz for the Wilsonian action:

$$S_k\left[\Psi,\bar{\Psi},\Phi\right]=\int d^dx\left[-\bar{\Psi}\left(x\right)\partial\!\!\!/\,\Psi\left(x\right)+\frac{1}{2}(\partial_\mu\Phi(x))^2+U_k\left(\bar{\Psi}\Psi\Phi\right)\right]. \tag{5.1}$$

A straightforward application of the procedure, just introduced in Sec. 3.3.3, leads to the RG equation for the Wilsonian potential U_k. For completeness, some tricks used for the integration of the fast fermion and boson degrees of freedom are reported in App. D.3. The equation for the dimensionless Wilsonian potential $V\left(\sigma,\phi,t\right)$, where $\sigma=\bar{\psi}\psi$ and the fields $\psi,\bar{\psi}$ and ϕ are dimensionless quantities too, turns out to be:

$$\begin{aligned}\frac{\partial}{\partial t}V &= dV-\frac{d-2}{2}\phi V_\phi-\left(d-1\right)\sigma V_\sigma\\ &+ C_d\left[\log\left(1+V_{\phi\phi}\right)-N'\log\left(1+V_\sigma^2\right)+\log\left(1+\Sigma\right)\right],\end{aligned} \tag{5.2}$$

where:

$$\Sigma=\frac{2\sigma V_\sigma\left(V_{\sigma\sigma}-\frac{V_{\sigma\phi}V_{\phi\sigma}}{1+V_{\phi\phi}}\right)}{1+V_\sigma^2}. \tag{5.3}$$

5.2 Equations for the Yukawa theory in the LPA

First of all, by using Eq. (5.2) the RG equations for the Yukawa model in the LPA are found.

On the one hand they give us the possibility of estimating the range of validity of the LPA near $d=4$, on the other hand they provide the starting point for further analysis. The Wilsonian potential for the Yukawa theory has the form:

$$V=\frac{M^2}{2}\phi^2+\frac{\lambda}{4!}\phi^4-g\phi\sigma. \tag{5.4}$$

By plugging this expression in Eq. (5.2) the following equations can be found:

$$\beta_\lambda = (4-d)\lambda - 2C_d\left(\frac{3\lambda^2}{2(1+M^2)^2} - 6N'g^4\right), \tag{5.5}$$

$$\beta_{g^2} = (4-d)g^2 - 2C_d\frac{2g^4}{1+M^2}, \tag{5.6}$$

$$\beta_{M^2} = 2M^2 + 2C_d\left(\frac{\lambda}{2(1+M^2)} - N'g^2\right). \tag{5.7}$$

Now a comparison with the Eqs. (3.51),(3.52),(3.53) can be performed easily. Indeed, near $d = 4$ each running coupling near the critical region flows around the origin. Thus by replacing $2C_4 = 1/8\pi^2$ and by setting $N' = 4N$, the Eqs. (5.5), (5.6),(5.7) can be consistently approximated by the following expressions:

$$\beta_\lambda = \epsilon\lambda - \frac{1}{8\pi^2}\left(\frac{3}{2}\lambda^2 - 24Ng^4\right), \tag{5.8}$$

$$\beta_{g^2} = \epsilon g^2 - \frac{1}{8\pi^2}2g^4, \tag{5.9}$$

$$\beta_{M^2} = 2M^2 - \frac{1}{8\pi^2}\frac{\lambda}{2}M^2, \tag{5.10}$$

Now it is easy to recognize which contributions are lacking in the LPA. According to the prescriptions given in Eqs.(3.19), (3.20), (3.21), the beta functions of the bare couplings, given in Eqs. (5.8),(5.9),(5.10), should be modified by the following replacements:

$$\beta_\lambda \to \beta_\lambda - 4\gamma_\phi\lambda, \tag{5.11}$$

$$\beta_{g^2} \to \beta_{g^2} - 2\gamma_\phi g^2 - 4\gamma_\psi g^2, \tag{5.12}$$

$$\beta_{M^2} \to \beta_{M^2} - 2\gamma_\phi M^2. \tag{5.13}$$

$$\tag{5.14}$$

Using the anomalous dimensions given in Eqs (3.54),(3.55) the beta functions in Eqs. (3.51), (3.52),(3.53), calculated by means of the epsilon expansion method, are recovered. Since γ_ϕ is of $\mathcal{O}(N)$, important contributions are lost in the LPA for large N values if g^2 is of $\mathcal{O}(1/N)$. Thus Hartree approximation cannot be consistently obtained. Returning to Eqs. (5.5), (5.6),(5.7) and performing an appropriate rescaling, which is equivalent to set

$C_d = 1$, the following equations are obtained:

$$\lambda' = (4-d)\lambda - \frac{3\lambda^2}{(1+M^2)^2} + 12N'g^4, \tag{5.15}$$

$$g^{2'} = (4-d)g^2 - \frac{4g^4}{1+M^2}, \tag{5.16}$$

$$M^{2'} = 2M^2 + \frac{\lambda}{1+M^2} - 2N'g^2. \tag{5.17}$$

Four fixed point solutions can be found for $d < 4$: the Gaussian one, the Wilson-Fisher fixed point and the other two fixed points analyzed in Sec. 3.51. It can be simply verified how these equations describe well the behaviour of the system around the Wilson-Fisher fixed point. Indeed, by linearizing the system around the fixed point:

$$g^2 = 0, \tag{5.18}$$

$$M^2 = \frac{4-d}{d-10} \simeq -\frac{\epsilon}{6}, \tag{5.19}$$

$$\lambda = \frac{12(4-d)}{(d-10)^2} \simeq \frac{\epsilon}{3}, \tag{5.20}$$

one finds the eigenvalues:

$$\lambda_\tau = \frac{1}{3}\left(\sqrt{7d^2-62d+145}+2d-5\right) \simeq 2 - \frac{\epsilon}{3}, \tag{5.21}$$

$$\lambda_2 = \frac{1}{3}\left(-\sqrt{7d^2-62d+145}+2d-5\right) \simeq -\epsilon, \tag{5.22}$$

$$\lambda_3 = 4 - d = \epsilon, \tag{5.23}$$

consistent with the results in Eqs. (3.60),(3.61),(3.62). Such a result is a simple extension of the analysis performed in [72], for a purely scalar theory. However one more comment is needed, when also fermions are included. In such a case, the anomalous dimensions of the scalar and fermion fields can be discarded since the fixed point value for g^2 is strictly zero. Unfortunately, this is not the case, for the fixed point associated with the χSB. After that, an epsilon expansion is performed near $d = 4$, this fixed point turns out to be:

$$g^2 \simeq \frac{\epsilon}{4}, \tag{5.24}$$

$$\lambda \simeq \frac{1+\sqrt{1+9N'}}{6}\epsilon, \tag{5.25}$$

$$M^2 \simeq \frac{1}{12}\left(-1+3N'-\sqrt{1+9N'}\right)\epsilon \tag{5.26}$$

Similarly, by linearizing around this fixed point and by expanding the result near $d = 4$, one finds the eigenvalues:

$$\lambda_\tau = 2 - \frac{1+\sqrt{1+9N'}}{6}\epsilon, \tag{5.27}$$

$$\lambda_2 = -\epsilon, \tag{5.28}$$

$$\lambda_3 = -\sqrt{1+9N'}\epsilon. \tag{5.29}$$

One relevant and two irrelevant directions are found, however since important contributions are missed in the LPA, the large N limit cannot be performed in a consistent way. On the other hand when $d = 4$ one finds that, near the origin, the coupling g^2 behaves as:

$$g^2(t) = \frac{4\pi^2}{t+c}. \tag{5.30}$$

By comparing this result with that given in Eq. (3.71) one can see that the same scaling, although quantitatively different, is predicted.

5.3 Fermi and Yukawa theories coupled together

In the previous section the Wilsonian *RG* method was applied for the description of the Yukawa theory, while in cap.3 it was used for the analysis of the GN model. In the following a system involving both the Fermi and the Yukawa interaction is taken into account. The beta functions of such a theory can be immediately calculated by extending the ansatz in Eq. (5.4) in order to include a fermion mass term and the Fermi coupling. One obtains:

$$V = \frac{M^2}{2}\phi^2 + \frac{\lambda}{4!}\phi^4 - g\phi\sigma - m\sigma - \frac{G}{2}\sigma^2. \tag{5.31}$$

Thus, inserting this expression in Eq. (5.2), the following set of equations is found:

$$\frac{dm}{dt} = m + \frac{2N'Gm}{1+m^2} - \frac{2Gm}{1+m^2} - \frac{2mg^2}{(1+m^2)(1+M^2)}, \tag{5.32}$$

$$\frac{dG}{dt} = (2-d)G + \frac{2N'G^2(1-m^2)}{(1+m^2)^2} - \frac{4G^2(1-2m^2)}{(1+m^2)^2} + \frac{4m^2g^4}{(1+m^2)(1+M^2)^2} + \frac{4Gg^2(-1+3m^2)}{(1+m^2)^2(1+M^2)}, \tag{5.33}$$

$$\frac{dg^2}{dt} = (4-d)g^2 + \frac{4N'Gg^2(1-m^2)}{(1+m^2)^2} - \frac{4Gg^2(1-m^2)}{(1+m^2)^2} - \frac{4g^4(1-m^2)}{(1+m^2)^2(1+M^2)}, \tag{5.34}$$

$$\frac{dM^2}{dt} = 2M^2 + \frac{\lambda}{1+M^2} - \frac{2N'g^2(1-m^2)}{(1+m^2)^2}, \tag{5.35}$$

$$\frac{d\lambda}{dt} = (4-d)\lambda - \frac{3\lambda^2}{(1+M^2)^2} + \frac{12N'g^4(1-6m^2+m^4)}{(1+m^2)^4}. \tag{5.36}$$

By freezing all the couplings in the r.h.s of each equation at their bare values the one loop contribution to the $1PI$ functions with the external momenta set to zero is obtained. In such a way, the equations can be easily checked.

In order to handle this complicated system one can start with the search of the fixed points. For $d < 4$ several fixed point solutions are found. Many of these are just extensions of those reported in Sec. 5.2. The Gaussian solution, the Wilson-Fisher fixed point, and the two non-Gaussian fixed point, presented in Sec. 3.2.4 and Sec. 5.2, are recovered. In all these cases an explicit mass term provides a new relevant direction, while the Fermi coupling, as expected, behaves as an additional irrelevant direction, which can be consistently discarded near the critical region.

In addition, two new interesting non-Gaussian solutions are found.

5.3.1 Two non-Gaussian solutions

The first fixed point is given by:

$$
\begin{aligned}
m &= 0, && (5.37)\\
G &= \frac{d-2}{2(N'-2)}, && (5.38)\\
g^2 &= 0, && (5.39)\\
M^2 &= 0, && (5.40)\\
\lambda &= 0. && (5.41)
\end{aligned}
$$

It seems to be a simple extension of the result found in Sec. (3.4.2), but it shows an interesting feature. Indeed, by linearizing around this solution and performing an expansion around $d = 4$ one finds the following eigenvalues:

$$
\begin{aligned}
\lambda_1 &= 3 - \epsilon + \frac{2-\epsilon}{N'-2}, && (5.42)\\
\lambda_2 &= 2 - \epsilon, && (5.43)\\
\lambda_3 &= 4 - \epsilon + \frac{2(2-\epsilon)}{N'-2}, && (5.44)\\
\lambda_4 &= 2, && (5.45)\\
\lambda_5 &= \epsilon. && (5.46)
\end{aligned}
$$

The eigenvalues λ_1 and λ_2 are associated with the two relevant operators, characterizing the non-perturbative behaviour of the GN model, which, roughly speaking, can be identified with the composite fields $\bar{\psi}\psi$ and $(\bar{\psi}\psi)^2$. On the other hand, the eigenvalues λ_4 and λ_5 are nothing but those provided by the Gaussian scaling of the operators ϕ^2 and ϕ^4. Finally the eigenvalue λ_3 is a new relevant direction which can be associated with the behaviour of the squared Yukawa coupling g^2.

One of the most interesting aspects of these results precisely concerns the behaviour of this coupling at $d = 4$. Indeed, by setting $\epsilon = 0$ one finds that g^2 is no longer trivial. The non-Gaussian FP (see Eqs. from (5.37) to (5.41)) is an UV attractor for the v_3 direction. Conversely the last one departs towards the IR region following a simple power law scaling.

Before proceeding with further analysis at $d = 4$ the other non-Gaussian solution is presented.

This is:

$$
\begin{aligned}
m &= 0, && (5.47)\\
G &= \frac{d-2}{2(N'-2)}, && (5.48)\\
g^2 &= 0, && (5.49)\\
M^2 &= \frac{4-d}{d-10}, && (5.50)\\
\lambda &= \frac{12(4-d)}{(d-10)^2}. && (5.51)
\end{aligned}
$$

The non-Gaussian fixed point, given in Eqs. from (5.37) to (5.41), joins the values obtained in the Gaussian fixed point solution of the Yukawa theory with those of m and G at the non-Gaussian fixed point found in Sec. 3.5. While, the fixed point solution given in Eqs. from (5.47) to (5.51) combines the non-Gaussian FP of the GN model with the Wilson-Fisher one of the Yukawa theory.

Both the FP in Eqs. from (5.37) to (5.41) and that in Eqs. from (5.47) to (5.51) coincide at $d = 4$. By linearizing the system around the non-Gaussian solution in in Eqs. from (5.47) to (5.51) one finds:

$$
\begin{aligned}
\lambda_1 &= 3 - \epsilon + \frac{2-\epsilon}{N'-2}, && (5.52)\\
\lambda_2 &= 2 - \epsilon, && (5.53)\\
\lambda_3 &= 4 - \epsilon + \frac{2(2-\epsilon)}{N'-2}, && (5.54)\\
\lambda_4 &= 2 - \frac{\epsilon}{3}, && (5.55)\\
\lambda_5 &= -\epsilon. && (5.56)
\end{aligned}
$$

The values of λ_1, λ_2 and λ_3 are the same as those given in Eqs. (5.42),(5.43) and (5.44) respectively. Conversely λ_4 and λ_5 coincide with the eigenvalues of the Wilson-Fisher model near $d = 4$. Some interesting information about the nature of this fixed point is obtained by calculating the scaling dimension of some operators in the Hartree approximation. It

is found:

$$
\begin{aligned}
[\mathcal{O}_1] &= \left[\bar{\psi}\psi\right]_0 - \gamma_1 = d - 1 - (d-2) = 1, && (5.57)\\
[\mathcal{O}_2] &= \left[(\bar{\psi}\psi)^2\right]_0 - \gamma_2 = 2 \\
&= 2\left[\mathcal{O}_1\right], && (5.58)\\
[\mathcal{O}_3] &= \left[\phi\bar{\psi}\psi\right]_0 - \frac{\gamma_3}{2} = \frac{d-2}{2} + d - 1 - (d-2) \\
&\simeq [\phi] + [\mathcal{O}_1]\,. && (5.59)
\end{aligned}
$$

The first two relations resemble the classical result of the GN model given Eqs. (3.119), (3.120). On the other hand the last equality, which is based on the assumption made in the LPA that $\gamma_\phi \simeq 0$, suggests a simple statistical interpretation. Near this fixed point the boson degrees of freedom weakly interact with a strong coupled fermion mixture, as also shown by the fact that $g^2 << 1$ and $G \simeq G_c$. In this sense, it is the opposite situation to that found near the strong coupled Yukawa theory in which $g^2 \simeq g_c^2$ and $G = 0$.

5.3.2 Non-trivial scaling of the Yukawa coupling near and at $d = 4$

In closing a numerical study of the system described by Eqs. from (5.32) to (5.36) is performed at $d = 4$. More precisely, the triviality of the Yukawa coupling, found in the perturbative region, is compared with an unusual scaling which is triggered by the presence of the non-Gaussian fixed point:

$$
\begin{aligned}
m &= 0, && (5.60)\\
G &= \frac{1}{(N'-2)}, && (5.61)\\
g^2 &= 0, && (5.62)\\
M^2 &= 0, && (5.63)\\
\lambda &= 0. && (5.64)
\end{aligned}
$$

As anticipated, both the fixed point in Eqs. from (5.37) to (5.41) and the one in Eqs. from (5.47) to (5.51) coincide with the solution in Eqs. from (5.60) to (5.64) at $d = 4$.

At $d = 4$ and for $N = 2$, the behaviour of the Yukawa coupling near the Gaussian fixed point is compared with the unusual scaling of the same parameter near the non-Gaussian solution.

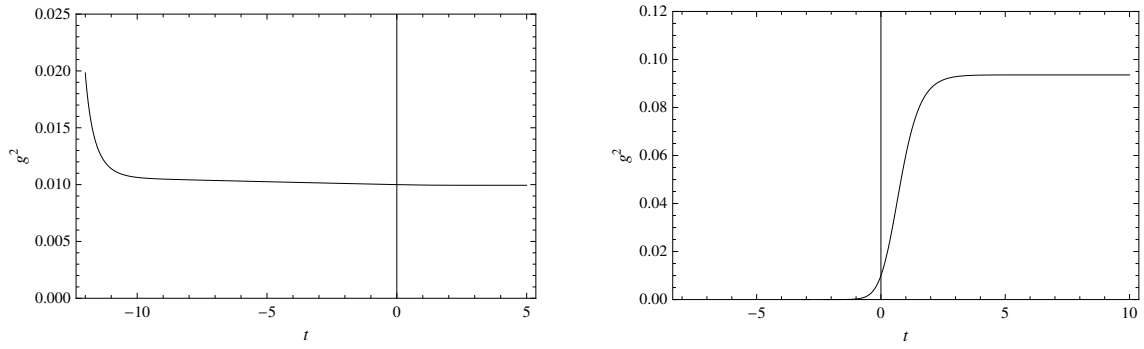

(a) (b)

Figure 5.1: (a) The flow of running Yukawa coupling $g^2(t)$, near the perturbative region, is shown. It was obtained by numerical solving the Eqs. from (5.32) to (5.36), at $d = 4$ and $N' = 8$, with the boundaries at $t = 0$: $m(t = 0) = 10^{-3}, M^2(t = 0) = 0.1, \lambda(t = 0) = 0.2, g^2(t = 0) = 0.01$ and $G(t = 0) = 0$. (b) The flow of running Yukawa coupling $g^2(t)$, around the non-Gaussian fixed point (Eqs. from (5.37) to (5.41)) , is shown. It was obtained by numerical solving the Eqs. from (5.32) to (5.36), at $d = 4$ and $N' = 8$, with the boundaries at $t = 0$: $m(t = 0) = 10^{-3}, M^2(t = 0) = 0.1, \lambda(t = 0) = 0.2, g^2(t = 0) = 0.01$ and $G(t = 0) = 0.833$.

The Gaussian region (Fig. 5.1 (a)) is obtained by setting the running Fermi constant $G(k)$ strictly at zero on the boundary. The running coupling $g^2(k)$ follows its usual perturbative behaviour. Taking a finite value in the IR region it reaches the Landau pole at a finite UV scale. On the other hand by choosing a non-zero value for $G(k)$ at the boundary, the $g^2(k)$, while saturates to a constant value in the IR region, flows towards zero when $k \to \infty$ as shown in Fig. 5.1 (b). According to the result given in Eq. (5.54), for large N values, the dimensionless coupling $g^2(t)$ scales as k^d, thus the dimensioned one behaves as: $g^2(k) \sim k^{4-2d}$. In this way the dimensioned Yukawa coupling behaves as:

$$g(k) \sim \frac{1}{k^{d-2}}, \tag{5.65}$$

which is far from triviality also at $d = 4$.

CHAPTER 6

SUMMARY AND CONCLUSIONS

In the present work the non-perturbative renormalizability of self-interacting fermion models has been investigated for a generic dimension $2 \leq d \leq 4$, with the help of a fermion Wilsonian *RG* method. The *RG* picture of the χSB has been compared with the descriptions provided by other analytical techniques. Moreover, regions unreachable by standard analytical tools have also been investigated. In this context, the GN model has been chosen as a paradigm for theories which allow for a dynamical mechanism for the generation of the masses for its simplicity and for the reliability of the known results. A comparison with theories involving the explicit use of elementary scalars has also been performed.

The first part of this work (chapters one and two) is mainly a review of the usual tools used for investigating fermion QFTs and of some features of the critical behaviour of such models. Although much useful literature on this subject already exists, this part makes it possible to contextualize our original *RG* results in a coherent way. Moreover some new, albeit simple, results have been worked out in this context. The perturbative techniques for calculating the Green's functions of elementary and composite fermion fields are also reviewed. More specifically, the role of the composite operator $\bar{\psi}\psi$ was emphasized as an essential ingredient for the description of the χSB and for the appearance of scalar collective excitations in fermion theories. Some amplitudes are explicitly computed in order to get useful expressions to be compared with our later *RG* results. The renormalizability of the Yukawa theory in $d = 4$ dimensions is discussed, which helps in showing later the

non-perturbative (actually $1/N$) renormalizability of the GN model and its triviality in $d = 4$ dimensions. Indeed, as is well known, the usual bosonization techniques and the $1/N$ expansion method allow the amplitudes of a four fermion theory to be rewritten in terms of diagrams of a Yukawa model.

A typical tool to analyze the non-perturbative behaviour of the GN model is the DS formalism. As at our knowledge a systematic derivation of these equations for four-fermion theories is missing, in the present work the DS equations for the $1PI$ two point and four point Green's functions for the GN model have been explicitly worked out. Then at leading order of the $1/N$ expansion, which corresponds to the so called "Hartree approximation", the well known results are recovered, namely, a non-vanishing fermion mass m for values of the Fermi constant G greater than a critical value G_c and the mass M of the composite boson, with $M = 2m$. The DS equations for the correlators of a theory with elementary and composite operators are then related to the DS equations of the bosonized version of the theory.

Successively, the critical behaviour of the GN and Yukawa models is reviewed for $2 \leq d \leq 4$ by using the mapping between an euclidean QFT and a SFT. The critical exponents (related to the χSB of these models), as obtained at the next to leading order in the $1/N$ expansion, are also listed. As a useful tool for such an analysis, the effective action for the bosonized version of the GN model is explicitly worked out here at the same order.

Finally, the beta functions of the Yukawa model coupling constants and the corresponding critical exponents, derived with the help of field theoretical renormalization group methods (implemented in the framework of the epsilon expansion), are presented. These latter methods provide a useful bridge for the transition to our Wilsonian RG approach.

By starting with the appropriate scale dependent action S_k for fermion models and performing a non-trivial extension of previous techniques, a new RG equation for a generalized N flavors GN model in $2 \leq d \leq 4$ is established. This equation provides a non-perturbative analytical tool to study this model in *any dimension*, with no reference to $1/N$ or small coupling or epsilon expansions. Indeed, within the Wilsonian approach, no expansion in any "small parameter" is needed as the width δk of the infinitesimal shell, over which the RG elimination of modes is performed, provides the *natural* small term

which makes the corresponding Gaussian integration exact.

This opens the way to analytical studies which cannot be performed with any of the other analytical techniques typically used. The approximation adopted here is the gradient expansion for the action S_k in its the lowest order, the Local Potential Approximation, which consists in neglecting the fluctuations induced by derivative operators. The range of validity of such an approximation is also investigated.

As a check for the validity of our approach by comparison with known results, the large N case is first considered. Actually, the RG equation for the Wilsonian potential contains "Hartree" and "Fock" contributions. Neglecting the latter, the leading order in the $1/N$ expansion to our RG equation is obtained.

By truncating the potential to the Fermi and mass terms, the RG equations for the running mass $m(k)$ and Fermi constant $G(k)$ are derived and it is found that the theory possesses a non-trivial fixed point. By linearizing these equations around this fixed point, the critical exponents are computed.

Successively, the coupled RG equations for $G(k)$ and $m(k)$ are numerically studied in the whole (G, m) plane. From this analysis, in turns out that the physics of the chiral phase transition can be described well in terms of a cross-over phenomenon triggered by the presence of an infinitesimal bare mass. Interestingly, it is found that, when the bare value of the Fermi constant is greater than the fixed point value G_c, the running of $m(k)$ from the UV to the IR shows a "steep" cross-over and a finite value of the fermion mass is generated. As in the case of the strict unbroken-broken phase transition, for values of G greater than G_c, the system is unstable against quantum fluctuations: the presence of an even infinitesimal bare mass gives rise to an amplification mechanism which resolves the instability through the generation of a finite physical mass.

It is also interesting to note that the knowledge of $m(k)$ in the whole range of k provides a very good example of IR-UV connection. The same is true for $G(k)$. Our RG approach makes this connection possible in a natural way. Typically, the behaviour of these functions is known only in the scaling region.

This IR-UV connection, which is first studied numerically, can also be investigated by means of some analytical approximations to $m(k)$ and $G(k)$. First of all, by considering a simple approximation to the RG equation for $m(k)$, the well known NJL result is reproduced. However, although this approximation is able to grasp qualitatively the

main features of the RG equations (which, due to quantum fluctuations, lead to the chiral phase transition), quantitatively more accurate analytical profiles for $m(k)$ and $G(k)$ require more sophisticated approximations.

As our results are obtained by referring directly to a purely fermion language, it is not difficult to find issues which can be handled within our approach but are out of reach of other analytical techniques. For instance, the critical exponents can be computed even for small values of N and also when the coupling constant space is larger than the one spanned by only the mass and the Fermi constant. As for the computation of the critical exponents for small values of N, it is clearly necessary to include also the Fock's contributions.

Within our *RG* approach, the critical exponents for generic values of N and d are then computed. In order to test the validity of our results, they are compared, when possible, with well established results obtained by other techniques. Such analysis shows the failure of the LPA near the upper-critical dimension ($d = 4$) of the model. Indeed, near $d = 4$, only at the leading order of the large N expansion (Hartree approximation) our results agree with those obtained with the help of other methods.

On the other hand, for $2 \leq d \leq 3$, the *LPA* provides results which, for large values of N, agree with those obtained at the next to leading in the large N expansion. At the same time, our results, for small values of N, agree with those obtained with MC numerical simulations at $d = 3$.

Successively, the impact of higher powers of the $\bar{\psi}\psi$ operators has been considered. In the previous literature, this is obtained (in the framework of the $1/N$ expansion) by including higher powers of the auxiliary scalar field. In that context, it was shown that the quartic operator plays an important role at $d = 4$, where corrections to scaling are important. Similarly, by means of our *RG* technique, it is now shown that a marginal operator arises (in $d = 4$) due to the presence of the $(\bar{\psi}\psi)^4$ term. In the Hartree approximation, when the *LPA* works, it is also shown how to translate the triviality of the bosonized version of the model into the purely fermion language. The new and somehow unexpected result is that, in this language, such logarithmic behaviour (at $d = 4$) is obtained around a non-Gaussian fixed point, while this kind of scaling is typically observed around a Gaussian fixed point. However, from the large N picture the *GN* model seems to be trivial even beyond the leading order. How this result could be achieved or, even-

tually, disproved by means of our RG approach is an interesting development for further analysis.

The impact of the operator $(\bar{\psi}\psi)^3$ is also investigated. In particular, at $d = 3$, the marginality of this operator in the the Hartree approximation is reproduced with our RG method. Similarly, also the irrelevance of this same operator, beyond the leading order in the $1/N$ expansion, is recovered. A way of computing the anomalous dimension is also introduced and the result turns out to be in agreement, for large N values, with that found in literature.

Finally the Wilsonian RG equation is extended to theories which involve both fermions and bosons. For $N = 1$ and $d = 4$ this equation coincides with that found in literature. First of all the equations for the Yukawa theory, for $2 \leq d \leq 4$, are worked out in the LPA. A non-trivial FP which should describe the chiral transition for $d < 4$ is then found. However, by comparing with known well established results, it is shown the LPA does not provide a good description of the scaling. On the other hand, when the theory is expressed in purely fermion language, its corresponding LPA provides good results for the scaling laws.

If, however, a four Fermi interaction term is added to the Yukawa theory, an intriguing and unexpected result is found. Namely, the non-perturbative scaling of the running Fermi constant $G(k)$ triggers the appearance of a non-Gaussian fixed point which heals the triviality running of the Yukawa coupling. The latter shows a power law scaling in the UV region near this fixed point, which makes it vanish at this point.

Clearly, several questions need to be further investigated. First of all, the impact of higher derivative terms should be considered. This target is motivated by different reasons. For $2 \leq d \leq 3$, several works have been devoted to investigate the properties of condensed matter systems via the RG techniques for fermions. In this respect, the inclusion of higher derivative terms in our approach would clearly bring an important improvement.

On the other hand, it has just been shown that the inclusion of these terms is necessary in order to study the region near and at $d = 4$. Already starting with the Hartree approximation, their presence should allow the computation of the logarithmic corrections to the scaling at the upper critical dimension. Moreover, the behaviour of the GN model and eventually its triviality could be analyzed for small values of N.

It has also been shown that, when a Fermi operator is considered in addition to a Yukawa interaction term, the appearance of a non-Gaussian fixed point drastically changes the scaling of the Yukawa coupling. It is very interesting to further analyze this result beyond the LPA.

In the authors' opinion, the suggestion concerning the presence of a non-Gaussian fixed point at $d = 4$ is one of the most interesting results of the present work. Far from representing a simple rephrasing of well known results, it could provide new perspectives for the non-perturbative analysis of QFTs.

APPENDIX A

PERTURBATIVE TRICKS IN FERMION MODELS

A.1 One loop contributions to the $1PI$ four fermion vertex

In this appendix the diagrams shown in Fig 1.14 are computed. The contributions of the coupling G appearing in each diagram and the Dirac delta functions, ensuring the total momentum conservation, are both included in the coefficients:

$$\mathcal{C}_1 = -\frac{G}{2}\delta^d\left(k_1+k_2+k_3+k_4\right), \tag{A.1}$$

$$\mathcal{C}_2 = +\frac{G^2}{8}\delta^d\left(k_1+k_2+k_3+k_4\right), \tag{A.2}$$

By defining the following abbreviations:

$$\int_k = \int \frac{d^dk}{(2\pi)^d}, \tag{A.3}$$

$$D_p = \frac{\left(-i\not{p}+m_B\right)}{p^2+m_B^2}, \tag{A.4}$$

the tree level and the one-loop amplitude turn out to be:

$$\begin{aligned}
I &= \mathcal{C}_1\,(-1)\,\delta_{41} \quad \delta_{23},\\
II &= \mathcal{C}_1\,(+1)\,\delta_{21} \quad \delta_{43},\\
a &= \mathcal{C}_2\,(-4)\int_p \delta_{41} \quad tr\,(D_p\cdot D_{p+q_s}) \quad \delta_{23},\\
b_1 &= \mathcal{C}_2\,(+4)\int_p (D_p\cdot D_{p+q_s})_{41} \quad \delta_{23},\\
b_2 1 &= \mathcal{C}_2\,(+4)\int_p \delta_{41} \quad (D_{p+q_s}\cdot D_p)_{23},\\
c &= \mathcal{C}_2\,(-4)\int_p (D_p)_{21} \quad (D_{p+q_s})_{43},\\
d &= \mathcal{C}_2\,(-4)\int_p (D_p)_{21} \quad (D_{-p+q_u})_{43}\\
e &= \mathcal{C}_2\,(+4)\int_p \delta_{21} \quad tr\,(D_p\cdot D_{p+q_s}) \quad \delta_{43},\\
f_1 &= \mathcal{C}_2\,(-4)\int_p (D_{p+q_t}\cdot D_p)_{21} \quad \delta_{43},\\
f_2 &= \mathcal{C}_2\,(-4)\int_p \delta_{21} \quad (D_p\cdot D_{p+q_t})_{43},\\
g &= \mathcal{C}_2\,(+4)\int_p (D_p)_{41} \quad (D_{p+q_t})_{23},\\
h &= \mathcal{C}_2\,(+4)\int_p (D_p)_{41} \quad (D_{-p+q_u})_{23},
\end{aligned} \tag{A.5}$$

where: $q_s = k_1 + k_4$, $q_t = k_1 + k_2$,$q_u = k_1 - k_3$. Thus by setting $q_s = q_t = q_u = 0$ the result in Eq. (1.101) is recovered.

A.2 Correlators of the GN model in the bosonized version

The two point correlation function of the composite operator is given by:

$$\left\langle (\bar\psi\psi)_1(\bar\psi\psi)_2\right\rangle^{\eta,\bar\eta,K} = \frac{1}{Z_f}\frac{\delta^2}{\delta K_1\delta K_2}Z_f, \tag{A.6}$$

while the two point function of the auxiliary field is obtained through:

$$\langle\sigma_1\sigma_2\rangle^{\eta,\bar\eta,J} = G^2\frac{1}{Z_b}\frac{\delta^2}{\delta K_1\delta K_2}Z_b. \tag{A.7}$$

Still deriving the result in Eq. (1.151) it is obtained:

$$\begin{aligned}\frac{\delta^2}{\delta K_1 \delta K_2} Z_f &= \mathcal{N}\left[-\frac{\delta_{21}}{G}\exp\left(-\int\frac{K^2}{2G}\right)Z_b + \frac{1}{G^2}K_2K_1\exp\left(-\int\frac{K^2}{2G}\right)Z_b\right.\\ &- \frac{K_1}{G}\exp\left(-\int\frac{K^2}{2G}\right)\frac{\delta Z_b}{\delta K_2} - \frac{K_1}{G}\exp\left(-\int\frac{K^2}{2G}\right)\frac{\delta Z_b}{\delta K_1}\\ &+ \left.\exp\left(-\int\frac{K^2}{2G}\right)\frac{\delta Z_b}{\delta K_2\delta K_1}\right], \end{aligned} \tag{A.8}$$

moreover dividing by Z_f the expression becomes:

$$\begin{aligned}\frac{1}{Z_f}\frac{\delta^2}{\delta K_1\delta K_2}Z_f &= -\frac{\delta_{21}}{G} + \frac{1}{G^2}K_1K_2 - \frac{K_1}{G}\frac{1}{Z_b}\frac{\delta Z_b}{\delta K_2}\\ &- \frac{K_2}{G}\frac{1}{Z_b}\frac{\delta Z_b}{\delta K_1} + \frac{1}{Z_b}\frac{\delta^2 Z_b}{\delta K_2\delta K_1}. \end{aligned} \tag{A.9}$$

By this way the two point correlation functions are related according to the equation:

$$\begin{aligned}\left\langle(\bar\psi\psi)_1(\bar\psi\psi)_2\right\rangle^{\eta,\bar\eta,K} &= -\frac{\delta_{21}}{G} + \frac{1}{G^2}K_1K_2 - \frac{K_1}{G^2}\left\langle\sigma_2\right\rangle^{\eta,\bar\eta,J}\\ &- \frac{K_2}{G^2}\left\langle\sigma_1\right\rangle^{\eta,\bar\eta,J} + \frac{1}{G^2}\left\langle\sigma_1\sigma_2\right\rangle^{\eta,\bar\eta,J}. \end{aligned} \tag{A.10}$$

Setting at zero all the external sources one finds:

$$\left\langle\sigma_1\sigma_2\right\rangle = G\delta_{12} + G^2\left\langle(\bar\psi\psi)_1(\bar\psi\psi)_2\right\rangle. \tag{A.11}$$

The function $\mathcal{G}_f^{(1;1;1)}$ can be also calculated. It involves both elementary and composite fields. It is obtained by the relation:

$$\left\langle\psi\ \bar\psi\ (\bar\psi\psi)\right\rangle^{\eta,\bar\eta,K} = \frac{1}{Z_f}\frac{\delta}{\delta\bar\eta}\frac{\delta}{\delta\eta}\frac{\delta}{\delta K}Z_f. \tag{A.12}$$

Deriving the Eq. (1.151) it is found:

$$\frac{1}{Z_f}\frac{\delta^3 Z_f}{\delta\bar\eta\delta\eta\delta K} = -\frac{K}{G}\frac{1}{Z_b}\frac{\delta^2 Z_b}{\delta\bar\eta\delta\eta} + \frac{1}{Z_b}\frac{\delta^3 Z_b}{\delta\bar\eta\delta\eta\delta K}, \tag{A.13}$$

immediately implying:

$$\left\langle\psi\ \bar\psi\ (\bar\psi\psi)\right\rangle^{\eta,\bar\eta,K} = -\frac{K}{G}\left\langle\psi\,\bar\psi\right\rangle^{\eta,\bar\eta,J} + \frac{1}{G}\left\langle\psi\,\bar\psi\,\sigma\right\rangle^{\eta,\bar\eta,J}. \tag{A.14}$$

On the right hand side of Eq. (A.14) the fermion propagator, calculated in the bosonized version of the theory, is represented.

Finally the effective action of the GN model can be rewritten with the help of Eq. (1.155) as:

$$\begin{aligned}\Gamma_f &= \int \frac{K^2}{2G} - W_b + \int \frac{K}{G}(\sigma_c - K) + \int \bar{\eta}\psi_c - \int \eta\bar{\psi_c} \\ &= -\int \frac{K^2}{2G} + \Gamma_b, \end{aligned} \tag{A.15}$$

again by squaring Eq. (1.155) one obtains:

$$\Gamma_f[\psi_c, \bar{\psi}_c, \bar{\psi}\psi_c] + \int \frac{G}{2}(\bar{\psi}\psi_c)^2 = \Gamma_b[\psi_c, \bar{\psi}_c, \sigma_c] - \int \frac{\sigma_c^2}{2G} + \int \sigma_c\, \bar{\psi}\psi_c. \tag{A.16}$$

Since:

$$\frac{\delta\Gamma_b}{\delta\sigma_c} = \frac{K}{G}, \tag{A.17}$$

it is immediately found:

$$\frac{\delta\Gamma_f}{\delta\bar{\psi}\psi_c} = G\frac{\delta\Gamma_b}{\delta\sigma_c}. \tag{A.18}$$

A.3 Properties of local Grassmann vertices

A property, arising in the computation of diagrams with local fermion vertices contributions, is analyzed in the following appendix. An action involving only local interactions which are powers of the $\bar{\psi}\psi$ operator has the form:

$$S = \int d^dx \left(\bar{\psi}_\alpha i\gamma^\mu_{\alpha\beta}\partial_\mu\psi_\beta + \sum_n \frac{g_n}{n!}\left(\bar{\psi}_\alpha\psi_\alpha\right)^n \right), \tag{A.19}$$

with $\alpha, \beta = 1, ..., I_{max}$, which are the indices charactering the tensorial product of the Dirac space with the flavour one. For simplicity one can just consider the $N = 1$ case without affecting the general result. Thus $I_{max} = 2^{k+1}$ where the index k is defined by means of the relation $d = 2k + 2$ for even d dimensions and by $d = 2k + 3$ for odd D dimensions.

The Grassmann functions describing the fermion fields satisfies the anti-commutation rules: $\left\{\bar{\psi}_\alpha, \psi_\beta\right\} = 0$, $\left\{\bar{\psi}_\alpha, \bar{\psi}_\beta\right\} = 0$, $\{\psi_\alpha, \psi_\beta\} = 0$ At $d = 4$ where $\alpha = 1, ..., 4$, one finds:

$$\begin{aligned}\left(\sum_\alpha \bar{\psi}_\alpha\psi_\alpha\right)^n &= \left(\bar{\psi}_1\psi_1 + ... + \bar{\psi}_4\psi_4\right)^n = \\ = \left(\bar{\psi}_1\psi_1 + ... + \bar{\psi}_4\psi_4\right) &... \left(\bar{\psi}_1\psi_1 + ... + \bar{\psi}_4\psi_4\right) = \\ = \bar{\psi}_1\psi_1\bar{\psi}_1\psi_1 &...\bar{\psi}_1\psi_1 + \bar{\psi}_1\psi_1\bar{\psi}_2\psi_2...\bar{\psi}_1\psi_1 + ... \,. \end{aligned} \tag{A.20}$$

Just terms involving a product of all distinct ψ_i components survive. But if $n \geq 5$ each term will contain at least a pair of identical components so that all the contribution vanish. Generally a fermion theory with an $U(N)$ flavour symmetry cannot involve in the Lagrangian any power of the $\bar{\psi}\psi$ operator greater then $I_{max} = N2^{k+1}$. if this property does not matter in the large N limit where the decoherence makes the $\bar{\psi}\psi$ operator looks like a scalar field. Interesting results could arise for small N values.

APPENDIX B

DS EQUATIONS FOR THE GN MODEL

B.1 DS equations for connected Green's functions

In this appendix some DS equations of the GN model are computed by applying the methods presented in Sec. 2.1.2) and in Sec. 2.1.4. For convenience, the elementary fermion fields are grouped in the multiplet $\theta = (\psi, \bar{\psi})$ while the source terms are rewritten as $\xi = (\bar{\eta}, \eta)$. According to these positions, the action of the Gross Neveu model in Eq. (1.1) takes the form:

$$S = \sum_{ab} \frac{1}{2} \theta_a \theta_b S^2_{ab} + \frac{1}{4!} \sum_{abcd} \theta_a \theta_b \theta_c \theta_d S^4_{abcd}. \tag{B.1}$$

where a and b are generic indices characterizing both discrete and continuous variables.

According to the Eqs. (2.16),(2.17), the DS equations for the W_f functional are:

$$\frac{\delta S}{\delta \theta_i} \left[\frac{\delta}{\delta \xi} + \frac{\delta W}{\delta \xi} \right] = \xi_i \tag{B.2}$$

By deriving the action in Eq. (B.1) one finds:

$$\frac{\delta S}{\delta \theta_i} = \sum_{b} \theta_b S^2_{ib} + \frac{1}{3!} \sum_{abc} \theta_a \theta_b \theta_c S^4_{abc}, \tag{B.3}$$

thus with the substitution:

$$\theta \to \frac{\delta}{\delta \xi} + \frac{\delta W}{\delta \xi}, \tag{B.4}$$

the equation for the one point connected function turns out to be:

$$\begin{aligned}\frac{\delta S}{\delta\theta_i} &= \sum_b \frac{\delta W}{\delta\xi_b} S^2_{ib} \\ &+ \frac{1}{3!}\sum_{abc}\left[\frac{\delta W}{\delta\xi_a}\frac{\delta W}{\delta\xi_b}\frac{\delta W}{\delta\xi_c} - 3\frac{\delta^2 W}{\delta\xi_a\xi_b}\frac{\delta W}{\delta\xi_c} + \frac{\delta^3 W}{\delta\xi_a\delta\xi_b\delta\xi_c}\right] S^4_{iabc},\end{aligned} \tag{B.5}$$

where several terms have been grouped by renaming the indices and by using antisymmetric properties of the coefficients.

By performing the second derivative of the expression in Eq. (B.5) with respect to the θ_i field one finds:

$$\begin{aligned}\delta_{ij} &= \sum_b \frac{\delta^2 W}{\delta\xi_j\delta x_b} S_{ib} \\ &+ \frac{1}{3!}\sum_{abc}\left[3\frac{\delta^2 W}{\delta\xi_j\delta\xi_a}\frac{\delta W}{\delta\xi_b}\frac{\delta W}{\delta\xi_c}\right. \\ &- \left. 3\frac{\delta^3 W}{\delta\xi_j\delta\xi_a\delta\xi_b}\frac{\delta W}{\delta\xi_c} - 3\frac{\delta^2 W}{\delta\xi_j\delta\xi_a}\frac{\delta^2 W}{\delta\xi_b\delta\xi_c} + \frac{\delta^4 W}{\delta\xi_j\delta\xi_a\xi_b\delta\xi_c}\right] S^4_{iabc},\end{aligned} \tag{B.6}$$

The third equation is obtained by deriving one more time the previous expression:

$$\begin{aligned}&\sum_b \frac{\delta^3 W}{\delta\xi_k\delta\xi_j\delta\xi_b} S_{ib} + \frac{1}{3!}\sum_{abc}\left[3\frac{\delta^3 W}{\delta\xi_k\delta\xi_j\delta\xi_a}\frac{\delta W}{\delta\xi_b}\frac{\delta W}{\delta\xi_c}\right. \\ &+ 6\frac{\delta^2 W}{\delta\xi_j\xi_a}\frac{\delta^2 W}{\delta\xi_k\delta\xi_b}\frac{\delta W}{\delta\xi_c} - 3\frac{\delta^4 W}{\delta\xi_k\delta\xi_j\delta\xi_a\delta\xi_b}\frac{\delta W}{\delta\xi_c} \\ &+ 3\frac{\delta^3 W}{\delta\xi_j\delta\xi_a\delta\xi_b}\frac{\delta^2 W}{\delta\xi_k\delta\xi_c} - 3\frac{\delta^3 W}{\delta\xi_k\delta\xi_j\delta\xi_a}\frac{\delta^2 W}{\delta\xi_b\delta\xi_c} \\ &- \left. 3\frac{\delta^3 W}{\delta\xi_k\delta\xi_a\delta\xi_b}\frac{\delta^2 W}{\delta\xi_j\delta\xi_c} + \frac{\delta^5 W}{\delta\xi_k\delta x_j\delta\xi_a\delta\xi_b\delta\xi_c}\right] S^4_{iabc} = 0,\end{aligned} \tag{B.7}$$

Finally the fourth derivative reads:

$$\begin{aligned}
& \sum_b \frac{\delta^4 W}{\delta\xi_h\delta\xi_k\delta\xi_j\delta\xi_b} S^2_{ib} + \frac{1}{3!}\sum_{abc}\left[3\frac{\delta^4 W}{\delta\xi_h\xi_k\delta\xi_j\delta\xi_a}\frac{\delta W}{\delta\xi_b}\frac{\delta W}{\delta\xi_c}\right. \\
- \; & 6\frac{\delta^3 W}{\delta\xi_k\delta\xi_j\delta\xi_a}\frac{\delta^2 W}{\delta\xi_h\delta\xi_b}\frac{\delta W}{\delta\xi_c} + 6\frac{\delta^3 W}{\delta\xi_h\delta\xi_j\delta\xi_a}\frac{\delta^2 W}{\delta\xi_h\delta\xi_b}\frac{\delta W}{\delta\xi_c} \\
- \; & 6\frac{\delta^3 W}{\delta\xi_h\delta\xi_k\delta\xi_a}\frac{\delta^2 W}{\delta\xi_j\delta\xi_b}\frac{\delta W}{\delta\xi_c} + 6\frac{\delta^2 W}{\delta\xi_j\delta\xi_a}\frac{\delta^2 W}{\delta\xi_k\delta\xi_b}\frac{\delta^2 W}{\delta\xi_h\delta\xi_c} \\
+ \; & 3\frac{\delta^5 W}{\delta\xi_h\delta\xi_k\delta\xi_j\delta\xi_a\delta\xi_b}\frac{\delta W}{\delta\xi_c} - 3\frac{\delta^4 W}{\xi_k\delta\xi_j\delta\xi_a\delta\xi_b}\frac{\delta^2 W}{\delta\xi_h\delta\xi_c} \\
+ \; & 3\frac{\delta^4 W}{\delta\xi_h\delta\xi_j\delta\xi_a\delta\xi_b}\frac{\delta^2 W}{\delta\xi_k\delta\xi_c} - 3\frac{\delta^4 W}{\delta\xi_h\xi_k\delta\xi_j\delta\xi_a}\frac{\delta^2 W}{\delta\xi_b\delta\xi_c} \\
-3 \; & \frac{\delta^4 W}{\delta\xi_h\xi_k\delta\xi_a\delta\xi_b}\frac{\delta^2 W}{\delta\xi_j\delta\xi_c} - 3\frac{\delta^3 W}{\delta\xi_j\delta\xi_a\delta\xi_b}\frac{\delta^3 W}{\delta\xi_h\delta\xi_k\delta\xi_c} \\
+ \; & 3\frac{\delta^3 W}{\delta\xi_k\delta\xi_j\delta\xi_a}\frac{\delta^3 W}{\delta\xi_h\delta\xi_b\delta\xi_c} + 3\frac{\delta^3 W}{\delta\xi_k\delta\xi_a\delta\xi_b}\frac{\delta^3 W}{\delta\xi_h\delta\xi_j\delta\xi_c} \\
+ \; & \left.\frac{\delta^6 W}{\delta\xi_h\delta\xi_k\delta\xi_j\delta\xi_a\delta\xi_b\delta\xi_c}\right] S^4_{iabc} = 0
\end{aligned} \tag{B.8}$$

B.2 DS equations for $1PI$ correlators

The DS for the $1PI$ functions can also be calculated. The equation for the one point correlator is:

$$\begin{aligned}
\frac{\delta\Gamma}{\delta\theta_i} &= \sum_b \theta_b S^2_{ib} + \frac{1}{3!}\sum_{abc}\left[\theta_a\theta_b\theta_c - 3\left(\frac{\delta\Gamma}{\delta\theta\delta\theta}\right)^{-1}_{ab}\theta_c\right. \\
&- \left.\sum_{mnl}\left(\frac{\delta\Gamma}{\delta\theta\delta\theta}\right)^{-1}_{am}\left(\frac{\delta\Gamma}{\delta\theta\delta\theta}\right)^{-1}_{bn}\left(\frac{\delta\Gamma}{\delta\theta\delta\theta}\right)^{-1}_{lc}\frac{\delta^3\Gamma}{\delta\theta_m\delta\theta_n\delta\theta_l}\right] S^4_{iabc}
\end{aligned} \tag{B.9}$$

where the relation:

$$\frac{\delta}{\delta\theta_m}\left(\frac{\delta\Gamma}{\delta\theta\delta\theta}\right)^{-1}_{bc} = -\sum_{nl}\left(\frac{\delta\Gamma}{\delta\theta\delta\theta}\right)^{-1}_{bn}\frac{\delta^3\Gamma}{\delta\theta_m\delta\theta_n\delta\theta_l}\left(\frac{\delta\Gamma}{\delta\theta\delta\theta}\right)^{-1}_{lc}, \tag{B.10}$$

was used. The Eq. (B.9) can also be written as:

$$\begin{aligned}
\Gamma^1_i &= \sum_b \theta_b S^2_{ib} + \frac{1}{3!}\sum_{abc}[\theta_a\theta_b\theta_c - 3\Delta_{ab}\theta_c \\
&- \left.\sum_{mnl}\Delta_{am}\Delta_{bn}\Delta_{lc}\Gamma^3_{mnl}\right] S^4_{iabc},
\end{aligned} \tag{B.11}$$

thus, for the two point function, one obtains:

$$\begin{aligned}\Gamma^2_{ji} &= S^2_{ij} + \frac{1}{3!}\sum_{abc}\Bigg[3\delta_{aj}\theta_b\theta_c + 3\sum_{lm}\Delta_{nl}\Delta_{mb}\Gamma^3_{jlm}\theta_c \\ &- 3\Delta_{ab}\delta_{jc} + 3\sum_{mlnrst}\Delta_{ar}\Delta_{sm}\Delta_{bn}\Delta_{lc}\Gamma^3_{jrs}\Gamma^3_{mnl} \\ &- \sum_{mnl}\Delta_{am}\Delta_{bn}\Delta_{lc}\Gamma^4_{jmnl}\Bigg]S^4_{iabc}. \end{aligned} \tag{B.12}$$

The third derivative provides the following equation:

$$\begin{aligned}\Gamma^3_{kji} &= \frac{1}{3!}\sum_{abc}\Bigg[6\delta_{aj}\delta_{bk}\theta_c - 6\sum_{lmrs}\Delta_{ar}\Delta_{sl}\Delta_{mb}\Gamma^3_{krs}\Gamma^3_{jlm}\theta_c \\ &+ 3\sum_{lm}\Delta_{al}\Delta_{mb}\Gamma^4_{kjlm}\theta_c - 3\sum_{lm}\Delta_{al}\Delta_{mb}\Gamma^3_{jlm}\delta_{ck} \\ &+ 3\sum_{lm}\Delta_{al}\Delta_{mb}\Gamma^3_{klm}\delta_{jc} \\ &+ \sum_{lmnrs}^{pq}\big[-3\Delta_{ap}\Delta_{qr}\Delta_{sm}\Delta_{ba}\Delta_{lc}\Gamma^3_{kpq}\Gamma^3_{jrs}\Gamma^3_{mnl} \\ &\quad -3\Delta_{ar}\Delta_{sp}\Delta_{qm}\Delta_{bn}\Delta_{lc}\Gamma^3_{kpq}\Gamma^3_{jrs}\Gamma^3_{mnl} \\ &\quad -3\Delta_{ar}\Delta_{sm}\Delta_{bp}\Delta_{qn}\Delta_{lc}\Gamma^3_{kpq}\Gamma^3_{jrs}\Gamma^3_{mnl} \\ &\quad -3\Delta_{ar}\Delta_{sm}\Delta_{bn}\Delta_{lp}\Delta_{qc}\Gamma^3_{kpq}\Gamma^3_{jrs}\Gamma^3_{mnl}\big] \\ &\quad \sum_{lmnrs}\big[+3\Delta_{ar}\Delta_{sm}\Delta_{bn}\Delta_{lc}\Gamma^4_{kjrs}\Gamma^3_{mnl} \\ &\quad +3\Delta_{ar}\Delta_{sm}\Delta_{bn}\Delta_{lc}\Gamma^3_{jrs}\Gamma^4_{kmnl}\big] \\ &+ \sum_{lmn}^{pq}\big[\Delta_{ap}\Delta_{qm}\Delta_{bn}\Delta_{lc}\Gamma^4_{jmnl}\Gamma^3_{kpq} \\ &\quad +\Delta_{am}\Delta_{bp}\Delta_{qn}\Delta_{lc}\Gamma^4_{jmnl}\Gamma^3_{kpq} \\ &\quad +\Delta_{am}\Delta_{bn}\Delta_{lp}\Delta_{qc}\Gamma^4_{jmnl}\Gamma^3_{kpq}\big] \\ &\quad \sum_{lmn}\Delta_{am}\Delta_{bn}\Delta_{lc}\Gamma^5_{kjmnl}\Bigg]. \end{aligned} \tag{B.13}$$

Finally by deriving one more time the previous expression the equations for the $1PI$ four point correlators it is found. This is:

$$
\begin{aligned}
\Gamma^4_{hkji} &= \frac{1}{3!}\sum_{abc}\left[6\delta_{aj}\delta_{bk}\delta_{hc} - 6\frac{\delta}{\delta\theta_h}\left(\sum_{lmrs}\Delta_{ar}\Delta_{sl}\Delta_{mb}\Gamma^3_{krs}\Gamma^3_{jlm}\theta_c\right)\right.\\
&+ 3\sum_{lm}\Delta_{al}\Delta_{mb}\Gamma^4_{kjlm}\delta_{hc} - 3\sum_{lm}\Delta_{al}\Delta_{mb}\Gamma^4_{hjlm}\delta_{kc}\\
&+ 3\sum_{lm}\Delta_{al}\Delta_{mb}\Gamma^4_{hklm}\delta_{jc}\\
&+ 3\frac{\delta}{\delta\theta_h}\left(\sum_{lm}\Delta_{al}\Delta_{mb}\Gamma^4_{kjlm}\right)\theta_c - 3\frac{\delta}{\delta\theta_h}\left(\sum_{lm}\Delta_{al}\Delta_{mb}\right)\delta_{ck}\Gamma^3_{jlm}\\
&+ \frac{\delta}{\delta\theta_h}\sum_{lmnrs}^{pq}\left[-3\Delta_{ap}\Delta_{qr}\Delta_{sm}\Delta_{ba}\Delta_{lc}\Gamma^3_{kpq}\Gamma^3_{jrs}\Gamma^3_{mnl}\right.\\
&\quad -3\Delta_{ar}\Delta_{sp}\Delta_{qm}\Delta_{bn}\Delta_{lc}\Gamma^3_{kpq}\Gamma^3_{jrs}\Gamma^3_{mnl}\\
&\quad -3\Delta_{ar}\Delta_{sm}\Delta_{bp}\Delta_{qn}\Delta_{lc}\Gamma^3_{kpq}\Gamma^3_{jrs}\Gamma^3_{mnl}\\
&\quad \left.-3\Delta_{ar}\Delta_{sm}\Delta_{bn}\Delta_{lp}\Delta_{qc}\Gamma^3_{kpq}\Gamma^3_{jrs}\Gamma^3_{mnl}\right]\\
&+ \sum_{lmnrs}\left[3\frac{\delta}{\delta\theta_h}\left(\Delta_{ar}\Delta_{sm}\Delta_{bn}\Delta_{lc}\Gamma^4_{kjrs}\right)\Gamma^3_{mnl}\right.\\
&\quad \left.+ 3\frac{\delta}{\delta\theta_h}\left(\Delta_{ar}\Delta_{sm}\Delta_{bn}\Delta_{lc}\Gamma^4_{kmnl}\right)\Gamma^3_{jrs}\right]\\
&+ \sum_{lmnrs}\left[3\Delta_{ar}\Delta_{sm}\Delta_{bn}\Delta_{lc}\Gamma^4_{kjrs}\Gamma^4_{hmnl}\right.\\
&\quad \left.+ 3\Delta_{ar}\Delta_{sm}\Delta_{bn}\Delta_{lc}\Gamma^4_{kmnl}\Gamma^4_{hjrs}\right]\\
&+ \sum_{lmn}^{pq}\left[\Delta_{ap}\Delta_{qm}\Delta_{bn}\Delta_{lc}\Gamma^4_{jmnl}\Gamma^4_{hkpq}\right.\\
&\quad +\Delta_{am}\Delta_{bp}\Delta_{qn}\Delta_{lc}\Gamma^4_{jmnl}\Gamma^4_{hkpq}\\
&\quad \left.+\Delta_{am}\Delta_{bn}\Delta_{lp}\Delta_{qc}\Gamma^4_{jmnl}\Gamma^4_{hkpq}\right]\\
&+ \sum_{lmn}^{pq}\left[\frac{\delta}{\delta\theta_h}\left(\Delta_{ap}\Delta_{qm}\Delta_{bn}\Delta_{lc}\Gamma^4_{kmnl}\right)\Gamma^3_{kpq}\right.\\
&\quad +\frac{\delta}{\delta\theta_h}\left(\Delta_{am}\Delta_{bp}\Delta_{qn}\Delta_{lc}\Gamma^4_{jmnl}\right)\Gamma^3_{kpq}\\
&\quad \left.+\frac{\delta}{\delta\theta_h}\left(\Delta_{am}\Delta_{bn}\Delta_{lp}\Delta_{qc}\Gamma^4_{jmnl}\right)\Gamma^3_{kpq}\right]\\
&\quad \left.\sum_{lmn}\frac{\delta}{\delta\theta_h}\left(\Delta_{am}\Delta_{bn}\Delta_{lc}\Gamma^5_{kjmnl}\right)\right].
\end{aligned}
\tag{B.14}
$$

Because of the symmetries of the theory the derivative giving odd green's functions are not explicitly performed, they have to vanish ensuring the Lorentz invariance of the effective action.

APPENDIX C

CALCULATION OF THE IMPROVED PROPAGATOR

Different methods for calculating the function $\mathcal{G}(q^2)$ are presented in the following. The computation is performed at $d = 3$, at $2 < d < 4$ and at $d = 4$. The different types of divergences arising in each calculus are explicitly stressed.

C.1 Calculation at $d = 3$

The improved propagator at $d = 3$ is calculated starting from the Eq. (2.75). By replacing the value of $1/G$ given by the gap equation (Eq. (2.73)) one finds:

$$\begin{aligned}
\mathcal{G}^{-1} = I &= \int \frac{d^3k}{(2\pi)^3} \left(\mathrm{Tr}\left[\frac{1/m}{i\not{k} + m}\right] + \mathrm{Tr}\left[\frac{1}{(i\not{k} + m)\left[i\left(\not{k} + \not{q}\right) + m\right]}\right] \right) \\
&= \mathrm{Tr}\,(1) \int \frac{d^3k}{(2\pi)^3} \left(\frac{1}{k^2 + m^2} + \frac{-k^2 - k\cdot q + m^2}{(k^2 + m^2)\left[(k+q)^2 + m^2\right]} \right) \\
&= \mathrm{Tr}\,(1) \int \frac{d^3k}{(2\pi)^3} \left(\frac{k^2 + q^2 + 2k\cdot q - k\cdot q - k^2 + 2m^2}{(k^2 + m^2)\left[(k+q)^2 + m^2\right]} \right) \\
&= \mathrm{Tr}\,(1) \int \frac{d^3k}{(2\pi)^3} \left(\frac{q^2 + k\cdot q + 2m^2}{(k^2 + m^2)\left[(k+q)^2 + m^2\right]} \right), \qquad \text{(C.1)}
\end{aligned}$$

Since the integral is no more divergent the cut-off Λ can be sent to infinity near the scaling region. Thus the following Feynmann trick can be applied:

$$\begin{aligned} l &= k + (1-x)\, q, \\ k \cdot q &= l \cdot q - (1-x)\, q^2, \qquad \text{(C.2)} \\ \frac{1}{AB} &= \int_0^1 dx \frac{1}{\left[xA + (1-x)\, B\right]^2}, \qquad \text{(C.3)} \end{aligned}$$

so that:

$$\begin{aligned} & \left(k^2+m^2\right)\left[(k+q)^2+m^2\right] \\ \rightarrow \quad & \left[x\left(k^2+m^2\right) + (k+q)^2 + m^2 - x\left(k^2+m^2\right) - xq^2 - 2xk\cdot q\right]^2 \\ = \quad & \left[l^2 + x\,(1-x)\, q^2 + m^2\right]^2. \qquad \text{(C.4)} \end{aligned}$$

As a consequence one obtains:

$$\begin{aligned} I &= \mathrm{Tr}\,(1) \int_0^1 dx \int \frac{d^3 l}{(2\pi)^3} \left(\frac{q^2 - (1-x)\, q^2 + 2m^2}{\left[l^2 + x\,(1-x)\, q^2 + m^2\right]^2} \right) \\ &= \mathrm{Tr}\,(1) \int_0^1 dx \int \frac{d^3 l}{(2\pi)^3} \left(\frac{xq^2 + 2m^2}{\left[l^2 + x\,(1-x)\, q^2 + m^2\right]^2} \right), \qquad \text{(C.5)} \end{aligned}$$

The integrals can thus be calculated by applying the formula:

$$\begin{aligned} B\,(q) &= \int \frac{d^3 k}{(2\pi)^3} \frac{1}{\left(k^2+m^2\right)\left[(k+q)^2+m^2\right]} \\ &= \int_0^1 dx \int \frac{d^3 l}{(2\pi)^3} \frac{1}{\left[l^2 + x\,(1-x)\, q^2 + m^2\right]^2} \int \\ &= \frac{1}{8\pi} \int_0^1 \frac{1}{\sqrt{x\,(1-x)\, q^2 + m^2}}, \qquad \text{(C.6)} \end{aligned}$$

and by performing the shift:

$$\begin{aligned} \alpha &= 2x - 1 \\ \int_0^1 dx \frac{1}{\sqrt{x\,(1-x)\, q^2 + m^2}} &= \int_{-1}^1 d\alpha \frac{1}{\sqrt{\left(1 + 4\frac{m^2}{q^2}\right) - \alpha^2}} \frac{1}{q} \\ &= \frac{2}{q} \arctan\left(\frac{q}{2m}\right) \\ \int_0^1 dx \frac{xq^2}{\sqrt{x\,(1-x)\, q^2 + m^2}} &= \int_{-1}^1 d\alpha \frac{(1/2 + \alpha/2)\, q^2}{\sqrt{\left(1 + 4\frac{m^2}{q^2}\right) - \alpha^2}} \frac{1}{q} \\ &= \frac{q^2}{2} \frac{2}{q} \arctan\left(\frac{q}{2m}\right). \qquad \text{(C.7)} \end{aligned}$$

Finally one finds:

$$\begin{aligned} I &= \mathrm{Tr}\,(1)\int_0^1 dx \frac{1}{8\pi}\left(\frac{xq^2+2m^2}{\sqrt{x\,(1-x)\,q^2+m^2}}\right) \\ &= \mathrm{Tr}\,(1)\,\frac{1}{8\pi}\left(2m^2\frac{2}{q}\arctan\left(\frac{q}{2m}\right)+\frac{q^2}{2}\frac{2}{q}\arctan\left(\frac{q}{2m}\right)\right) \\ &= \left(q^2+4m^2\right)\arctan\left(\frac{q}{2m}\right)\frac{\mathrm{Tr}\,(1)}{8\pi q}. \end{aligned} \tag{C.8}$$

This is the result shown in Eq. (2.76).

C.2 Sharp cut-off calculation $2 < d < 4$

Here the calculation of the improved propagator is performed for a generic dimension $2 < d < 4$. Starting fro Eq. (2.84) and by replacing the value of $1/G$ given by the gap equation (Eq. (2.73)) it is found:

$$\begin{aligned} \mathcal{G}^{-1} = I &= N'\int\frac{d^dp}{(2\pi)^d}\left(\frac{q^2+p\cdot q+2m^2}{(p^2+m^2)\left[(p+q)^2+m^2\right]}\right) \\ &= \frac{N'}{2}\int\frac{d^dp}{(2\pi)^d}\left[\frac{1}{p^2+\sigma_0^2}-\frac{1}{(p+q)^2+\sigma_0^2}\right] \\ &+ \frac{N'}{2}(q^2+4\sigma_0^2)\int\frac{d^dp}{(2\pi)^d}\frac{1}{(p^2+\sigma_0^2)[(p+q)^2+\sigma_0^2]}. \end{aligned} \tag{C.9}$$

The rules for integration in polar coordinates are:

$$\begin{aligned} \int\frac{d^dp}{(2\pi)^d}f(p^2,p\cdot q) &= \int\frac{d\Omega_{d-1}}{(2\pi)^d}\int_0^\Lambda dpp^{d-1}\int_0^\pi(\sin\theta)^{d-2}f(p^2,pq\cos\theta) \\ &= \int\frac{d\Omega_{d-1}}{(2\pi)^d}\int_0^\Lambda dpp^{d-1}\int_{-1}^1(1-x^2)^{\frac{d-3}{2}}f(p^2,pqx). \end{aligned} \tag{C.10}$$

Thus the following expansion it is found:

$$\begin{aligned} \int\frac{d^dp}{(2\pi)^d}\frac{1}{(p+q)^2+\sigma_0^2} &= \int\frac{d\Omega_{d-1}}{(2\pi)^d}\int_{-1}^1(1-x^2)^{\frac{d-3}{2}}\int_0^\Lambda dpp^{d-1} \\ &\quad\left[\frac{1}{p^2+\sigma_0^2}-\frac{2px}{(p^2+\sigma_0^2)}q\right. \\ &+ \left.\left(-\frac{1}{(p^2+\sigma_0^2)^2}+\frac{4p^2x^2}{(p^2+\sigma_0^2)^3}\right)q^2+\ldots\right]. \end{aligned} \tag{C.11}$$

The contribution to the integral with odd powers in x vanish for for the parity of the integrand function. On the other hand terms of order q^4 provide only finite contributions

for $2 < d \leq < 4$. Also the coefficient of q^2 gives a finite contribution in this region. Indeed at $d = 4$, where possible divergent contributions could arise, it is found:

$$\begin{aligned} & \int \frac{d\Omega_3}{(2\pi)^4} \int_{-1}^{1} (1-x^2)^{\frac{1}{2}} \int_0^{\Lambda} dp p^3 \left(-\frac{1}{(p^2+\sigma_0^2)^2} + \frac{4p^2x^2}{(p^2+\sigma_0^2)^3} \right) \\ = & \frac{1}{16\pi^2} \ln\left(1+\frac{\Lambda^2}{\sigma_0^2}\right) - \frac{1}{16\pi^2} \ln\left(1+\frac{\Lambda^2}{\sigma_0^2}\right) = 0. \end{aligned} \tag{C.12}$$

Since the difference in Eq. (C.9) is finite it vanishes in the continuous limit. it is found:

$$\mathcal{G}^{-1} = \frac{N'}{2}(q^2+4\sigma_0^2) \int \frac{d^dp}{(2\pi)^d} \frac{1}{(p^2+\sigma_0^2)[(p+q)^2+\sigma_0^2]}. \tag{C.13}$$

The present result highlights the presence of a pole at $q^2 = -4\sigma_0^2$.

Then, one finds the result:

$$\begin{aligned} & \int \frac{d^dp}{(2\pi)^d} \frac{1}{(p^2+\sigma_0^2)[(p+q)^2+\sigma_0^2]} \\ = & \int_0^1 dx \frac{d^dl}{(2\pi)^d} \frac{1}{[l^2+x(1-x)q^2+\sigma_0^2]^2} \\ = & \int_0^1 dx \frac{1}{(4\pi)^{d/2}} \Gamma(2-d/2)(x(1-x)q^2+\sigma_0^2)^{d/2-2} \\ = & \frac{2^{4-d}}{(4\pi)^{d/2}} \Gamma(2-d/2)(q^2+4\sigma_0^2)^{\frac{d-4}{2}} \, 2F_1\left(\frac{1}{2}, 2-\frac{d}{2}; \frac{3}{2}; \frac{q^2}{q^2+4\sigma_0^2}\right) \\ = & \frac{\Gamma(2-d/2)}{(4\pi)^{d/2}} \frac{1}{\sigma_0^{4-d}} 2F_1\left(1, 2-\frac{d}{2}; \frac{3}{2}; -\frac{q^2}{4\sigma_0^2}\right), \end{aligned} \tag{C.14}$$

where the following tricks were applied in the computation:

$$x = y + 1/2, \tag{C.15}$$

$$\int_{-1/2}^{1/2} dy \, (ay^2+b)^{\frac{d-4}{2}} = b^{\frac{d-4}{2}} 2F_1\left(\frac{1}{2}, 2-\frac{d}{2}, 3/2, -\frac{a}{4b}\right), \tag{C.16}$$

$$a = -q^2, b = q^2/4 + \sigma_0^2, \tag{C.17}$$

$$\int \frac{d^dl}{(2\pi)^d} \frac{1}{(l^2+\Delta)} = \frac{1}{(4\pi)^{d/2}} \Gamma\left(2-\frac{d}{2}\right) \Delta^{\frac{d}{2}-2}, \tag{C.18}$$

$$\int_0^1 dx \, x^{\alpha-1}(1-x)^{\beta-1} = \frac{\Gamma[\alpha]\Gamma[\beta]}{\Gamma[\alpha+\beta]}, \tag{C.19}$$

and also:

$$2F_1(a,b;c;z) = (1-z)^{-b} 2F_1\left(c-a, b; c; \frac{z}{z-1}\right), \tag{C.20}$$

$$z = -q^2/4\sigma_0^2. \tag{C.21}$$

The result in Eq. (2.86) is recovered.

C.3 Sharp cut-off calculation at $d = 4$

At $d = 4$ an additional sub-leading divergence appears in the improved propagator. The integral in Eq. (C.14) is logarithmically divergent thus in order to evaluate it, with the help of a sharp-cut off regularization scheme, some additional tools are required. One can split this integral as:

$$\int \frac{d^4p}{(2\pi)^4} \frac{1}{(p^2+\sigma_0^2)[(p+q)^2+\sigma_0^2]} \tag{C.22}$$

$$= \int \frac{d^4p}{(2\pi)^4} \frac{1}{(p^2+\sigma_0^2)^2} - \int \frac{d^4p}{(2\pi)^4} \frac{q^2+p\cdot q+\sigma_0^2}{(p^2+\sigma_0^2)^2[(p+q)^2+\sigma_0^2]}, \tag{C.23}$$

so that the divergence part merges into an integral which is independent from the external momentum q. By using the Feynmann trick:

$$\int_0^1 \frac{2(1-x)}{(xA+(1-x)B)^3} = \frac{1}{AB^2}, \tag{C.24}$$

the finite part of the integral in Eq. (C.22) can be easily computed. One finds:

$$- \int \frac{d^4p}{(2\pi)^4} \frac{q^2+2p\cdot q}{(p^2+\sigma_0^2)^2[(p+q)^2+\sigma_0^2]} \tag{C.25}$$

$$= -2\int_0^1 dx(1-x) \int \frac{d^4l}{(2\pi)^4} \frac{(2x-1)q^2}{(l^2+x(1-x)q^2+\sigma_0^2)^3} \tag{C.26}$$

$$= -\frac{1}{16\pi^2}\int_0^1 dx(1-x)\frac{(2x-1)q^2}{x(1-x)q^2+\sigma_0^2} \tag{C.27}$$

$$= -\frac{1}{8\pi^2} - \frac{1}{16\pi^2}\frac{\sqrt{q^2+4\sigma_0^2}}{q}\ln\left(\frac{1+\frac{q}{\sqrt{q^2+4\sigma_0^2}}}{1-\frac{q}{\sqrt{q^2+4\sigma_0^2}}}\right). \tag{C.28}$$

The identity $i\text{Arctan}\,(-ix) = 1/2\log\left(\frac{1+x}{1-x}\right)$ was applied. The logarithmic divergent contribution in Eq. (C.22) regularized with a sharp cut-off Λ gives:

$$\int \frac{d^4p}{(2\pi)^4}\frac{1}{(p^2+\sigma_0^2)^2} = \frac{1}{16\pi^2}\ln\left(1+\frac{\Lambda^2}{\sigma_0^2}\right) - \frac{1}{16\pi^2}. \tag{C.29}$$

Thus at $d = 4$, by setting $N' = 4N$ and $\sigma_0 = m$ one finds:

$$\mathcal{G}(q)^{-1} = \frac{1}{8\pi^2}\left(q^2+4m^2\right)\left[\log\left(\frac{\Lambda^2}{m^2}\right)\right.$$
$$\left. - \frac{\sqrt{q^2+4m^2}}{q}\log\left(\frac{1+\frac{q}{\sqrt{q^2+4m^2}}}{1-\frac{q}{\sqrt{q^2+4m^2}}}\right) - 3\right], \tag{C.30}$$

being the result in Eq. (2.31).

In order to reach the scaling region the following expansion should be followed:

$$\begin{aligned} \ln\left(\frac{1+\frac{q}{\sqrt{q^2+4m^2}}}{1-\frac{q}{\sqrt{q^2+4m^2}}}\right) &= \ln\left(\frac{1+\sqrt{q^2+4m^2}}{-1+\sqrt{q^2+4m^2}}\right) \\ &\simeq \ln\left(\frac{2+\frac{1}{2}\frac{4m^2}{q^2}}{\frac{1}{2}\frac{4m^2}{q^2}}\right) = \log\left(\frac{q^2}{m^2}\right), \end{aligned} \tag{C.31}$$

thus getting the result in Eq. (2.33).

APPENDIX D

FUNCTIONAL DETERMINANT COMPUTATIONS

D.1 First order corrections to the Effective action in the $1/N$ expansion

In the following appendix the one loop contribution arising in Eq. (2.68) is calculated. It represents the next-to-leading-order correction correction in the $1/N$ expansion. The rules for the super-algebra manipulations are applied following [25]. Thus one finds:

$$\begin{aligned}
\frac{1}{2}S\mathrm{Trln}(S^{(2)}_{eff.}) &= \frac{1}{2}\mathrm{Trln}(S_{\sigma\sigma}) \\
&- \frac{1}{2}\mathrm{Trln}\left[\begin{pmatrix} 0 & \Delta_\sigma^{-1} \\ -(\Delta_\sigma^{-1})^T & 0 \end{pmatrix} + S^{-1}_{\sigma\sigma}\begin{pmatrix} \psi\psi & -\psi\bar{\psi} \\ -\bar{\psi}\psi & \bar{\psi}\bar{\psi} \end{pmatrix}\right] \\
&= \frac{1}{2}\mathrm{Trln}(S_{\sigma\sigma}) - \mathrm{Trln}\left[\Delta_\sigma^{-1}\right] \\
&- \frac{1}{2}\mathrm{Trln}\left[\begin{pmatrix} 1 & 0 \\ 0 & 1 \end{pmatrix} + \begin{pmatrix} 0 & -\Delta_\sigma^T \\ \Delta_\sigma & 0 \end{pmatrix} S^{-1}_{\sigma\sigma}\begin{pmatrix} \psi\psi & -\psi\bar{\psi} \\ -\bar{\psi}\psi & \bar{\psi}\bar{\psi} \end{pmatrix}\right] \\
&= \frac{1}{2}\mathrm{Trln}(S_{\sigma\sigma}) - \mathrm{Trln}\left[\Delta_\sigma^{-1}\right] + \frac{1}{2}\mathrm{Trln}\left(1 - 2S^{-1}_{\sigma\sigma}\bar{\psi}\Delta_\sigma\psi\right). \qquad \text{(D.1)}
\end{aligned}$$

D.2 The *RG* equation for the Wilsonian potential in fermion model

In this Appendix the expression $\mathrm{tr}\ln\Delta^{-1}$ which has been encountered in Eq. (3.98) is calculated, where Δ^{-1} is the operator defined in Eq. (3.97):

$$\Delta^{-1} = \begin{pmatrix} \frac{\delta^2 U}{\delta\psi^b_\beta \delta\bar{\psi}^a_\alpha} & -i\not{p}_{\alpha\beta}\delta^{ab} + \frac{\delta^2 U}{\delta\psi^b_\beta \delta\bar{\psi}^a_\alpha} \\ -i\not{p}_{\beta\alpha}\delta^{ba} + \frac{\delta^2 U}{\delta\bar{\psi}^b_\beta \delta\psi^a_\alpha} & \frac{\delta^2 U}{\delta\psi^b_\beta \delta\psi^a_\alpha} \end{pmatrix} . \tag{D.2}$$

As compared to Eq. (3.97), the subscript "0" is now omitted in ψ and the subscript k in U_k, while all the other indexes are explicitly indicated: Greek letters are for Dirac indexes, Latin letters for flavor ones. Now, defining $\rho = \bar{\psi}\psi = \sum_{c,\gamma} \bar{\psi}^c_\gamma \psi^c_\gamma$ and using the chain rule for functions of Grassmann numbers, all the derivatives can be expressed in terms of the field ρ:

$$\begin{aligned} \frac{\delta^2 U}{\delta\psi^b_\beta \delta\psi^a_\alpha} &= -\bar{\psi}^a_\alpha \bar{\psi}^b_\beta U_{\rho\rho}, \\ \frac{\delta^2 U}{\delta\psi^b_\beta \delta\bar{\psi}^a_\alpha} &= \delta_{\alpha\beta}\delta^{ab} U_\rho + \psi^a_\alpha \bar{\psi}^b_\beta U_{\rho\rho}, \\ \frac{\delta^2 U}{\delta\bar{\psi}^b_\beta \delta\psi^a_\alpha} &= -\delta_{\beta\alpha}\delta^{ba} U_\rho + \bar{\psi}^a_\alpha \psi^b_\beta U_{\rho\rho}, \\ \frac{\delta^2 U}{\delta\bar{\psi}^b_\beta \delta\bar{\psi}^a_\alpha} &= -\psi^a_\alpha \psi^b_\beta U_{\rho\rho}. \end{aligned} \tag{D.3}$$

The operator Δ^{-1} then becomes:

$$\begin{aligned} \Delta^{-1} &= \begin{pmatrix} -\psi^a_\alpha \psi^b_\beta U_{\rho\rho} & -i\not{p}_{\alpha\beta}\delta^{ab} + \delta_{\alpha\beta}\delta^{ab} U_\rho + \psi^a_\alpha \bar{\psi}^b_\beta U_{\rho\rho} \\ -i\not{p}_{\beta\alpha}\delta^{ba} - \delta_{\beta\alpha}\delta^{ba} U_\rho + \bar{\psi}^a_\alpha \psi^b_\beta U_{\rho\rho} & -\bar{\psi}^a_\alpha \bar{\psi}^b_\beta U_{\rho\rho} \end{pmatrix} \\ &= \begin{pmatrix} -\psi\psi U_{\rho\rho} & -i\not{p} + U_\rho + \psi\bar{\psi} U_{\rho\rho} \\ -i\not{p}^T - U_\rho + \bar{\psi}\psi U_{\rho\rho} & -\bar{\psi}\bar{\psi} U_{\rho\rho} \end{pmatrix}^{ab}_{\alpha\beta} \\ &= \begin{pmatrix} 0 & -i\not{p} + U_\rho \\ -i\not{p}^T - U_\rho & 0 \end{pmatrix}^{ab}_{\alpha\beta} + U_{\rho\rho} \begin{pmatrix} -\psi\psi & \psi\bar{\psi} \\ \bar{\psi}\psi & -\bar{\psi}\bar{\psi} \end{pmatrix}^{ab}_{\alpha\beta} \\ &= \begin{pmatrix} 0 & -i\not{p} + U_\rho \\ -i\not{p}^T - U_\rho & 0 \end{pmatrix}^{ac}_{\alpha\gamma} \\ &\quad \left[\begin{pmatrix} 1 & 0 \\ 0 & 1 \end{pmatrix} + \begin{pmatrix} 0 & \frac{i\not{p}^T - U_\rho}{p^2 + U_\rho^2} \\ \frac{i\not{p} + U_\rho}{p^2 + U_\rho^2} & 0 \end{pmatrix} U_{\rho\rho} \begin{pmatrix} -\psi\psi & \psi\bar{\psi} \\ \bar{\psi}\psi & -\bar{\psi}\bar{\psi} \end{pmatrix} \right]^{cb}_{\gamma\beta} \\ &= (\Delta_0^{-1})^{ac}_{\alpha\gamma} \left[1 + \Delta_0 \Sigma\right]^{cb}_{\gamma\beta} , \end{aligned} \tag{D.4}$$

where:

$$\Delta_0^{-1} = \begin{pmatrix} 0 & -i\not{p} + U_\rho \\ -i\not{p}^T - U_\rho & 0 \end{pmatrix}, \tag{D.5}$$

and

$$\Sigma = U_{\rho\rho} \begin{pmatrix} -\psi\psi & \psi\bar{\psi} \\ \bar{\psi}\psi & -\bar{\psi}\bar{\psi} \end{pmatrix}. \tag{D.6}$$

The matrix Δ^{-1} has been split in the product of two matrices: Δ_0^{-1} and $[1 + \Delta_0\Sigma]$. From Δ_0 the Hartree contribution to the RG equation (see the text) is obtained, from the other factor the Fock's one. From Eq. (D.18) one finds:

$$\mathrm{trln}\left(\Delta^{-1}\right) = \mathrm{trln}\left(\Delta_0^{-1}\right) + \mathrm{trln}\left(1 + \Delta_0\Sigma\right). \tag{D.7}$$

As for the Hartree term, $\mathrm{trln}\left(\Delta_0\right)$, one immediately gets:

$$\mathrm{trln}\left(\Delta_0^{-1}\right) = \mathrm{tr}\,\mathbb{I}\, N \ln(p^2 + U_\rho^2), \tag{D.8}$$

where $\mathbb{I}$ is the identity matrix in the Dirac space and the value of $\mathrm{tr}\,\mathbb{I}$ depends on the specific representation chosen for the Dirac spinors (see Section 2).

In order to evaluate the Fock contribution, $\mathrm{trln}\left(1 + \Delta_0\Sigma\right)$,the following expansion is performed:

$$\mathrm{trln}\left(1 + \Delta_0\Sigma\right) = \mathrm{tr}\left(\Delta_0\Sigma\right) - \frac{1}{2}\mathrm{tr}\left(\Delta_0\Sigma\Delta_0\Sigma\right) + \ldots \tag{D.9}$$

with:

$$\Delta_0\Sigma = \begin{pmatrix} \frac{i\not{p}^T - U_\rho}{p^2+U_\rho^2} U_{\rho\rho}\bar{\psi}\psi & -\frac{i\not{p}^T - U_\rho}{p^2+U_\rho^2} U_{\rho\rho}\bar{\psi}\bar{\psi} \\ -\frac{i\not{p} + U_\rho}{p^2+U_\rho^2} U_{\rho\rho}\psi\psi & \frac{i\not{p} + U_\rho}{p^2+U_\rho^2} U_{\rho\rho}\psi\bar{\psi} \end{pmatrix}. \tag{D.10}$$

The traces in Eq. (D.9) are easily computed by choosing a multiplet of the $U(N)$ group with just one non-vanishing component. Then, if $d \leq 4$, only terms up to the fourth order in powers of $\bar{\psi}\psi$ survive, (see App. A.3). For the Fock contribution, with the help of the identity:

$$\left(\Delta_0\Sigma\right)^n = \left(\frac{2\sigma U_\sigma U_{\sigma\sigma}}{p^2 + U_\sigma^2}\right)^{n-1} \Delta_0\Sigma, \tag{D.11}$$

one finds:

$$\mathrm{trln}\left(1 + \Delta_0\Sigma\right) = -\ln\left(1 + \frac{2\rho U_\rho U_{\rho\rho}}{p^2 + U_\rho^2}\right), \tag{D.12}$$

which is the expression used in the text (see Eq. (3.99)).

D.3 Wilsonian RG equation for fermions and bosons

In the following appendix the Wilsonian RG equations for the effective potential of a chiral theory involving both boson and fermion fields is calculated.

In order to obtain the flow equation for this potential the same passages sketched in Sec. 3.3.3 must be followed. After the Gaussian integration over the fast components, a functional super-determinant of the matrix:

$$\begin{pmatrix} S_{\phi\phi} & S_{\phi\bar{\psi}} & S_{\phi\psi} \\ S_{\bar{\psi}\phi} & S_{\bar{\psi}\bar{\psi}} & S_{\bar{\psi}\psi} \\ S_{\psi\phi} & S_{\psi\bar{\psi}} & S_{\psi\psi} \end{pmatrix} = \begin{pmatrix} M_{BB} & M_{BF} \\ M_{FB} & M_{FF} \end{pmatrix}, \tag{D.13}$$

it is found. Generally a super-determinant can be calculated by applying the rule:

$$\mathrm{sdet}\,(M) = \frac{\det\,(M_{BB})}{\det\,(N_{FF})}, \tag{D.14}$$

where: $N_{FF} = M_{FF} - M_{FB}M_{BB}^{-1}M_{BF}$. Thus for the matrix in Eq. (D.13) one finds:

$$M_{FB}M_{BB}^{-1}M_{BF} = \begin{pmatrix} S_{\bar{\psi}\phi} \\ S_{\psi\phi} \end{pmatrix} \cdot S_{\phi\phi}^{-1} \cdot \left(S_{\phi\bar{\psi}}, S_{\phi\psi}\right) = \begin{pmatrix} S_{\bar{\psi}\phi}S_{\phi\phi}^{-1}S_{\phi\bar{\psi}} & S_{\bar{\psi}\phi}S_{\phi\phi}^{-1}S_{\phi\psi} \\ S_{\psi\phi}S_{\phi\phi}^{-1}S_{\bar{\phi}\psi} & S_{\psi\phi}S_{\phi\phi}^{-1}S_{\phi\psi} \end{pmatrix}. \tag{D.15}$$

By applying the chain rules for functions of Grassmann numbers the matrix N_{FF} can be evaluated. Since:

$$\begin{aligned} S_{\phi\phi} &= p^2 + U_{\phi\phi}, \\ S_{\phi\psi} &= U_{\phi\psi}, \quad \text{etc.} \\ U_{\phi\psi^\alpha} &= -U_{\phi\rho}\bar{\psi}^\alpha, \\ U_{\psi^\alpha\phi} &= -U_{\rho\phi}\bar{\psi}^\alpha, \\ U_{\phi\bar{\psi}^\beta} &= U_{\phi\rho}\psi^\beta, \\ U_{\bar{\psi}^\beta\phi} &= U_{\rho\phi}\psi^\beta, \end{aligned} \tag{D.16, D.17}$$

it turns out to be:

$$N_{FF} \;=\; \begin{pmatrix} -\psi\psi(U_{\rho\rho} - \frac{U_{\rho\phi}U_{\phi\rho}}{p^2+U_{\phi\phi}}) & -i\not{p} + U_\rho + \psi\bar{\psi}(U_{\rho\rho} - \frac{U_{\rho\phi}U_{\phi\rho}}{p^2+U_{\phi\phi}}) \\ -i\not{p}^T - U_\rho + \bar{\psi}\psi(U_{\rho\rho} - \frac{U_{\rho\phi}U_{\phi\rho}}{p^2+U_{\phi\phi}}) & -\bar{\psi}\bar{\psi}(U_{\rho\rho} - \frac{U_{\rho\phi}U_{\phi\rho}}{p^2+U_{\phi\phi}}) \end{pmatrix} \tag{D.18}$$

Finally the trace of the logarithm of this matrix is given by:

$$\ln\det N_{FF} = N'\ln\left(p^2 + U_\rho^2\right) - \ln\left(1 + \frac{2\rho U_\rho\left(U_{\rho\rho} - \frac{U_{\rho\phi}U_{\phi\rho}}{p^2+U_{\phi\phi}}\right)}{p^2 + U_\rho^2}\right) \tag{D.19}$$

For generic d dimension the Wilsonian RG equation for dimensionless quantities is then:

$$\begin{aligned}\frac{\partial}{\partial t}U &= dU - \frac{d-2}{2}\phi U_\phi - (d-1)\,\sigma U_\sigma \\ &+ \frac{1}{2}\frac{2^{1-d}}{\pi^{d/2}\Gamma\left(\frac{d}{2}\right)}\left[\log\left(1+U_{\phi\phi}\right) - N'\log\left(1+U_\sigma^2\right) + \log\left(1+\Sigma\right)\right], \end{aligned} \tag{D.20}$$

where:

$$\Sigma = \frac{2\sigma U_\sigma\left(U_{\sigma\sigma} - \frac{U_{\sigma\phi}U_{\phi\sigma}}{1+U_{\phi\phi}}\right)}{1+U_\sigma^2}. \tag{D.21}$$

BIBLIOGRAPHY

[1] D.J.Gross, A.Nuveu, *Phys. Rev.* D **10**, 10 (1974) .

[2] C. Itzykson, J-M. Drouffe, "Statistical Field Theory: Strong Coupling, Monte Carlo Methods, Conformal Field Theory, And Random Systems", Cambridge University Press, 2nd ed., (1991).

[3] E. Fermi, Z. Phys. **88**, 161 (1934).

[4] S.Glashow, Nucl. Phys. **22**, 579 (1961); S.Weinberg, *Phys. Rev. Lett.* **19**, 1264 (1967); A.Salam In: *Proc. 8th Nobel Symp.*, Almqvist and Wiksell, Stockholm (1968).

[5] F.Englert, R.Brout, *Phys. Rev. Lett.* **13**, 321 (1964); P.Higgs, *Phys. Rev. Lett.* **13**, 508 (1964); G.Guralnik,C.Hagen, T.Kibble *Phys. Rev. Lett.* **13**, 585 (1964).

[6] Y.Nambu, G.Jona-Lasinio, *Phys. Rev.* **122**, 345 (1961); Y.Nambu, G.Jona-Lasinio, *Phys. Rev.* **124**, 246 (1961).

[7] G.Cvetic, Rev.Mod.Phys. **71**, 513 (1999).

[8] E. Brezin, J. Le Guillou, J. Zinn-Justin, Phys. Rev. D8 **434**, 1973 (;) E. Brezin, J. Zinn-Justin, Phys. Rev.Lett. **691**, 1976 (;) E. Brezin, J. Le Guillou, J. Zinn-Justin,Phys. Rev.D **1544**, 1977 (.)

[9] K. Wilson,*Phys. Rev. Lett.* **28**, 240 (1972); K. Wilson and J. Kogut, *Phys. Rep.* C **12**, 75 (1974); K. Wilson, *Rev. Mod. Phys.* **47**, 773 (1975).

[10] D.Lurie, A.Macfarlane, *Phys. Rev.* **136**, 3B (1964).

[11] K.Wilson, *Phys. Rev.* D **7**, 10 (1973).

[12] G.Parisi *Nucl. Phys.* B **100**, 368 (1975).

[13] K.Shizuya, *Phys. Rev.* D **21**, 8 (1980).

[14] C.Bender, F.Cooper, G.Guralnik, Annals of Physics **109**, 165 (1977).

[15] K.Tamvakis, G. Guralnik, *Phys. Rev.* D **18**, 4551 (1978).

[16] B.Rosenstein, B.J.Warr, S.H.Park, *Phys. Rev. Lett.* **62**, 13 (1989).

[17] J.Zinn-Justin,*Nucl. Phys.* B **B367**, 105 (1991).

[18] A.Hasenfratz, P.Hasenfratz, K.Jansen, J.Kuti, Y.Shen, *Nucl. Phys.* B **365**, 79 (1991).

[19] S.Hands, A.Kocić, J.B. Kogut *Phys. Lett.* B **273**, 111 (1991).

[20] W.Bardeen, C.Hill, M.Lindner *Phys. Rev.* D **41**, 5 (1990).

[21] A.Miransky, M.Tanabashi, K.Yamawaki, Mod. Phys. Lett. **A4**, 1043 (1989); A.Miransky, M.Tanabashi, K.Yamawaki, Phys. Lett. **B221**, 177 (1989).

[22] S.Hands, A.Kocić, J.B.Kogut, Annals of Physics **224**, 29 (1993).

[23] S.Hands, J.B. Kogut *Nucl. Phys.* B **B520**, 382 (1998).

[24] F.Wegner, A.Houghton, *Phys. Rev.* **A8**, 401 (1972).

[25] T.Clark, B.Haeri, S.Love, *Nucl. Phys.* B **402**, 3 (1993).

[26] See for instance: R. Rivers, "Phat Integral methods in quantum field theory", Cambridge University Press, (1987).

[27] See for instance: J. Zinn-Justin, "Quantum Field Theory and Critical Phenomena", Claredon Press, (1996).

[28] J. Zinn-Justin, "Phase Transitions and Renormalization Group", Oxford University Press, (2007).

[29] See for instance: M. Maggiore, "A Modern Introduction to Quantum Field Theory", Oxford University Press, (2005).

[30] A. Pich, Lectures at the 1997 Les Houches Summer School "Probing the Standard Model of Particle Interactions."

[31] J. Cornwall, R. Jackiw, E. Tomboulis, Phys.Rev. **D10**, 2428 (1974); E. Gorbar, Annals Phys. **277**, 255 (1999).

[32] W. Zimmermann, Annals of Phys. **77**, 570 (1973); See for instance: S. Weinberg, "The Quantum Theory of Fields", v.2, Cambridge University Press, (1996).

[33] See for instance: W.Greiner, J. Reinhardt, "Field Quantization", Springer Ed., (1996).

[34] See for instance: A. Fetter, J.Walecka, "Quantum Theory of Many-Particle Systems", McGraw-Hill Ed., (1980).

[35] See for instance: N. Goldenfeld, "Lectures on Phase Transitions and the Renormalization Group", Perseus (1992).

[36] J. Wess, B. Zumino,Nucl. Phys.B **70**, 39 (1974); J. Wess, B. Zumino B, Nucl. Phys.B **49**, 52 (1974).

[37] S. Adler,Phys. Rev. **177**, 2426 (1969); J. Bell, R. Jackiw,Il Nuovo Cimento A **60**, 47 (1969).

[38] S. Coleman,"Aspect of Symmetry", Cambridge University Press, (1985).

[39] See for instance: J. Weiss, J. Bagger, "Supersymmetry and Supergravity", Princetone Series 2^{nd} Ed.,(1992); P. Kopietz, L. Bartosch, F.Schutz, "Introduction to the Functional Renormalization Group",Springer Ed., (2010), p.169-171.

[40] See for instance: C. Itzykson, J.-M. Drouffe, "Statistical field theory", Cambridge University Press (1989): K. Huang "Statistical Mechanics", 2^{nd} Ed.,(1987); R. Pathria "Statistical Mechanics", Butterworth-Heinemann 2^{nd} Ed.,(1996).

[41] See for instance: M. Peskin, D. Schroeder, "An Introduction To Quantum Field Theory", Addison-Wesley (1995).

[42] F. Dyson, Phys. Rev. **75**, 1736 (1949); J. Schwinger, PNAS **37**, 452 (1951).

[43] N. Bogoliubov, Jour. of Phys.USSR **10**, 265 (1946); J. Kirkwood, The Jour. of Chem. Phys. **14**, 180 (1946); J. Kirkwood, The Jour. of Chem. Phys. **15**, 72 (1947); M. Born, H. Green, Proc. Roy. Soc. A **188**, 10 (1946).

[44] L. Kadanoff, G. Baym, "Quantum Statistical Mechanics", Benjamin, New York, (1962).

[45] G. 't Hooft, Nucl. Phys. B **72**, 461 (1974).

[46] L. Cooper, Phys. Rev. **104**, 1189 (1956); J. Bardeen, L. Cooper, J. Schrieffer,Phys. Rev. **106**, 162 (1957); J. Bardeen, L. N. Cooper, J. R. Schrieffer, Phys. Rev. **108**, 1175 (1957).

[47] Moshe-Moshe, J. Zinn-Justin, Phys. Rep. **385**, 69 (2003).

[48] See for instance: D. Stauffer, A. Aharony, "Introduction To Percolation Theory',2^{nd} Ed.,(1991)

[49] J. Polonyi, Centr. Eur. Journ. of Phys. **1**, 1 (2003); C. Bagnuls, C. Bervillier, Phys.Rept. **348**, 2001 (;)

[50] K. Wilson, M. Fisher, *Phys. Rev. Lett.* **28**, 240 (1972).

[51] See for instance: J. Amit "Renormalization Group and Critical Phenomena", World Scientific,(1984);

[52] C.G. Callan, Jr.,*Phys. Rev.* D **2**, 1541 (1970)

[53] K. Symanzik, Commun. Math. Phys. **18**, 227 (1970).

[54] K. Symanzik,Commun. Math. Phys. **23**, 49 (1971).

[55] E. Focht, J. Jersáka, J. Paul, *Nucl. Phys.* B **47**, 709 (1996).

[56] V.Branchina, *Phys. Lett.* B **549**, 1 (2002).

[57] See for instance: C. Domb, M.S. Green, "Phase Transitions and Critical Phenomena", v.6, Academic Press, (1976); S.-K. Ma, "Modern Theory of Critical Phenomena", Benjamin, Reading (1976).

[58] J.Alexandre, V.Branchina, J.Polonyi, *Phys. Rev.* D **58**, 016002 (1998).

[59] S.Weinberg, Critical Phenomena for Field Theorists, Lectures presented at Int. School of Subnuclear Physics, Ettore Majorana, Erice, Sicily, Jul 23 - Aug 8, 1976. Published in Erice Subnucl.Phys.1976:1 (QCD161:I65:1976); S. Weinberg, Ultraviolet Divergences In Quantum Theories Of Gravitation, p.790, in "General Relativity", Eds. S.W.Hawking and W.Israel (1980).

[60] L. Karkkainen, R. Lacaze, P. Lacock, B. Petersson, Nucl.Phys.B **415**, 781 (1994); ERRATUM-Nucl.Phys.B **438**, 650 (1995).

[61] S. Christofi, C. Strouthos, Journ. of High En. Phys. **0705**, 088 (2007).

[62] L. Rosa, P. Vitale, C. Wetterich,Phys. Rev. Lett. **86**, 958 (2001).

[63] S. Kim, A. Kocic, J. Kogut, Nucl.Phys. B **429**, 407 (1994).

[64] G. Gat, A. Kovner, B. Rosenstein Nucl.Phys. B **385**, 76 (1992).

[65] K. Aoki (Kanazawa U.), K. Morikawa, J. Sumi , H. Terao, M. Tomoyose Prog.Theor.Phys. **102**, 1151 (1999); K. Aoki, M. Bando, K. Hasebe, T. Kugo, H. Nakatani Progr. of Theor. Phys. **82**, 1151 (1989).

[66] A. Bonanno, V. Branchina, H. Mohrbach, D. Zappalá, Phys. Rev. D **60**, 065009 (1999).

[67] S. Hands, Nucl.Phys. B **63**, 673 (1998).

[68] R. Pisarski, *Phys. Rev. Lett.* **48**, 574 (1982).

[69] W. Bardeen, Moshe Moshe, *Phys. Rev.* D **28**, 1372 (1983), W. Bardeen, Moshe Moshe, M. Bander, *Phys. Rev. Lett.* **52**, 1188 (1984).

[70] F. David, D. Kessler, H. Neuberger, Nucl.Phys.B **257**, 695 (1985).

[71] T. Appelquist, U. Heinz, *Phys. Rev.* D **24**, 2169 (1981), T. Appelquist, U. Heinz, *Phys. Rev.* D **25**, 2620 (1982).

[72] K. Aoki, K. Morikawa, W. Souma, J.Sumi, H. Terao,Prog.Theor.Phys. **95**, 409 (1996).

[73] R.Shankar, Rev. Mod. Phys. **66**, 129 (1994).

[74] M. Salmhofer, C. Honerkamp ,Prog. Theor. Phys. **105**, 1 (2001).